

Part A: Rhodium-Catalyzed Synthesis of Heterocycles
Part B: Mechanistic Studies on Tethering Organocatalysis Applied to
Cope-Type Alkene Hydroamination

Nicolas Guimond

A thesis submitted to the
Faculty of Graduate and Postdoctoral Studies
In partial fulfillment of the requirements
For the Philosophiae Doctor (Ph.D.) degree in chemistry

Ottawa-Carleton Chemistry Institute
Faculty of Science
University of Ottawa

Abstract

The last decade has been marked by a large increase of demand for green chemistry processes. Consequently, chemists have focused their efforts on the development of more direct routes toward different classes of targets. In that regard catalysis has played a crucial role at enabling key bond formations that were otherwise inaccessible or very energy and resources consuming. The central theme of this body of work concerns the formation of C–N bonds, either through transition metal catalysis or organocatalysis. These structural units being highly recurrent in biologically active molecules, the establishment of more efficient routes for their construction is indispensable.

The first part of this thesis describes a new method for the synthesis of isoquinolines from the oxidative coupling/annulation of alkynes with *N-tert*-butyl benzaldimines via Rh(III) catalysis (Chapter 2). Preliminary mechanistic investigations of this system pointed to the involvement of Rh(III) in the C–H bond cleavage step as well as in the C–N bond reductive elimination that provides the desired heterocycle.

Following this oxidative process, a Rh(III)-catalyzed redox-neutral approach to isoquinolones from the reaction of benzhydroxamic acids with alkynes is presented (Chapter 3). The discovery that an N–O bond contained in the substrate can act as an internal oxidant was found to be very enabling. Indeed, it allowed for milder reaction conditions, broader scope (terminal alkyne and alkene compatible) and low catalyst loadings (0.5 mol%). Mechanistic investigations on this system were also conducted to identify the nature of the C–N bond formation/N–O bond cleavage as well as the rate-determining step.

The second part of this work presents mechanistic investigations performed on a recently developed intermolecular hydroamination reaction catalyzed through tethering

organocatalysis (Chapter 4). This transformation operates via the reversible covalent attachment of two reactants, a hydroxylamine and an allylamine, to an aldehyde catalyst by the formation of a mixed aminal. This allows a difficult intermolecular Cope-type hydroamination to be performed intramolecularly. The main kinetic parameters associated with this reaction were determined and they allowed the generation of a more accurate catalytic cycle for this transformation. Attempts at developing new families of organocatalysts are also discussed.

Acknowledgments

I think that whether you like a place or not is not related to the place itself, but to the people with who you are. If I loved my time in Ottawa, I owe it in big part to all the people I had the chance to spend my time with over the years.

First of all, I want to thank the Fagnou Factory for welcoming me in their group when I joined the University of Ottawa. You guys have been awesome from the beginning till the end. Special thanks to Dave, great friend from who I learned so much and who made my passion for chemistry even greater with all those discussions we had together at the chalkboard. Thanks to Derek, you were like my big brother in the lab. I appreciate all the help you gave me with chemistry and the fun with had playing foosball. Christina, you have been an awesome labmate with sweet musical tastes. If ever you meet J.-Q., don't forget to tell him to hold on to his pants! Sophie, j'ai tellement d'estime pour toi. Merci d'avoir été mon amie et ma confidente pour si longtemps. Merci pour toute ton aide avec la chimie aussi. J'ai déjà hâte de te revoir en Europe. T-Rash, you are probably the guy with who I spent the most time with over my Ph.D.. Thanks for being so nice all the time. I still hope I'll see you with unsymmetrical facial hair at some point. Mégan, j'ai passé les plus beaux moments de ma vie à tes côtés. Merci pour tout. Thanks to all the other members of the Fagnou Factory, or should I say Fagnou Family. Malcolm and Olivier: thanks for the proof-reading and all the fun with had together. Ben: merci d'avoir été si rassembleur avec le groupe, ça a été très important, surtout dans les moments les plus dures. Dan: you are the funniest guy I know, thanks for all the laughs. David: merci pour tout le fun qu'on a eu ensemble, que ce soit au foosball ou en voyageant à Montréal. Thanks to Ho-Yan, Lina, Ivan, Elisia, Marieke and Chris who made my experience in the Fagnou lab as nice as it was.

Keith, I wish I could tell you how much of an honour and a privilege it was for me to study under your supervision. You have impacted my life positively in so many aspects and in a magnitude that no one has ever done before in such a short period of time. Your attitude toward chemistry and life in general will remain a model for me forever. Thanks for all.

Thanks to the Beauchemin group for welcoming me in their lab toward the end of my Ph. D. I really appreciated being with you all that time. Thanks Mel for all the great times and the nice discussions while my lunch was heating or while walking to go get a Funky Monkey ;) . One day I will see you again and I will be able to speak English, I promise. Amanda, you have been an awesome labmate. I know it is unlikely, but I truly wish we will be labmate again at some point in the future (then we can take over the world). You made a difference in everyday I spent working beside you, thanks for that. Frank, ça a été un plaisir de partager mes dernières années de doc avec toi. Tu as été un bon ami et un bon confident. Merci pour tout. Colin, I really liked sharing chemistry ideas with you. I hope you'll keep up with that. Oh by the way, do a Ph. D! :P. Chris, merci pour les discussions de chimie. C'est toujours le fun de pouvoir s'entraider comme on l'a fait. Subordonné Vincent-Rocan, j'ai bien aimé passer du temps avec toi dans le lab ou sur le court de badminton. Thanks to all the other Beauchemin members: Nic, Shubin, and Wei, the only post-doc trio which can get drunk using only one beer :P. Just kidding, you guys are great scientists and it was a pleasure working with you. Bashir, Keira, Mat, Isa, and Ashley, I had a lot of fun working with all of you. Thanks for being so nice with me. Finally, I want to thank Pat Moon, Charlotte and Kashif, who were amazing undergrads with awesome attitude and personality. I wish you the best of luck with the rest of your studies.

Le dernier et non le moindre, André. Tu a été un superviseur remarquable. Ton enthousiasme et ta passion envers la chimie ont fait que mon expérience dans ton groupe a

été des plus agréable. J'ai adoré parler de chimie avec toi et j'espère pouvoir transmettre la même passion autour de moi plus tard dans ma carrière. Je veux te remercier aussi pour toute l'aide et le réconfort que tu m'as apporté dans les moments les plus difficiles. Les choses n'ont pas toujours été faciles après le décès de Keith, mais tu as toujours été là pour me supporter à 100%, sans compromis et sans compter ton temps. Merci pour tout, je n'oublierai jamais tout ce que tu as fait pour moi.

Table of Content

Abstract	ii
Acknowledgments	iv
Table of Content	vii
List of Figures	x
List of Schemes	xii
List of Tables	xv
Glossary of Abbreviations	xvi
Chapter 1	1
Introduction	1
1.1 C–N Bonds From Transition Metal-Mediated Reductive Elimination.....	2
1.2 Mechanistic Considerations For Transition Metal-Mediated C–H Bond Functionalization	9
1.3 Mechanistic Aspects of Different Hydroamination Systems	13
Chapter 2	22
Rhodium(III)-Catalyzed Oxidative Synthesis of Isoquinolines	22
2.1 Introduction.....	22
2.1.1 Traditional Routes to Isoquinolines.....	23
2.1.2 Larock Isoquinoline Synthesis.....	25
2.1.3 Heterocycle Synthesis Via C–H Functionalization	27
2.2 Results and Discussion	31
2.2.1 Reaction Development and Exploration of Coupling Partners Compatibility	31
2.2.2 Mechanistic Insights	38
2.3 Summary and Outlook	41
Chapter 3	42
Rhodium(III)-Catalyzed Redox-Neutral Synthesis of Nitrogen-Containing Heterocycles	42
3.1 Introduction.....	42
3.1.1 Rhodium(III)-Catalyzed Oxidative Heterocycle Synthesis.....	44
3.1.2 N–O Bond as Oxidant in Transition Metal Catalysis.....	51
3.2 Results and Discussion	57
3.2.1 Initial Reaction Development and Scope	57
3.2.2 Preliminary Mechanistic Investigations.....	64
3.2.3 Internal Oxidant Modification	68
3.2.4 Improved reaction scope	71
3.2.5 Computational and experimental mechanistic investigations	78
3.2.6 Isoquinoline synthesis	85
3.3 Summary and Outlook	93
Chapter 4	95
Mechanistic Investigations on Cope-Type Hydroamination Through Tethering Organocatalysis	95
4.1 Introduction.....	95
4.1.1 Catalysis Through Temporary Intramolecularity	97
4.1.2 Cope-Type Hydroamination of Alkenes as a Mean for C–N Bond Formation	101
4.1.3 Merging Tethering Organocatalysis with Cope-Type Hydroamination Reactivity.....	106

4.2 Results and Discussion	107
4.2.1 Exploration of Different Competent Aldehyde Catalysts	108
4.2.2 Kinetic Experiments	110
4.2.3 Exploration of Ketone Catalysts	117
4.2.4 Bifunctional Organocatalysts	120
4.2.5 Formaldehyde as a More Active Catalyst	123
4.3 Summary and Outlook	127
Chapter 5.....	129
Supporting Information.....	129
5.1 General Methods.....	129
5.2 Rhodium(III)-Catalyzed Oxidative Synthesis of Isoquinolines	129
5.2.1 SYNTHESIS OF BENZALDIMINES.....	130
5.2.2 SYNTHESIS OF UNSYMMETRICAL ALKYNES.....	134
5.2.3 SYNTHESIS OF ISOQUINOLINES.....	137
5.3 Rhodium(III)-Catalyzed Redox-Neutral Synthesis of Nitrogen-Containing Heterocycles.....	144
5.3.1 MECHANISTIC EXPERIMENTS OF SECTION 3.2.2	144
5.3.2 SYNTHESIS OF <i>O</i> -METHYL HYDROXAMATES	149
5.3.3 SYNTHESIS OF UNSYMMETRICAL ALKYNES.....	152
5.3.4 SYNTHESIS OF SUBSTITUTED ISOQUINOLONES.....	154
5.3.5 PREPARATION OF THE SUBSTRATES BEARING DIFFERENT INTERNAL OXIDANTS.....	160
5.3.6 ISOQUINOLONE SCOPE SUBSTRATES	164
5.3.7 SYNTHESIS OF DISUBSTITUTED ISOQUINOLONES FROM <i>N</i> -(OPiv) BENZAMIDES.....	166
5.3.8 SYNTHESIS OF MONOSUBSTITUTED ISOQUINOLONES	171
5.3.9 SYNTHESIS OF 3,4-DIHYDROISOQUINOLONES.....	174
5.3.10 MECHANISTIC EXPERIMENTS.....	179
5.3.11 ISOQUINOLINE SYNTHESIS RELATED EXPERIMENTS.....	182
5.3.12 DFT CALCULATIONS	188
5.4 Mechanistic Investigations on Cope-Type Hydroamination Through Tethering Organocatalysis	201
5.4.1 ALDEHYDE SCREENING	202
5.4.2 MOLECULES FOR MECHANISTIC EXPERIMENTS	206
5.4.3 KINETIC EXPERIMENTS.....	207
5.4.4 DEUTERIUM KINETIC ISOTOPE EFFECT (DKIE) EXPERIMENTS	213
5.4.5 EYRING PLOT.....	214
5.4.6 KETONE SCREENING.....	217
5.4.7 "BIFUNCTIONAL" ORGANOCATALYSTS PREPARATION	221
5.4.8 RATE COMPARISON FOR 4.3T AND 4.3W	223
5.4.8 PARAFORMALDEHYDE-CATALYZED COPE-TYPE HYDROAMINATION OF ALLYLIC AMINES WITH <i>N</i> -ALKYLHYDROXYLAMINES	225
Appendix 1	228
Initial Steps Toward the Development of an Organocatalyzed Azide-Alkyne Huisgen Cycloaddition	228
A1.1 Introduction	228
A1.2 Results and Discussion	232
A1.3 Summary and Outlook	237
Supporting Information for Appendix 1	239
SYNTHESIS OF CYCLOADDITION PRECURSORS.....	239
Appendix 2	242
Claims to Original Research	242

Publications from this Work	243
Presentations from this Work	243
Oral presentation.....	243
Poster Presentations.....	244

List of Figures

Figure 1.1 Proposed mechanism for C(<i>sp</i> ²)-H bond functionalization	10
Figure 1.2 Distortion-interaction analysis for the CMD transition state; benzene is shown as a representative substrate	13
Figure 2.1 Representative isoquinolines in chemistry and medicine	23
Figure 2.2 Traditionnal approaches toward the isoquinoline heterocycle	24
Figure 2.3 Hydroaryation/electrocyclization/oxidation potential mechanistic pathway.....	38
Figure 2.4 Potential Rh(IV) reductive elimination pathway	39
Figure 3.1 Rh(III)-catalyzed oxidative heterocycle formation.....	43
Figure 3.2 Different heterocycles accessible through a rhodium(III)-catalyzed cross-coupling/cyclization strategy	45
Figure 3.3 Arene rhodation regioselectivity.....	46
Figure 3.4 Regioselectivity of the alkyne insertion.....	49
Figure 3.5 Strategies for heterocycle formation.....	57
Figure 3.6 Mechanistic hypothesis for potential Rh(I)-catalyzed isoquinolone synthesis.....	59
Figure 3.7 Monitoring of the reaction of 3.1a with 3.2a	61
Figure 3.8 Revised structure of 3.3a	62
Figure 3.9 Initially proposed catalytic cycle	68
Figure 3.10 Proposed stabilized intermediate in the catalytic cycle	69
Figure 3.11 Mechanistic hypotheses for the C-N bond forming/N-O bond cleaving event. .	79
Figure 3.12 Explanation for the observation of the methyl ester side-product	92
Figure 4.1 Log plot of the initial rate dependence on the concentration of the diverse reaction components showing (a) a first order dependence in organocatalyst (4.3t), (b) a first order dependence in allylbenzylamine (4.1b), and (c) an inverse order dependence in benzylhydroxylamine (4.2a).	112
Figure 4.2 Reaction profile over 13 h period	113
Figure 4.3 Competing 1,2-addition of 4.2a and 4.1b on 4.5a , which explains the inverse order behavior in 4.2a	114
Figure 4.4 Eyring plot generated at intervals of 10 °C between 25 and 55 °C for the reaction of 4.1b (0.75 mmol, 1.5 equiv.) and 4.2a (0.5 mmol, 1 equiv) in C ₆ D ₆ (1 M) using 4.3t (20 mol%) as catalyst.	115
Figure 4.5 Proposed catalytic cycle.....	117
Figure 4.6 Possible Lewis acid activation of the nitron intermediate	120

Figure 4.7 Initial rate comparison in DMSO- <i>d</i> ₆ using 4.1b (1.5 equiv.), 4.2a (1 equiv.), catalyst 4.3t or 4.3w (20 mol%), DMSO- <i>d</i> ₆ (1 M), 25 °C.	125
Figure A1.1 Design plan for an organocatalytic Huisgen 1,3-dipolar azide-alkyne cycloaddition	231
Figure A1.2 Potential Thorpe-Ingold effect to allow for a lower temperature cyclization..	236
Figure A1.3 Internal hydrogen bonding activation	237

List of Schemes

Scheme 1.1 Buchwald-Hartwig Amination and General Mechanism.....	4
Scheme 1.2 Electronic Effects on Rate of Reductive Elimination	5
Scheme 1.3 Palladium(IV)-mediated C-N Bond Reductive Elimination	6
Scheme 1.4 Rate of Cu(III)-Mediated Reductive Elimination as Function of Electronic Factors	7
Scheme 1.5 Cu(III) Intermediate Detected During Catalysis	8
Scheme 1.6 Example of Brønsted Acid-Catalyzed Hydroamination and Mechanism	15
Scheme 1.7 Enantioselective Brønsted Acid-Catalyzed Hydroamination	16
Scheme 1.8 Example of Base-Catalyzed Alkene Hydroamination and Mechanism.....	17
Scheme 1.9 Early Transition Metal-Catalyzed Hydroamination and Corresponding Mechanism	19
Scheme 1.10 Late Transition Metal-Catalyzed Hydroamination and Corresponding Mechanism	20
Scheme 2.1 Larock Isoquinoline Synthesis ⁵⁴	26
Scheme 2.2 Bergman and Ellman and Jun Heterocycle Synthesis.....	27
Scheme 2.3 Rhodium(III)-Mediated Isoquinoline Salt Formation by Jones.....	29
Scheme 2.4 Fagnou Indole Synthesis	30
Scheme 2.5 Initial Hit	31
Scheme 2.6 Product Inhibition Testing	37
Scheme 2.7 Reaction Outcome with Different Leaving Groups.	38
Scheme 2.8 Ruling Out of the Electrocyclization/Oxidation Pathway.....	39
Scheme 2.9 Verification of the Rh(IV) Hypothesis.....	40
Scheme 2.10 Proposed Catalytic Cycle	41
Scheme 3.1 Kinetics for Arene Rhodation Regioselectivity	47
Scheme 3.2 Palladium-Catalyzed Amino-Heck Reactions	52
Scheme 3.3 Isoquinoline Derivatives Via Palladium-Catalyzed Amino-Heck Reaction.....	53
Scheme 3.4 Liebeskind <i>N</i> -Imination of Organometallic Species	54
Scheme 3.5 Copper-Mediated Amidation Reaction From Hydroxamic Acid Derivatives	55
Scheme 3.6 Use of N–O bond as Oxidant in a C–H Alkenylation Reaction.....	55
Scheme 3.7 Palladium-Catalyzed Intramolecular Direct Amination Reaction	56
Scheme 3.8 Use of Hydroxamic Acids for Direct C–H Bond Amination.....	58

Scheme 3.9 Initial Result Using Oxidative Conditions	58
Scheme 3.10 Cheng Rh(I)-Catalyzed Isoquinoline Synthesis	64
Scheme 3.11 Rh(III)-Catalyzed Hydroarylation.....	65
Scheme 3.12 Electrocyclization Hypothesis Verification	66
Scheme 3.13 Preliminary Mechanistic Insights.....	67
Scheme 3.14 Unsubstituted Isoquinolone Via Retro-Diels-Alder.....	77
Scheme 3.15 Irreversibility of Alkyne Insertion	79
Scheme 3.16 DKIE Measurements.....	80
Scheme 3.17 Rate Measurements for Substrates With a Different Internal Oxidant	81
Scheme 3.18 Free Energy Diagram (ΔG_{298K} , kcal mol ⁻¹ in methanol) for the Relevant Intermediates, Transition States and Products for the Reaction of 3.11 with Acetylene. The Neutral and Cationic Pathway Energies Are Shown in Black and Red, Respectively.	84
Scheme 3.19 DFT Calculated Catalytic Cycle	85
Scheme 3.20 Unsuccessful Isoquinoline Synthesis From Aldoxime Derived Substrates	86
Scheme 3.21 Initial Hit Using Oxime Derivatives as Starting Material.....	87
Scheme 3.22 Isoquinolines from Acetophenone Oxime Derivative 3.10d	89
Scheme 3.23 Observation of a Methyl ester Side-Product	91
Scheme 3.24 Free Oxime as Substrate	92
Scheme 3.25 Control Experiments	93
Scheme 4.1 Organocatalyzed Nitrile Hydration	99
Scheme 4.2 Carbonyl-Catalyzed Ester Hydrolysis.....	100
Scheme 4.3 Formaldehyde-Catalyzed Amide Hydrolysis.....	100
Scheme 4.4 Ketone-Catalyzed Enantioselective Nitrile Hydrolysis	101
Scheme 4.5 House Alkene Hydroamination Product	102
Scheme 4.6 Ciganek Mechanistic Proposal ¹²⁸	103
Scheme 4.7 Knight's Synthesis of Vicinal Diamines.....	104
Scheme 4.8 Intermolecular Cope-Type Hydroamination	105
Scheme 4.9. Intermolecular Organocatalyzed Cope-Type Hydroamination.....	107
Scheme 4.10 DKIE Experiments.....	114
Scheme 4.11 Confirmation of an Inhibition Pathway	116
Scheme 4.12 Steric Effects Using Ketone.....	119
Scheme 4.13 Effect of Thiourea Co-Catalyst.....	121
Scheme 4.14 Attempts at Internal Lewis Acid Activation.....	123

Scheme A1.1 Huisgen 1,3-Dipolar Cycloaddition of Azides and Terminal Alkynes	229
Scheme A1.2 Intramolecular 1,3-Dipolar Azide-Alkyne Cycloaddition	231
Scheme A1.3 Individual Steps Leading to the Formation of Triazole A1.5a.....	233
Scheme A1.4 Initial Attempts Toward Organocatalyzed Triazole Formation	234

List of Tables

Table 2.1 Solvent Screening.....	32
Table 2.2 Oxidant Screening	33
Table 2.3 Optimization of Catalyst Loading and Reaction Concentration	34
Table 2.4 Scope of Substituted <i>N-tert</i> -Butylbenzaldimines.	35
Table 2.5 Reaction Compatibility with Unsymmetrical Alkynes	36
Table 3.1 Alkyne Scope with Various Heterocycles.....	48
Table 3.2 Overview of Reaction Conditions for Various Rh(III)-Catalyzed Heterocycle Syntheses.....	50
Table 3.3 Screening of Rh(I) Catalysts ^a	60
Table 3.4 Selected Observations During Reaction Development ^a	62
Table 3.5 Reaction Scope ^a	63
Table 3.6 Internal Oxidant Optimization ^{a,b}	70
Table 3.7 Increased Reactivity Provided by the Pivalate Internal Oxidant. ^a	71
Table 3.8 Internal Alkyne Scope ^{a,b}	72
Table 3.9 Terminal Alkyne Scope ^a	74
Table 3.10 Alkene Scope ^a	76
Table 3.11 Base Screening	88
Table 3.12 Solvent Screening ^{a,b}	88
Table 3.13 Internal Oxidant Optimization.....	90
Table 4.1 Selected Examples of Aldehydes Tested for Catalytic Activity ^a	109
Table 4.2 Screen of Ketone Catalysts.....	118
Table 4.3 Comparative Reaction Scope for the Formaldehyde-Catalyzed Cope-Type Hydroamination ^{a,b}	126
Table A1.1 Lewis Acid Screen for an Intramolecular 1,3-Dipolar Cycloaddition Leading to a 5,5-Fused Heterocycle.....	234
Table A1.2 Lewis Acid Screen for an Intramolecular 1,3-Dipolar Cycloaddition Leading to a 5,6-Fused Heterocycle.....	236

Glossary of Abbreviations

Ac – acetyl
AcO – acetate
AcOH – acetic acid
t-AmOH – *tert*-amylalcohol
aq – aqueous
Ar – generic aryl group
B3LYP – Becke-3-Lee-Yang-Parr
Bn – benzyl
Boc – *tert*-butoxycarbamate
n-Bu – *n*-butyl
t-Bu – *t*-butyl
Bz – benzoyl
cal – calorie
cat. – catalytic
CDCl₃ – chloroform-*d*₃
CMD – concerted-metallation-deprotonation
COD – 1,5-cyclooctadiene
coe – cyclooctene
COSY – correlation spectroscopy
Cp* – 1,2,3,4,5-pentamethylcyclopentadiene
Cy – cyclohexyl
δ – chemical shift in part per million
dba – dibenzylideneacetone
DCE – 1,2-dichloroethane
DFT – density functional theory
DKIE – deuterium kinetic isotope effect
DMAD – dimethylacetylenedicarboxylate
DMAP – *N,N*-dimethylaminopyridine
DMF – *N,N*-dimethylformamide
DMSO – dimethylsulfoxide
DPPF – 1,1'-*bis*(diphenylphosphino)ferrocene
E_{dist} – energy of distortion
ee – enantiomeric excess
E_{int} – energy of interaction
equiv. – equivalent
Et – ethyl
FG – generic functional group
FTIR – Fourier transform infrared
g – gram
GCMS – gas chromatography mass spectrometry
h – hour
HMDS – hexamethyldisilazide
HRMS – high resolution mass spectrometry
Hz – hertz

IR – infrared
 J – coupling constant
 K – equilibrium constant
 L – generic ligand
 M – generic metal; Molar
 Me – methyl
 $MeCN$ – acetonitrile
NMR – nuclear magnetic resonance
NOESY – nuclear overhauser effect spectroscopy
 Nu – nucleophile
[O] – generic oxidant
 Ph – phenyl group
 Piv – pivaloyl group
 $PivOH$ – pivalic acid
 PMB – *para*-methoxybenzyl
 n -Pr – *n*-propyl
 py – pyridine
 R – generic carbon containing group
 R_L – generic large organic fragment
 R_S – generic small organic fragment
 rt – room temperature
 $sat.$ – saturated
 S_EAr – electrophilic aromatic substitution
 TBS – *tert*-butyldimethylsilyl
 $TBDPS$ – *tert*-butyldiphenylsilyl
 THF – tetrahydrofuran
 THP – 2-tetrahydropyran
TLC – thin layer chromatography
 TMB – 1,3,5-trimethoxybenzene
 $TMEDA$ – tetramethylethylenediamine
 TMS – trimethylsilyl
 TPS – triphenylsilyl
 Ts – *para*-toluenesulfonyl
 μW – microwave
 X – generic halide
 $^{\circ}C$ – degrees Celsius

Introduction

The importance of developing methods to form C–N bonds can hardly be overstated. Considering that the vast majority of drugs and natural products with biological activity contain at least one nitrogen atom bound to a carbon atom, it is not surprising that chemists, over the years, have developed many families of reactions that form this important bond. Indeed, current state-of-the-art methods include nucleophilic substitutions, condensations/additions, hydroaminations, electrophilic aminations, nitrene insertion and reductive elimination from a transition metal. Although these are all very important classes of reaction, this thesis will focus mainly on recent developments regarding reductive elimination from a transition metal and tethered hydroamination. This chapter will thus provide important background information about these two types of reactions. Also, given that all C–N bond forming reactions made via reductive elimination presented in this thesis are preceded by a C–H bond functionalization, a brief description of the mechanism of this particular step will be provided in this introductory chapter.

1.1 C–N Bonds From Transition Metal-Mediated Reductive Elimination

Compared to most other ways of forming C–N bonds, reductive elimination from a transition metal is a relatively recent strategy. In the context of palladium catalysis, the first report on this transformation was a palladium-catalyzed aromatic amination of aryl bromides with *N,N*-diethylamino-tributyltin. This advance was published in 1983.¹ Another early and pertinent example of such a transformation is the Larock indole synthesis reported in 1991.² This is a cross-coupling/annulation reaction of *ortho*-iodo anilines with alkynes. The mechanism of this catalytic reaction was proposed to go through 1) an oxidative insertion of palladium(0) into the aryl iodide bond, 2) insertion of the alkyne into the Pd(II)-C bond and 3) C-N bond reductive elimination from Pd(II). Although this mechanistic proposal seems reasonable, no in depth investigations were performed on this system.

In 1994, the early palladium-catalyzed aryl bromide amination reaction mentioned above was further developed³ and its mechanism was clarified.⁴ Hartwig was able, through isolation of reaction intermediates, to strongly suggest that the C–N bond-forming event was occurring via transmetallation from a tin amide followed by reductive elimination.⁵ This hetero cross-coupling reaction (Scheme 1.1, Eq. 1) was thus mechanistically very analogous to the well-known Stille cross-coupling reaction. Soon after the reports using tin amides, Buchwald and Hartwig showed that these types of aryl halide amination could be performed directly from amines in the presence of a non-coordinating base (Scheme 1.1, Eq. 2).⁶ This

¹ Kosugi, M.; Kameyama, M.; Migita, T. *Chem. Lett.* **1983**, *12*, 927.

² Larock, R. C.; Yum, E. K.; *J. Am. Chem. Soc.* **1991**, *113*, 6689.

³ Guram, A. S.; Buchwald, S. L. *J. Am. Chem. Soc.* **1994**, *116*, 7901.

⁴ For a review, see: Hartwig, J. F. *Nature* **2008**, *455*, 314.

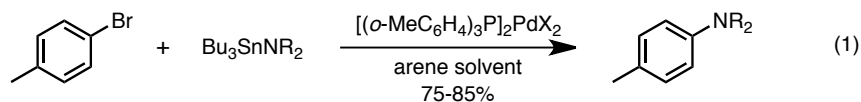
⁵ Paul, F.; Patt, J.; Hartwig, J. F. *J. Am. Chem. Soc.* **1994**, *116*, 5969.

⁶ (a) Guram, A. S.; Rennels, R. A.; Buchwald, S. L. *Angew. Chem., Int. Ed. Engl.* **1995**, *34*, 1348. (b) Louie, J.; Hartwig, J. F. *Tetrahedron Lett.* **1995**, *36*, 3609.

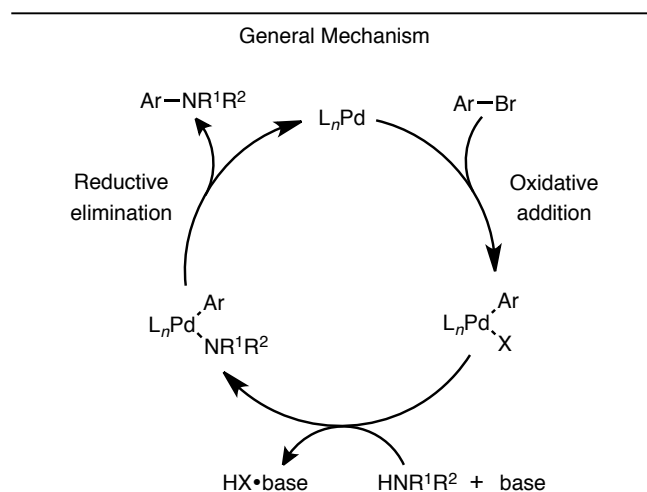
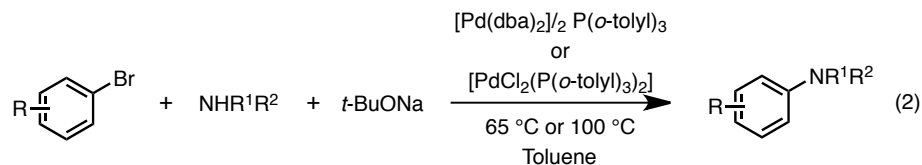
gave rise to what we refer today as the Buchwald-Hartwig amination reaction.⁷ The general mechanism for this reaction is depicted in Scheme 1.1. Starting from a palladium(0) species, oxidative addition into an aryl halide occurs first. An arylpalladium-amido complex is then formed with concomitant amine deprotonation. From this intermediate, the desired aniline is obtained via reductive elimination. The very broad scope that this reaction now features is due to an important ancillary ligand engineering that occurred over the years. Side reactions such as β -hydride elimination are now outcompeted by reductive elimination. Selective monoarylation using primary amines or even ammonia can also be easily achieved. In addition, less reactive aryl chlorides are now perfectly suited coupling partners.

⁷ For reviews, see: (a) Surry, D. S.; Buchwald, S. L. *Chem. Sci.* **2011**, *2*, 27. (b) Muci, A. R.; Buchwald, S. L. *Topics in Curr. Chem.* **2002**, *219*, 131. (c) Hartwig, J. F. *Acc. Chem. Res.* **1998**, *31*, 852. (d) Wolfe, J. P.; Wagaw, S.; Marcoux, J.-F.; Buchwald, S. L. *Acc. Chem. Res.* **1998**, *31*, 805. (e) Hartwig, J. F. *Angew. Chem., Int. Ed.* **1998**, *37*, 2046. (f) Hartwig, J. F. *Acc. Chem. Res.* **2008**, *41*, 1534. (g) Surry, D. S.; Buchwald, S. L. *Angew. Chem., Int. Ed.* **2008**, *47*, 6338. (h) Hartwig, J. F. *Synlett* **1997**, 329.

Hartwig 1994



Buchwald 1995

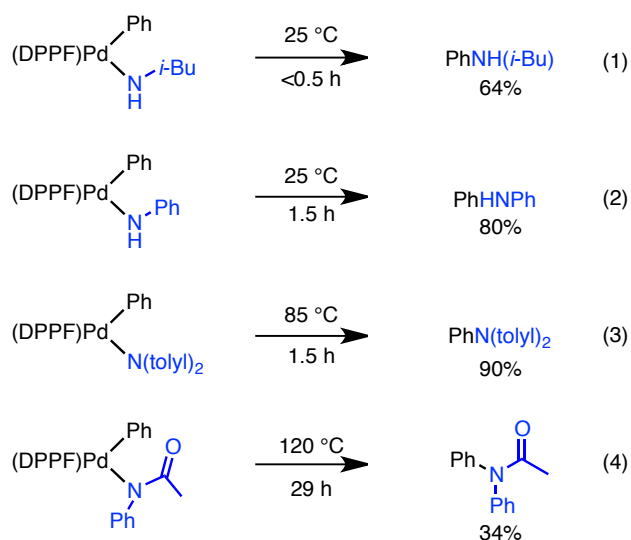


Scheme 1.1 Buchwald-Hartwig Amination and General Mechanism

Detailed mechanistic investigations have been performed on this transformation. More specifically, the reductive elimination step of the mechanism has been thoroughly explored by Hartwig.⁸ It was shown that the electronic properties of both the amine and the arene coupling partners have an important impact on the rate of the reductive elimination step. Regarding the arene, the more electron-withdrawing it is, the faster the reductive elimination occurs. As for the amine, the more electron-rich it is, the faster the reaction. Scheme 1.2 qualitatively illustrates this trend. A series of palladium(II)-amido complexes have been synthesized with the same ancillary ligand, 1,1'-bis(diphenylphosphino)ferrocene

⁸ (a) Driver, M. S.; Hartwig, J. F. *J. Am. Chem. Soc.* **1997**, *119*, 8232. (b) Fujita, K.-I.; Yamashita, M.; Puschmann, F.; Alvarez-Falcon, M. M.; Incarvito, C. D.; Hartwig, J. F. *J. Am. Chem. Soc.* **2006**, *128*, 9044.

(DPPF). The reductive elimination from an alkylamine (Eq. 1) was found to be faster than the one from an arylamine (Eq. 2), which is faster than the one from a diarylamine (Eq. 3), which, in turn, is considerably faster than from an palladium-amidato complex (Eq. 4). These results thus suggest that the aryl group acts as an electrophile and the amido ligand acts as a nucleophile in palladium(0)-catalyzed C–N bond-forming reactions. Of note, the ability to isolate stable precursors to reductive elimination is a precious advantage of palladium complexes for the study of C–N bond reductive elimination that most other metals do not present.



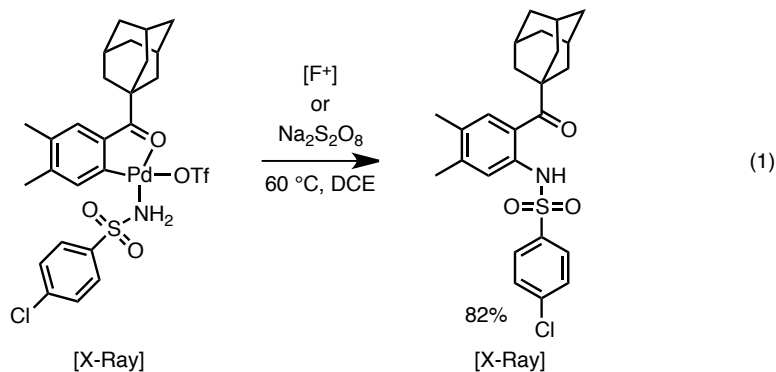
Scheme 1.2 Electronic Effects on Rate of Reductive Elimination

Amination reactions via reductive elimination from a Pd(IV) intermediate has also been proposed in a few recent systems. Liu established the best proof of this reactivity in 2011 by isolating an intermediate of the catalytic oxidative amination reaction he had developed (Scheme 1.3, Eq. 1).⁹ Oxidation of this Ar-Pd(II)-NHSO₂Ar species using strong oxidants such as Na₂S₂O₈ or Selectfluor afforded the desired aminated product likely via a

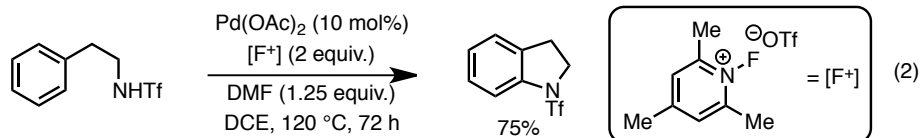
⁹ Xiao, B.; Gong, T.-J.; Xu, J.; Liu, Z.-J.; Liu, L. *J. Am. Chem. Soc.* **2011**, *133*, 1466.

highly reactive Pd(IV) intermediate. Yu also reported a direct amination system which presumably goes through a high-valent palladium(IV) species (Scheme 1.3, Eq. 2).¹⁰

Liu 2011



Yu 2009



Scheme 1.3 Palladium(IV)-mediated C-N Bond Reductive Elimination

Other metals also proved to be competent to promote C–N bond reductive elimination. Low-valent copper complexes have been employed for decades for the formation of C–N bonds.¹¹ It is only recently, however, that some high-valent organo-copper(III) complexes have been isolated and that their involvement in C–N bond reductive elimination has been demonstrated.¹² Stahl did pioneering work in this area by studying the stoichiometric reaction of aryl copper(III) complexes with amides.¹³ The reactions illustrated in Scheme 1.4 represent the first direct investigation of C–N bond reductive elimination

¹⁰ Mei, T.-S.; Wang, X.; Yu, J.-Q. *J. Am. Chem. Soc.* **2009**, *131*, 10806.

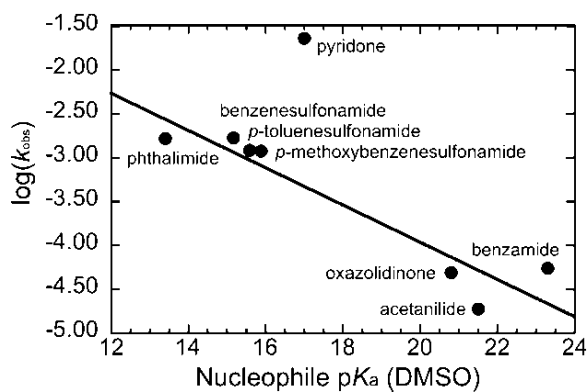
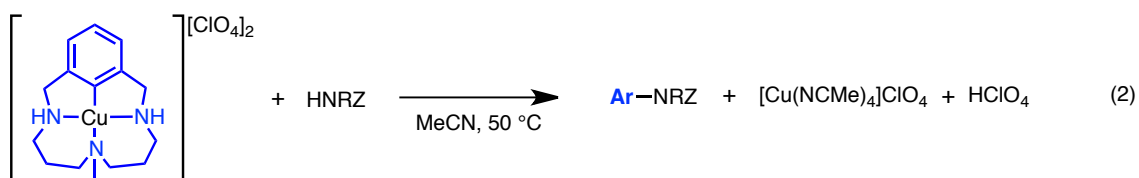
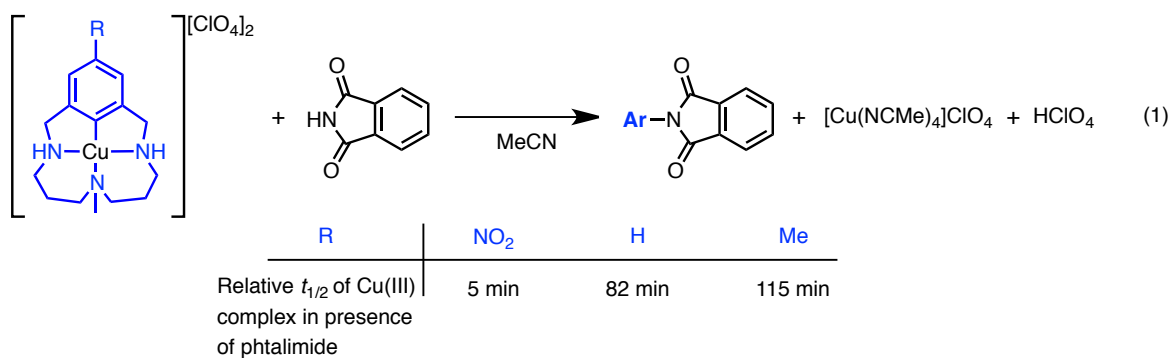
¹¹ For reviews, see: (a) Lindley, J. *Tetrahedron* **1984**, *40*, 1433. (b) Ley, S. V.; Thomas, A. W. *Angew. Chem., Int. Ed.* **2003**, *42*, 5400. (c) Kunz, K.; Scholz, U.; Ganzer, D. *Synlett* **2003**, 2428. (d) Beletskaya, I. P.; Cheprakov, A. V. *Coord. Chem. Rev.* **2004**, *248*, 2337.

¹² For a review, see: Hickman, A. J.; Sanford, M. S. *Nature* **2012**, *484*, 177.

¹³ Huffman, L. M.; Stahl, S. S. *J. Am. Chem. Soc.* **2008**, *130*, 9196.

reactions from copper(III) species. It was noted that the rate of the reaction was related to the electronic properties of the coordinated arene undergoing amidation. Electron-withdrawing groups were shown to accelerate the reaction with phthalimide whereas slightly electron-donating substrates were found to slow it down (Scheme 1.4, Eq. 1). This tendency is in accordance with the observations previously discussed with palladium catalysis.

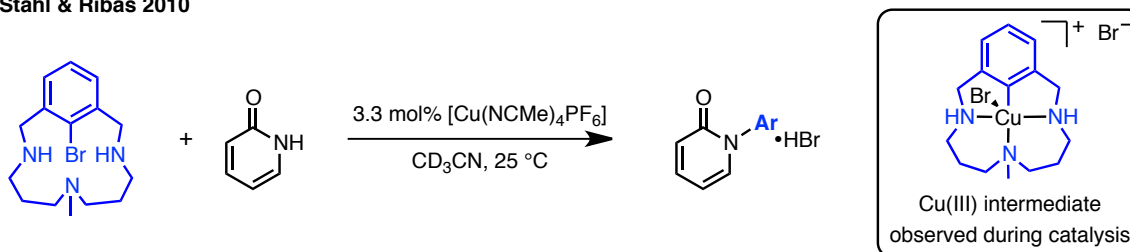
Stahl 2008



Scheme 1.4 Rate of Cu(III)-Mediated Reductive Elimination as Function of Electronic Factors

The electronic effect of the amide coupling partner was also probed (Scheme 1.4, Eq. 2). In this case, a correlation was found between the pKa of the amide and the reaction rate. More acidic amides proved to react faster. This goes against the expected outcome in a case where the neutral amide would react with the copper(III)-aryl compound. These results are thus consistent with a scenario where deprotonation of the amide occurs prior to or at the C–N bond forming event. In 2010, Stahl and Ribas disclosed a version of this reaction that is catalytic in copper (Scheme 1.5).¹⁴ Interestingly, a copper(III) intermediate preceding C–N bond formation was stable enough to be detected using ¹H NMR and UV-visible spectrometry. This is due to the macrocyclic ligand employed. It allows for a fast oxidative addition that leads to a stable high-valent copper(III)-aryl complex. This experiment represented the first direct observation of a copper(III) intermediate in the catalytic cycle of a Goldberg reaction (copper-catalyzed amination of aryl halide).

Stahl & Ribas 2010



Scheme 1.5 Cu(III) Intermediate Detected During Catalysis

Other metals such as nickel,¹⁵ iron¹⁶ and cobalt¹⁷ are also known to participate in catalytic C–N bond forming reactions. Although the scope of these reactions has been well

¹⁴ Casitas, A.; King, A. E.; Parella, T.; Costas, M.; Stahl, S. S.; Ribas, X. *Chem. Sci.* **2010**, *1*, 326.

¹⁵ For selected examples, see: (a) Wolfe, J. P.; Buchwald, S. L. *J. Am. Chem. Soc.* **1997**, *119*, 6054. (b) Gradel, B.; Brenner, E.; Schneider, R. L.; Fort, Y. *Tetrahedron Lett.* **2001**, *42*, 5689. (c) Omar-Amrani, R.; Thomas, A.; Brenner, E.; Schneider, R.; Fort, Y. *Org. Lett.* **2003**, *5*, 2311. (d) Gao, C. Y.; Cao, X. B.; Yang, L. M. *Org. Biomol. Chem.* **2009**, *7*, 3922. (e) Iglesias, M. J.; Prieto, A.; Nicasio, M. C. *Adv. Synth. Catal.* **2010**, *352*, 1949.

¹⁶ For selected examples, see: (a) Correa, A.; Bolm, C. *Angew. Chem., Int. Ed.* **2007**, *46*, 8862. (b) Correa, A.; Carril, M.; Bolm, C. *Chem. Eur. J.* **2008**, *14*, 10919. (c) Guo, D. L.; Huang, H.; Xu, J. Y.; Jiang, H. L.; Liu, H. *Org. Lett.* **2008**, *10*, 4513.

described, their mechanisms, including the nature of the C–N bond forming step, have yet to be investigated.

In 2010, Chang reported an aryl bromide amination reaction catalyzed by a Rh(I)/NHC complex.¹⁸ This first example of a rhodium-catalyzed Buchwald-Hartwig amination likely proceeds through a mechanism similar to the one outline in Scheme 1.1, where C–N bond formation via reductive elimination would occur from a Rh(III) intermediate. Nevertheless, no mechanistic detail has been reported to support this possibility. In the following chapters, what are believed to be the first examples of Rh(III)-mediated C–N bond reductive elimination in a catalytic cycle will be described. Experimental and computational investigations were conducted on these systems and the results obtained are consistent with such a mechanistic pathway.

1.2 Mechanistic Considerations For Transition Metal-Mediated C–H Bond Functionalization

The functionalization of C(*sp*²)–H bond using late transition metals as catalysts has become a topic of great interest in organic and organometallic chemistry. Indeed, the possibility to directly transform a rather inert covalent bond into a value added product such as a biaryl, an aryl halide, or an aryl boronate is very appealing from a green chemistry perspective. As the need for new transformations of this type becomes more important, the understanding of the underlying mechanistic aspects of C(*sp*²)–H functionalization is essential. In that regard, many mechanisms have been proposed to account for these

¹⁷ For selected examples, see: (a) Toma, G.; Fujita, K.; Yamaguchi, R. *Eur. J. Org. Chem.* **2009**, 4586. (b) Teo, Y. C.; Chua, G. L. *Chem. Eur. J.* **2009**, *15*, 3072.

¹⁸ Kim, M.; Chang, S. *Org. Lett.* **2010**, *12*, 1640.

transformations. Most of them relate to palladium-catalyzed reactions.¹⁹ The main four types of mechanistic proposals in biaryl formation reactions are outlined in Figure 1.1.

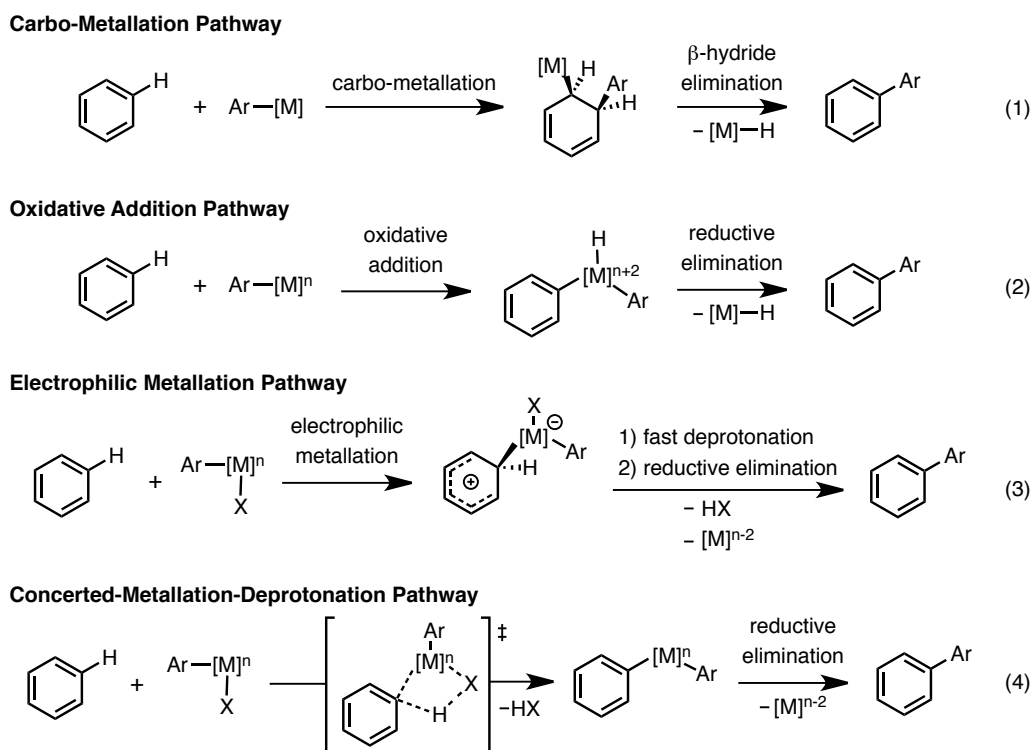


Figure 1.1 Proposed mechanism for C(sp^2)-H bond functionalization

The first one (Figure 1.1, Eq. 1) is a carbo-metallation, or a so-called Heck-type mechanism.²⁰ It is characterized by the *syn*-addition of a metal-aryl (or -alkenyl) species across the double bond of an aromatic system. This pathway had originally been proposed for the palladium-catalyzed arylation of 5-membered electron-rich heterocycles. Given that an *anti*-beta-hydride elimination would be of very high energy, it was suggested in some instances that the π -allyl system generated would isomerize to allow a *syn*- β -hydride

¹⁹ For a relevant discussion on the different mechanisms proposed in palladium-catalyzed C-H functionalization reactions, see: Engle, K. M.; Wang, D.-H.; Yu, J.-Q. *J. Am. Chem. Soc.* **2010**, *132*, 14137.

²⁰ For publications discussing this mechanistic proposal, see: (a) Sezen, B.; Sames, D. *J. Am. Chem. Soc.* **2003**, *125*, 5274. (b) Glover, B.; Harvey, K. A.; Liu, B.; Sharp, M. J.; Tymoschenko, M. F. *Org. Lett.* **2003**, *5*, 301. (c) Toyota, M.; Ilangoan, A.; Okamoto, R.; Masaki, T.; Arakawa, M.; Ihara, M. *Org. Lett.* **2002**, *4*, 4293. (d) Hughes, C. C.; Trauner, D. *Angew. Chem., Int. Ed.* **2002**, *41*, 1569. (e) Hennessy, E. J.; Buchwald, S. L. *J. Am. Chem. Soc.* **2003**, *125*, 12084.

elimination to be performed. The mechanism shown in Eq. 2 goes through an oxidative addition into a C–H bond. This type of C–H activation is more common with low-valent late transition metal such as Rh(I).²¹ Examples applied to palladium catalysis are rare and lack mechanistic evidence.²² In Eq. 3, an electrophilic metallation mechanism is put forward. This mechanism, also known as an electrophilic aromatic substitution (S_EAr), is definitely one of the most proposed pathways to account for palladium-catalyzed C–H bond functionalization.²³ It is characterized by the attack of a nucleophilic arene onto an electrophilic metal species. This generates a Wheland-type intermediate, which then undergoes a fast deprotonation to afford the desired metallo-arene. While this mechanism is often proposed based on the faster reactivity of electron-rich arenes, strong experimental evidence remains rare.

The last mechanistic proposal outlined in Figure 1 (Eq. 4) is a concerted-metallation-deprotonation (CMD).²⁴ This pathway is very similar to the electrophilic metallation mechanism, with the exception that the proton abstraction occurs at the same time as the arene metallation. Depending on the base employed, the mechanism can go through a 6- (i.e. with an acetate) or a 4-membered transition state. In the latter case, it is also referred to as a σ -bond metathesis. Since this is a concerted mechanism, it is typical to observe a primary deuterium kinetic isotope effect for the C–H bond cleavage. This contrasts with the S_EAr mechanism, where the proton abstraction from the Wheland intermediate is thought to be fast due to the thermodynamic driving force associated with re-aromatization. Recent

²¹ Colby, D. A.; Bergman, R. G.; Ellman, J. A. *Chem. Rev.* **2010**, *110*, 624.

²² Canty, A. J.; van Koten, G. *Acc. Chem. Res.* **1995**, *28*, 406.

²³ For a seminal contribution, see: Ryabov, A. D.; Sakodinskaya, I. K.; Yatsimirsky, A. K. *J. Chem. Soc., Dalton Trans.* **1985**, 2629.

²⁴ For recent reviews on metal carboxylate-catalyzed C-H bond cleavage, see: (a) Boutadla, Y.; Davies, D. L.; Macgregor, S. A.; Poblador-Bahamonde, A. I. *Dalton Trans.* **2009**, 5820. (b) Lapointe, D.; Fagnou, K. *Chem. Lett.* **2011**, *111*, 1315.

investigations by the Fagnou group on palladium-catalyzed direct arylation pointed out the involvement of the CMD mechanism with systems having a wide range of electronic properties. In fact, the CMD pathway is now considered accurate to predict not only the reactivity and regioselectivity of electron-neutral and electron-deficient substrates,²⁵ but also electron-rich arenes,²⁶ which reactivity was previously rationalized mostly through a $S_{E}Ar$ mechanism.²⁷ Computational analyses performed on these various systems coupled with experimental results allowed Fagnou and co-workers to point out important physical parameters related to the reactivity of aromatic molecules toward C–H bond cleavage. Figure 1.2 illustrates these findings by breaking down the overall energy of the CMD transition state (ΔE) into two main components: the distortion energy (E_{dist}) and the interaction energy (E_{int}). E_{dist} represents the energy required to distort the palladium catalyst and the arene from their respective ground state (**I** and **II**) to adopt their conformation at the calculated transition state (**III** and **IV**). This energy cost is typically higher for electron-rich than for electron-poor substrates. E_{int} represents the stabilization energy gained through the electronic interaction of **III** with **IV**, which leads to transition state **V**. Since electron-rich substrates allow a greater interaction with the metal center, the stabilization of the transition state is typically greater with these substrates. The balance between E_{dist} and E_{int} was found to explain and allow the prediction of the energy required to undergo C–H functionalization. This concept was

²⁵ (a) Lafrance, M.; Rowley, C. N.; Woo, T. K.; Fagnou, K. *J. Am. Chem. Soc.* **2006**, *128*, 8754. (b) Lafrance, M.; Fagnou, K. *J. Am. Chem. Soc.* **2006**, *128*, 16496. (c) Garcia-Cuadrado, D.; Braga, A. A. C.; Maseras, F.; Echavarren, A. M. *J. Am. Chem. Soc.* **2006**, *128*, 1066. (d) Garcia-Cuadrado, D.; de Mendoza, P.; Braga, A. A. C.; Maseras, F.; Echavarren, A. M. *J. Am. Chem. Soc.* **2007**, *129*, 6880. (e) Sun, H.-Y.; Gorelsky, S. I.; Stuart, D. R.; Campeau, L.-C.; Fagnou, K. *J. Am. Chem. Soc.* **2010**, *132*, 8180.

²⁶ (a) Liégault, B.; Petrov, I.; Gorelsky, S. I.; Fagnou, K. *J. Org. Chem.* **2010**, *75*, 1047. (b) Liégault, B.; Lapointe, D.; Caron, L.; Vlassova, A.; Fagnou, K. *J. Org. Chem.* **2008**, *74*, 1826. (c) René, O.; Fagnou, K. *Adv. Synth. Catal.* **2010**, *352*, 2116.

²⁷ For accurate reactivity/regioselectivity prediction using DFT, see (a) Gorelsky, S. I.; Lapointe, D.; Fagnou, K. *J. Am. Chem. Soc.* **2008**, *130*, 10848. (b) Gorelsky, S. I.; Lapointe, D.; Fagnou, K. *J. Org. Chem.* **2012**, *77*, 658. (c) Lapointe, D.; Markiewicz, T.; Whipp, C. J.; Toderian, A.; Fagnou, K. *J. Org. Chem.* **2011**, *76*, 749.

recently demonstrated with a vast diversity of aromatic substrates in the context of palladium-catalyzed direct arylation.²⁷

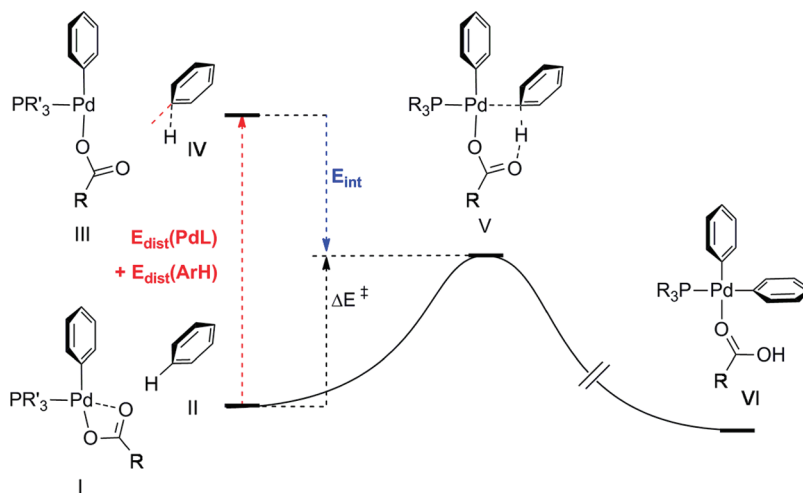


Figure 1.2 Distortion-interaction analysis for the CMD transition state; benzene is shown as a representative substrate

The CMD mechanism is also believed to be operative in catalysis employing other metals such as rhodium(III) for instance. Examples will be briefly discussed in the following chapters.

1.3 Mechanistic Aspects of Different Hydroamination Systems

A hydroamination reaction can be defined as the addition of a N–H bond across an alkene or an alkyne. This conceptually very simple process has nonetheless challenged chemists for decades.²⁸ Many aspect of this transformation such as selectivity (Markovnikov vs anti-Markovnikov), functional group compatibility, enantioselectivity and intermolecular reactivity are still problems to which no general solution exists, regardless of the tremendous amount of work that has been accomplished in this area. As one may expect, the challenge of

²⁸ For comprehensive reviews, see: (a) Müller, T. E.; Beller, M. *Chem. Rev.* **1998**, *98*, 675. (b) Müller, T. E.; Hultsch, K. C.; Yus, M.; Foubelo, F.; Tada, M. *Chem. Rev.* **2008**, *108*, 3795.

hydroamination has been approached from numerous standpoints. In fact, catalysis of this reaction was successfully performed with acid, base, early and late transition metals, etc.²⁹ Each of these modes of catalysis operates in a different manner. This section will describe briefly these types of catalysis by highlighting selected recent examples and presenting their mechanisms and limitations.

1.3.1 Acid-Catalyzed Hydroamination

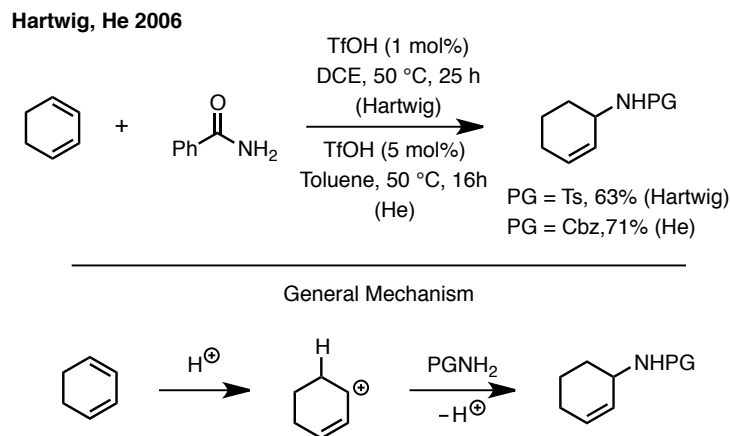
Perhaps the simplest, cheapest and most easily scalable method for hydroamination goes through a Brønsted acid activation of the alkene. The Ritter reaction,³⁰ which consists of reacting acid-activated alkenes with nitriles, is definitely a classic example of this type of chemistry. As more recent examples, Hartwig³¹ and He³² reported in 2006 a practical method employing low catalyst loadings to perform alkene hydroamination with protected amines (Scheme 1.6). An inherent characteristic of this method is the high Markovnikov amination selectivity. This is due to the mechanism via which the reaction operates, where the most stable carbocation of the protonated alkene undergoes amination. Drawbacks of this hydroamination strategy include the incompatibility of acid-sensitive moieties as well as the need to employ protected nitrogen atoms that are non-basic.

²⁹ Alkene hydroamination has also been performed using rare-earth metals, actinides, alkaline earth metals and through radical pathways. These aspects will not be covered in this thesis. For relevant reviews on the topic, see ref 28.

³⁰ For a review, see: Krimen, L. I.; Cota, D. J. *Org. React.* **1969**, *17*, 213.

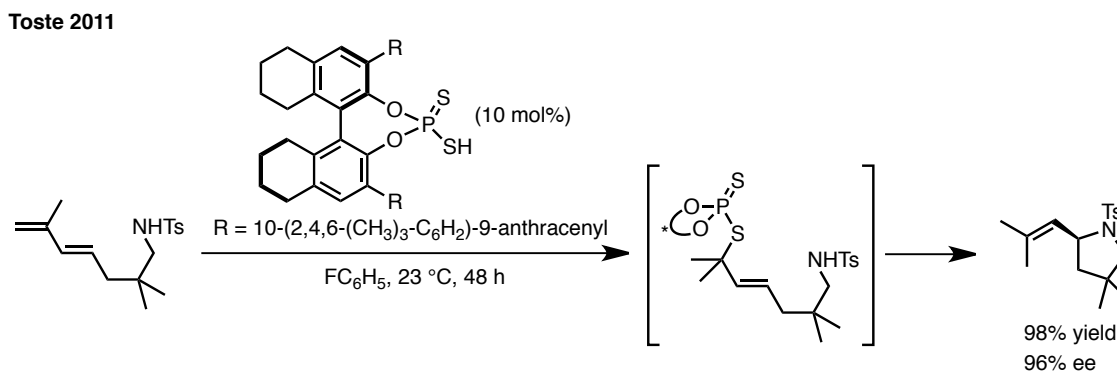
³¹ Rosenfeld, D. C.; Sekhar, S.; Takemiya, A.; Utsunomiya, M.; Hartwig, J. F. *Org. Lett.* **2006**, *8*, 4179.

³² Li, Z.; Zhang, J.; Brouwer, C.; Yang, C.-G.; Reich, N. W.; He, C. *Org. Lett.* **2006**, *8*, 4175.



Scheme 1.6 Example of Brønsted Acid-Catalyzed Hydroamination and Mechanism

Possibly the most sophisticated example of an acid-catalyzed hydroamination reaction was established by Toste in 2011 (Scheme 1.7).³³ This reports deals with the use of a chiral dithiophosphoric acid to activate a 1,3-diene and promote intramolecular hydroamination. This important advancement constitutes the first chiral Brønsted acid-catalyzed enantioselective Markovnikov addition onto an unactivated alkene. An example of this reaction is outlined in Scheme 1.7. The proposed mechanism is slightly different from the one presented above. In this case, a Markovnikov addition of the chiral acid occurs first and then displacement of this good leaving group is made enantioselectively via a S_N2' reaction using the amine as nucleophile.



³³ (a) Shapiro, N. D.; Rauniyar, V.; Hamilton, G. L.; Wu, J.; Toste, F. D. *Nature* **2011**, *470*, 245. For a highlight, see: Dion, I.; Beauchemin, A. M. *Angew. Chem., Int. Ed.* **2011**, *50*, 8233

Scheme 1.7 Enantioselective Brønsted Acid-Catalyzed Hydroamination

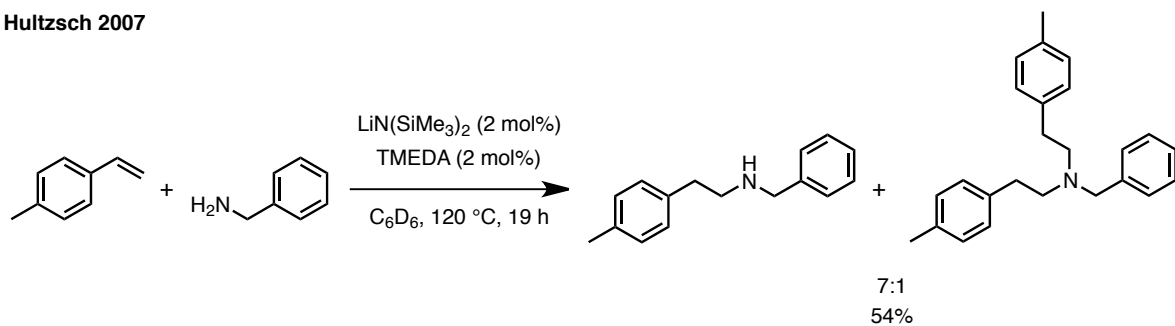
1.3.2 Base-Catalyzed Hydroamination

Another very simple and low cost method to perform an alkene hydroamination is to employ base catalysis.³⁴ Contrary to acid catalysis, where the alkene becomes a good electrophile, this type of catalysis transforms the amine into a much more powerful nucleophile via deprotonation. Using this method, anti-Markovnikov selectivity is generally observed. Inherent limitations comprise the incompatibility of base sensitive substrates, electrophile-containing substrates and the need for slightly activated or electron-poor alkenes such as styrenes or 1,3-dienes. As shown in the example from Hultsch outlined in Scheme 1.8,³⁵ the use of primary amines can lead to mixture of secondary and tertiary amines resulting from multiple additions of vinylarenes.

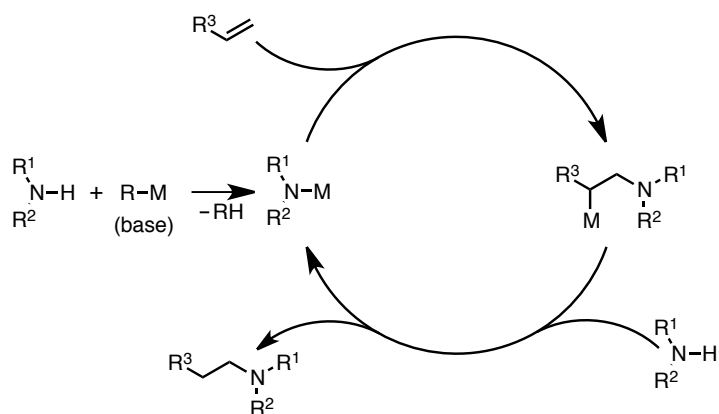
³⁴ For a review on base-catalyzed hydroamination of olefin, see: Seayad, J.; Tillack, A.; Hartung, C. G.; Beller, M. *Adv. Synth. Catal.* **2002**, *344*, 795.

³⁵ Horrillo-Martínez, P.; Hultsch, K. C.; Gil, A.; Branchadell, V. *Eur. J. Org. Chem.* **2007**, 3311.

Hultsch 2007



General Mechanism



Scheme 1.8 Example of Base-Catalyzed Alkene Hydroamination and Mechanism

1.3.3 Early Transition Metal-Catalyzed Hydroamination

Among the large variety of systems that have been developed for the hydroamination of alkenes, important contributions have recently been reported using early transition metal catalysts. Given their low cost and toxicity, these methods can prove advantageous over late-transition metal-catalyzed systems. In a recent report from Schafer, zirconium complexes were shown to catalyze the intramolecular hydroamination of terminal and 1,2-disubstituted alkenes (Scheme 1.9).³⁶ Of note, secondary amines were shown to be suitable substrates. This contrasts with most previous early transition metal-catalyzed methods, where only primary amines were tolerated. This is due to the mechanism through which these

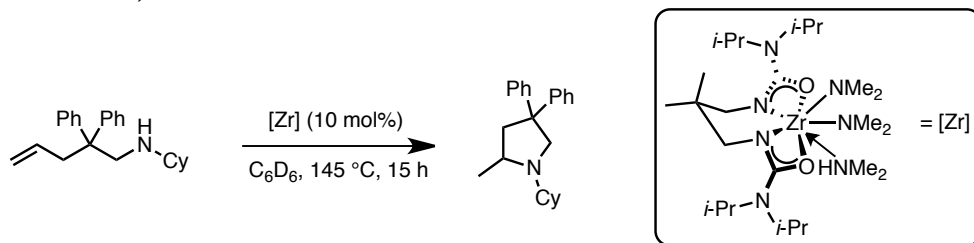
³⁶ Leitch, D. C.; Payne, P. R.; Dunbar, C. R.; Schafer, L. L. *J. Am. Chem. Soc.* **2009**, *131*, 18246.

transformations would operate, where a [2+2] addition of an alkene onto a metal-imido species would be responsible for the formation of the hydroamination product.³⁷ Schafer performed thorough mechanistic investigations on the system she reported in 2009 and a simplified version of the catalytic cycle she proposed is shown in Scheme 1.9.³⁸ Following aminolysis of the precatalyst using a molecule of substrate, intramolecular hydroamination can occur via a six-membered transition state using a coordinated secondary amine as a source of proton. The resulting heterocycle is then decoordinated and replaced by a new molecule of substrate, which concomitantly undergoes proton transfer with the amine coordinated to the catalyst. This affords the initial intermediate, which can go through a subsequent turnover.

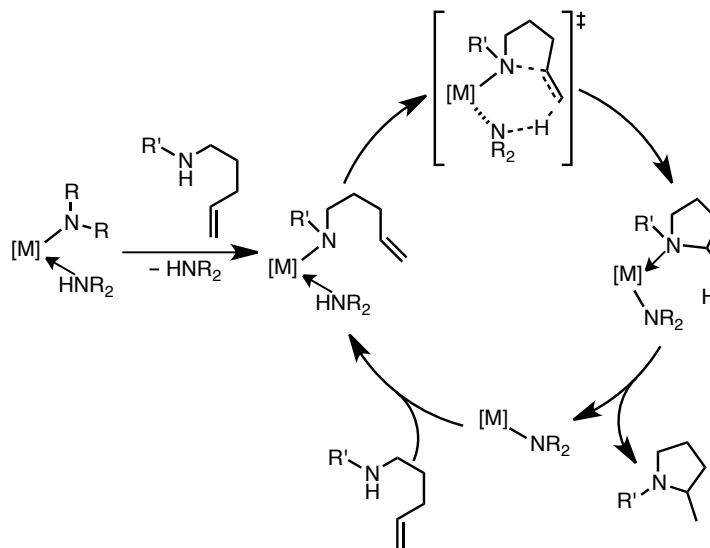
³⁷ (a) Walsh, O. J.; Baranger, A. M.; Bergman, R. G. *J. Am. Chem. Soc.* **1992**, *114*, 1708. (b) Thomson, R. K.; Bexrud, J. A.; Schafer, L. L. *Organometallics*, **2006**, *25*, 4069. (c) Gott, A. L.; Clarke, A. J.; Clarkson, G. J.; Scott, P. *Chem. Commun.* **2008**, 1422. (d) Allan, L. E. N.; Clarkson, G. J.; Fox, D. J.; Gott, A. L.; Scott, P. *J. Am. Chem. Soc.* **2010**, *132*, 15308.

³⁸ Leitch, D. C.; Platel, R. H.; Schafer, L. L. *J. Am. Chem. Soc.* **2011**, *133*, 15453.

Schafer 2009, 2011



Simplified Mechanism



Scheme 1.9 Early Transition Metal-Catalyzed Hydroamination and Corresponding Mechanism

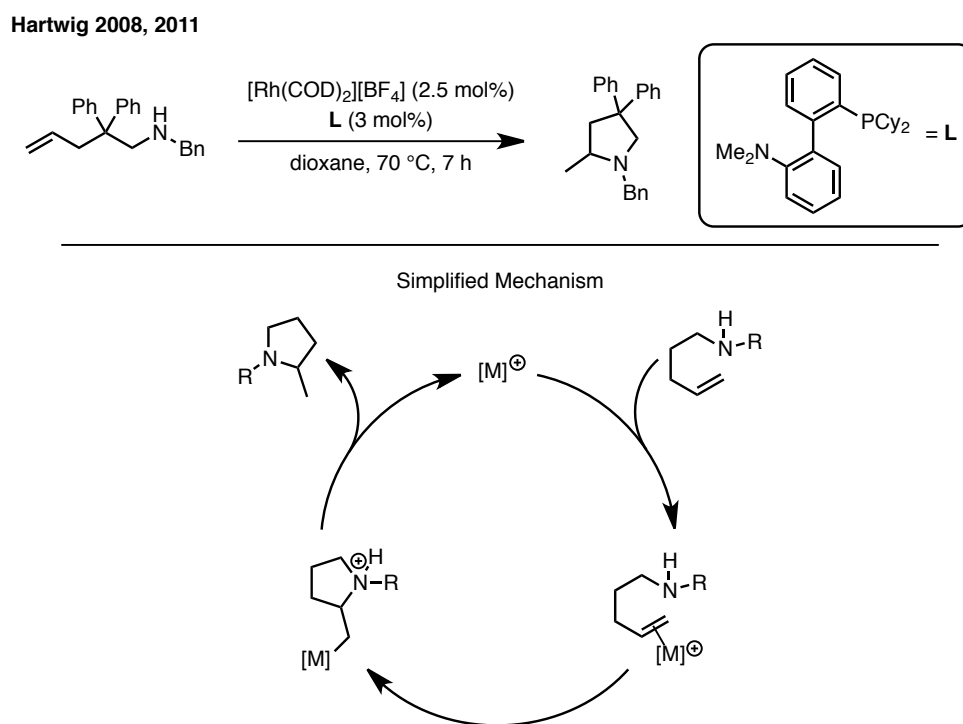
Typical issues associated with this type of early transition metal catalysis include the need for high reaction temperatures, the absence of intermolecular reactivity³⁹ and the sensitivity to most common functional groups.

1.3.4 Late Transition Metal-Catalyzed Hydroamination

The hydroamination of alkenes using late transition metals has been accomplished with many different metals, and via a variety of mechanisms. Of these mechanisms, two of

³⁹ Intermolecular reactivity could be achieved using alkynes in place of alkenes

them seem to appear more frequently. The first one proceeds through the oxidative addition of a metal into a N–H bond, followed by alkene migratory insertion and C–H bond reductive elimination.⁴⁰ The second one proceeds via a nucleophilic attack of an amine onto a coordinated alkene. A following proton transfer yields the desired hydroamination product.⁴¹ For example, Hartwig reported in 2008 a Rh(I)-catalyzed transformation that was later found to operate via the latter mechanism (Scheme 1.10).⁴² This interesting transformation constitutes a rare example of Rh(I) activation of alkene toward an amine nucleophile.



Scheme 1.10 Late Transition Metal-Catalyzed Hydroamination and Corresponding Mechanism

⁴⁰ For a seminal example, see: Casalnuovo, A. L.; Calabrese, J. C.; Milstein, D. *J. Am. Chem. Soc.* **1988**, *110*, 6738.

⁴¹ For selected examples, see: (a) Bender, C. F.; Widenhoefer, R. A. *J. Am. Chem. Soc.* **2005**, *127*, 1070. (b) Cochran, B. M.; Micheal, F. E. *J. Am. Chem. Soc.* **2008**, *130*, 2786.

⁴² (a) Liu, Z.; Hartwig, J. F. *J. Am. Chem. Soc.* **2008**, *130*, 1570.

Hydroamination via late transition metal catalysis can be an advantageous strategy as it tolerates the presence of many functional groups, it can display intermolecular enantioselectivity⁴³ and it is fairly resistant to air or moisture in most instances when compared to early transition metals. Nonetheless, the use of these precious metals typically makes for more expensive reactions, a characteristic that becomes more concerning when working on large scale. Additionally, even though many systems have shown excellent intramolecular reactivity, the restrictive use of biased substrates such as strained bicyclic alkenes, styrenes or 1,3 dienes in the intermolecular variant remains a limitation to address.⁴⁴ In the cases where unbiased alkenes are employed, protected amines or very forcing conditions are generally required.⁴⁵

In summary, despite the advances that have been achieved using base, acid, transition metal or rare earth metal catalysis, the limitations highlighted in this section call for new modes of catalysis and/or reaction pathways. Our advances regarding a conceptually distinct strategy, namely the Cope-type hydroamination, will be discussed in more depth in the fourth chapter of this thesis. We hope that this approach will provide a good alternative to the current state-of-the-art hydroamination methods.

⁴³ For examples, see: (a) Kawatsura, M.; Hartwig, J. F.; *J. Am. Chem. Soc.* **2000**, *122*, 9546. (b) Löber, O.; Kawatsura, M.; Hartwig, J. F. *J. Am. Chem. Soc.* **2001**, *123*, 4366. (c) Dorta, R.; Egli, P.; Zürcher, F.; Togni, A. *J. Am. Chem. Soc.* **1997**, *119*, 10857. (d) Zhou, J.; Hartwig, J. F. *J. Am. Chem. Soc.* **2008**, *130*, 12220.

⁴⁴ For recent examples, see: (a) Shaffer, A. R.; Schmidt, J. A. R. *Organometallics* **2008**, *27*, 1259. (b) Sakai, N.; Ridder, A.; Hartwig, J. F. *J. Am. Chem. Soc.* **2006**, *128*, 8134. (c) Johns, A. M.; Liu, Z.; Hartwig, J. F. *Angew. Chem., Int. Ed.* **2007**, *46*, 7259. (d) Brouwer, C.; He, C. *Angew. Chem., Int. Ed.* **2006**, *45*, 1744. (e) Kovács, G.; Ujaque, G.; Lledós, A. *J. Am. Chem. Soc.* **2008**, *130*, 853. (f) Utsunomiya, M.; Hartwig, J. F. *J. Am. Chem. Soc.* **2003**, *125*, 14286. (g) Utsunomiya, M.; Hartwig, J. F. *J. Am. Chem. Soc.* **2004**, *126*, 2702.

⁴⁵ For examples, see: (a) Yi, C. S.; Yun, S. Y. *Org. Lett.* **2005**, *7*, 2181. (b) Baudequin, C.; Brunet, J.-J.; Rodriguez-Zubiri, M. *Organometallics* **2007**, *26*, 5264. (c) Diamond, S. E.; Szalkiewicz, A.; Mares, F. *J. Am. Chem. Soc.* **1979**, *101*, 490. (d) Coulson, D. R. *Tetrahedron Lett.* **1971**, *12*, 429. (e) Brunet, J.-J.; Cadena, M.; Chu, N. C.; Diallo, O.; Jacob, K.; Mothes, E. *Organometallics* **2004**, *23*, 1264. (f) Wang, X.; Widenhofer, R. A. *Organometallics* **2004**, *23*, 1649. (g) Brunet, J.-J.; Chu, N.-C.; Diallo, O. *Organometallics* **2005**, *24*, 3104. (h) Brunet, J.-J.; Chu, N.-C.; Rodriguez-Zubiri, M. *Eur. J. Inorg. Chem.* **2007**, 4711.

Rhodium(III)-Catalyzed Oxidative Synthesis of Isoquinolines

2.1 Introduction

Nitrogen-containing heterocycles are among the most important motifs found in biologically active molecules. A recent survey of the top 200 most prescribed drugs in the US in 2010 revealed that over 47% of these molecules contain one or more of these structures embedded in their core.⁴⁶ As member of this nitrogen-containing heterocycle family, the isoquinoline motif is an important sub-unit found in natural products and synthetic molecules that display biological activity. In fact, 1,2-dihydroisoquinolines and 1,2,3,4-tetrahydroisoquinilines were found particularly active due to their capacity to transport drugs through the otherwise hardly penetrable blood-brain barrier.⁴⁷ They also display sedative,⁴⁸ antidepressant,⁴⁹ antitumor and antimicrobial activity.⁵⁰ Due to its

⁴⁶ Information gathered by the Jon Njardarson research group with sales data from DrugTopics.

⁴⁷ For examples, see: (a) Pop, E.; Wu, W.-M.; Shek, E.; Bodor, N. *J. Med. Chem.* **1989**, *32*, 1774. (b) Prokai, L.; Prokai-Tatrai, K.; Bodor, N. *Med. Res. Rev.* **2000**, *20*, 367.

⁴⁸ Lukevics, E.; Segal, I.; Zablotskaya, A. Germane, S. *Molecules*, **1997**, *2*, 180.

aromatic nature and basic nitrogen, the isoquinoline motif has also found application in many other fields of chemistry: material science (dyes and paints), organocatalysis and transition metal catalysis. Figure 2.1 displays representative examples of the use of the isoquinoline motif in chemistry and medicine.

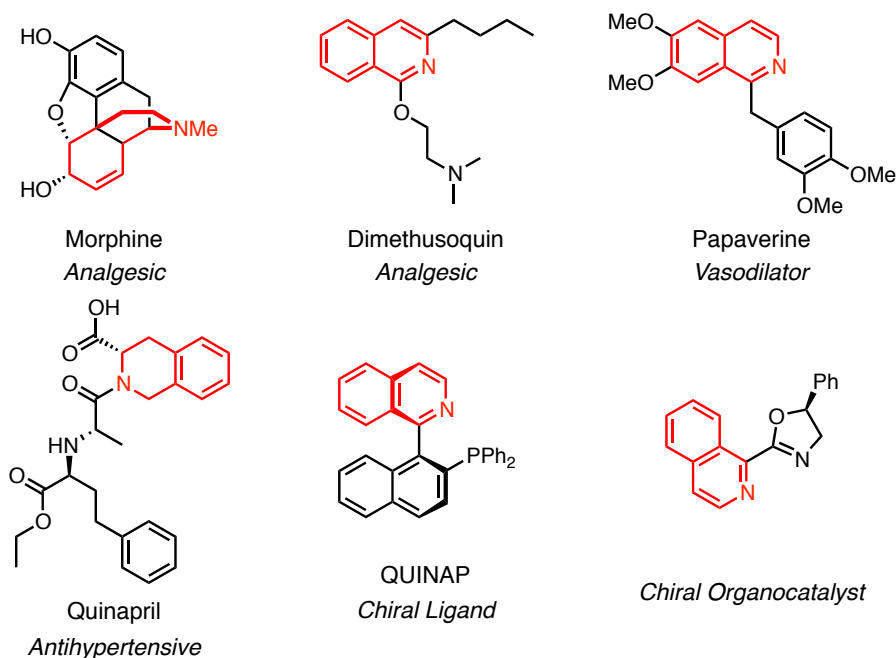


Figure 2.1 Representative isoquinolines in chemistry and medicine

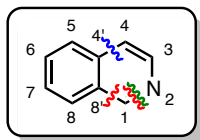
2.1.1 Traditional Routes to Isoquinolines

Given the frequent occurrence of the isoquinoline heterocycle in natural products, chemists established very early diverse dehydrative cyclization methods to synthetically access its structure. In 1893, two well-known methods emerged. One of them, the Bischler-

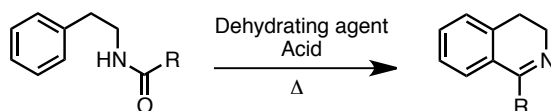
⁴⁹ (a) Maryanoff, B. E.; McComsey, D. F.; Gardocki, J. F.; Shank, R. P.; Costanzo, M. J.; Nortey, S. O.; Schneider, C. R.; Setler, P. E. *J. Med. Chem.* **1987**, *30*, 1433. (b) Sorgi, K. L.; Maryanoff, C. A.; McComsey, D. F.; Graden, D. W.; Maryanoff, B. D. *J. Am. Chem. Soc.* **1990**, *112*, 3567.

⁵⁰ (a) Scott, J. D.; Williams, R. M. *Chem. Rev.* **2002**, *102*, 1669. (b) Tietze, L. F.; Rackemann, N.; Müller, I. *Chem. Eur. J.* **2004**, *10*, 2722. (c) Knöllner, H.-J.; Agarwal, S. *Tetrahedron Lett.* **2005**, *46*, 1173.

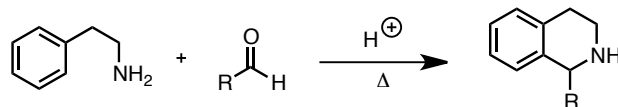
Napieralski isoquinoline synthesis (Figure 2.2),⁵¹ can be seen retrosynthetically as arising from a disconnection between carbons 1 and 8'. The starting material for this cyclization is a β -arylethylamide. It usually proceeds under rather harsh conditions using a mixture of acid and strong dehydrating agent. Since the proposed mechanism goes through an intramolecular electrophilic aromatic substitution, the reaction works best using electron-rich aryl groups.



Bischler-Napieralski 1893



Pictet-Spengler 1909



Pomeranz-Fritsch 1893

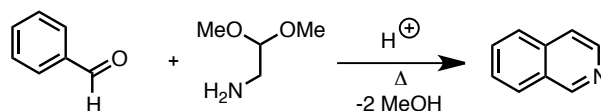


Figure 2.2 Traditionnal approaches toward the isoquinoline heterocycle

The Pictet-Spengler reaction (Figure 2.2),⁵² developed in 1909, is also a robust way to access the isoquinoline core. It also allows retrosynthetic disconnections to be made between atoms 1 and 8' and 1 and 2. The reaction involves the condensation of a β -arylethylamine onto an aldehyde followed by an acid catalyzed ring closure that yields a

⁵¹ For selected examples, see: (a) Xu, X.; Guo, S.; Dang, Q.; Chen, J.; Bai, X. *J. Comb. Chem.* **2007**, *9*, 773. (b) Ishikawa, T.; Shimooka, K.; Narioka, T.; Noguchi, S.; Saito, T.; Ishikawa, A.; Yamazaki, E.; Harayama, T.; Seki, H.; Yamaguchi, K. *J. Org. Chem.* **2000**, *65*, 9143. (c) Bischler, A.; Napieralski, B. *Ber. Dtsch. Chem. Ges.* **1893**, *26*, 1903.

⁵² For reviews, see: (a) Whaley, W. M.; Govindachari, T. R. *Org. React.* **1951**, *6*, 151. (b) Cox, E. D.; Cook, J. M. *Chem. Rev.* **1995**, *95*, 1797. (c) Royer, J.; Bonin, M.; Micouin, L. *Chem. Rev.* **2004**, *104*, 2311. For selected examples, see: (d) Youn, S. W. *J. Org. Chem.* **2006**, *71*, 2521. (e) Pictet, A.; Spengler, T. *Chem. Ber.* **1911**, *44*, 2030.

tetrahydroisoquinoline. Similar to the Bischler-Napieralski reaction, the cyclization step proceeds through an electrophilic aromatic substitution, which is made easier using electron-donating substituents on the aromatic moiety.

Pomeranz and Fritsch⁵³ also reported an isoquinoline synthesis in 1893 (figure 2.2). As opposed to the Bischler-Napieralski and Pictet-Spengler syntheses, the retrosynthetic disconnection is made between carbons 4 and 4'. This reaction involves the condensation of an amino acetaldehyde acetal onto a benzaldehyde molecule, followed by an electrophilic cyclization in an acidic medium. Again, the nature of the mechanism prevents electron-poor benzaldehydes to be employed efficiently in the reaction.

2.1.2 Larock Isoquinoline Synthesis

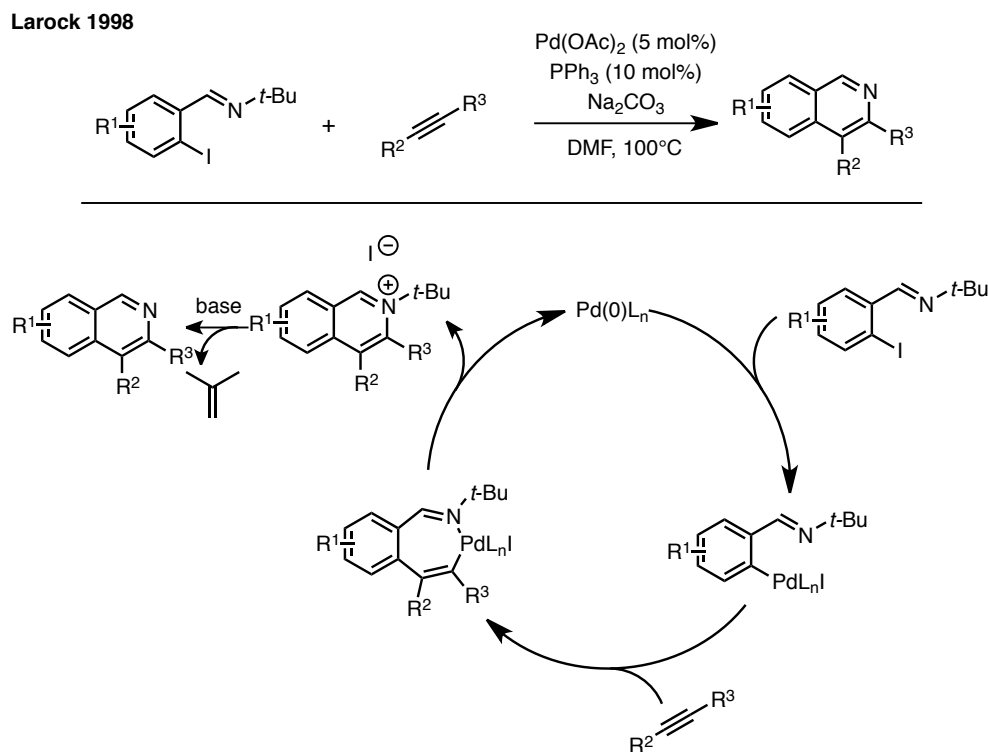
To avoid the elevated temperatures and strongly acidic conditions as well as the poor functional group compatibility characteristic of the traditional approaches toward isoquinolines, several transition metal catalyzed methods have recently begun to emerge.⁵⁴ The Larock isoquinoline synthesis is a very good example of a mild, efficient and functional group tolerant approach, where *ortho*-iodoaldimines and alkynes are coupled in the presence of a palladium catalyst.⁵⁵ The intermolecular nature of this reaction allows for simple the formation of a very diverse array of substituted isoquinolines. The mechanism for this

⁵³ For selected examples, see : (a) Brown, E. V. *J. Org. Chem.* **1977**, *42*, 3208. (b) Herz, W.; Tocker, S. *J. Am. Chem. Soc.* **1955**, *77*, 6355. (c) Fritsch, P. *Ber. Dtsch. Chem. Ges.* **1893** *26*, 419. (d) Pomeranz, C. *Monatsh. Chem.* **1893**, *14*, 116.

⁵⁴ For selected recent metal-catalyzed isoquinoline synthesis, see : (a) Hwang, S.; Lee, Y.; Lee, P. H.; Shin, S. *Tet. Lett.* **2009**, *50*, 2305. (b) Gao, H.; Zhang, J. *Adv. Synth. Catal.* **2009**, *351*, 85. (c) Fischer D.; Tomeba H.; Pahadi N. K.; Patil N. T.; Yamamoto Y. *Angew. Chem.* **2007**, *119*, 4848. (d) Konno, T.; Chae, J.; Miyabe, T.; Ishihara, T. *J. Org. Chem.* **2005**, *70*, 10172. (e) Korivi, R. P.; Cheng, C.-H. *Org. Lett.* **2005**, *7*, 5179. Dai, G.; (f) Larock, R. C.; *J. Org. Chem.* **2003**, *68*, 920. (g) Huang, Q.; Larock, R. C. *J. Org. Chem.* **2003**, *68*, 980. (h) Roesch, K. R.; Larock, R. C. *J. Org. Chem.* **2002**, *67*, 86. (i) Dai, G.; Larock, R. C. *Org. Lett.* **2002**, *4*, 193. (j) Huang, Q.; Hunter, J. A.; Larock, R. C. *J. Org. Chem.* **2002**, *67*, 3437. (k) Huang, Q.; Larock, R. C. *Tet. Lett.* **2002**, *43*, 3557.

⁵⁵ (a) Roesch, K. R.; Zhang, H.; Larock, R. C. *J. Org. Chem.* **2001**, *66*, 8042. (b) Roesch, K. R.; Larock, R. C. *Org. Lett.* **1999**, *1*, 553. (c) Roesch, K. R.; Larock, R. C. *J. Org. Chem.* **1998**, *63*, 5306.

transformation is depicted in Scheme 2.1. Starting from a palladium(0) species, an oxidative addition can occur into the carbon-iodine bond of the aldimine substrate. The resulting intermediate can then undergo alkyne insertion to provide a seven membered palladacycle. Upon reductive elimination, the catalyst is regenerated and an isoquinolinium salt is produced. The latter expels isobutene and the desired isoquinolone after deprotonation.



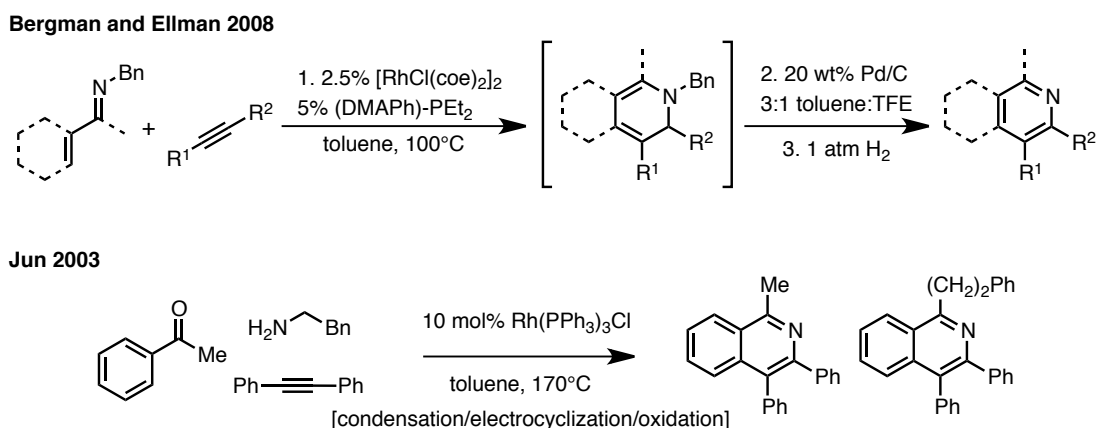
Scheme 2.1 Larock Isoquinoline Synthesis⁵⁵

The scope of the Larock isoquinoline synthesis is very broad, given that the *ortho*-iodoaldimine is accessible. It provides good reactivity with a range of substituted alkynes, regardless of whether the substituents are alkyl or aryl groups. Even though terminal alkynes are not tolerated, silyl-substituted alkynes can be employed to access the corresponding 4-unsubstituted isoquinoline. Of note, when alkyl-aryl disubstituted alkynes are employed, the sp^2 centre goes regioselectively at the 3-position. Overall, the major limitation of this approach is the requirement of a pre-activated substrate, namely the *ortho*-iodobenzaldimine.

These starting materials are generally very expensive or difficult to prepare, adding time and cost to the isoquinoline synthesis.

2.1.3 Heterocycle Synthesis Via C–H Functionalization

Our interest in the minimization of substrate pre-activation in metal-catalyzed processes lead us to question whether a similar reaction mode might be possible where the aryl C–I functional group of the *ortho*-iodobenzimine used in the Larock isoquinoline synthesis could be replaced by a simple C–H bond. A number of challenges are inherent in this approach. Bergman and Ellman have described a Rh(I)-catalyzed C–H enamine vinylation that may be followed by electrocyclic/oxidation steps to generate functionalized pyridines.⁵⁶ Application of a similar approach in isoquinoline synthesis by Jun necessitated the use of highly elevated temperatures (150 °C) due to loss of aromaticity during the electrocyclic, however, and resulted in product mixtures and diminished yields (Scheme 2.2).⁵⁷



Scheme 2.2 Bergman and Ellman and Jun Heterocycle Synthesis

⁵⁶ Colby, D. A.; Bergman, R. G.; Ellman, J. A. *J. Am. Chem. Soc.* **2008**, *130*, 3645.

⁵⁷ Lim, S.-G.; Lee, J. H.; Moon, C. W.; Hong, J.-B.; Jun, C.-H. *Org. Lett.* **2003**, *5*, 2759.

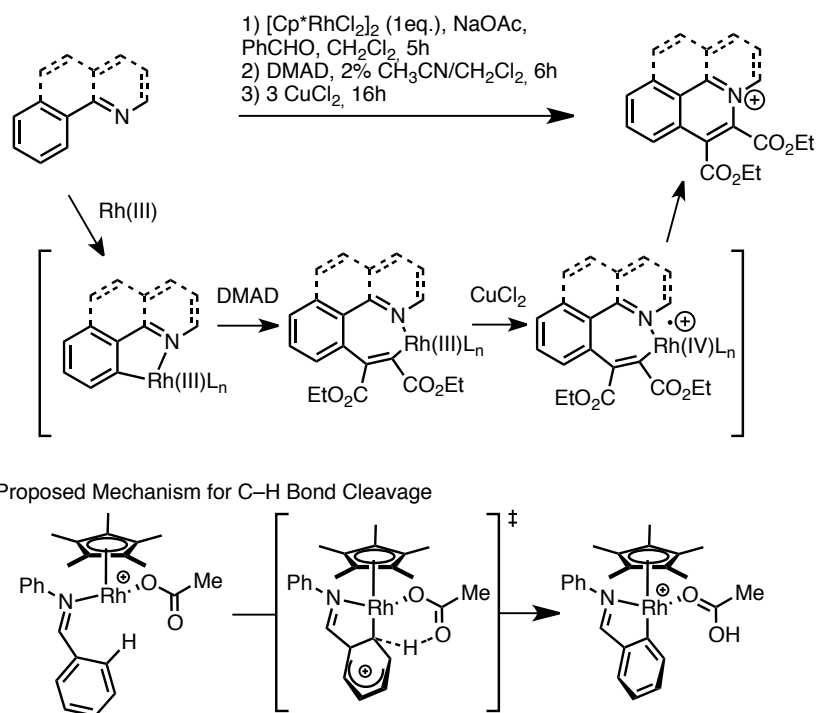
To avoid this unfavorable second step, a catalytic process where the metal catalyst would be involved in both the C–C and the C–N bond forming steps would be preferable.⁵⁸ Also pertinent, Jones reported that isoquinolinium salts can be generated under mild conditions in three steps via (1) stoichiometric Rh(III) induced C–H bond cleavage of 2-phenylpyridine, benzo[*h*]quinoline or *N*-benzylidenemethylamine, (2) alkyne carbometallation and (3) Cu(II) induced C–N reductive elimination.⁵⁹ In the last step, the Cu(II) was proposed to engage in single electron transfer to form a Rh(IV) intermediate more disposed to reductive elimination (Scheme 2.3). In a subsequent report, Jones also proposed a mechanism for the rhodium(III)-mediated C–H bond cleavage. Given the presence of a deuterium kinetic isotope effect and the faster cyclometallation of electron-rich substrates, a mechanism involving a concerted-metallation-deprotonation (CMD),⁶⁰ where the rhodium has a strong electrophilic character, was proposed. It was also found that the regioselectivity of the benzaldimine rhodation was governed by steric interactions, the least encumbered site being metallated preferentially.

⁵⁸ For rhodium(III)-catalyzed formation of C-C and C-O bond, see: Ueura, K.; Satoh, T.; Miura, M. *Org. Lett.* **2007**, *9*, 1407.

⁵⁹ (a) Li, L.; Brennessel, W. W.; Jones, W. D. *J. Am. Chem. Soc.* **2008**, *130*, 12414. (b) Li, L.; Brennessel, W. W.; Jones, W. D. *Organometallics*. **2009**, *28*, 3492.

⁶⁰ For a review on the CMD mechanism, see: (a) Lapointe, D.; Fagnou, K. *Chem. Lett.* **2010**, *39*, 1118. For other selected leading references, see: (b) Gorelsky, S. I.; Lapointe, D.; Fagnou, K. *J. Am. Chem. Soc.* **2008**, *130*, 10848. (c) Gorelsky, S. I.; Lapointe, D.; Fagnou, K. *J. Org. Chem.* **2012**, *116*, 199. (d) Sun, H.-Y.; Gorelsky, S. I.; Stuart, D. R.; Campeau, L.-C.; Fagnou, K. *J. Org. Chem.* **2010**, *75*, 8180. (e) Brown, H. C.; McGray, Jr., C. W. *J. Am. Chem. Soc.* **1955**, *77*, 2306. (f) de la Mare, P. B. D.; Hilton, I. C.; Varma, S. *J. Chem. Soc.* **1960**, 4044. (g) Kresge, A. J.; Dubeck, M.; Brown, H. C. *J. Org. Chem.* **1966**, *32*, 745. (h) Kresge, A. J.; Brennan, J. F. *J. Org. Chem.* **1966**, *32*, 752. (i) Ryabov, A. D.; Sakodinskaya, I. K.; Yatsimirsky, A. K. *J. Chem. Soc., Dalton Trans.* **1985**, 2629. (j) Davies, D. L.; Donald, S. M. A.; MacGregor, S. A. *J. Am. Chem. Soc.* **2005**, *127*, 13754. (k) Davies, D. L.; Donald, S. M. A.; Al-Duaiji, O.; MacGregor, S. A.; Pölleth, M. *J. Am. Chem. Soc.* **2006**, *128*, 4210.

Jones 2008



Scheme 2.3 Rhodium(III)-Mediated Isoquinoline Salt Formation by Jones

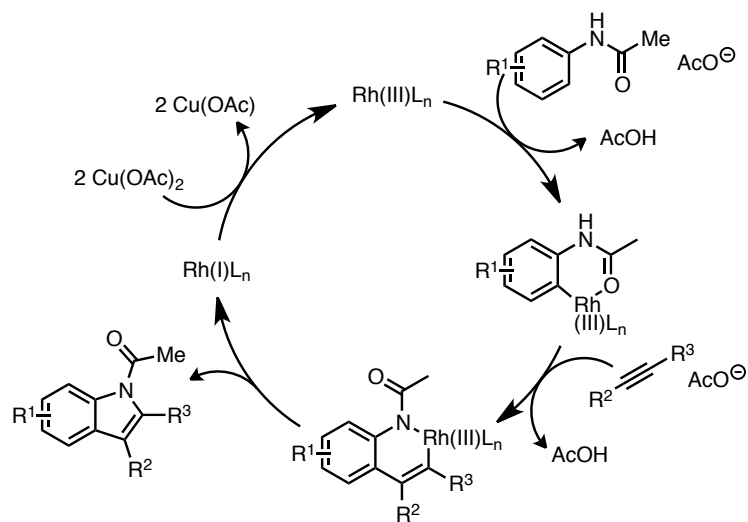
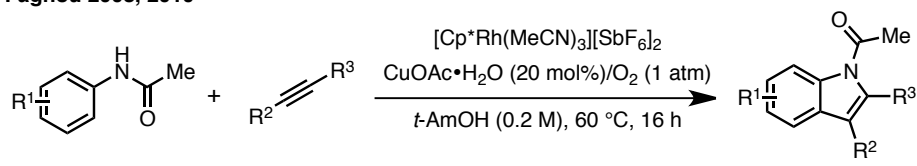
Our group had recently reported another relevant advance for the formation of nitrogen-containing heterocycles where the metal participates in the C–H bond cleavage as well as the C–C and C–N bond formation.⁶¹ This reaction uses a catalytic amount of Rh(III) to access the indole motif from the oxidative coupling of acetanilides with alkynes (Scheme 2.4). The mechanism of this transformation was later subjected to rigorous investigation,⁶² where it was determined that the rhodium catalyst, after coordination with the substrate's directing group, was involved in a rate-determining cyclometallation. Following this step, addition across the alkyne occurs, and then a reductive elimination takes place. The reduced Rh(I) species is re-oxidized using either stoichiometric copper or catalytic copper with oxygen as the terminal oxidant. This catalytic and environmentally friendly indole synthesis

⁶¹ (a) Stuart, D. R.; Bertrand-Laperle, M.; Burgess, K. M. N.; Fagnou, K. *J. Am. Chem. Soc.* **2008**, 130, 16474
For another related example, see: (b) Umeda, N.; Tsurugi, H.; Satoh, T.; Miura, M. *Angew. Chem. Int. Ed.* **2008**, 47, 4019.

⁶² Stuart, D. R.; Alsabeh, P.; Kuhn, M.; Fagnou, K. *J. Am. Chem. Soc.* **2010**, 132, 18326.

features a broad scope with both coupling partners. It also displays predictable regioselectivity with both the arene rhodation and alkyne insertion step. The rhodation typically occurs on the least hindered site. Regarding the alkyne insertion, both steric and electronic factors were found to have an important role. The most electron poor substituent generally ends up at the proximal position relative to the nitrogen. In a case where the electronic nature of the substituents is similar, the bigger group will be positioned away from the nitrogen atom.

Fagnou 2008, 2010



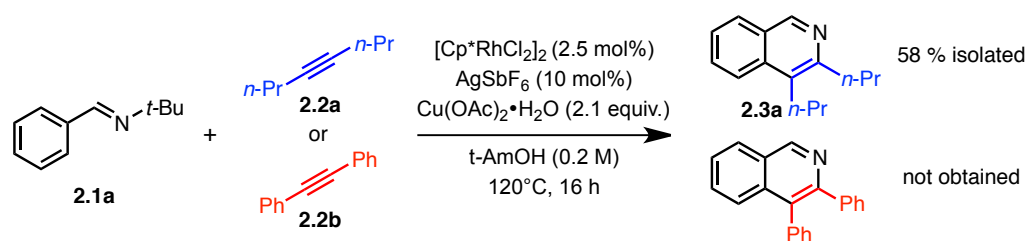
Scheme 2.4 Fagnou Indole Synthesis

2.2 Results and Discussion

2.2.1 Reaction Development and Exploration of Coupling Partners

Compatibility

Inspired by the Larock's isoquinoline synthesis,⁵⁵ the Jones stoichiometric isoquinoline salt formation⁵⁹ and the Fagnou indole synthesis,^{61a,62} we wondered if a hybrid of these reactions could potentially provide *catalytically* a variety of substituted isoquinolines from the reaction of non-pre-activated benzaldimines with alkynes. Building on the success of Rh(III) for the synthesis of indoles, we first attempted to obtain the isoquinoline motif from the reaction of *N*-*tert*-butyl benzaldimine (**2.1a**) with two different alkynes: 4-octyne (**2.2a**) and diphenylacetylene (**2.2b**). The conditions developed in our laboratory for the indole synthesis were first tested. The active catalyst was generated *in situ* by the abstraction of chlorine atoms from the commercially available $[\text{Cp}^*\text{RhCl}_2]_2$ complex using AgSbF_6 . The resulting cationic complex was found to be much more reactive in the indole system. Results from the first attempt were both very encouraging and unexpected at the same time (Scheme 2.5).

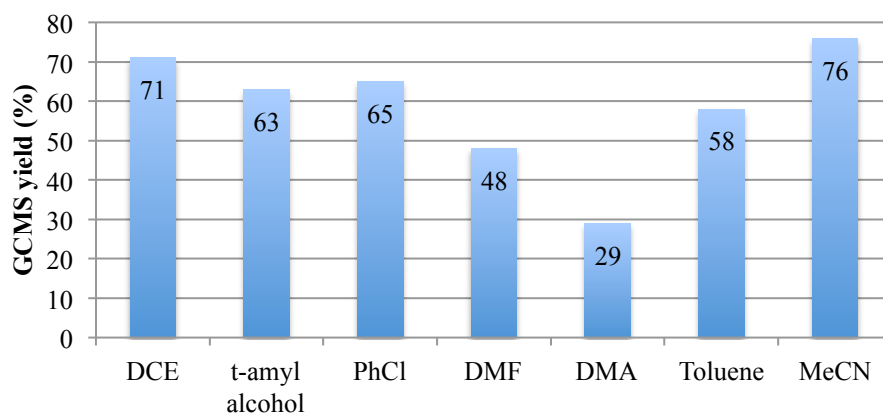
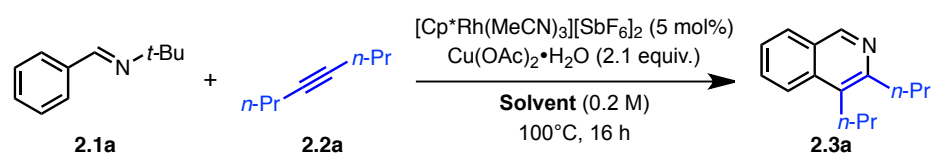


Scheme 2.5 Initial Hit

An isolated yield of 58% was obtained for the reaction of a dialkyl substituted alkyne whereas no reaction was observed using diphenylacetylene. This interesting result went against what was observed with the corresponding indole synthesis, where diphenylacetylene

was a substrate of choice for the coupling reaction. We therefore embarked on the reaction optimization using **2.1a** and **2.2.a** as coupling partners. To accomplish this task, the precatalyst $[\text{Cp}^*\text{Rh}(\text{MeCN})_3][\text{SbF}_6]_2$ was used instead of $[\text{Cp}^*\text{RhCl}_2]_2$ and AgSbF_6 as it is a bench stable solid that proved to give similar results with the oxidative indole synthesis. At first, a screening of solvent was performed (Table 2.1). Where all solvents tried gave at least a small amount of product, 1,2-dichloroethane (DCE) and acetonitrile gave slightly higher yields: 71% and 76% respectively. Given the acetonitrile shortage at the time when this discovery was made, we thought that the use of DCE would be more appealing. The optimization was thus further conducted using this more available solvent.

Table 2.1 Solvent Screening

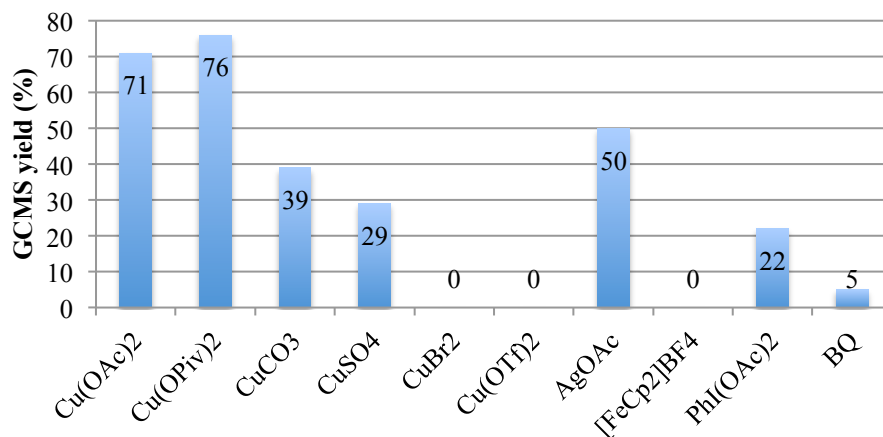
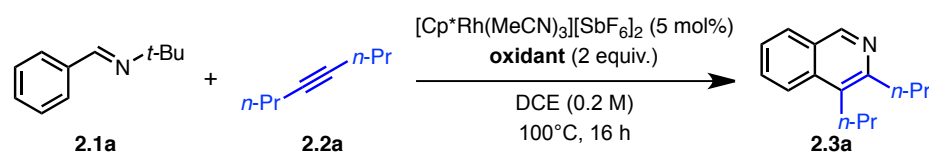


Conditions: **2.1a** (1 equiv.), **2.2a** (1.2 equiv.), $[\text{Cp}^*\text{Rh}(\text{MeCN})_3][\text{SbF}_6]_2$ (5 mol%), $\text{Cu}(\text{OAc})_2 \cdot \text{H}_2\text{O}$ (2 equiv.), solvent (0.2 M), 100 °C, 16 h. Reactions performed in sealed vials. Yields determined by GCMS using 1,3,5-trimethoxybenzene as internal standard

Next, an oxidant screening was performed. As shown in Table 2, a variety of 1 and 2-electrons oxidants were tested. In the case where 2-electron oxidants were employed, 1 equiv. was used in the reaction mixture. From this screening, copper(II)-based oxidants were

found to be ideal. Interestingly, the reaction seems to be very sensitive to the counteranion on the copper. Using counteranions that are very weakly basic (or not basic at all) gave very low yields. This is probably due to the requisite of a base to effect the functionalization of the C–H bond, as previously shown by Jones (see section 2.1.3). Organic oxidants such as iodobenzenediacetate or benzoquinone were also not suitable for the reaction, giving yields of 22% and 5% respectively. Even though the best result was obtained with $\text{Cu}(\text{OPiv})_2$ (76%), the small difference in yield compared to the second best oxidant ($\text{Cu}(\text{OAc})_2 \cdot \text{H}_2\text{O}$, 71%) did not justify its use given the fact that it is not readily available.

Table 2.2 Oxidant Screening

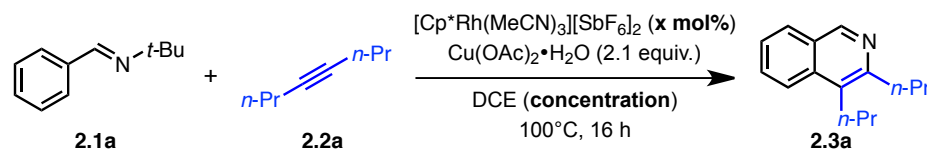


Conditions: **2.1a** (1 equiv.), **2.2a** (1.2 equiv.), $[\text{Cp}^*\text{Rh}(\text{MeCN})_3][\text{SbF}_6]_2$ (5 mol%), oxidant (2 equiv.), DCE (0.2 M), 100 °C, 16 h. Yields determined by GCMS using 1,3,5-trimethoxybenzene as internal standard

A temperature screen was also performed at intervals of 10 °C between 50 °C and 90 °C. While good reactivity could still be obtained at temperatures as low as 50 °C (67%), the optimal yield was obtained at 80 °C (78%). We therefore decided to conduct the reaction under reflux since the boiling point of DCE is 83 °C. Next, we evaluated the impact of

catalyst loading and concentration on the reaction outcome (Table 2.3). While keeping the catalyst loading at 5 mol%, the reduction of concentration from 0.2 M to 0.1 M was able to increase the yield by 13% (entries 1 and 2). Interestingly, a lower catalyst loading of 2.5 mol% compared to 5 mol% also gave an increase in yield (entries 1 and 3). Using a 0.1 M concentration along with a diminished catalyst loading of 2.5 mol% provided the optimal conditions (entry 4). Further reducing of either the concentration or the catalyst loading did not lead to any yield improvement (entries 5 and 6).

Table 2.3 Optimization of Catalyst Loading and Reaction Concentration

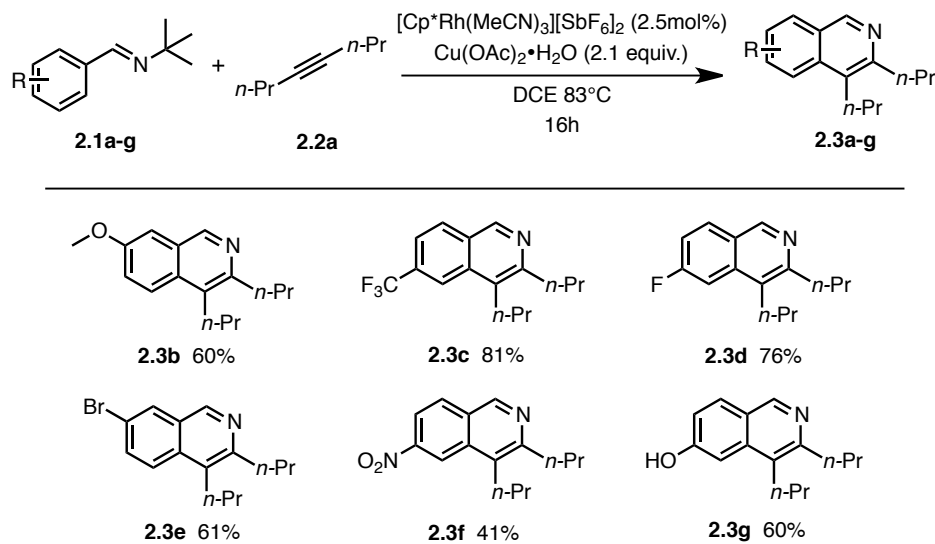


Entry	Concentration (M)	Catalyst loading (mol%)	GCMS yield (%)
1	0.2	5	71
2	0.1	5	84
3	0.2	2.5	88 (76)
4	0.1	2.5	90 (80)
5	0.05	2.5	88
6	0.1	1	36

Conditions: **2.1a** (1 equiv.), **2.2a** (1.2 equiv.), [Cp*Rh(MeCN)₃][SbF₆]₂ (x mol%), Cu(OAc)₂·H₂O (2 equiv.), DCE (concentration), 100 °C, 16 h. Yields determined by GCMS using 1,3,5-trimethoxybenzene as internal standard. Isolated yield in parentheses.

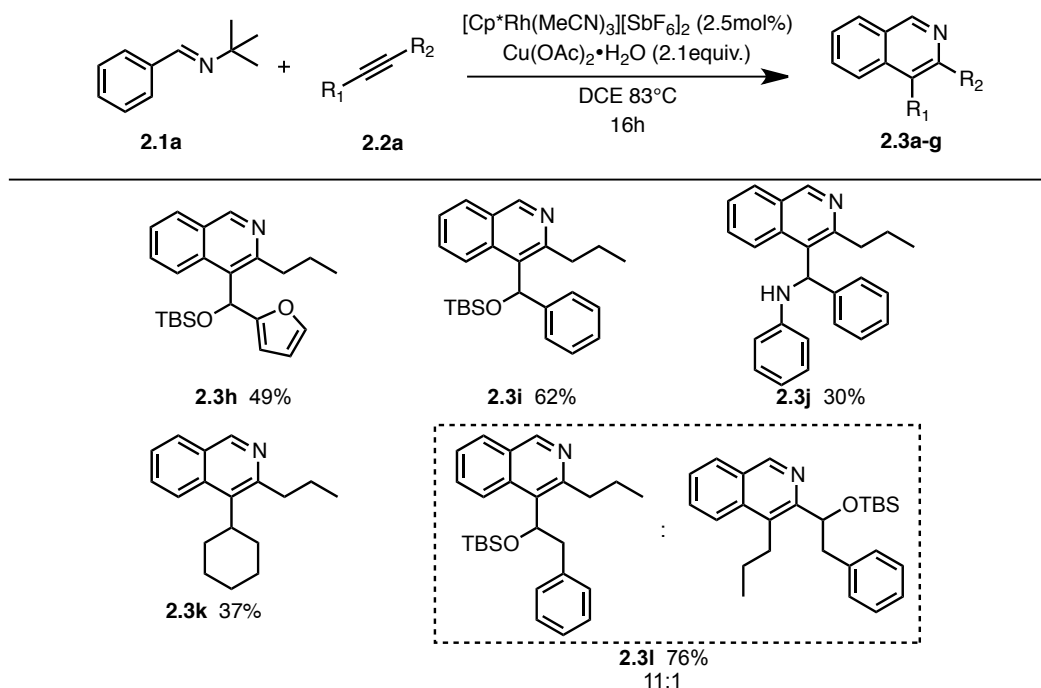
Using alkyne **2.2a**, we have found the reaction to be compatible with a variety of substituents on the benzaldimine coupling partner. As shown in Table 4, both electron-donating and electron-withdrawing groups are tolerated. Furthermore, when the substituent is at the *meta* position relative to the imine moiety, the rhodation occurs exclusively at the least hindered position (**2.3b** and **2.3e**). An arylbromide substituent remains intact during the reaction (**2.3e**), providing a useful handle for further elaboration. Of note, a phenol OH group does not need protection as illustrated by the formation of **2.3g**.

Table 2.4 Scope of Substituted *N*-*tert*-Butylbenzaldimines.



Conditions: **2.1** (1 equiv.), **2.2a** (1.2 equiv.), $[\text{Cp}^*\text{Rh}(\text{MeCN})_3][\text{SbF}_6]_2$ (2.5 mol%), $\text{Cu}(\text{OAc})_2 \cdot \text{H}_2\text{O}$ (2 equiv.), DCE (0.1 M), 83 °C, 16 h. Isolated yields are reported

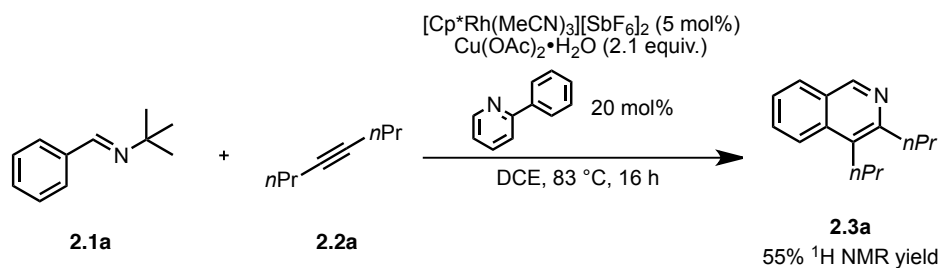
The use of unsymmetrical alkynes is also possible as exemplified in Table 2.5. The larger substituent is regioselectively placed at the benzylic position away from the nitrogen atom. For example, isoquinolines **2.3h-j** are all formed as the exclusive regioisomers. In the case of **2.3i**, the two isomers are produced in an 11:1 ratio. Terminal alkynes were found to lead to alkyne dimerization (Glaser coupling) most likely due to the presence of copper under the reaction conditions. Silyl-substituted alkynes or 2-(2-hydroxypropyl)-protected terminal alkynes did not lead to any product formation.

Table 2.5 Reaction Compatibility with Unsymmetrical Alkynes

Conditions: **2.1a** (1 equiv.), **2.2** (1.2 equiv.), $[\text{Cp}^*\text{Rh}(\text{MeCN})_3][\text{SbF}_6]_2$ (2.5 mol%), $\text{Cu}(\text{OAc})_2 \cdot \text{H}_2\text{O}$ (2 equiv.), DCE (0.1 M), 83 °C, 16 h. Isolated yields are reported

The generally lower yields observed are due to incomplete conversion of the starting material. No decomposition would typically occur under these reaction conditions. As opposed to the indole synthesis previously reported by our group and the isoquinoline synthesis reported by Larock, aryl substituents on the alkyne were not tolerated, even under the optimized conditions. It was first thought that this lack of reactivity could be due to product inhibition. Indeed, the product obtained, given that the aryl group would go at the 3-position, would contain a 2-phenylpyridine motif. These structures are well known to yield cyclometallated species with a variety of transition metals. To test whether this could be the problem in our system, benzaldimine **2.1a** was reacted with alkyne **2.2a** under the optimal reaction conditions (however with 5 mol% cat. loading) and in presence of 20 mol% of 2-phenylpyridine. The ^1H NMR yield obtained from this reaction after 16 h was 55% (Scheme

2.6). This result thus goes against the hypothesis of product inhibition, even though a small decrease in reaction yield was observed.

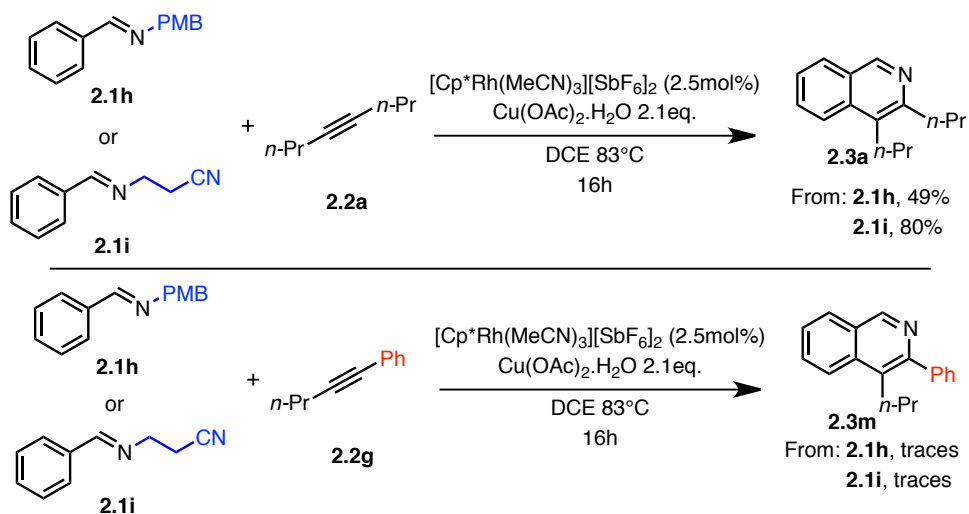


Scheme 2.6 Product Inhibition Testing

Being uncertain of whether the large *tert*-butyl group on the benzaldimine nitrogen was optimal in terms of size for the positioning of a larger substituent at the 3-position, we tested a few alternative groups that could subsequently form stable carbocations (i.e. better positive "leaving group"). The rationale was that if aryl groups would adopt a proximal position relative to the nitrogen,⁶³ a smaller positive "leaving group" would provide more space for their incorporation. As such, a *para*-methoxybenzyl (PMB) and a propionitrile group (leaving as acrylonitrile) were made and used as *N*-substituents on the benzaldimine. To make sure these were suitable leaving groups for this isoquinoline synthesis, they were first tested with alkyne **2.2a**. GCMS yields of 49% and 80% were obtained for the reaction of **2.1h** and **2.1i** respectively. However, when the same reaction was run with alkyne **2.2g**, only traces of product could be detected by GCMS (Scheme 2.7).⁶⁴ Further screening of solvents (*t*-AmOH, mesitylene, DMF, dioxane, cyclohexanone, chlorobenzene) or base additives (Na₂CO₃, NaHCO₃, NaOH, Et₃N) did not lead to any significant improvements.

⁶³ Electronic factors were found to direct *sp*² centres at the proximal position relative to the nitrogen atom for the formation of indoles and pyrroles: (a) Ref 61a (b) Ref. 62 (c) Huestis, M. P.; Chan, L.; Stuart, D. R. *Angew. Chem. Int. Ed.* **2011**, *50*, 1338.

⁶⁴ In the case of **2.1i** an unknown product that seems to arise from the alkyne hydroarylation was isolated. For an example of Rh(III)-catalyzed hydroarylation reaction, see: Schipper, D. J.; Hutchinson, M.; Fagnou, K. *J. Am. Chem. Soc.* **2010**, *132*, 6910.



Scheme 2.7 Reaction Outcome with Different Leaving Groups.

2.2.2 Mechanistic Insights

One mechanism that could explain the formation of the desired isoquinolones is analogous to the proposal of Bergman and Ellman and Jun described previously (Scheme 2.2). Hydroarylation of the alkyne could occur first to afford intermediate **2.4**, which could then undergo electrocyclization and oxidation to furnish isoquinolone **2.3a** (Figure 2.3).

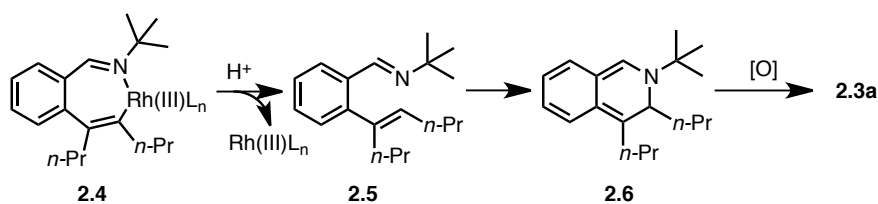
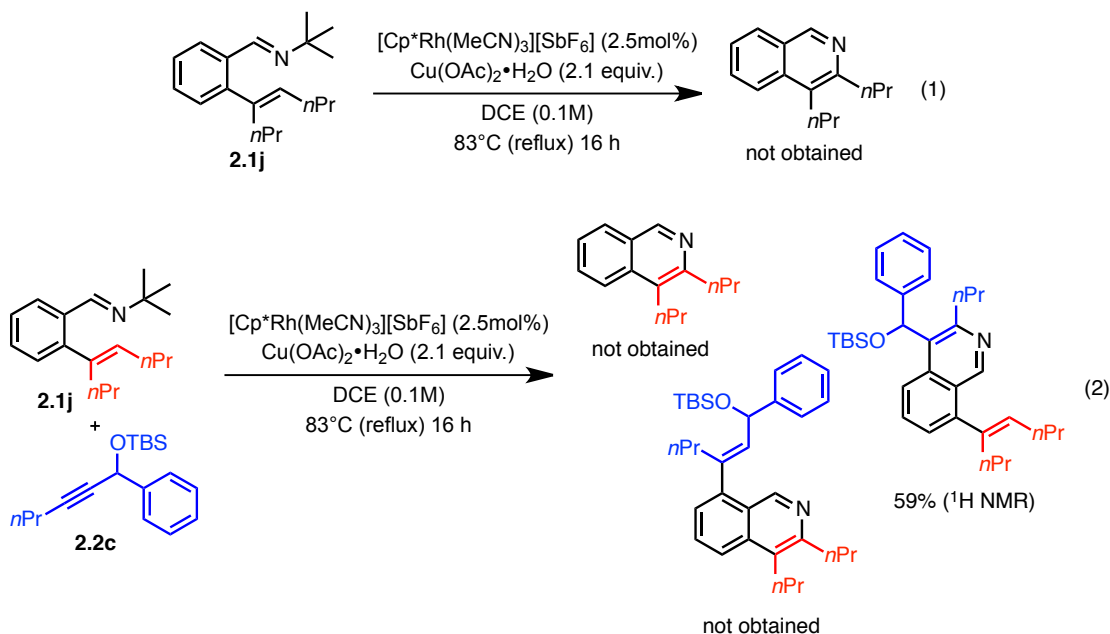


Figure 2.3 Hydroarylation/electrocyclization/oxidation potential mechanistic pathway

In order to probe this mechanistic pathway, aldimine **2.1j**, bearing an alkene substituent, was subjected to the standard reaction conditions (Scheme 2.8, Eq. 1). No product was obtained from this experiment. In a similar fashion, when **2.1j** was reacted in the presence of alkyne **2.2c**, the only product detected in the crude reaction mixture is **10**

(Scheme 2.8, Eq. 2). The absence of cyclization with the pre-installed olefinic moiety, both in the absence and presence of added alkyne, strongly indicates that an electrocyclization/oxidation pathway does not account for product formation.



Scheme 2.8 Ruling Out of the Electrocyclization/Oxidation Pathway

Another mechanistic pathway that could account for the formation of isoquinolones using a Rh(III) catalyst is depicted in Figure 2.4. From the seven-membered rhodacycle intermediate **2.4**, copper-mediated oxidation of Rh(III) to Rh(IV) could happen, which would trigger a C–N reductive elimination.

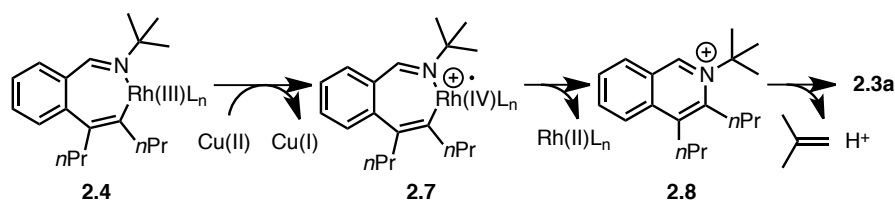
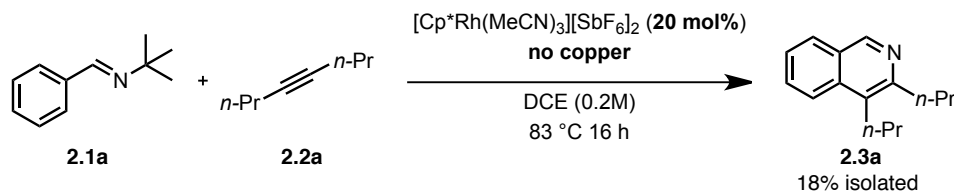


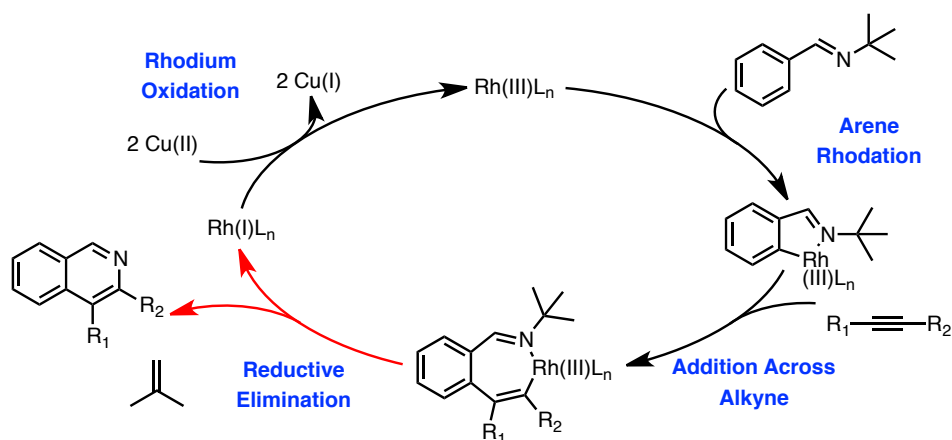
Figure 2.4 Potential Rh(IV) reductive elimination pathway

In addition to this Rh(IV) pathway, which was proposed by Jones for stoichiometric experiments,^{59a} C-N reductive elimination may also occur directly from the Rh(III) intermediate **2.4**. To probe the nature of the reaction mechanism, the reaction of **2.1a** was performed in the presence of 20 mol% Rh(III) catalyst in the absence of added Cu(OAc)₂•H₂O (Scheme 2.9).



Scheme 2.9 Verification of the Rh(IV) Hypothesis

In this case, **2.3a** is obtained in 18% yield. Similarly, if a reaction is performed with 2.5 mol% [Cp*Rh(MeCN)₃][SbF₆]₂ without added Cu(OAc)₂•H₂O, **2.3a** is generated in 2.2 % GCMS yield after 16 hours. After this time, addition of 2.1 equiv. Cu(OAc)₂•H₂O induces catalyst turnover resulting in a 79% GCMS yield after 24 hours. These results indicate that Cu(II) is not essential for C-N bond formation. In light of these studies, we currently favour the reaction pathway outlined in Scheme 2.10 whereby a Rh(III) species first forms a metallacycle with an aldimine substrate. This intermediate can then engage in an alkyne insertion followed by a C-N reductive elimination directly from Rh(III). The findings gleaned from our mechanistic experiments allowed us to propose for the first time this type of reductive elimination from Rh(III) in a catalytic cycle. The reduced Rh(I) species can then be re-oxidized by copper(II) to reform the active Rh(III) species.



Scheme 2.10 Proposed Catalytic Cycle

2.3 Summary and Outlook

The ability of rhodium(III) to catalytically induce C–H bond cleavage, C–C bond formation and importantly, C(sp^2)–N(sp^2) bond reductive elimination under relatively mild reaction conditions with a range of different aldimines and alkynes should not only find application in the preparation of other isoquinoline molecules, but also serve as a useful source of inspiration for the development of other novel rhodium(III)-catalyzed transformations in heterocycle synthesis. In fact, the following chapter will describe significant new advances that were made building on the concepts put forward in this chapter.

Rhodium(III)-Catalyzed Redox-Neutral Synthesis of Nitrogen-Containing Heterocycles

3.1 Introduction

Recognizing the value of nitrogen-containing heterocyclic compounds, chemists continue to devise novel methods for their synthesis. The past few years have witnessed a very rapid increase of methods to access these coveted structures from minimally pre-activated starting materials. Rhodium(III)-catalyzed methods are illustrative (Figure 3.1), whereby a nitrogen-containing directing group allows the direct *ortho*-functionalization of arenes (or alkenes) and subsequent alkyne insertion. A following reductive elimination typically furnishes the desired heterocycle. In order to put into context the importance of the work that will be discussed in this chapter, more background information about the general trends observed in these oxidative annulation methods will be provided. Additionally, some inherent limitations of the current approaches will be discussed.

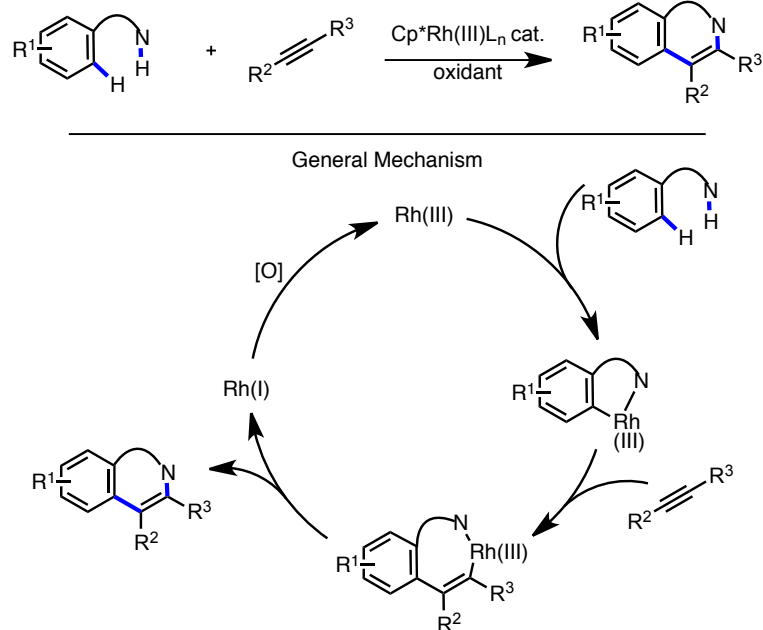


Figure 3.1 Rh(III)-catalyzed oxidative heterocycle formation

The formation of C–N bonds via reductive elimination from a transition metal has traditionally been achieved from a metal being bonded to both coupling partners. In almost all examples of such bond forming reactions, the nitrogen component is initially coordinated to the metal by means of a simple deprotonation. After reductive elimination, the catalyst is then re-oxidized via either oxidative addition into a C–X bond or with the help of an external oxidant (in oxidative reactions). Besides these more common approaches, an orthogonal strategy, which consists of performing an oxidative addition into an N–O bond, has also been developed. After a brief review on the general trends in Rh(III)-catalyzed heterocycle synthesis, this section will discuss more thoroughly this strategy as well as how it can be applied for the formation of nitrogen-containing heterocycles.

3.1.1 Rhodium(III)-Catalyzed Oxidative Heterocycle Synthesis

While rhodium(III)-catalyzed transformations were recently shown to promote a rich diversity of reactions (oxidative Heck reactions,⁶⁵ 1,2-addition reactions,⁶⁶ oxygen-containing heterocycle formation,⁶⁷ various benzannulation reactions⁶⁸ and dehydrogenative couplings⁶⁹),⁷⁰ the following discussion will focus on oxidative nitrogen-containing heterocycle formation.

As exemplified in the preceding chapter, oxidative rhodium(III)-catalyzed cross-coupling/annulation reactions are efficient strategies to construct nitrogen-containing

⁶⁵ For selected examples, see: (a) Ueura, K.; Satoh, T.; Miura, M. *Org. Lett.* **2007**, *9*, 1407. (b) Umeda, N.; Hirano, K.; Satoh, T.; Miura, M. *J. Org. Chem.* **2009**, *74*, 7094. (c) Mochida, S.; Hirano, K.; Satoh, T.; Miura, M. *J. Org. Chem.* **2011**, *76*, 3024. (d) Li, X.; Zhao, M. *J. Org. Chem.* **2011**, *76*, 8530. (e) Park, S. H.; Kim, J. Y.; Chnag, S. *Org. Lett.* **2011**, *13*, 2372. (f) Tsai, A. S.; Brasse, M.; Bergman, R. G.; Ellman, J. A. *Org. Lett.* **2011**, *13*, 540. (g) Chen, J.; Song, G.; Pan, C.-L.; Li, X. *Org. Lett.* **2010**, *12*, 5426. (h) Wang, F.; Song, G.; Li, X. *Org. Lett.* **2010**, *12*, 5430. (i) Wang, F.; Song, G.; Du, Z.; Li, X. *J. Org. Chem.* **2011**, *76*, 2926. (j) Patureau, F. W.; Glorius, F. *J. Am. Chem. Soc.* **2010**, *132*, 9982. (k) Patureau, F. W.; Besset, T.; Glorius, F. *Angew. Chem., Int. Ed.* **2011**, *50*, 1064. (l) Rakshit, S.; Grohmann, C.; Besset, T.; Glorius, F. *J. Am. Chem. Soc.* **2011**, *133*, 2350. (m) Besset, T.; Kuhl, N.; Patureau, F. W.; Glorius, F. *Chem. Eur. J.* **2011**, *17*, 7167. (n) Li, H.; Li, Y.; Zhang, X.-S.; Chen, K.; Wang, X. Shi, Z.-J. *J. Am. Chem. Soc.* **2011**, *133*, 15244. (o) Willwacher, J.; Rakshit, S.; Glorius, F. *Org. Biomol. Chem.* **2011**, *9*, 4736.

⁶⁶ For selected examples, see: (a) Hesp, K. D.; Bergman, R. G.; Ellman, J. A. *Org. Lett.* **2012**, *14*, 2304. (b) Tauchert, M. E.; Incarvito, C. D.; Rheingold, A. L.; Bergman, R. G.; Ellman, J. A. *J. Am. Chem. Soc.* **2012**, *134*, 1482. (c) Hesp, K. D.; Bergman, R. G.; Ellman, J. A. *J. Am. Chem. Soc.* **2011**, *133*, 11430. (d) Tsai, A. S.; Tauchert, M. E.; Bergman, R. G.; Ellman, J. A. *J. Am. Chem. Soc.* **2011**, *133*, 1248. (e) Li, Y.; Li, B.-J.; Wang, W.-H.; Huang, W.-P.; Zhang, X.-S.; Chen, K.; Shi, Z.-J. *Angew. Chem., Int. Ed.* **2011**, *50*, 2115. (f) Yang, L.; Correia, C. A.; Li, C.-J. *Adv. Synth. Catal.* **2011**, *353*, 1269. (g) Park, J. Park, E.; Kim, A.; Lee, Y.; Chi, K.-W.; Kwak, J. H.; Jung, Y. H.; Kim, I. S. *Org. Lett.* **2011**, *13*, 4390.

⁶⁷ (a) Ueura, K.; Satoh, T.; Miura, M. *J. Org. Chem.* **2007**, *72*, 5362. (b) Ueura, K.; Satoh, T.; Miura, M. *Org. Lett.* **2007**, *9*, 1407. (c) Mochida, S.; Hirano, K.; Satoh, T.; Miura, M. *J. Org. Chem.* **2009**, *74*, 3478. (d) Satoh, T.; Ueura, K.; Miura, M.; *Pure Appl. Chem.* **2008**, *80*, 1127. (e) Shimizu, M.; Hirano, K.; Satoh, T.; Miura, M. *J. Org. Chem.* **2009**, *74*, 3478. (f) Mochida, S.; Shimizu, M.; Hirano, K.; Satoh, T.; Miura, M. *Chem. Asian-J.* **2010**, *5*, 847. (g) Wang, F.; Song, G.; Du, Z.; Li, X. *J. Org. Chem.* **2011**, *76*, 2926. (h) Song, G.; Chen D.; Pan, C.-L.; Crabtree, R. H.; Li, X. *J. Org. Chem.* **2010**, *75*, 7487.

⁶⁸ For selected examples, see: (a) Song, G.; Gong, X.; Li, X. *J. Org. Chem.* **2011**, *76*, 7583. (b) Umeda, N.; Tsurugi, H.; Satoh, T.; Miura, M. *Angew. Chem., Int. Ed.* **2008**, *47*, 4019. (c) Umeda, N.; Hirano, K.; Satoh, T.; Miura, M. *J. Org. Chem.* **2011**, *76*, 13. (d) see ref. 67f.

⁶⁹ (a) Wencel-Delord, J.; Nimphius, C.; Patureau, F. W.; Glorius, F. *Chem. Asian J.* **2012**, DOI: 10.1002/asia.201101018. (b) Wencel-Delord, J.; Nimphius, C.; Patureau, F. W. *Angew. Chem., Int. Ed.* **2012**, *51*, 1710.

⁷⁰ For reviews, see: (a) Song, G.; Wang, F.; Li, X. *Chem. Soc. Rev.* **2012**, *41*, 3651. (b) Satoh, T.; Miura, M. *Chem. Eur. J.* **2010**, *16*, 11212. (c) Colby, D. A.; Tsai, A. S.; Bergman, R. G.; Ellman, J. A. *Acc. Chem. Res.* **2012**, DOI: 10.1021/ar200190g.

heterocycles from minimally pre-activated starting materials. Apart from isoquinolines⁷¹ and indoles,⁷² which were presented in Chapter 2, several other heterocycles can be obtained using this strategy.⁷³ Figure 3.2 showcases the scaffolds that are currently accessible using rhodium(III) catalysis. Besides the nature of the directing group, many similarities or general trends exist between the multiple syntheses established thus far. These common behaviours can be observed in 1) the arene rhodation regioselectivity, 2) the alkyne insertion regioselectivity, as well as 3) the general reaction conditions.

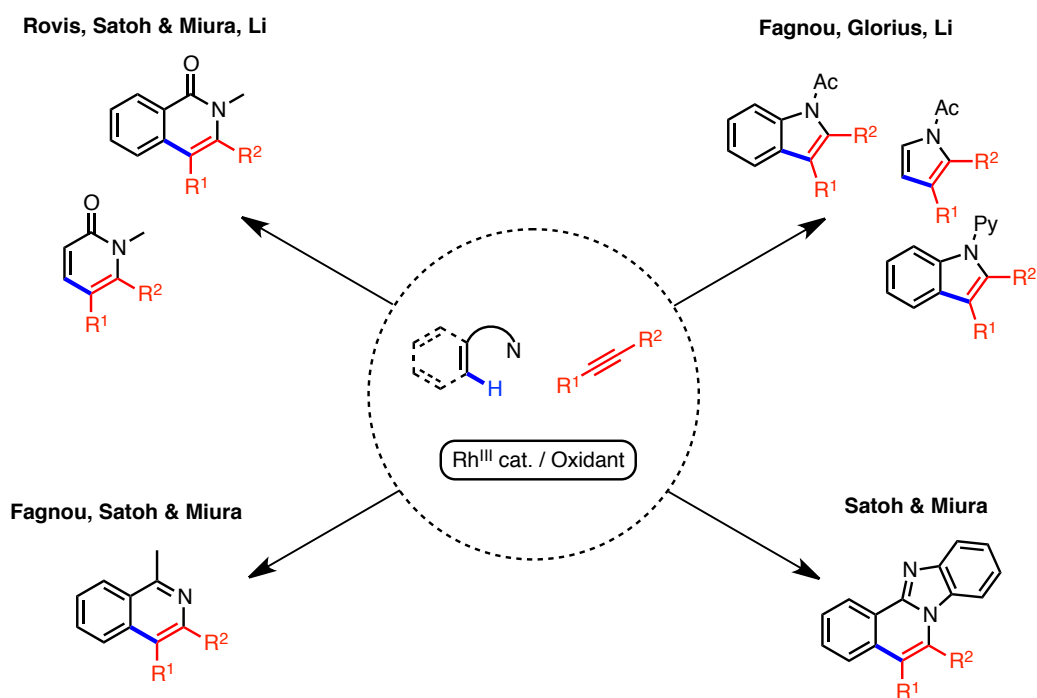


Figure 3.2 Different heterocycles accessible through a rhodium(III)-catalyzed cross-coupling/cyclization strategy

⁷¹ Guimond, N.; Fagnou, K. *J. Am. Chem. Soc.* **2009**, *131*, 12050.

⁷² (a) Stuart, D. R.; Bertrand-Laperle, M.; Burgess, K. M. N.; Fagnou, K. *J. Am. Chem. Soc.* **2008**, *130*, 16474. (b) Stuart, D. R.; Alsabeh, P.; Kuhn, M.; Fagnou, K. *J. Am. Chem. Soc.* **2010**, *132*, 18326.

⁷³ For isoquinoline syntheses, see: (a) Fukutani, T.; Umeda, N.; Hirano, K.; Satoh, T.; Miura, M. *Chem. Commun.* **2009**, 5141. (b) Morimoto, K.; Hirano, K.; Satoh, T.; Miura, M. *Chem. Lett.* **2011**, *40*, 600. For pyrrole syntheses, see: (c) Ref 72b (d) Rakshit, S.; Patureau, F. W.; Glorius, F. *J. Am. Chem. Soc.* **2010**, *130*, 9585. For isoquinolone syntheses, see: (e) Hyster, T. K.; Rovis, T. *J. Am. Chem. Soc.* **2010**, *132*, 10565. (f) Mochida, S.; Umeda, N.; Hirano, K.; Satoh, T.; Miura, M. *Chem. Lett.* **2010**, *39*, 744. (g) Song, G.; Chen, D.; Pan, C.-L.; Crabtree, R. H.; Li, X. *J. Org. Chem.* **2010**, *75*, 7487. For pyridone syntheses, see: (h) Su, Y.; Zhao, M.; Han, K.; Song, G.; Li, X. *Org. Lett.* **2010**, *12*, 5462. (i) Hyster, T. K.; Rovis, T. *Chem. Sci.* **2011**, *2*, 1606.

Arene rhodation regioselectivity. After coordination of the catalyst to the directing group of the substrate, the first step of the catalytic cycle responsible for the various Rh(III)-catalyzed heterocycle syntheses usually involves arene rhodation via C–H bond cleavage (Figure 3.1). When employing aromatic substrates that are substituted at the *meta* position relative to the directing group, C–H functionalization can occur at two possible sites. Typically, the least hindered site will undergo rhodation with high levels of regioselectivity. This has been demonstrated in a variety of systems, as illustrated in Figure 3.3.

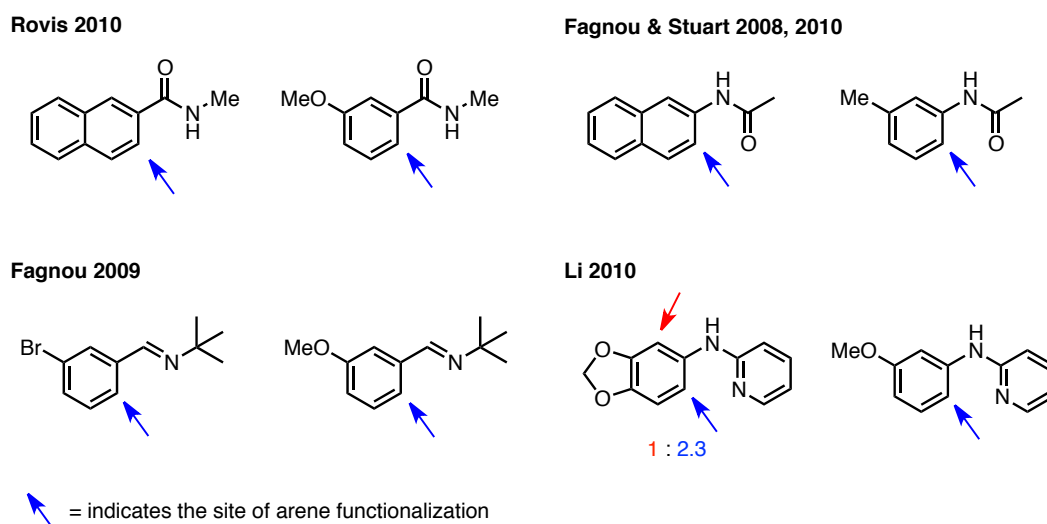
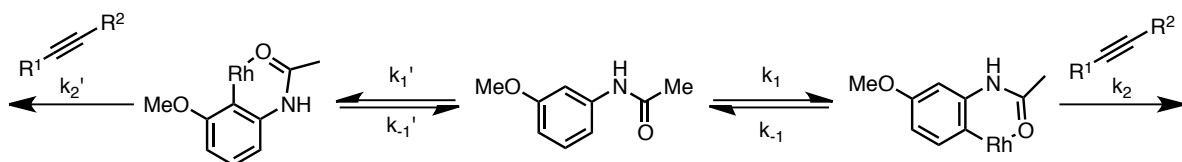


Figure 3.3 Arene rhodation regioselectivity

Fagnou and Stuart noted in their recent report on the synthesis of indoles that this regioselectivity can be dependent on the nature of the alkyne substituents as well as its concentration.^{72b} In fact, it was shown for the indole system that the arene rhodation regioselectivity is governed by the relative rates of the reversibility of cyclorhodation and alkyne insertion. It is therefore under Curtin-Hammet kinetic control. Scheme 3.1 summarizes this behaviour. With faster inserting alkynes,⁷⁴ the regioselectivity was found to be lower. This is due to the greater rate of alkyne insertion relative to the arene proto-

⁷⁴ It was found that diaryl-substituted alkynes react faster than dialkyl-substituted alkynes.

derhodation (i.e. $k_2, k_2' \gg k_{-1}, k_{-1}'$). The resulting regioselectivity is thus closer to the initial arene metallation ratio k_1/k_1' . The same effect can be observed by varying the alkyne concentration. At higher alkyne loadings, k_2, k_2' becomes much greater than k_{-1}, k_{-1}' . Consequently, the regioselectivity also reflect the ratio k_1/k_1' . This hypothesis was further supported by the fact that slow addition of the alkyne substrate to the reaction mixture (i.e. lower k_2, k_2' values) provided higher regioselectivities, perhaps due to the higher concentration of the least hindered rhodacycle when equilibrium can be reached between these two structural isomers.



Scheme 3.1 Kinetics for Arene Rhodation Regioselectivity

Alkyne scope and regioselectivity of insertion. The variety of heterocycles that can be obtained through Rh(III) catalysis is directly related to the scope of alkynes that can undergo the insertion and cyclization steps. Table 3.1 summarizes the tolerance of various alkyne substitution patterns with the heterocycle syntheses developed to date with many similarities noted between several heterocycle classes. At the exception of the isoquinoline synthesis discussed in Chapter 2,⁷¹ the previously established methods tolerate the use of diaryl- and alkyl,aryl-substituted alkynes. The reason for this particular restriction in our isoquinoline system is still unknown. With regard to dialkyl-substituted alkynes, at least one method has been developed to access every corresponding heterocycle.^{72,73} Hence, the

synthesis of disubstituted heterocycles through oxidative rhodium(III) catalysis can more or less be considered as a solved problem. Monosubstituted heterocycles, on the other hand, are much more difficult to obtain. In fact, none of the oxidative syntheses established thus far allow for the use of terminal alkynes. In cases where these substrates were tried, alkyne dimerization was reported as being the major product. Nonetheless, Fagnou and Stuart have recently described strategies to overcome this limitation.^{72b} It was indeed found that TMS-protected alkynes were tolerated in some instances. Subsequent deprotection would typically afford the monosubstituted heterocycle. While only one example was reported for an indole synthesis with a yield of 20%, this strategy proved much more useful for the synthesis of pyrroles, where yields ranging from 55 to 76% were reported with alkyl, TMS- and aryl, TMS-substituted alkynes.

Table 3.1 Alkyne Scope with Various Heterocycles

R ₁	R ₂					
Ar	Ar	✓ (Sato & Miura) ✗ (Fagnou)	✓	✓	✓	✓
Alk	Ar	✓ (Sato & Miura) ✗ (Fagnou)	✓	✓	✓	✓
Alk	Alk	✓	✓	✓ (Rovis) ✗ (Li)	✓	✓ (Fagnou) ✗ (Glorius)
TMS	Ar	✗	✗	✗	✗	✓ (Fagnou) ✗ (Glorius)
Alk	TMS	✗	✗	✗	✓ (Fagnou) ✗ (Li)	✓ (Fagnou) ✗ (Glorius)
H/R	H/R	✗	✗	✗	✗	✗

As for the regioselectivity of alkyne insertion, both electronic and steric factors were found to play a role (Figure 3.4). However electronic effects appear to have a stronger influence, with the sp^2 -substituted carbon being normally positioned next to the nitrogen of the heterocycle. This general trend was observed for all heterocycle syntheses, without exception. When reacting dialkyl-substituted alkynes, the larger substituent is typically installed at the distal position relative to the nitrogen atom. Of note Huestis and Fagnou nicely exploited these features for the regiocontrolled preparation of 2,3-aliphatic-substituted indoles and pyrroles employing enyne coupling partners.⁷⁵

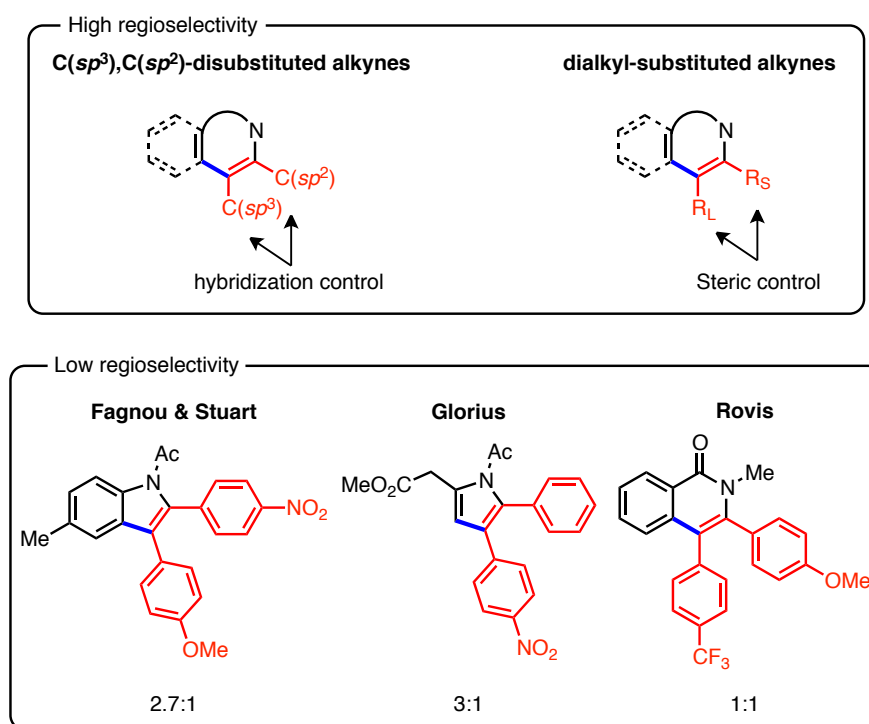


Figure 3.4 Regioselectivity of the alkyne insertion. The major regioisomer is displayed, and the ratio is given under the structure.

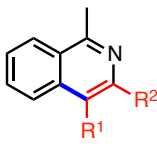
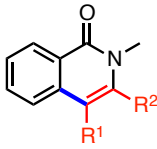
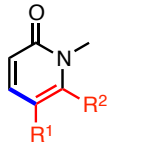
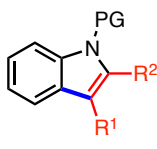
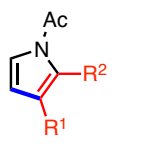
The only case where the regioselectivity is inconsistent from one heterocycle synthesis to another is when diaryl-substituted alkynes with different electronic properties on

⁷⁵ Huestis, M. P.; Chan, L.; Stuart, D. R.; Fagnou, K. *Angew. Chem., Int. Ed.* **2011**, *50*, 1338.

each aryl group are employed. The regioselectivity obtained with these substrates is usually low and hardly predictable. Some examples are displayed in Figure 3.4. No general explanation has been given to account for these divergent results.

General Conditions. The conditions developed for the synthesis of various nitrogen-containing heterocycles using Rh(III) catalysis contain several similarities. Table 3.2 outlines the main reaction parameters for these different methods. Although the pyrrole synthesis developed by Fagnou and Stuart was shown to proceed at room temperature in high yield,^{72b} most other reactions necessitate higher temperatures, typically ranging from 60 to 130 °C. Regarding the catalyst loadings, amounts of around 5 mol% are typical. One example with a relatively low loading (1 mol%) was nonetheless demonstrated by Li for the synthesis of pyridones.^{73h} With respect to the external oxidant, stoichiometric amounts of Cu(OAc)₂ have been successfully used for the synthesis of all heterocycles. Some alternatives were also shown to be suitable. For example, Li employed Ag₂CO₃ as a stoichiometric oxidant for the synthesis of pyridones and isoquinolones.^{73g,h} Additionally, Fagnou and Stuart have used a catalytic amount of Cu(OAc)₂ with oxygen as a terminal oxidant.^{72b}

Table 3.2 Overview of Reaction Conditions for Various Rh(III)-Catalyzed Heterocycle Syntheses

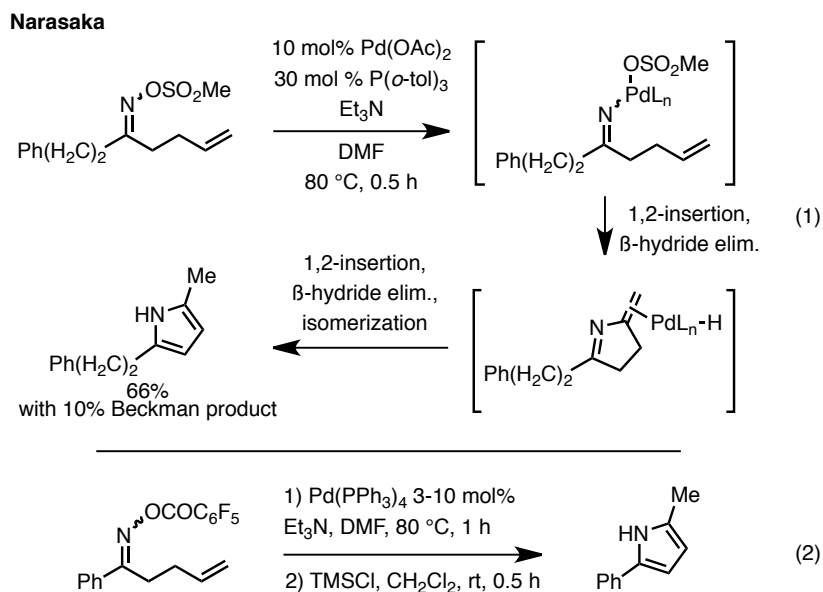
					
Temperature	80-130 °C	110-115 °C	80-120 °C	60-120°C	rt-120 °C
Rh(III) loading	2-4 mol%	4-8 mol%	1-8 mol%	4-5 mol%	5 mol%
Oxidant	Cu(OAc) ₂	Cu(OAc) ₂ or Ag ₂ CO ₃	Cu(OAc) ₂ or Ag ₂ CO ₃	Cu(OAc) ₂ or Cu(OAc) ₂ /O ₂	Cu(OAc) ₂ or Cu(OAc) ₂ /O ₂

Remaining Challenges. Prior to the work that will be presented in this section, a few important limitations remained in the Rh(III)-catalyzed synthesis of nitrogen-containing heterocycles. First of all, with the exception of the latest pyrrole synthesis^{72b} where a TMS substituted alkyne can be used as a terminal alkyne surrogate, all methods developed thus far provide disubstituted heterocycles. This is due to the intolerance for terminal alkynes under the typical reaction conditions. The establishment of a strategy allowing the coupling of terminal alkynes or acetylene is needed to increase the applicability of these Rh(III)-catalyzed heterocycle syntheses. Moreover, even though it was demonstrated that conditions with low temperatures and low catalyst loadings (≤ 1 mol%) could be used, no general method that combines these two characteristics has been developed. The realization of this challenge would enable future large-scale applications of this chemistry. Finally, unsaturated heterocycles have not been made from alkenes instead of alkynes as coupling partners. This development would considerably broaden the scope of accessible heterocycles.

3.1.2 N–O Bond as Oxidant in Transition Metal Catalysis

Since the first direct observation of oxidative addition into the N–O bond of an oxime,⁷⁶ the chemistry of this specific moiety toward transition metals has only been scarcely explored.

⁷⁶ Ferreira, C. M. P.; Guedes da Silva, M. F. C.; Kukushkin, V. Y.; Fraústo da Silva, J. J. R.; Pombeiro, A. J. L. *J. Chem. Soc., Dalton Trans.* **1998**, 325.

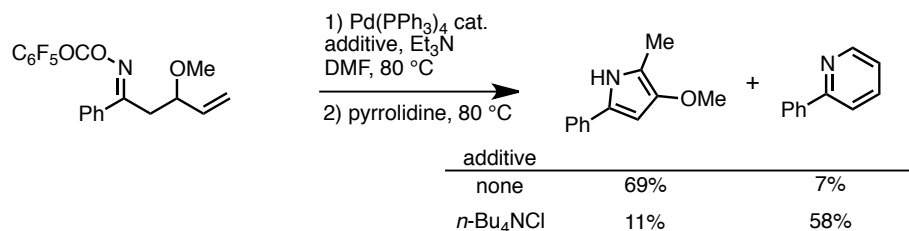


Scheme 3.2 Palladium-Catalyzed Amino-Heck Reactions

The Narasaka group was the first to investigate this reactivity in the context of catalysis.⁷⁷ They initially discovered that the intermediate resulting from the oxidative addition of palladium into the N–O bond of an oxime derivative could undergo intramolecular Heck-type reactions (Scheme 3.2). After isomerization, pyrrole derivatives could be obtained. Starting from methanesulfonyloximes, by-products arising from a Beckman rearrangement were also obtained. (Scheme 3.2, Eq. 1) In order to suppress this undesired pathway, different *O*-protecting groups were explored. It was found that the use of an *O*-pentafluorobenzoyloxime was optimal for the reaction (Scheme 3.2, Eq. 2). Following the intramolecular amino-Heck reaction, a TMSCl-mediated isomerization was typically performed to obtain the desired pyrrole. This method was also successfully employed for the formation of pyridine or isoquinoline derivatives. As outlined in Scheme 3.3, starting from an γ,δ -unsaturated ketoxime bearing a β -methoxy group, pyridine compounds could be

⁷⁷ For reviews, see: (a) Narasaka, K. *Pure Appl. Chem.* **2002**, *74*, 143. (b) Kitamura, M.; Narasaka, K. *Chem. Rec.* **2002**, *2*, 268. (c) Narasaka, K.; Kitamura, M. *Eur. J. Org. Chem.* **2005**, 4505.

obtained in good yields via a 6-*endo* cyclization using slightly different conditions. Of note, the chlorine atoms were crucial for the selective formation of pyridine over pyrrole compounds.⁷⁸

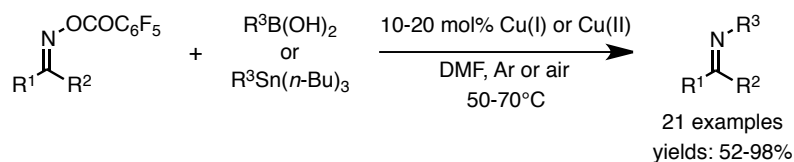


Scheme 3.3 Isoquinoline Derivatives Via Palladium-Catalyzed Amino-Heck Reaction

More recently, Liebeskind developed a copper-catalyzed amination of boronic acids and organostannanes where the N–O bond contained in the oxime substrate acts as an internal oxidant.⁷⁹ This reaction is similar to standard transition metal-catalyzed C–C cross coupling reactions, but instead of having an aryl halide as oxidant and coupling partner, an *O*-acyl oxime is employed (Scheme 3.4). Analogously to the previous work done by Narasaka, Liebeskind found that *O*-pentafluorobenzoyl oximes provide the best yields for this type of reaction.

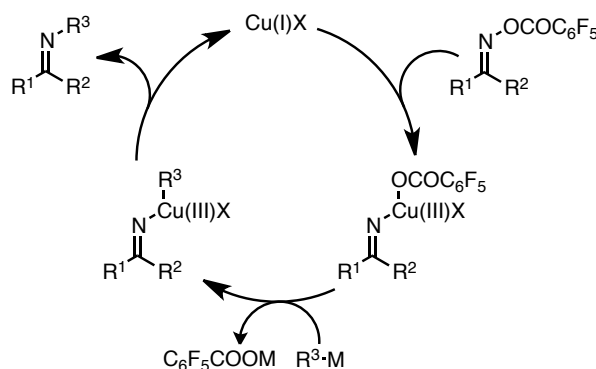
⁷⁸ A rationale for this particular chlorine atom effect has not been provided. Beneficial effect was however observed in other Heck cross-coupling reactions. See: Merlic, C. A.; Semmelhack, M. F. *J. Organomet. Chem.* **1990**, *391*, C23.

⁷⁹ (a) Liu, S.; Yu, Y.; Liebeskind, L. S. *Org. Lett.* **2007**, *9*, 1947. (b) For the use of this strategy applied to the synthesis of pyridines, see: (b) Liu, S.; Liebeskind, L. S. *J. Am. Chem. Soc.* **2008**, *130*, 6918.

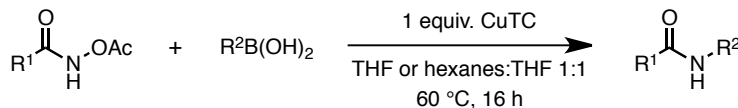
Liebeskind 2007

R¹, R² = aryl, heteroaryl, alkyl

R³ = aryl, alkenyl for B; aryl, heteroaryl and alkenyl for Sn

**Scheme 3.4** Liebeskind *N*-Imination of Organometallic Species

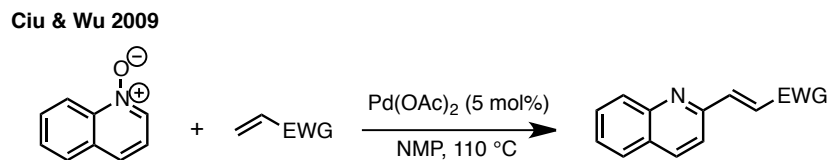
The mechanism proposed for this transformation is depicted in Scheme 3.4. Starting from a Cu(I) species, oxidative addition into the N–O bond gives a Cu(III) intermediate. From this point, transmetalation can take place followed by reductive elimination, which returns the catalyst to its initial oxidation state and yields the desired coupling product. Liebeskind was later able to use the N–O bond contained in a hydroxamic acid moiety to perform similar cross-couplings. These amidation reactions however need stoichiometric amounts of copper (Scheme 3.5). The authors speculated that this lack of turnover was due to a very sluggish transmetalation step.⁸⁰



⁸⁰ It was proposed that this slow transmetalation step is due to the formation of weakly electrophilic dimeric copper amido species. When *N*-substituted hydroxamic acids are employed, N–O bond cleavage occurs, but no cross-coupling is observed.

Scheme 3.5 Copper-Mediated Amidation Reaction From Hydroxamic Acid Derivatives

In the context of transition metal-catalyzed C–H functionalization, Cui and Wu were the first to demonstrate the multiple uses of an N–O bond as both an inductive platform *and* an oxidant (Scheme 3.6).⁸¹ Starting from quinoline *N*-oxides, they were able to perform a direct alkenylation reaction without the need for external oxidants. Even though the mechanism of this transformation has not been subjected to intensive investigation, it has set the stage for the use of an N–O bond as an internal oxidant in transition metal-catalyzed C–H functionalization processes. Of note, as opposed to the previously highlighted uses of N–O bonds, the *N*-oxide moiety in this case is not employed to initiate the process, but rather to re-oxidize the palladium(0) species after the Heck coupling.



Scheme 3.6 Use of N–O bond as Oxidant in a C–H Alkenylation Reaction

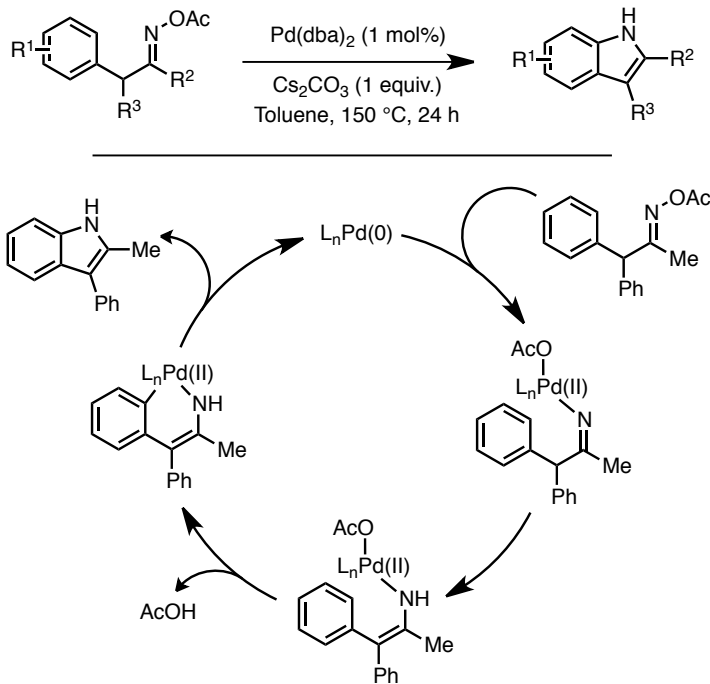
In 2010, Tan & Hartwig developed a method to prepare indoles starting from the oxime acetate derivative of 1,1'-diaryl ketones.⁸² This procedure featured both C–H bond functionalization and N–O bond oxidative addition reactions. Some mechanistic investigations were also performed, leading to the proposed a catalytic cycle outlined in Scheme 3.7. Oxidative addition of palladium(0) into the N–O bond initiates the reaction. The Pd(II) intermediate thus generated undergoes isomerization followed by arene palladation. Reductive elimination then yields the indole product along with the initial Pd(0) catalyst. To support this mechanism, Hartwig isolated the intermediate that underwent oxidative addition.

⁸¹ Wu, J.; Cui, X.; Chen, L.; Jiang, G.; Wu, Y. *J. Am. Chem. Soc.* **2009**, *131*, 13888.

⁸² Tan, Y.; Hartwig, J. F. *J. Am. Chem. Soc.* **2010**, *132*, 3676.

The use of this intermediate as a catalyst in an indole formation reaction did promote turnover, which suggested that this isolated species is part of the operative catalytic cycle.

Hartwig 2010



Scheme 3.7 Palladium-Catalyzed Intramolecular Direct Amination Reaction

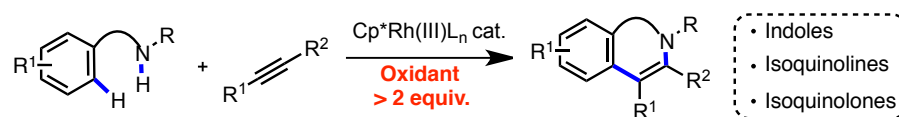
This reaction represented the first example of a non-nitrene⁸³ based redox-neutral intramolecular amination achieved from C(*sp*²)-H and N-O coupling partners. More recently, Yu developed an intermolecular variant of this reaction where aromatic substrates are aminated with pre-formed *O*-benzoylhydroxylamines using a Pd(II) catalyst.⁸⁴ While the exact mechanism of this transformation remains unclear, possible pathways include electrophilic amination and oxidative addition into the N-O bond. In this chapter, a

⁸³ For aromatic C-H bond amination via nitrenes, see: a) Diaz-Requejo, M. M.; Belderrain, T. R.; Nicasio, M. C.; Trofimenko, S.; Pérez, P. J. *J. Am. Chem. Soc.* **2003**, *125*, 12078. b) Thu, H.-Y.; Yu, W.-Y.; Che, C.-M. *J. Am. Chem. Soc.* **2006**, *128*, 9048. c) Li, Z.; Capretto, D. A.; Rahaman, R. O.; He, C. *J. Am. Chem. Soc.* **2007**, *129*, 12058. d) Stokes, B. J.; Dong, H.; Leslie, B. E.; Pumphrey, A. L.; Driver, T. G. *J. Am. Chem. Soc.* **2007**, *129*, 7500. e) Chiba, S.; Hattori, G.; Narasaka, K. *Chem. Lett.* **2007**, *36*, 52.

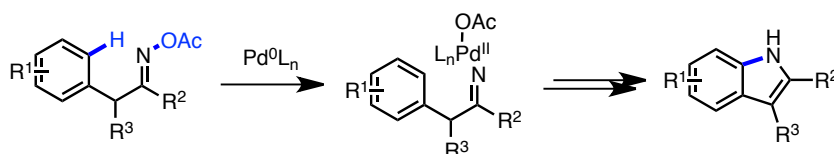
⁸⁴ Yoo, E. J.; Ma, S.; Mei, T.-S.; Chan, K. S. L.; Yu, J.-Q. *J. Am. Chem. Soc.* **2011**, *133*, 7652.

mechanistically distinct process that affords the isoquinolone motif⁸⁵ via Rh(III)-catalyzed annulation of benzhydroxamic acids with alkynes will be presented. This intermolecular external oxidant-free process strategically utilizes an N–O bond as an instrument for C–N bond formation and catalyst release. It therefore differs from oxidative processes as well as other reactions where N–O bond oxidative addition initiates the catalytic cycle (Figure 3.5).

Oxidative cross-coupling/cyclization strategy



Hartwig's indole formation



This work

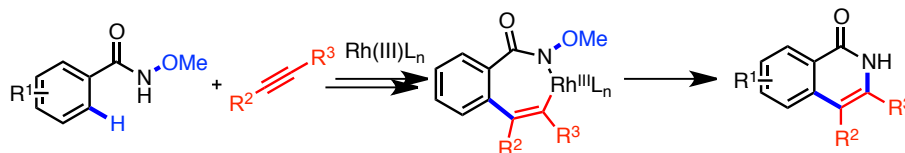


Figure 3.5 Strategies for heterocycle formation

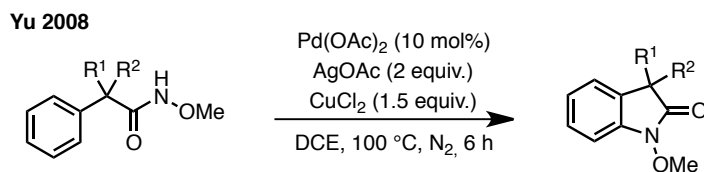
3.2 Results and Discussion

3.2.1 Initial Reaction Development and Scope

Pursuing our interest in heterocycle formation, we sought to use an oxidative coupling approach analogous to those previously discussed in this section to gain entry to different nitrogen-containing heterocycles. We postulated that the isoquinolone motif, which had not been reported yet, could be accessed using a benzamide-derived starting material.

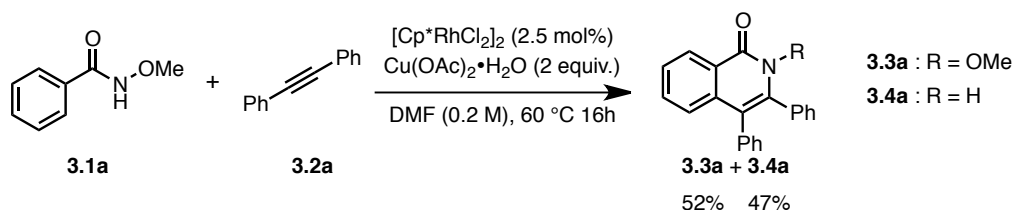
⁸⁵ For a review on recent isoquinolone syntheses, see: Glushkov, V. A.; Shklyayev, Y. V. *Chem. Heterocycl. Compd.* **2001**, *37*, 663.

Inspired by Yu's work on oxidative direct amination (Scheme 3.8),⁸⁶ we reasoned that benzhydroxamic acids could serve as a directing group for C–H functionalization⁸⁷ as well as predisposing the substrate toward C–N reductive elimination.



Scheme 3.8 Use of Hydroxamic Acids for Direct C–H Bond Amination

Initial attempts at the formation of isoquinolone **3.3a** resulted in product mixtures (Scheme 3.9). Interestingly, the major side-product (**3.4a**) of the reaction had undergone N–O bond cleavage.



Scheme 3.9 Initial Result Using Oxidative Conditions

Considering that an additional synthetic step is usually required to achieve this reduction,⁸⁶ we decided to further explore this direct transformation to obtain **3.4a** in one step. One of our first hypotheses to account for the formation of **3.4a** was based on a Rh(I)/Rh(III) catalytic cycle (analogous to the system of Hartwig, see scheme 3.7) initiated by an oxidative addition into an N–O bond. The catalytic cycle that describes this hypothesis is depicted in Figure 3.6. The active Rh(I) species could be generated by a first catalytic cycle involving C–N bond reductive elimination, which would afford one equivalent of **3.3a**.

⁸⁶ Wasa, M.; Yu, J.-Q. *J. Am. Chem. Soc.* **2008**, *130*, 14058.

⁸⁷ Wang, D.-H.; Wasa, M.; Giri, R.; Yu, J.-Q. *J. Am. Chem. Soc.* **2008**, *130*, 7190.

This Rh(I) complex could then undergo oxidative addition into the N–O bond of another substrate to afford a Rh(III) amidate intermediate, which could then undergo arene rhodation. Alkyne insertion would then take place followed by C–N reductive elimination to regenerate the Rh(I) species.

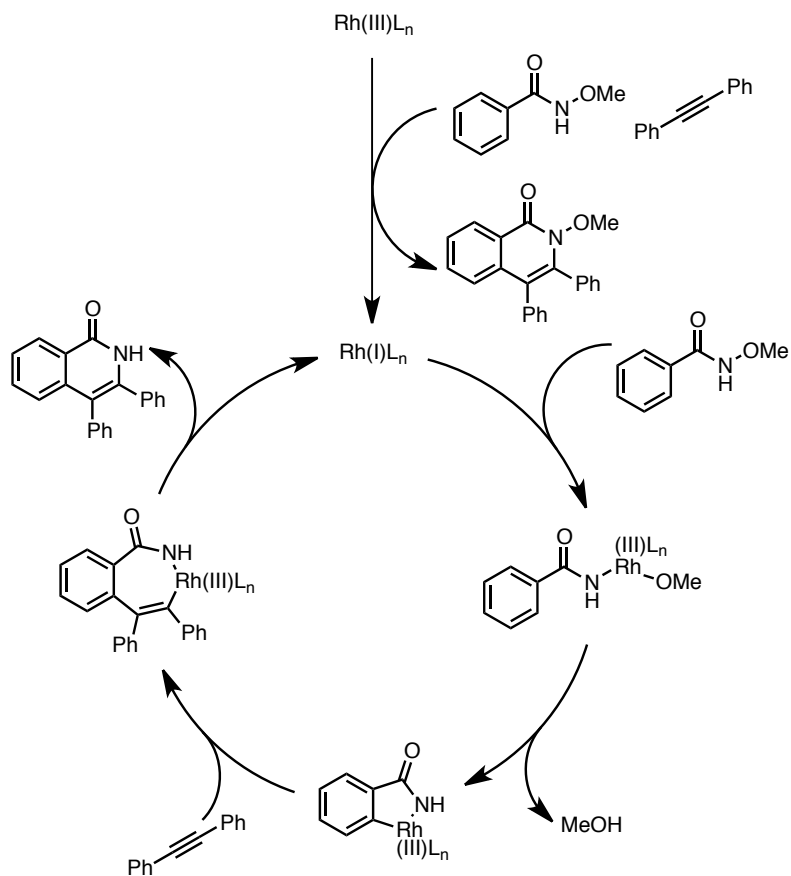
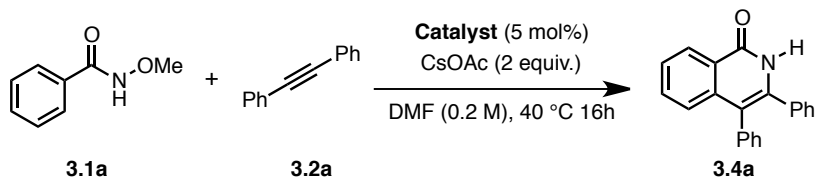


Figure 3.6 Mechanistic hypothesis for potential Rh(I)-catalyzed isoquinolone synthesis

To verify whether this pathway could account for the formation of compound **3.4a**, several experiments were conducted. First, a screening of Rh(I) catalysts in the absence of added copper(II) oxidant was performed to see if other monovalent rhodium species could afford the desired product. CsOAc was added as a base to mimic the effect of Cu(OAc)₂, but without oxidative properties. Results of this screen are shown in Table 3.3.

Table 3.3 Screening of Rh(I) Catalysts^a

Entry	Catalyst	¹ H NMR Yield (%)
1	Rh(COD)Cl	0
2	Rh(PPh ₃)Cl	0
3	Cp*Rh(CO) ₂	15
4	Cp*Rh(CO) ₂ + Me ₃ NO	8

^aConditions: **3.1a** (1 equiv.), **3.2a** (1.1 equiv), Catalyst (5 mol%), CsOAc (2 equiv.), DMF (0.2 M), 40 °C, 16 h.

The only catalysts that provided the desired product are based on a Cp*RhL_n motif. In the case of entry 4, trimethylamine *N*-oxide was employed to scavenge the carbon monoxide ligands. The results obtained from this screen suggest that a catalytic cycle based on Rh(I) is improbable. The small yields obtained in entries 3 and 4 are likely due to the presence of small amounts of Rh(III) contaminant present in our Rh(I) catalyst, as it is an air sensitive complex.⁸⁸ To further validate that the proposed Rh(I) hypothesis was not operative, a reaction using a Rh(III) catalyst in the absence of copper additive was studied by ¹H NMR. In a case where the reaction would proceed as shown in the catalytic cycle in Figure 3.3, a fast formation of ~5% of product **3.3a** should be observed at the beginning of the reaction, which would provide the necessary Rh(I) species that can account for the formation of **3.4a**. As shown in Figure 3.7, product **3.3a** is formed very slowly (0% yield until 130 min) and well after **3.4a** begins to be formed.⁸⁹ Again, this goes against the Rh(I)-catalyzed reaction hypothesis.

⁸⁸ If the reaction is redox-neutral and catalyzed by Rh(III), trace amounts of Rh(III) present in the pre-catalyst can account for the production of larger quantities of **3.4a**, as observed in entries 3 and 4.

⁸⁹ This experiment was conducted in MeOH instead of DMF. This explains the lower amount of **3.3a** observed after a 350 min

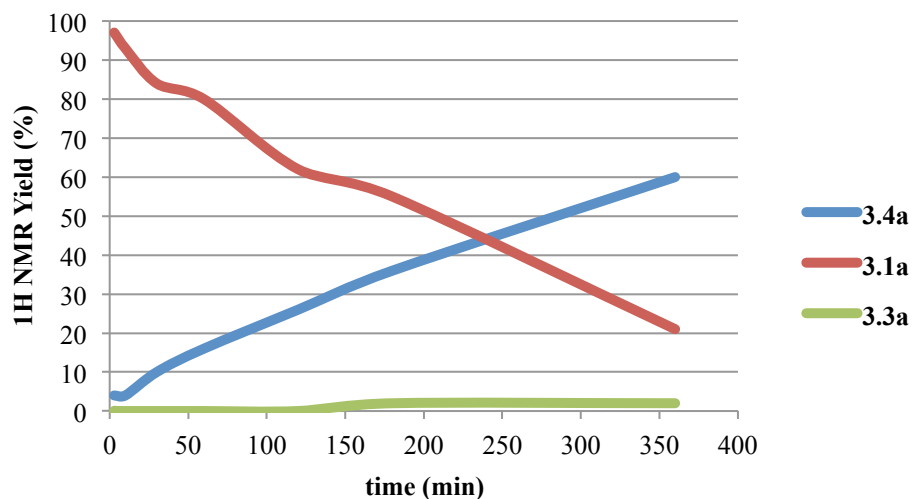
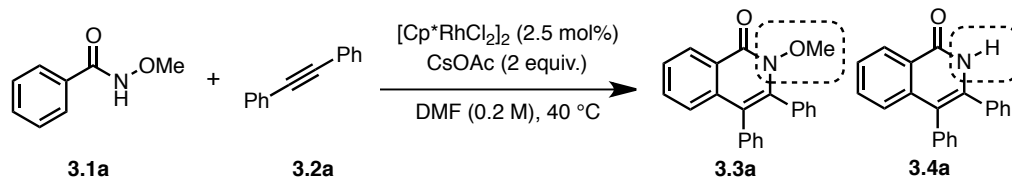
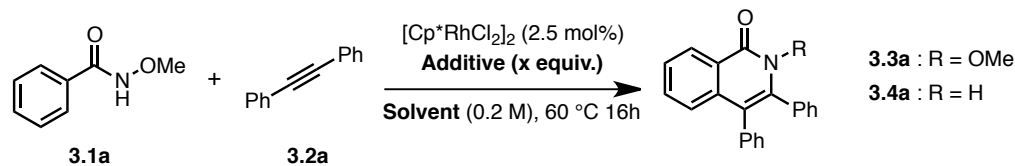


Figure 3.7 Monitoring of the reaction of **3.1a** with **3.2a**. Conditions: **3.1a** (1 equiv.), **3.2a** (1.1 equiv), $[\text{Cp}^*\text{RhCl}_2]_2$ (2.5 mol%), CsOAc (2 equiv.), MeOH (0.2 M), 40 °C.

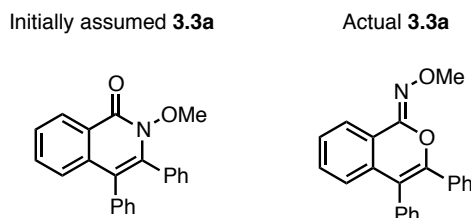
These interesting results seem to indicate that the formation of **3.4a** is catalyzed by a Rh(III) species and that the transformation is overall redox-neutral. We therefore focused our following efforts to find conditions that would promote this Rh(III)-catalyzed reaction. We thus replaced $\text{Cu}(\text{OAc})_2 \cdot \text{H}_2\text{O}$ by CsOAc. Doing so, the ratio of **3.3a**:**3.4a** went from 1.1:1 to 1:20 (Table 3.4, entry 2), albeit with a lower yield of 38%. A screen of solvents then revealed that methanol could provide a high yield of **3.4a** (Table 3.4, entry 3) while keeping the same product ratio. Finally, we were able to reduce the base loading to 30 mol% without any loss in yield (Table 3.4, entry 4). The scope of this reaction was thus ready to be further explored.

Table 3.4 Selected Observations During Reaction Development^a

Entry	Solvent	Additive (equiv.)	¹ H NMR yield (3.3a + 3.4a)	¹ H NMR ratio 3.3a:3.4a
1	DMF	Cu(OAc) ₂ •H ₂ O (2)	89	1.1:1
2	DMF	CsOAc (2)	38	1:20
3	MeOH	CsOAc (2)	97 (92) ^b	1:20
4	MeOH	CsOAc (0.3)	97 (90) ^b	1:20

^a 3.1a (1 equiv.), 3.2a (1.1 equiv.), [Cp*RhCl₂]₂ (2.5 mol%), additive (x equiv.), solvent (0.2 M), 60 °C, 16 h. ^b Isolated yield

It is worth mentioning that two years after reporting this chemistry, Huang *et al.*⁹⁰ showed that product **3.3a** was not the isoquinolone that underwent a C–N bond reductive elimination, but rather the heterocycle resulting from a C–O bond reductive elimination (Figure 3.8). Although this constitutes a valuable piece of information which could have been insightful earlier in the reaction development, it does not change the outcome of this study as we decided to concentrate our efforts toward the production of the isoquinolone **3.4a**, which underwent N–O bond cleavage.

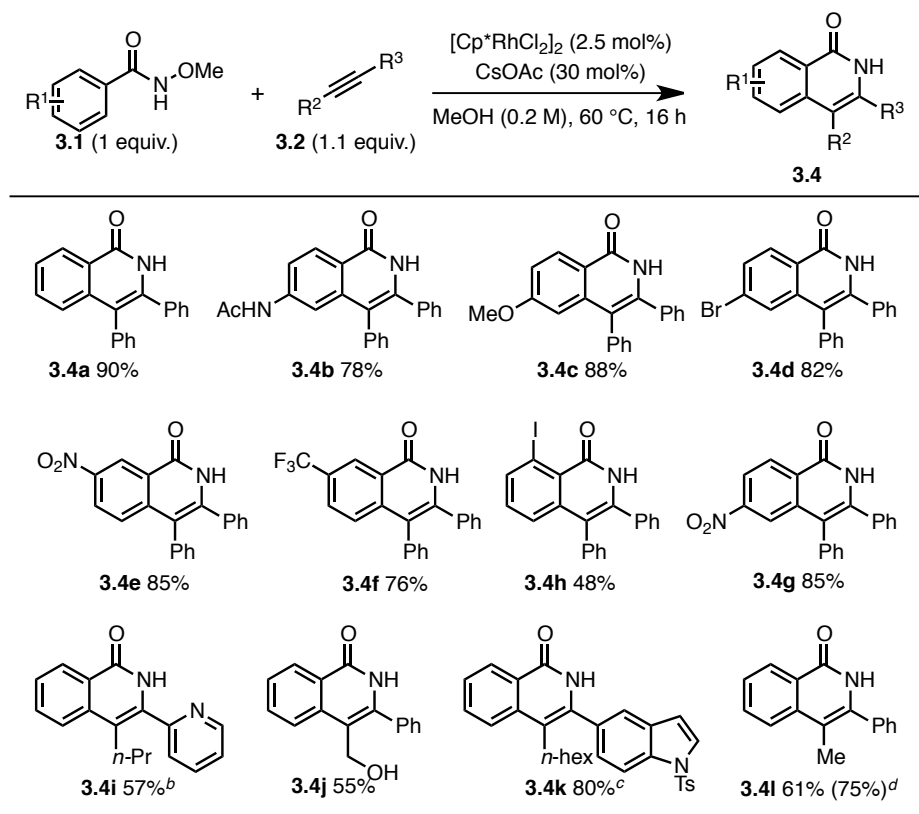
**Figure 3.8** Revised structure of **3.3a**

With a good set of conditions in hand, the scope of isoquinolone formation was demonstrated (with the help of Christina Gouliaras) with a variety of substituted

⁹⁰ Zhong, H.; Yang, D.; Wang, S.; Huang, J. *Chem. Commun.* **2012**, *48*, 3236.

benzhydroxamic acids. As shown in Table 3.5, the reaction provides the desired isoquinolones regardless of the electron donating or withdrawing character of the benzhydroxamic acid substituents. Additionally, when *meta*-substituted benzhydroxamic acids are used, arene rhodation occurs at the less hindered site, providing exclusively the C-7 substituted regioisomer (**3.4e**, **3.4f**). Also, both symmetrical and unsymmetrical alkynes are tolerated as coupling partners.⁹¹ Moreover, the insertion of an aryl-alkyl disubstituted alkyne occurs regioselectively with the *sp*² center being installed at the 3-position. Of note, these mild and copper free conditions allow an alkyne bearing a pyridyl group (**3.4i**) to undergo the isoquinolone formation albeit requiring slightly more forcing conditions (100 °C, 40 h).

Table 3.5 Reaction Scope^a

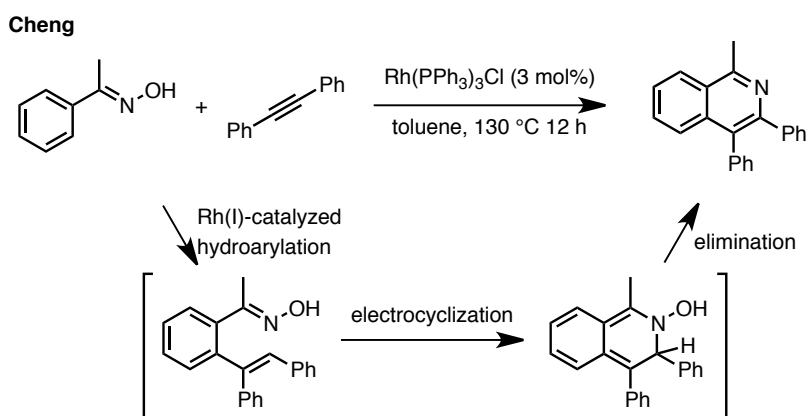


^a Isolated yields. ^b Reaction conducted in a sealed tube at 100 °C for 40 h. ^c Isolated as a 20:1 mixture of regioisomers. ^d 2 equiv. CsOAc used.

⁹¹ Under these reaction conditions, the use of terminal alkynes resulted in alkyne dimerization.

3.2.2 Preliminary Mechanistic Investigations

The absence of added oxidant and the loss of the *N*-methoxy substituent in the isoquinolone product prompted us to probe the mechanism of this redox neutral process. The first mechanistic hypothesis that was considered is analogous to the one that was proposed by Cheng for the formation of pyridines and isoquinolines via a hydroarylation/electrocyclization/elimination sequence (Scheme 3.10).⁹²



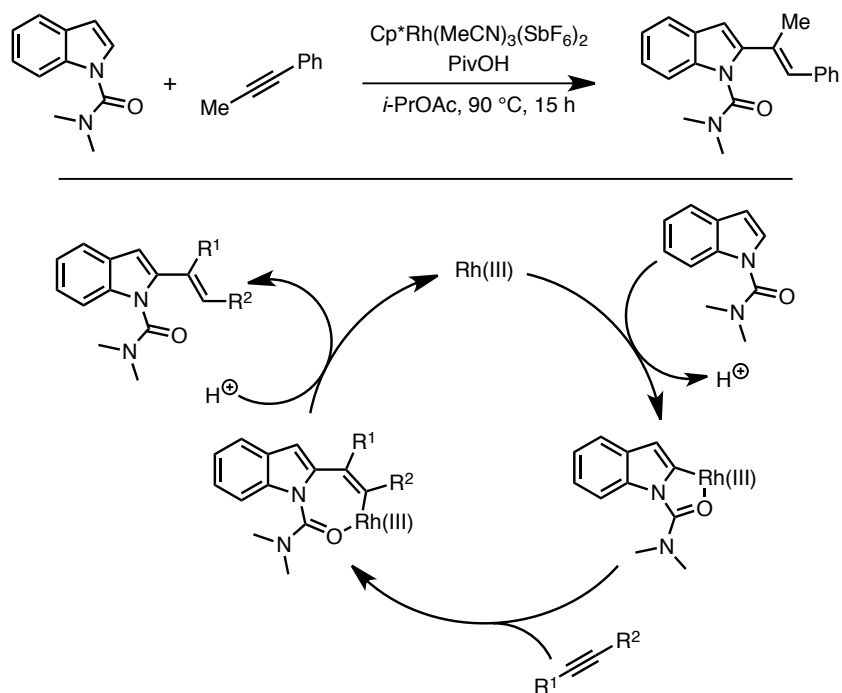
Scheme 3.10 Cheng Rh(I)-Catalyzed Isoquinoline Synthesis

As opposed to the system of Cheng, a rhodium(III) catalyst is required for our isoquinolone synthesis. Therefore, the hydroarylation that would yield the electrocyclization precursor would more likely operate through a different mechanism than the rhodium(I)-catalyzed analogous reaction (Scheme 3.11). This specific transformation was recently well described by our research group.⁹³

⁹² (a) Parthasarathy, K.; Cheng, C.-H. *J. Org. Chem.* **2009**, *74*, 9359. (b) Parthasarathy, K.; Jeganmohan, M.; Cheng, C.-H. *Org. Lett.* **2008**, *10*, 325. For oxidative heterocycle formation going through an hydroarylation/electrocyclization mechanism, see: (c) Colby, D. A.; Bergman, R. G.; Ellman, J. A. *J. Am. Chem. Soc.* **2008**, *130*, 3645. (d) Lim, S.-G.; Lee, J. H.; Moon, C. W.; Hong, J.-B.; Jun, C.-H. *Org. Lett.* **2003**, *5*, 2759.

⁹³ Schipper, D. J.; Hutchinson, M.; Fagnou, K. *J. Am. Chem. Soc.* **2010**, *132*, 6910.

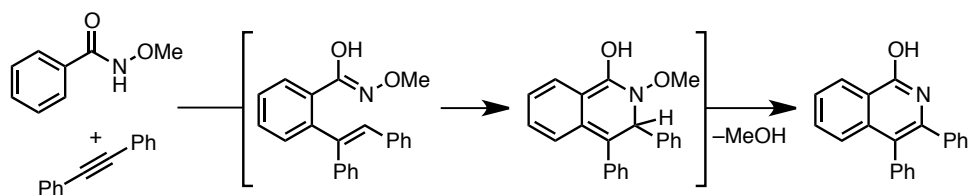
Fagnou & Schipper 2010



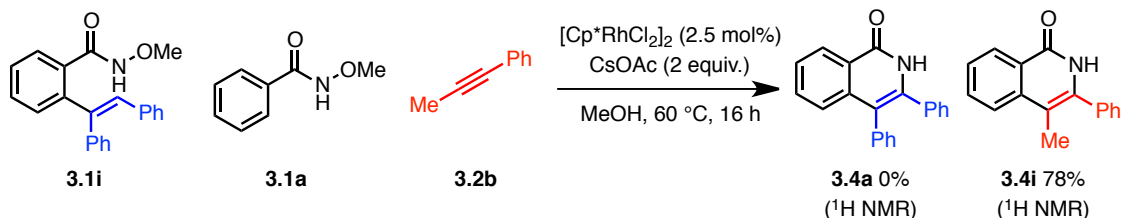
Scheme 3.11 Rh(III)-Catalyzed Hydroarylation

To verify whether this sequence could be operative for our isoquinolone synthesis, substrate **3.1i** was synthesized and reacted under the optimal reaction conditions along with substrates **3.1a** and **3.2b** (Scheme 3.12). From this experiment, no **3.3a** was obtained, which strongly suggests against this mechanistic hypothesis.

Mechanistic Hypothesis



Experimental Refutation



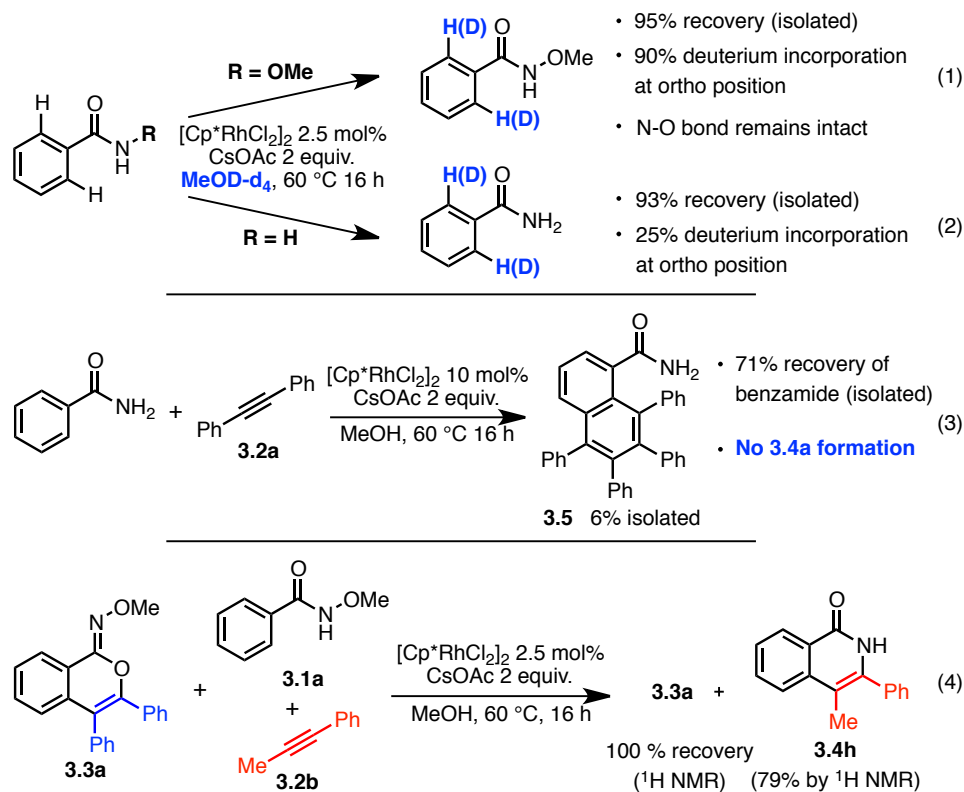
Scheme 3.12 Electrocyclization Hypothesis Verification

Considering these results, the intriguing role of the *N*-methoxy group was then evaluated by carrying out two experiments in deuterated methanol in the absence of alkyne, the first with **3.1a** as substrate and the second with benzamide. In both cases, deuterium was incorporated exclusively *ortho* to the directing group (Scheme 3.13, Eqs 1 and 2). In addition, no cleavage of the N–O bond was observed with **3.1a**. These results suggest that the first step of the mechanism is a reversible cyclometalation.⁹⁴ Also, the integrity of the *N*-methoxy group is inconsistent with a mechanism involving N–O bond oxidative addition prior to C–H bond cleavage as has previously been demonstrated in Hartwig’s palladium system.⁸² Next, a reaction starting from benzamide was run in the presence of **3.2a** and 20 mol% of Rh(III) (Scheme 3.13, Eq. 3). From this experiment, 71% of the starting material was recovered, along with 6% of the benzannulation product **3.5**.⁹⁵ No formation of isoquinolone **3.4a** was observed, signifying that the *N*-methoxy group is a prerequisite for C–N bond formation. Lastly, to determine whether the N–O bond acts as an oxidant for Rh(I)

⁹⁴ These results are consistent with Jones’ findings in related systems: a) Li, L.; Brennessel, W. W.; Jones, W. D. *Organometallics* **2009**, *28*, 3492. b) Li, L.; Brennessel, W. W.; Jones, W. D. *J. Am. Chem. Soc.* **2008**, *130*, 12414.

⁹⁵ Similar benzannulation reactions have been reported. For examples, see ref 68.

after C–N bond reductive elimination, **3.1a** and **3.2b** were reacted in the presence of **3.3a**. No cleavage of the N–O bond on substrate **3.3a** occurred (Scheme 3.13, Eq. 4), indicating that N–O bond cleavage happens intramolecularly with the substrate on which C–N bond formation occurs.



Scheme 3.13 Preliminary Mechanistic Insights

Based on these results, our postulated mechanism is presented in Figure 3.9. The mechanistic information revealed above is consistent with the first step being a reversible arene rhodation providing **3.6**. The alkyne can then undergo an insertion into the Rh–C bond, forming intermediate **3.7**. At this point, a concerted or stepwise C–N bond forming/N–O bond cleaving event can occur, affording the desired isoquinolone and releasing the catalyst. Computational and more experimental studies should help to further establish the nature of the last step of the catalytic cycle.

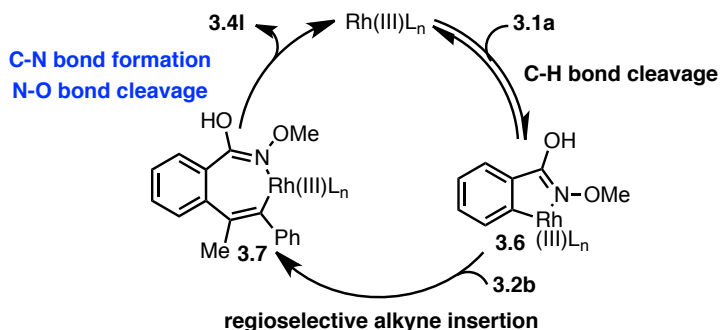


Figure 3.9 Initially proposed catalytic cycle

3.2.3 Internal Oxidant Modification

The results described above were the object of our initial report on the preparation of isoquinolones from benzamide-type starting materials.^{96,97} Since this isoquinolone synthesis does not require copper additives, we surmised that further development of the method could address some of the alkyne related limitations previously mentioned. This section will describe (1) the optimization of the internal oxidant/directing group that leads to the discovery of increased reactivity, which allows heterocycle formation to be performed at room temperature using low catalyst loading, (2) the expanded scope of the reaction which now enables the use of terminal alkynes and alkenes, the former yielding monosubstituted isoquinolones and the latter giving saturated heterocycles while furnishing C(*sp*³)-N bonds,⁹⁸ (3) computational and experimental studies which reveal important insights about the mechanism of the redox-neutral rhodium-catalyzed isoquinolone formation and (4) the application of these findings to the synthesis of isoquinolines.⁹⁹

⁹⁶ Guimond, N.; Gouliaras, C.; Fagnou, K. *J. Am. Chem. Soc.* **2010**, *130*, 6908.

⁹⁷ For a highlight, see: Patureau, F. W.; Glorius, F. *Angew. Chem., Int. Ed.* **2011**, *50*, 1977.

⁹⁸ During the preparation of the manuscript that relates to this section, Glorius reported similar results: Rakshit, S.; Grohmann, C.; Besset, T.; Glorius, F. *J. Am. Chem. Soc.* **2011**, *133*, 2350.

⁹⁹ Guimond, N.; Gorelsky, S. I.; Fagnou, K. *J. Am. Chem. Soc.* **2011**, *133*, 6449.

Although our previous discussion on the synthesis of isoquinolones from the coupling of *N*-methoxybenzamide with alkyne featured very mild conditions, we questioned whether it would be possible to achieve even better reactivity by modifying the nature of the built-in oxidant. We reasoned that using hydroxamic acids bearing better leaving groups, or groups that could better stabilize intermediates of the catalytic cycle (Figure 3.10), would be beneficial to the reaction.

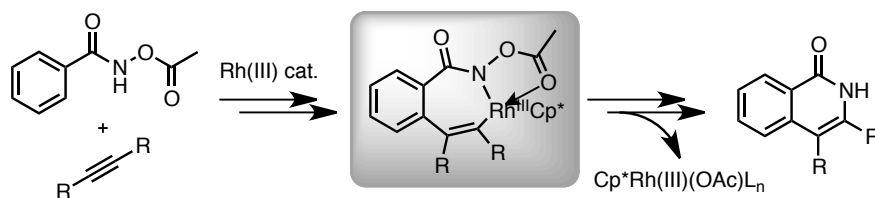
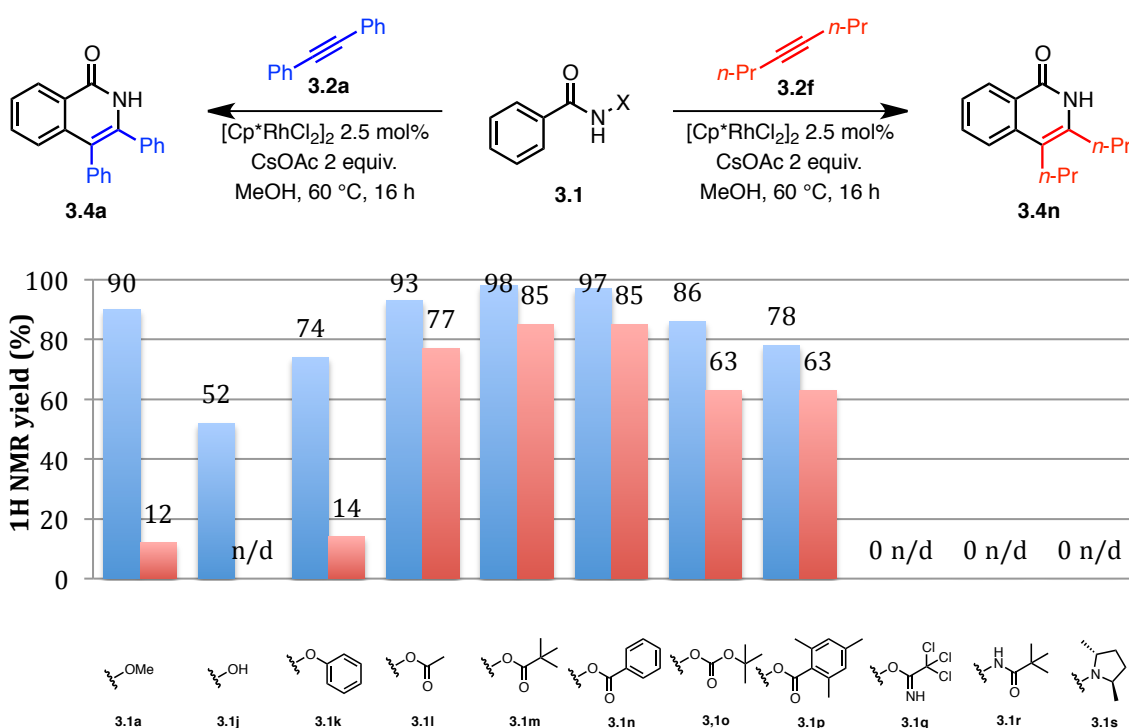


Figure 3.10 Proposed stabilized intermediate in the catalytic cycle

With that mind set, a variety of hydroxamic acid-type substrates were synthesized, each one having a different leaving group on the nitrogen atom. Since the reaction was known to be more challenging with internal alkynes substituted with two alkyl groups, substrate optimization was performed using both diaryl-substituted and dialkyl-substituted alkynes (Table 3.6). Being uncertain about the nature of the C–N bond forming/N–O bond cleaving process, we first surveyed built-in oxidants that have very similar leaving group ability as our original directing group. However, no yield improvement was observed with the hydroxy (**3.1j**) or the phenoxy (**3.1k**) groups. We then synthesized a variety of carboxylate-type internal oxidants. Such substrates provided a major yield improvement when using 4-octyne (**3.2f**). Both the pivalate (**3.1m**) and the benzoate (**3.1n**) gave an almost quantitative yield with **3.2a** and 85% yield using **3.2f**. A carbonate (**3.1o**) and a highly hindered mesityl (**3.1p**) leaving groups also gave good yields with **3.2a** and **3.2f**. This increased reactivity could potentially be due to the better leaving group ability of the acetate

or to an interaction of the carbonyl's oxygen lone pair with the rhodium catalyst (Figure 3.10). It is believed that the N–O bond cleaving/C–N bond forming step might be facilitated by such interactions. Following this idea, substrate **3.1q** was synthesized in order to have the trichloroacetimide's nitrogen to act as an even stronger intramolecular sigma donor for rhodium(III). However, no isoquinolone was observed when this substrate was used as starting material. Nitrogen leaving groups were also tested (**3.1r**, **3.1s**), yet were unsuccessful presumably due to the stronger N–N bonds in these moieties. Given these results, the pivaloyl group was selected for further reaction development.

Table 3.6 Internal Oxidant Optimization^{a,b}

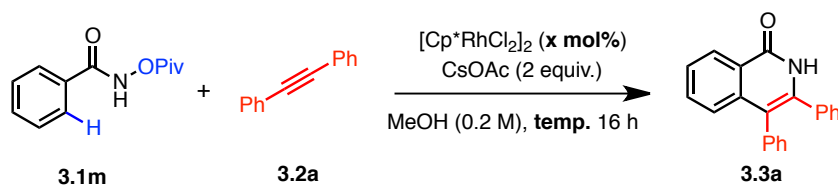


^aConditions: **3.1** (1 equiv., 0.2 mmol), **3.2a** or **3.2f** (1.1 equiv., 0.22 mmol), CsOAc (2 equiv., 0.4 mmol), [Cp*RhCl₂]₂ (2.5 mol%), MeOH (0.2 M), 60 °C, 16 h. ^b¹H NMR yield vs 1,3,5-trimethoxybenzene as internal standard.

Next, we sought to evaluate the improved reactivity provided by the new internal oxidant (Table 3.7). It was found that, while keeping the temperature at 60 °C, the catalyst loading could be reduced to 1 mol% Rh(III) without impacting the yield (Table 3.7, entry 2).

However, lowering the Rh(III) content to 0.1 mol% decreased the yield considerably (Table 3.7, entry 3). We were then pleased to find that running the reaction at room temperature could also provide nearly quantitative yields while using only 0.5 mol% Rh(III) (Table 3.7, entry 5). Lowering the catalyst loading to 0.1 mol% at this temperature resulted in an incomplete reaction affording 61% ¹H NMR yield after 16 h. Finally, it is noteworthy that the isoquinolone synthesis can be performed on gram-scale using 0.5 mol% Rh(III) to afford the 3,4-diphenylisoquinolone in 96% isolated yield (Table 3.7, entry 7).

Table 3.7 Increased Reactivity Provided by the Pivalate Internal Oxidant.^a



Entry	Temperature (°C)	Catalyst Loading (mol%)	¹ H NMR Yield 3.3a (%) ^b
1	60	2.50	97
2	60	0.50	99
3	60	0.05	33
4	rt	2.50	99
5	rt	0.25	99
6	rt	0.05	61
7 ^c	rt	0.25	96 (isolated)

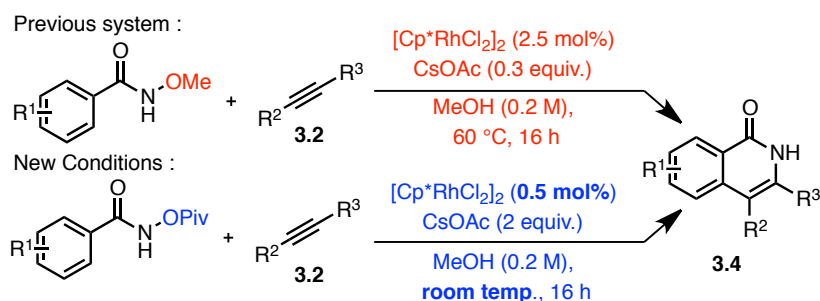
^aConditions: **3.1m** (1 equiv., 0.20 mmol), **3.2a** (1.1 equiv., 0.22 mmol), CsOAc (2 equiv., 0.40 mmol), [Cp*RhCl₂]₂ (x mol%), MeOH (0.2 M), specified temperature, 16h. ^b ¹H NMR yield vs 1,3,5-trimethoxybenzene as internal standard. ^c Reaction conducted on a 1.00 gram scale of **3.1m**.

3.2.4 Improved reaction scope

With the newly found optimal internal oxidant, a reinvestigation of the scope of the isoquinolone synthesis previously described was carried out. All the experiments were conducted with 0.5 mol% rhodium (III) dimer at room temperature. Table 3.8 presents the comparison of the previously reported conditions with the newly designed ones. With diaryl-substituted alkynes, yields remain high with both systems (Table 3.8, entries 1-3). The

electron withdrawing or donating character of the substituents on the hydroxamic acids does not seem to affect the outcome of the reaction. When a meta-substituted starting material is employed, the corresponding isoquinolone is obtained as a single regioisomer (Table 3.8, entry 4). Moreover, in contrast to the first generation system (N-OMe), the use of alkyl-aryl disubstituted alkynes gave high yields and high regioselectivity with the sp^2 center being installed at the 3-position of the heterocycle. Interestingly, a TMS-protected alkyne was also tolerated, which constitutes a useful handle for further functionalization (Table 3.8, entry 8). Additionally, while di-alkyl substituted alkynes were problematic with the previously reported conditions, they are now well suited using the pivaloyl group as internal oxidant. When unsymmetrical dialkyl-substituted alkynes are employed, the more sterically demanding group will typically be installed at the 4-position (Table 3.8, entry 9). This outcome is in agreement with the previous reports on rhodium-catalyzed heterocycle formation.

Table 3.8 Internal Alkyne Scope^{a,b}



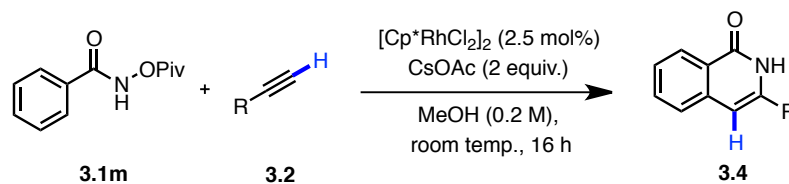
Entry	Substrate	Alkyne	Product	Red Conditions Yield (%)	Blue Conditions Yield (%)
1				90	96

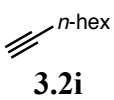
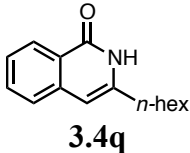
2				85	90
3				88	89
4				n/d	92
5				61	92
6				12 ^c	70
7				55	99
8				n/d	55
9				n/d	83

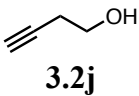
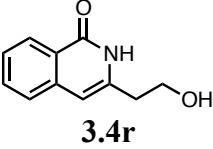
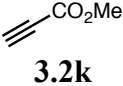
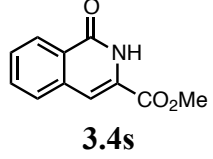

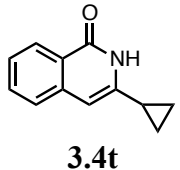
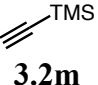
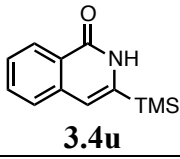
^aConditions: Previous system: **3.1m** (1 equiv., 0.20 mmol), **3.2** (1.1 equiv., 0.22 mmol), CsOAc (0.3 equiv., 0.06 mmol), [Cp**RhCl*₂]₂ (2.5 mol%), MeOH (0.2 M), 60 °C, 16 h. New system: **1e** (1 equiv., 0.20 mmol), **2** (1.1 equiv., 0.22 mmol), CsOAc (2 equiv., 0.40 mmol), [Cp**RhCl*₂]₂ (0.5 mol%), MeOH (0.2 M), room temp., 16 h. ^b Isolated yields are reported. ^c ¹H NMR yield vs 1,3,5-trimethoxybenzene as internal standard.

As mentioned earlier, an important limitation encountered with the recently developed rhodium-catalyzed oxidative synthesis of nitrogen-containing heterocycles is the inability to incorporate terminal alkynes. Their use has primarily lead to alkyne dimerization (Glaser coupling) due to the Cu(II) oxidant typically employed in these reactions. As a result, only disubstituted heterocycles have been synthesized using Rh(III)-catalyzed methods. With the newly designed copper-free conditions, a reinvestigation of this restraint was conducted. It was found that terminal alkynes were now tolerated and give the desired monosubstituted heterocycle in moderate to high yield. In addition, the regioselectivity of their insertion is highly predictable, with the terminal end being located at the 4-position. As shown in Table 3.9, with yields ranging from 85% to 95%, the reaction is compatible with alkyl-substituted terminal alkynes. Performing the heterocycle formation at 60°C also allowed for the formation of a 3-methylester monosubstituted isoquinolone (Table 3.9, entry 3). Moreover, we were pleased to observe that trimethylsilylacetylene is a suitable alkyne yielding an isoquinolone that can be subsequently functionalized (Table 3.9, entry 5). Phenylacetylene was also subjected to the reaction conditions, however none of the desired product was observed.

Table 3.9 Terminal Alkyne Scope^a



Entry	Alkyne	Product	Yield ^b (%)
1	 3.2i	 3.4q	92 ^c

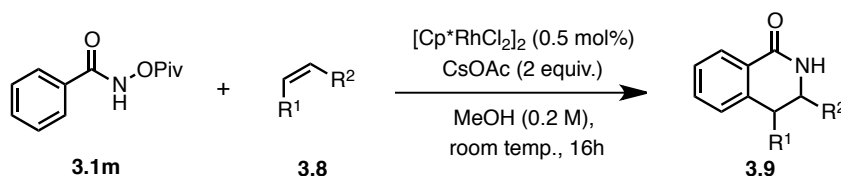
2	 3.2j	 3.4r	85 ^d
3	 3.2k	 3.4s	49 ^d
4	 3.2l	 3.4t	95
5	 3.2m	 3.4u	75

^aConditions: **3.1m** (1 equiv., 0.20 mmol), **3.2** (1.1 equiv., 0.22 mmol), CsOAc (2 equiv., 0.40 mmol), [Cp*RhCl₂]₂ (2.5 mol%), MeOH (0.2 M), room temperature, 16 h. ^bIsolated yields are reported. ^c0.5 mol% [Cp*RhCl₂]₂ was employed. ^dReaction ran at 60 °C.

With recent reports on oxidative olefinations using Cp*Rh(III)L_n as catalysts,⁶⁵ we were interested to investigate the use of alkenes under our new conditions to access the corresponding 3,4-dihydro heterocycle. The inherent challenge with this method is the formation of the C(*sp*³)-N bond while avoiding the well-documented β-hydride elimination which gives rise to Heck-type products. To do so, the C-N bond forming/N-O bond cleaving step must be lower in energy than β-hydride elimination. Considering the mild reaction conditions required for the isoquinolone synthesis, we presumed that the formation of the unsaturated heterocycle could occur preferentially. Indeed, it was found that alkenes do undergo insertion followed by C-N bond formation with no product arising from β-hydride elimination detectable (Table 3.10). Following the same trend as their alkyne counterparts, alkenes substituted with an *sp*² carbon center provide the 3,4-dihydroisoquinolone with the *sp*²-hybridized substituent generally located at the 3-position (Table 3.10, entry 1 and 2). With respect to *sp*³ substituted terminal alkenes, the products obtained were typically a

mixture of regioisomers which were separable by flash column chromatography (Table 3.10, entry 5, 6). A current limitation to the alkene scope is the poor reactivity of acyclic internal alkenes and unactivated cyclic alkenes. Both diarylsubstituted and dialkylsubstituted alkenes failed to react under our reaction conditions.¹⁰⁰ However, strained or activated cyclic substrates such as norbornadiene, 1,3-cyclohexadiene and 2,3-dihydrofuran were found to react readily providing tricyclic structures (Table 3.10, entry 2-4). Interestingly, the unsubstituted 3,4-dihydroisoquinolone can also be synthesized at ambient pressure and ambient temperature using a balloon of ethylene (Table 3.10, entry 8). It is of note that 3,4-dihydroisoquinolone **6c** can undergo a retro Diels-Alder reaction providing the unsubstituted isoquinolone **4f** in high yield (Scheme 3.14).¹⁰¹ The scope highlights the validity of the method to construct, in a minimal amount of steps, a wide variety isoquinolones having various substitution patterns while generating only pivalic acid as byproduct.


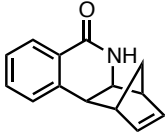
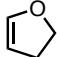
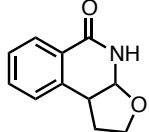
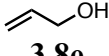
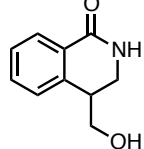
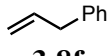
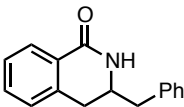
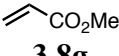
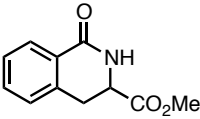
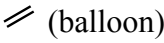
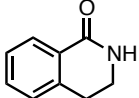
Table 3.10 Alkene Scope^a



Entry	Alkene	Product	Yield ^b (%)	Regioselectivity
1			90	>20:1
2			77	>20:1

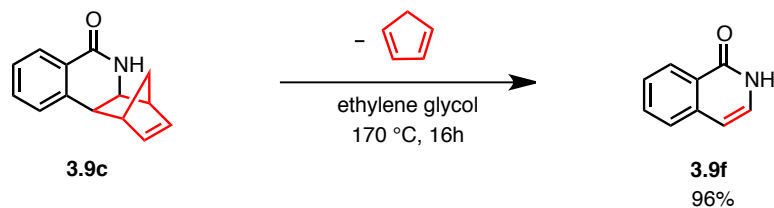
¹⁰⁰ *trans*-Stilbene, 3-hexene and cyclohexene failed to provide the desired 3,4-dihydroisoquinolone.

¹⁰¹ For similar examples of retro Diels-Alder, see: Thansandote, P.; Hulcoop, D. G.; Langer, M.; Lautens, M. *J. Org. Chem.* **2008**, *74*, 1673.

3	 3.8c	 3.9c	91	N/A
4	 3.8d	 3.9d	77	>20:1
5	 3.8e	 3.9e	85 ^c	1.3:1
6	 3.8f	 3.9f	85 ^c	2:1
7	 3.8g	 3.9g	95	1:4.5 ^d
8	 3.8h	 3.9h	95	N/A

^aConditions: **3.1m** (1.0 equiv., 0.20 mmol), **3.8** (1.1 equiv., 0.22 mmol), CsOAc (2.0 equiv., 0.40 mmol), [Cp*RhCl₂]₂ (0.5 mol%), MeOH (0.2 M), room temperature, 16 h. ^bIsolated yields are reported. ^cIsolated yield of both regioisomers. ^dUnseparable mixture of regioisomers.

Scheme 3. Access to Unsubstituted Isoquinolone via Retro Diels-Alder Reaction.



Scheme 3.14 Unsubstituted Isoquinolone Via Retro-Diels-Alder

3.2.5 Computational and experimental mechanistic investigations

The observed increase in reactivity provided by the *O*-pivaloylhydroxamic acid directing group/internal oxidant as well as the uncertain nature of the C–N bond forming/N–O bond cleaving step of the catalytic cycle prompted us to further investigate the mechanism of this transformation. We determined in our previous communications on the subject⁷¹ that the first step of the catalytic cycle was likely a reversible arene rhodation. We proposed that alkyne insertion was then occurring,¹⁰² which was followed by a concerted or stepwise C–N bond forming/N–O bond cleaving event. It was also demonstrated from cross-over experiments that the N–O bond cleavage happened in an intramolecular sense (Scheme 3.13). From this last piece of information, we reasoned that two mechanistic pathways could account for the last steps of the catalytic cycle (Figure 3.11). Pathway A consists of a concerted process where a highly organized six-membered cyclic transition state accounts for simultaneous C–N bond formation and N–O bond cleavage. The main characteristic of such a mechanism is that the Rh(III) catalyst remains at the +3 oxidation state throughout the entire catalytic cycle. Pathway B is a more common reductive elimination/oxidative addition process that would occur in a stepwise fashion. The C–N bond reductive elimination would yield an intermediate that would readily proceed to N–O bond oxidative addition. For such a mechanism to be operative and consistent with the experimental data, the oxidative addition would have to occur faster than decoordination of the substrate from the catalyst.

¹⁰² For studies of alkyne insertion with related cyclometalated substrates, see: (a) Ref. 94b (b) Boutadla, Y.; Davies, D. L.; Al-Duajji, O.; Fawcett, J.; Jones, R. C.; Singh, K. *Dalton Trans.* **2010**, 39, 10447.

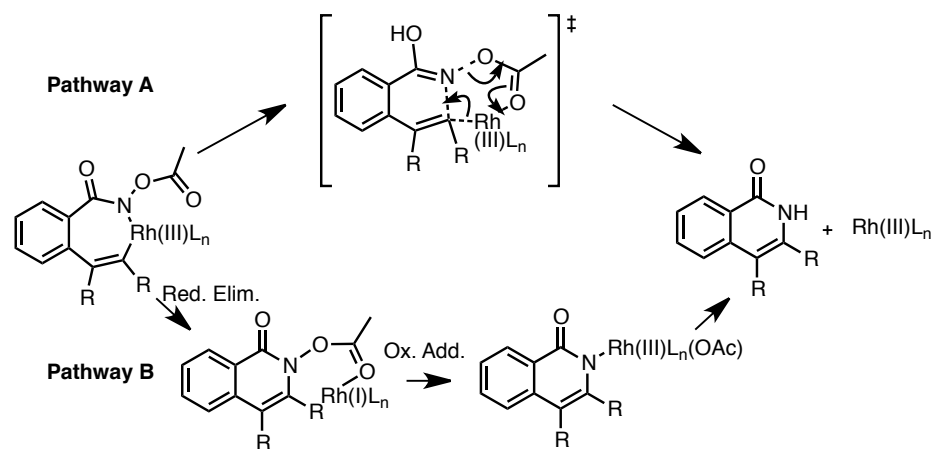
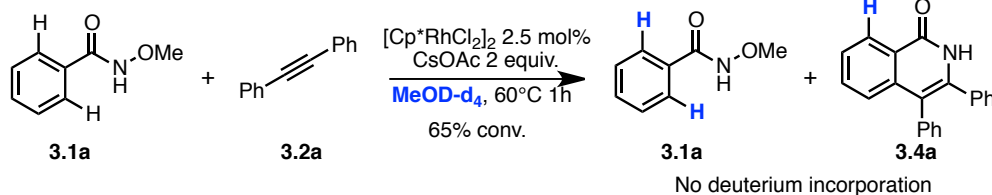


Figure 3.11 Mechanistic hypotheses for the C-N bond forming/N-O bond cleaving event.

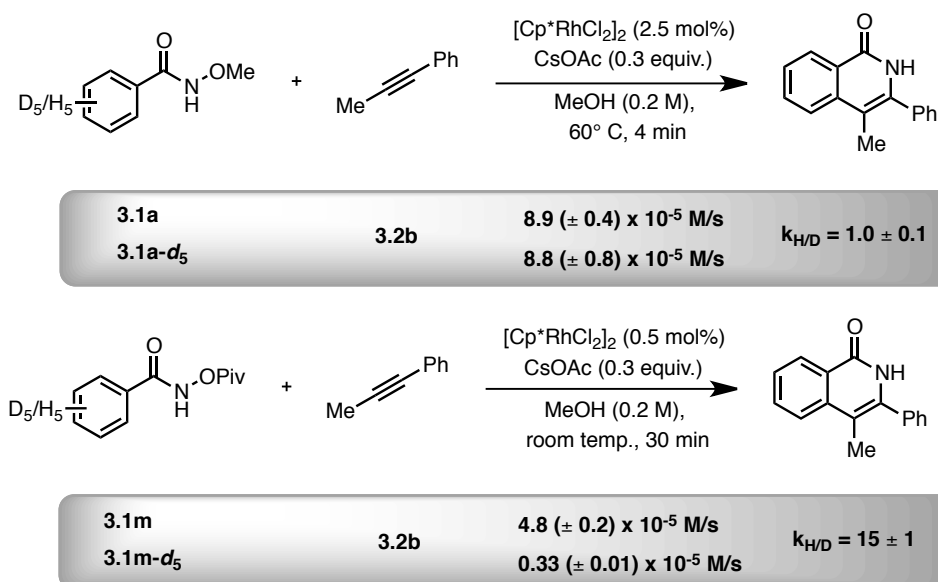
Drawing inspiration from the work of Rovis on a similar system,^{73e} a reaction was conducted to establish the reversibility of the cyclometalation in the presence of an alkyne (Scheme 3.15). Thus, the reaction of **3.1a** with **3.2a** using the standard reaction conditions in deuterated methanol was stopped before completion. Compounds **3.1a** and **3.4a** were isolated and their deuterium content was analyzed by ¹H NMR. With both recovered compounds, no deuterium incorporation was observed. This suggests that cyclometalation is irreversible in presence of **3.2a**.



Scheme 3.15 Irreversibility of Alkyne Insertion

From this point, we were intrigued to determine the turnover-limiting step of the catalytic cycle. Taking into account the new system's reactivity, it was also appropriate to determine whether the slow step is the same with both **3.1a** and **3.1m**. To do so, we

conducted deuterium kinetic isotope effect (DKIE) measurements by comparing the initial rates of both systems side by side. Scheme 3.16 summarizes the results of this study. No DKIE was observed with the *N*-methoxybenzamide substrate whereas a large primary DKIE of 15 ± 1 was found with **3.1m**. These results suggest that the nature of the rate-limiting step depends on the internal oxidant. With **3.1a**, the rate-limiting step remains uncertain whereas the use of **3.1m** renders the C–H bond cleavage to become rate-determining. The high DKIE of 15 ± 1 with **3.1e** can be explained by tunneling effects.¹⁰³

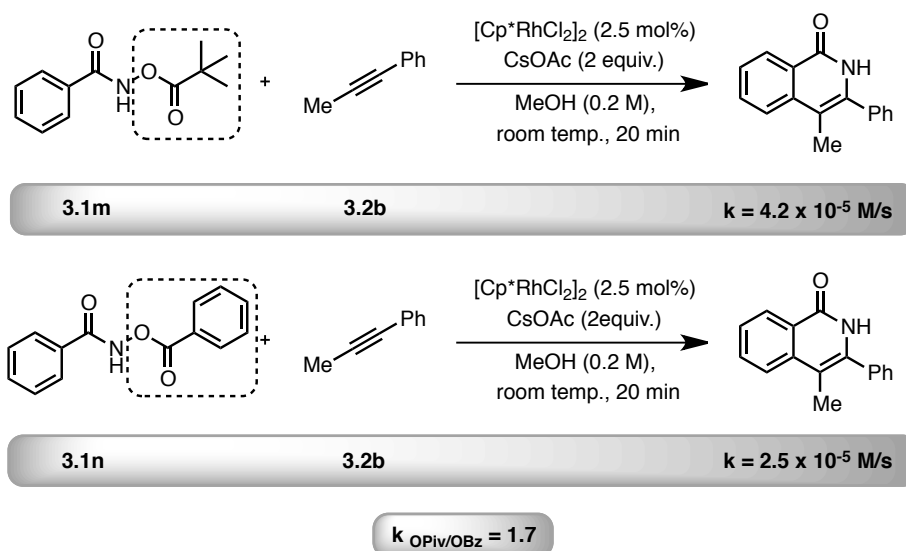


Scheme 3.16 DKIE Measurements

To corroborate this finding, a rate study of the reaction of **3.1m** and **3.1n** with **3.2b** using the new conditions was conducted (Scheme 3.17). It was found that while the leaving group ability of benzoate is greater than that of pivalate, the reaction occurred 1.7 times faster with the latter. If the N–O bond cleavage was the turnover-limiting step, one would expect the substituent with better leaving group ability to react faster. In this case, since the

¹⁰³ Garrett, B. C.; Truhlar, D. G., *J. Chem. Phys.* **1980**, *72*, 3460.

DKIE experiments suggest the slow step to be the C–H bond cleavage, it is reasonable to find the pivalate to be faster as it is most likely the stronger directing group.



Scheme 3.17 Rate Measurements for Substrates With a Different Internal Oxidant

In order to acquire a better understanding of the overall catalytic cycle, quantum chemical¹⁰⁴ density functional theory¹⁰⁵ (DFT) calculations were conducted for the reaction of substrate **3.11** (N-OAc) with acetylene using CpRh(OAc)₂ as catalyst. These chemical species were selected to simplify calculations while keeping the essential features of the catalytic cycle as accurate as possible. All computations were performed using the Hybrid B3LYP level functional^{106,107} with a TZVP¹⁰⁸ basis set for all atoms except rhodium, for which a DZVP¹⁰⁹ basis set was used. Gibbs free energy calculations were performed in both the gas phase and with a solvent correction for methanol at 298K (please refer to experimental section for full computational details). The goal of this exercise was to gain

¹⁰⁴ Ziegler, T.; Autschbach, I. *Chem. Rev.* **2005**, *105*, 2695.

¹⁰⁵ (a) Hohenberg, P.; Kohn, W. *Phys. Rev. B.* **1964**, *136*, 864. (b) Kohn, W.; Sham, L. *Phys. Chem. Rev. A*, **1965**, *140*, 1133.

¹⁰⁶ Lee, C.; Yang, W.; Parr, R. G. *Phys. Rev. B*, **1988**, *37*, 785.

¹⁰⁷ Becke, A. D. *J. Chem. Phys.* **1993**, *98*, 5648.

¹⁰⁸ Schafer, A.; Huber, C.; Ahlrichs, R. *J. Chem. Phys.* **1994**, *100*, 5829.

¹⁰⁹ Godbout, N.; Salahub, D. R.; Andzelm, J.; Wimmer, E. *Can. J. Chem.* **1992**, *70*, 560.

insight into the currently unknown nature of the C–N bond forming/N–O bond cleaving event. Scheme 3.19 shows the resultant catalytic cycle while Scheme 3.18 presents the relative Gibbs free energy for all the intermediates and transition states.

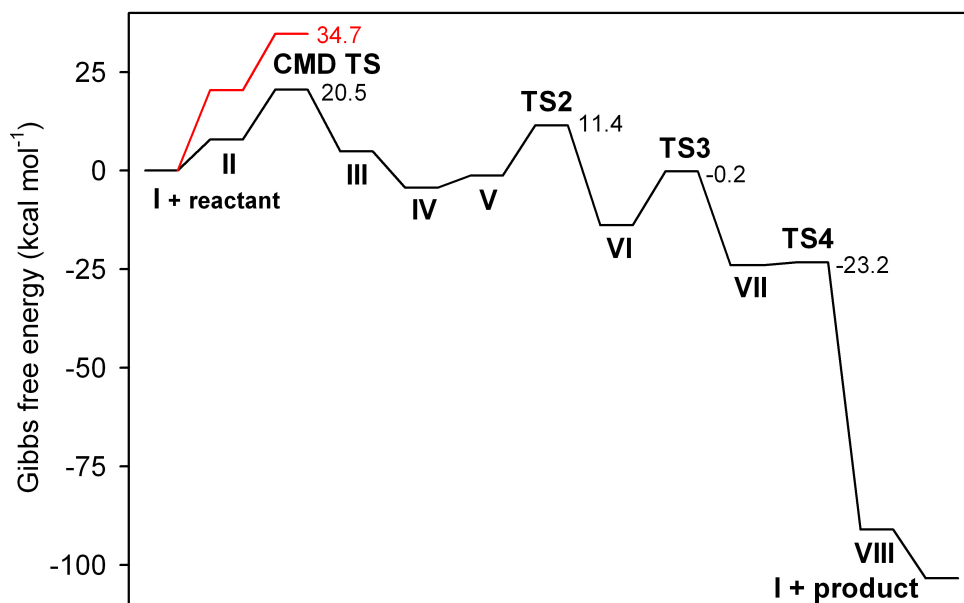
The catalytic cycle starts from CpRh(OAc)₂ (**I**), which is first coordinated to **3.11** with concomitant loss of acetic acid. Next, based on mechanistic investigations of closely related systems¹¹⁰ and our large primary DKIE, we assumed that C–H bond cleavage would occur via a concerted metalation-deprotonation (CMD) transition state (TS). This step affords intermediate **III**, where acetic acid is still bound to rhodium. The Gibbs free energy of the CMD TS is 20.5 kcal mol⁻¹ which is the highest barrier reached in the catalytic cycle.^{111,112} Calculations were also conducted with non-deprotonated **3.11** bonded to Rh(III) prior to the CMD step. However, a high CMD TS energy of 34.7 kcal mol⁻¹ (Scheme 3.18, red line) was found with this cationic complex for the CMD process. This pathway was consequently ruled out. This calculation however reveals the importance of substrate deprotonation for allowing a low-barrier catalytic cycle. Continuing with the lowest energy pathway, acetic acid ligand dissociates from intermediate **III** to give intermediate **IV** and then acetylene coordinates to Rh(III) to yield intermediate **V**. From this point, insertion of acetylene in the Rh–C bond can occur to give intermediate **VI**, a process where the TS energy is 11.4 kcal mol⁻¹. Then, reductive elimination via TS3 (ΔG^\ddagger is -0.2 kcal mol⁻¹) allows the C–N bond formation and

¹¹⁰ Li, L.; Brennessel, W. W.; Jones, W. D. *Organometallics* **2009**, *28*, 3492.

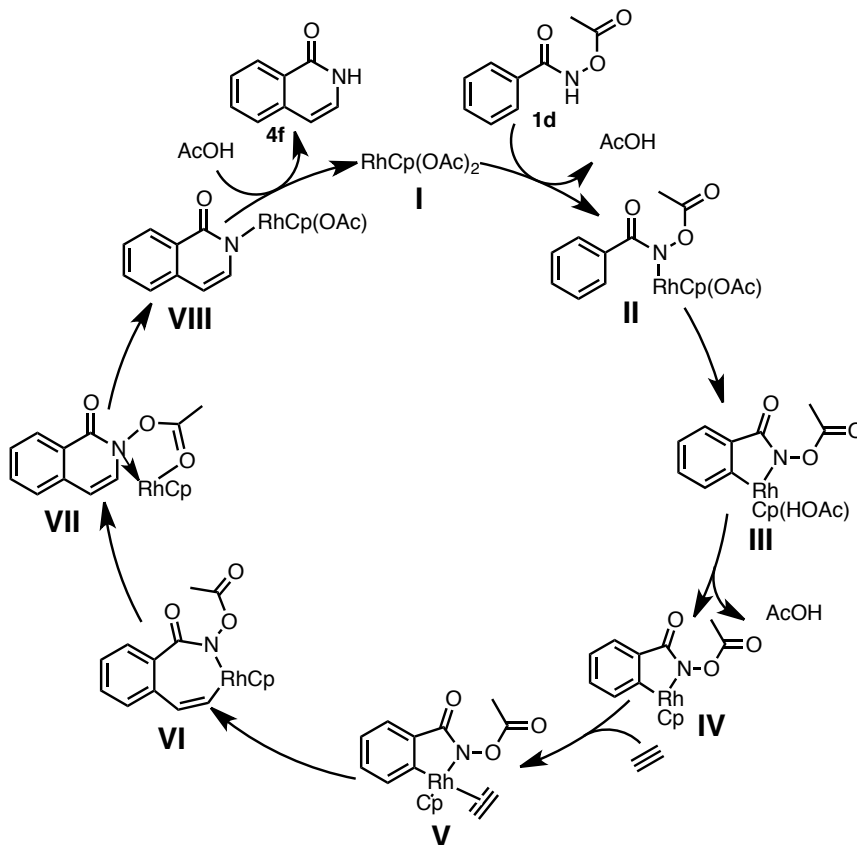
¹¹¹ For DFT calculations of CMD processes with Pd, see : a) Sun, H.-Y.; Gorelsky, S. I.; Stuart, D. R.; Campeau, L.-C.; Fagnou, K. *J. Org. Chem.* **2010**, *75*, 8180. b) Garcia-Cuadrado, D.; Braga, A. A. C.; Maseras, F.; Echavarren, A. M. *J. Am. Chem. Soc.* **2006**, *128*, 1066. c) Garcia-Cuadrado, D.; de Mendoza, P.; Braga, A. A. C.; Maseras, F.; Echavarren, A. M. *J. Am. Chem. Soc.* **2007**, *129*, 6880. d) Lafrance, M.; Rowley, C. N.; Woo, T. K.; Fagnou, K. *J. Am. Chem. Soc.* **2006**, *128*, 8754. e) Gorelsky, S. I.; Lapointe, D.; Fagnou, K. *J. Am. Chem. Soc.* **2008**, *130*, 10848. f) Liégault, B.; Petrov, I.; Gorelsky, S. I.; Fagnou, K. *J. Org. Chem.* **2010**, *75*, 1047-1060.

¹¹² The structural features of this TS (the C-H and O-H distances for the proton transfer are 1.30 Å and 1.36 Å, respectively, and the Rh-C distance is 2.23 Å) are fairly similar to those reported in Pd(II)-catalyzed CMD TS structures (the C-H and O-H distances for the proton transfer are 1.44 Å and 1.21 Å, respectively, and the Pd-C distance is 2.25 Å for the CMD TS for the reaction of C₆H₆ with [Pd(PMe₃)(Ph)(OAc)]) (ref 111e)

delivers intermediate **VII**. The low energy barrier for the reductive elimination step would explain its kinetic irrelevance under the new reaction conditions. Subsequently, a fast oxidative addition occurs via TS4 to form intermediate **VIII**, which is finally protonated by acetic acid. This last step releases the desired isoquinolone and regenerates the catalyst. Calculations were also attempted to find the lowest energy pathway of a concerted process analogous to pathway A presented in Figure 3.8, but no low energy pathway was found to match the experimental data. Consequently, we propose pathway B as being operative in the catalytic cycle. The low energy barrier calculated for the N–O bond oxidative addition correlates well with the experimental evidence showing that the cleavage of the N–O bond happens intramolecularly on the substrate on which the C–N bond is formed. It is also of note that a cationic pathway, where the substrate's directing group is not deprotonated (acting as a L ligand), is considerably higher in energy than a similar pathway where the complex is neutral.



Scheme 3.18 Free Energy Diagram ($\Delta G^\ddagger_{298\text{K}}$, kcal \cdot mol⁻¹ in methanol) for the Relevant Intermediates, Transition States and Products for the Reaction of **3.11** with Acetylene. The Neutral and Cationic Pathway Energies Are Shown in Black and Red, Respectively.



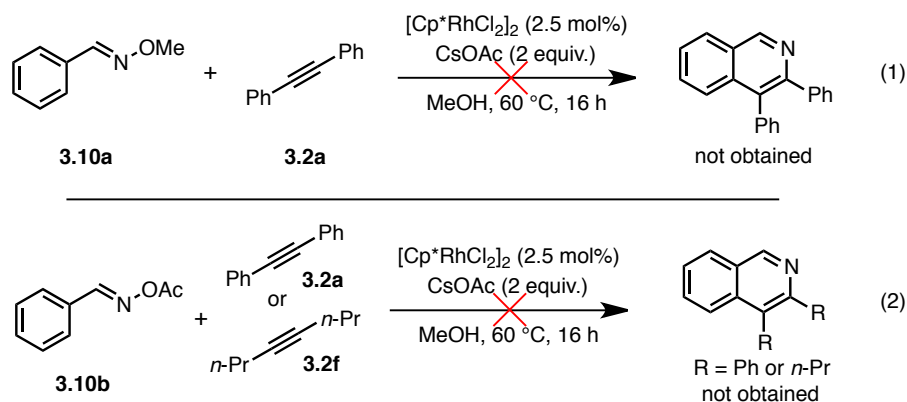
Scheme 3.19 DFT Calculated Catalytic Cycle

3.2.6 Isoquinoline synthesis¹¹³

With the development of a mild and robust redox-neutral isoquinolone synthesis, we sought to elaborate on this strategy to make it compatible with other heterocycle syntheses. Possessing a somewhat similar structure, we targeted the isoquinoline motif as a potential candidate. We surmised that this heterocycle could arise from the coupling of an *O*-protected oxime with an alkyne. Although we and others had previously reported (see chapter 2) an oxidative strategy to access this heterocycle, we were curious about the possibility to employ a redox-neutral strategy. Our goal was to allow for a broader scope and milder conditions

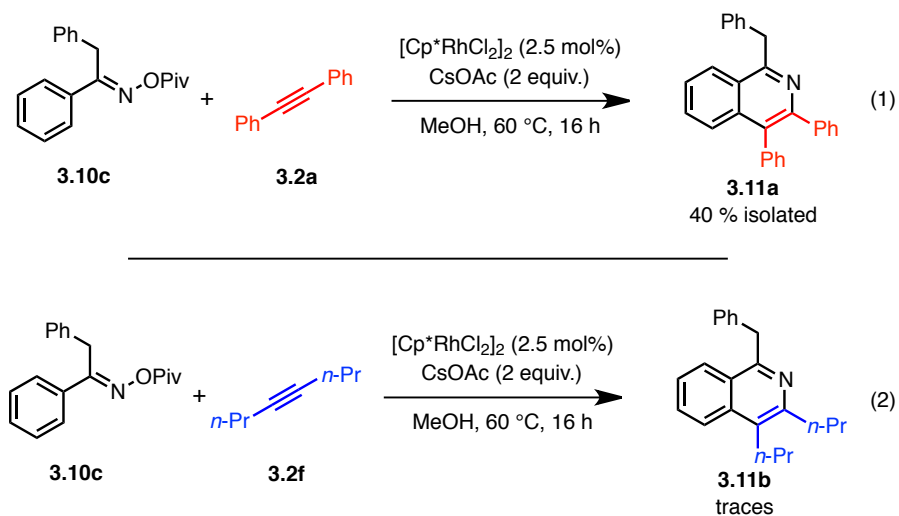
¹¹³ During the development of this chemistry, Chiba reported a similar reaction, see: Too, O. C.; Wang, Y.-F.; Chiba, S. *Org. Lett.* **2010**, *12*, 5688.

than the ones reported so far. Considering the success we had with the isoquinolone motif (terminal alkyne compatible, low temperature, low catalyst loading, alkene compatible), it seemed plausible and important to explore this concept for the synthesis of other heterocycles. Early on in this investigation, we tested the potential reactivity using an aldoxime starting material. As revealed in Scheme 3.20, using either an *O*-methyl oxime or an *O*-acyl oxime, no desired isoquinoline was obtained.



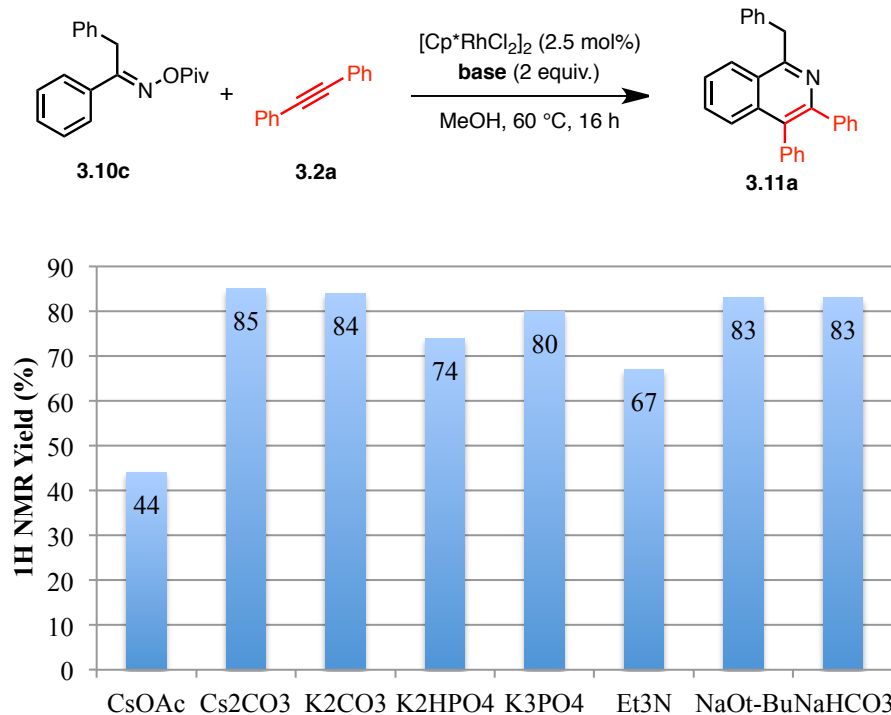
Scheme 3.20 Unsuccessful Isoquinoline Synthesis From Aldoxime Derived Substrates

According to the calculations that were performed on the isoquinolone system, it seemed very important to have a moderately acidic directing group on the substrate, which can, once deprotonated, act as an X ligand on rhodium. Otherwise, the activation energy for the initial arene rhodation is expected to be much higher (Scheme 3.18, red line). In order to elaborate on this assumption, oxime **3.10c**, which has acidic protons at the benzylic position was synthesized and submitted to the conditions developed for the isoquinolone synthesis (Scheme 3.21). Gratifyingly, an isolated yield of 40% was obtained for the reaction with diphenylacetylene (Scheme 3.21, Eq. 1). The reaction using 4-octyne as cross-coupling partner gave low conversion and only traces of product were detectable (Scheme 3.21, Eq. 2).



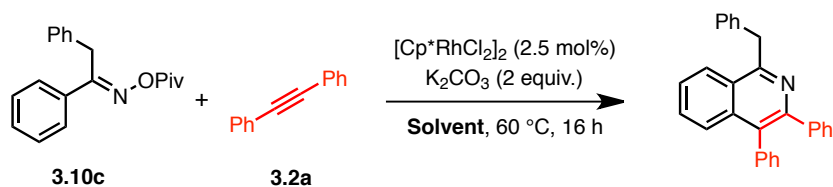
Scheme 3.21 Initial Hit Using Oxime Derivatives as Starting Material

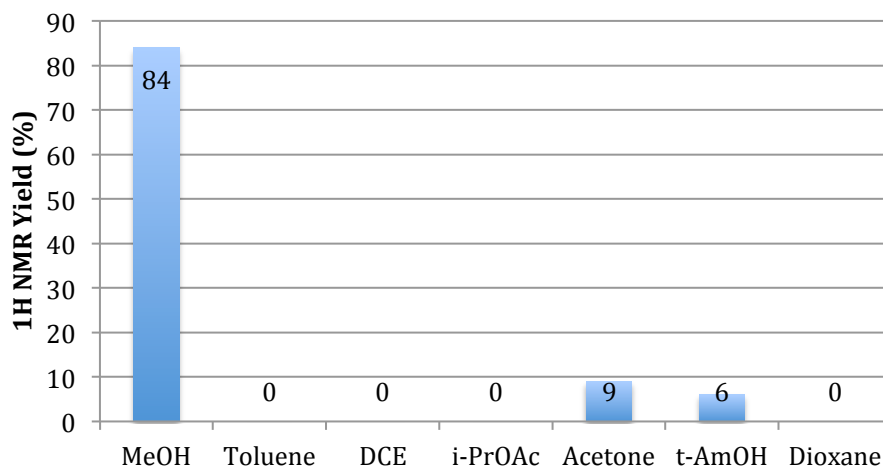
Encouraged by this initial reactivity, further optimization was conducted to obtain higher yields. Since we believed in the importance of having a deprotonated reaction intermediate, the first parameter that we decided to examine was the effect of base on the reaction. The results of this screen are outlined in Table 3.11. We were encouraged to find that exchanging cesium acetate for a slightly stronger base could increase the yield by a factor of 2.

Table 3.11 Base Screening

^aConditions: **3.10c** (1.0 equiv., 0.10 mmol), **3.2a** (1.1 equiv., 0.11 mmol), base (2.0 equiv., 0.20 mmol), [Cp^{*}RhCl₂]₂ (2.5 mol%), MeOH (0.2 M), 60 °C, 16 h. ^b¹H NMR yields vs 1,3,5-trimethoxybenzene as internal standard

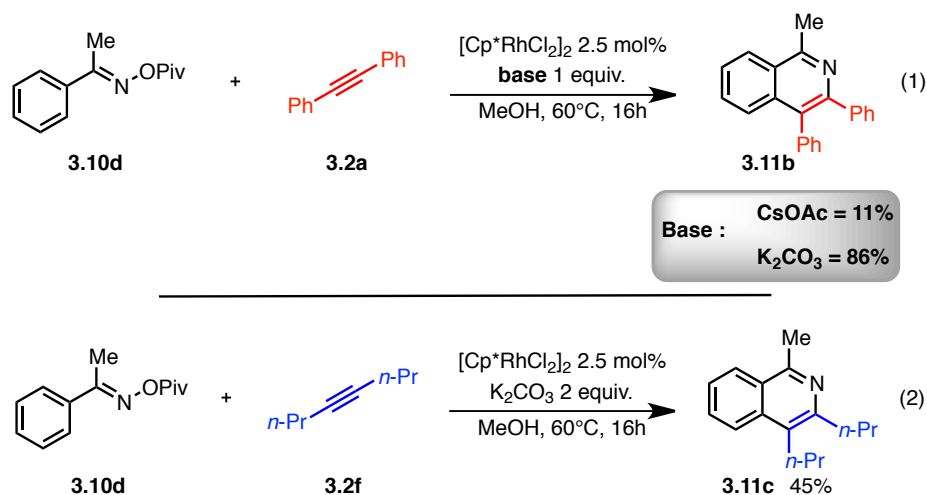
Due to the high yield and clean reaction mixture provided by potassium carbonate, as well as its low cost, further optimization was carried out with this base. A solvent screen was then performed, the results of which are outlined in Table 3.12. Interestingly, only MeOH provided high yields. All other solvents, regardless of their polarity, provided only traces of the desired isoquinolone.

Table 3.12 Solvent Screening^{a,b}



^aConditions: **3.10c** (1.0 equiv., 0.10 mmol), **3.2a** (1.1 equiv., 0.11 mmol), K₂CO₃ (2.0 equiv., 0.20 mmol), [Cp*RhCl₂]₂ (2.5 mol%), solvent (0.2 M), 60 °C, 16 h. ^b¹H NMR yields vs 1,3,5-trimethoxybenzene as internal standard

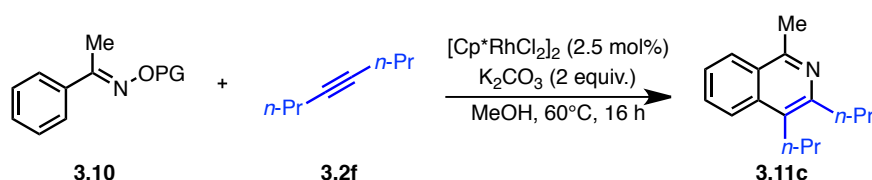
Next, we were curious to see if more acidic benzylic protons were necessary at the *alpha* position of the oxime. When substrate **3.10d**, derived from acetophenone was subjected to the newly optimized reaction conditions, we were pleased to observe that **3.11b** was formed in 86% by ¹H NMR (Scheme 3.22, Eq. 1). Changing the base from K₂CO₃ to the weaker CsOAc lowered the yield of **3.11b** significantly, which is consistent with the results obtained using **3.10c** as substrate.



Scheme 3.22 Isoquinolines from Acetophenone Oxime Derivative **3.10d**

Next, **3.10d** was reacted with the more challenging alkyne **3.2f** using K_2CO_3 as base (Scheme 3.22, Eq 2). This time, a lower yield of 45% was obtained (In our hands, conditions reported by Chiba (ref 113) afforded 42% 1H NMR yield instead of the reported 87%). Trying to improve this moderate yield, we embarked on the screening of other internal oxidants. Since an appreciable quantity of the free oxime resulting from the *O*-protecting group hydrolysis was always observed as side product, we focused our efforts toward the synthesis of substrates that would be more resilient to hydrolysis. Selected examples of this leaving group screening are presented in Table 3.13.

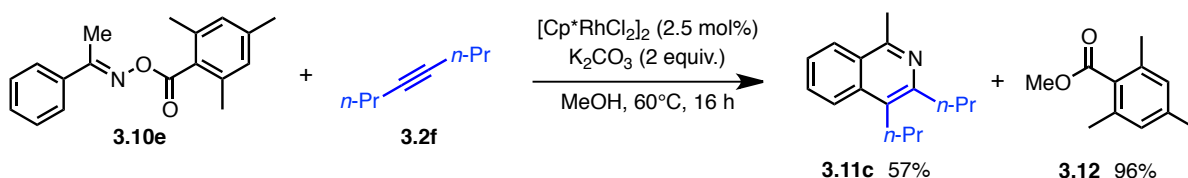
Table 3.13 Internal Oxidant Optimization



Entry	Substrate	Yield (%)	Entry	Substrate	Yield (%)
1		45	4		55
2		57	5		40
3		55	6		56

^aConditions: **3.10** (1.0 equiv., 0.10 mmol), **3.2f** (1.1 equiv., 0.11 mmol), K_2CO_3 (2.0 equiv., 0.20 mmol), $[\text{Cp}^*\text{RhCl}_2]_2$ (2.5 mol%), MeOH (0.2 M), 60 °C, 16 h. ^b 1H NMR yields vs trimethoxybenzene as internal standard

Interestingly, when *O*-mesitylacetophenone oxime (**7b**) was employed as starting material, a further investigation of the ^1H NMR spectrum of the crude reaction mixture revealed that an almost quantitative amount of ester **3.12** was produced (Scheme 3.23).



Scheme 3.23 Observation of a Methyl ester Side-Product

If the reaction was proceeding as expected, the corresponding benzoic acid should be observed in place of the methyl ester. The only way a quantitative amount of ester **3.12** can be produced is by simple basic methanolysis of **3.10e**, which would concomitantly afford the free acetophenone oxime (Figure 3.12). This interesting finding led us to question whether the simple free oxime could be the actual competent starting material in these isoquinoline syntheses. Thus, oxime **3.10j** was reacted with **3.2a** and **3.2f** in the standard reaction conditions (Scheme 3.24). The ^1H NMR yields obtained were found to be essentially the same as the ones obtained using the acyl protected oximes. This finding confirms that the free oxime is the active starting material. It should consequently simplify the preparation of the substrates undergoing this type of reaction.

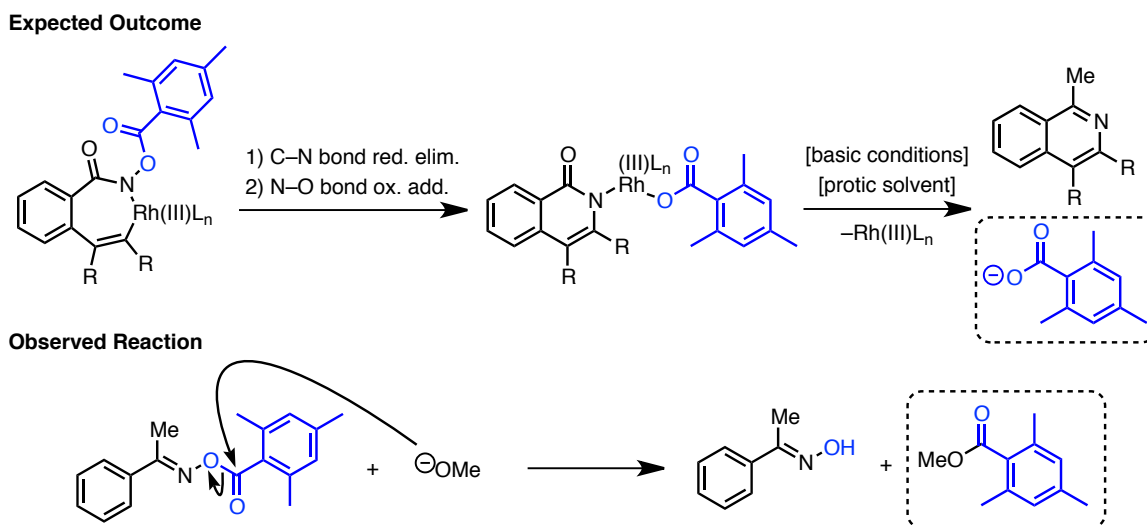
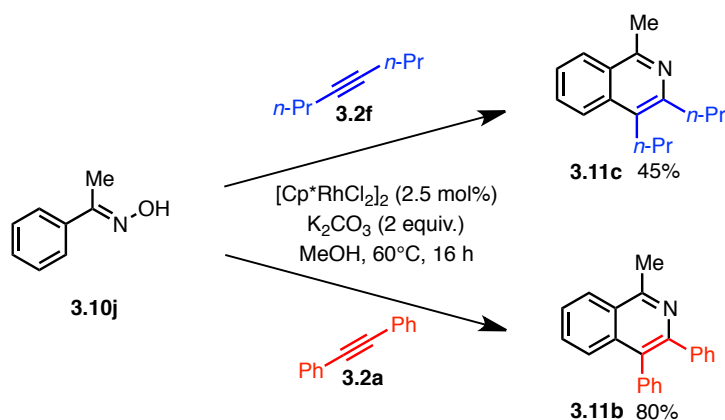


Figure 3.12 Explanation for the observation of the methyl ester side-product

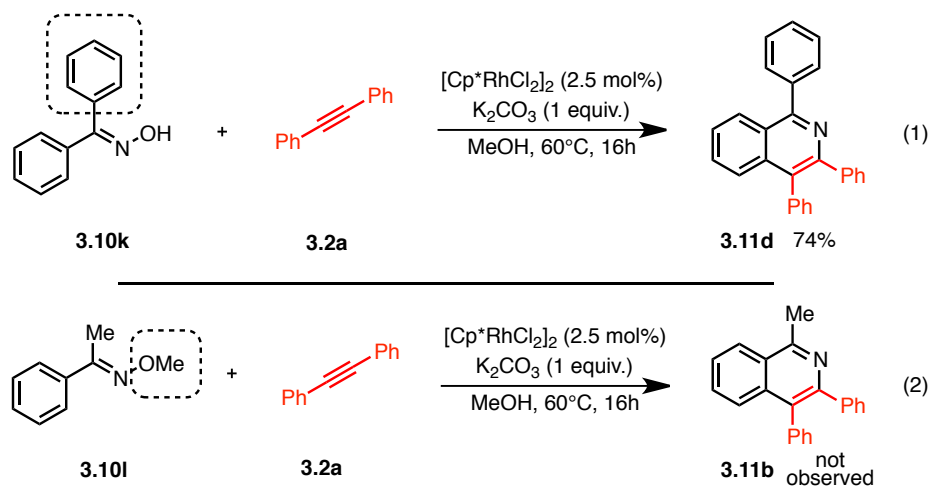


Scheme 3.24 Free Oxime as Substrate

Control experiments were then conducted to verify whether deprotonation of the starting material to obtain a neutral Rh(III) complex was indeed important with this system and if so, to reveal where the deprotonation occurs. Thus, oxime **3.10k** was first reacted with **3.2a** in the standard reaction conditions (Scheme 3.25, Eq 1).¹¹⁴ A ¹H NMR yield of 84% was obtained for this reaction, indicating that, in contrast with our initial assumption, deprotonation *alpha* to the oxime was not essential to undergo the desired transformation.

¹¹⁴ It was found that the use of 1 equiv. of K₂CO₃ provided the same results as 2 equiv.

Subsequently, a reaction of *O*-methyloxime **3.10l** with **3.2a** was run (Scheme 3.25, eq 2). From this experiment, no desired isoquinoline was observed. These results are consistent with deprotonation of the oxime oxygen as an important step in the reaction. They also clarify why only MeOH as solvent would provide good yields, as it is necessary for the methanolysis of the *O*-protecting group of the substrate. Additionally, these findings are in good agreement with the computational experiments done on the isoquinolone system, where it was shown that a deprotonated substrate bounded to rhodium lower the energy barriers of the CMD TS by providing a neutral Rh(III) complex.



Scheme 3.25 Control Experiments

3.3 Summary and Outlook

In conclusion, a conceptually new approach to C–N bond formation from benzhydroxamic acids was developed. This redox-neutral isoquinolone synthesis operates under mild conditions, is not sensitive to air or moisture and does not require an external oxidant. A refinement of this discovery through empirical screening of a variety of internal oxidants was also performed. This allowed for the mildest rhodium(III)-catalyzed

isoquinolone and 3,4-dihydroisoquinolone synthesis reported to date. The reaction is a rare example of an aromatic C–H bond functionalization reaction run at room temperature. It can also provide high yields with catalyst loadings as low as 0.5 mol%. Additionally, we have circumvented the limitations associated with the oxidative heterocycle syntheses reported recently where exclusively internal alkynes were tolerated. Indeed, the overall redox-neutral strategy presented herein allowed us to use terminal alkynes as well as alkenes to access isoquinolones with various substitution patterns. At present, it is still the only report of such a Rh(III)-catalyzed heterocycle synthesis where terminal alkynes are tolerated. Mechanistic insights revealed a change in the rate-limiting step depending on the internal oxidant used. In addition, DFT calculations were conducted, which shed light on the reductive C–N bond forming and oxidative N–O bond cleaving steps. These calculations also revealed the importance of substrate deprotonation throughout the catalytic cycle. This concept was shown to be readily applicable to rhodium(III)-catalyzed isoquinoline synthesis. As this chapter is being written, these findings already proved valuable in the design of various other related rhodium(III) and ruthenium(II)-catalyzed reactions that are mild and do not use external oxidants.¹¹⁵

¹¹⁵ For a highlight, see: (a) Patureau, F. W.; Glorius, F. *Angew. Chem., Int. Ed.* **2011**, *50*, 1977. For selected examples, see: (b) Hyster, T. K.; Rovis, T. *Chem. Commun.* **2011**, *47*, 11846. (c) Li, B; Feng, H.; Xu, S.; Wang, B. *Chem.–Eur. J.* **2011**, *17*, 12573. (d) Ackermann, L.; Fenner, S. *Org. Lett.* **2011**, *13*, 6548. (e) see ref. 11 (f) see ref. 113. (g) Too, O. C.; Chua, S. H.; Wong, S. H.; Chiba, S. *J. Org. Chem.* **2011**, *76*, 6159. (h) Zhang, X.; Chen, D.; Zhao, M.; Zhao, J.; Jia, A.; Li, X. *Adv. Synth. Catal.* **2011**, *353*, 719.

Mechanistic Investigations on Cope-Type Hydroamination Through Tethering Organocatalysis

4.1 Introduction

In thermodynamics, the Gibbs free energy can be defined by the following equation: $G = H - TS$, where H is enthalpy, T is temperature and S is entropy. When considering a chemical transformation, the overall change in free energy can be expressed as: $\Delta G = \Delta H - T\Delta S$. It is thus well known that, due to the entropy factor (ΔS), intermolecular reactions, which need to combine two reaction components (negative ΔS value), are energetically disfavoured relative to their intramolecular variant. This explains why catalysis, whether it is performed by enzymes, transition metals or smaller organic molecules, often operates by means of pre-association of the reaction components. Of course, pre-association is an important parameter, but the most efficient catalysts are also able to stabilize the transition state of chemical transformations via various other interactions. Nature, through the use of enzymes, displays the most efficient examples of such catalytic activity. Indeed these natural

catalysts are known to be able to increase reaction rates by a factor of up to 10^{17} .¹¹⁶ Trying to mimic this particular ability of Nature to achieve difficult reactions using preorganization, chemists have developed various directed, tethered or templated reactions.¹¹⁷ Although most of these tethering reactions proved useful, they generally suffer from the drawback that additional synthetic steps are required for the installation and cleavage of the tethering atom(s). To address this issue, different research groups have focused their efforts on the establishment of catalytic tethering strategies, where reversible association/dissociation events through covalent bonding occur throughout a reaction. The temporary intramolecularity achieved during the association event allows difficult intermolecular reactions to be executed intramolecularly.¹¹⁸ Examples relating to this strategy will be discussed in this section.¹¹⁹

Besides, owing to the abundance of nitrogen-containing moieties in biologically active molecules, tremendous progress has been accomplished over the past decades for the formation of carbon-nitrogen bonds. Among the plethora of methods now available to construct these coveted bonds, alkene hydroamination represents perhaps one of the simplest strategies that one can imagine. Although we saw in Chapter 1 that acid, base, early and late

¹¹⁶ Radzicka, A.; Wolfenden, R. *Science* **1995**, *267*, 90.

¹¹⁷ (a) For a review on substrate-directable chemical reactions, see: Hoveyda, A. H.; Evans, D. A.; Fu, G. C. *Chem. Rev.* **1993**, *93*, 1307-1370. (b) For a recent review on removable or catalytic directing groups, see: Rousseau, G.; Breit, B. *Angew. Chem., Int. Ed.* **2011**, *50*, 2450-2494.

¹¹⁸ For selected examples in which the catalytic systems operate via preassociation and substrate activation, see: (a) Sammakia, T.; Hurley, T. B. *J. Am. Chem. Soc.* **1996**, *118*, 8967. (b) Sammakia, T.; Hurley, T. B. *J. Org. Chem.* **1999**, *64*, 5652. (c) Sammakia, T.; Hurley, T. B. *J. Org. Chem.* **2000**, *65*, 974. (d) Bedford, R. B.; Coles, S. J.; Hursthouse, M. B.; Limmert, M. E. *Angew. Chem., Int. Ed.* **2003**, *42*, 112. (e) Lightburn, T. E.; Dombrowski, M. T.; Tan, K. L. *J. Am. Chem. Soc.* **2008**, *130*, 9210. (f) Grünanger, C. U.; Breit, B. *Angew. Chem., Int. Ed.* **2008**, *47*, 7346. (g) Fuchs, D.; Rousseau, G.; Diab, L.; Gellrich, U.; Breit, B. *Angew. Chem., Int. Ed.* **2012**, *51*, 2178. (h) Worthy, A. D.; Joe, C. L.; Lightburn, T. E.; Tan, K. L. *J. Am. Chem. Soc.* **2010**, *132*, 14757. (i) Sun, X.; Worthy, A. D.; Tan, K. L. *Angew. Chem., Int. Ed.* **2011**, *50*, 8167. (j) Murphy, S. K.; Coulter, M. M.; Dong, V. *Chem. Sci.* **2012**, *3*, 355. For a review, see: (k) Tan, K. L.; Sun, X.; Worthy, A. D. *Synlett* **2012**, *23*, 321

¹¹⁹ (a) For excellent reviews, see: Tan, K. L. *ACS Catalysis* **2011**, *1*, 877. (b) Pascal, R. *Eur. J. Org. Chem.* **2003**, 1813.

transition metals proved useful to catalyze this transformation in a number of instances,¹²⁰ many challenges still exist. For example, selectivity, functional group compatibility and intermolecular reactivity are still ongoing hurdles in the hydroamination area. Over the past few years, our group has been focusing on Cope-type hydroamination¹²¹ to undertake these problems from a different angle. Although we showed that intermolecular reactivity was achievable,¹²² restraints in terms of alkene scope and amount used as well as reaction temperature and selectivity still impede the widespread use of this metal-free hydroamination method. This section will discuss in more details the accomplishments and the remaining challenges associated with Cope-type hydroamination.

4.1.1 Catalysis Through Temporary Intramolecularity

The utilization of small organic molecules to accomplish difficult intermolecular reactions via temporary intramolecularity is not a new concept. However, given the small number of transformations that have benefited from such catalysis, it seems like this area of research has been slightly overlooked. This type of catalysis has mainly been applied to simple hydrolysis reactions, and expansion of this concept to more complex systems has not been reported in the organocatalysis field. Nevertheless, transition metal-catalysis did take advantage of temporary intramolecularity in some instances.¹²³ This emerging area of

¹²⁰ For selected reviews on hydroamination see: (a) Müller, T. E.; Hultzs, K. C.; Yus, M.; Foubelo, F.; Tada, M. *Chem. Rev.* **2008**, *108*, 3795. (b) Aillaud, I.; Collin, J.; Hannedouche, J.; Schulz, E. *Dalton Trans.* **2007**, 5105. (c) Hultzs, K. C. *Adv. Synth. Catal.* **2005**, *347*, 367. (d) Nobis, M.; Drießen-Hölscher, B. *Angew. Chem., Int. Ed.* **2001**, *40*, 3983. (e) Müller, T. E.; Beller, M. *Chem. Rev.* **1998**, *98*, 675.

¹²¹ For an excellent review on Cope-type hydroamination see: Cooper, N. J.; Knight, D. W. *Tetrahedron*, **2004**, *60*, 243.

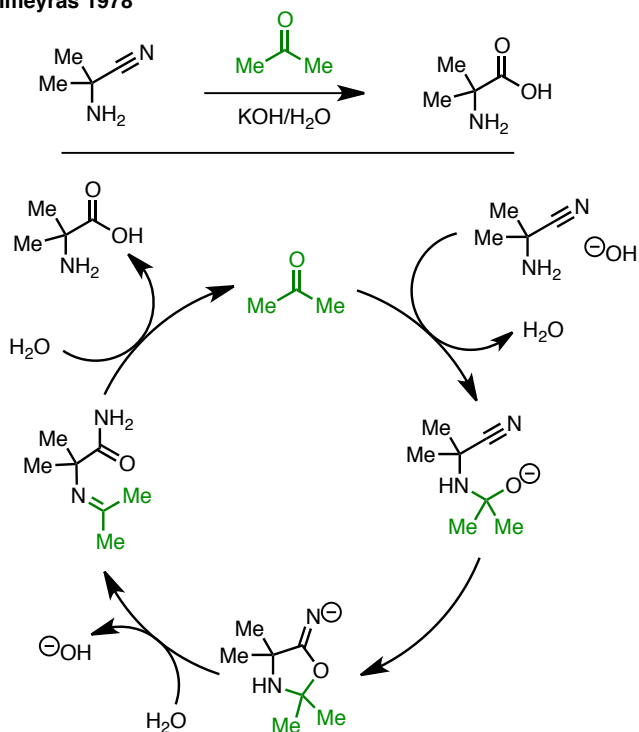
¹²² (a) Beauchemin, A. M.; Moran, J.; Lebrun, M.-E.; Séguin, C.; Dimitrijevic, E.; Zhang, L.; Gorelsky, S. I. *Angew. Chem., Int. Ed.*, **2008**, *47*, 1410. (b) Moran, J.; Gorelsky, S. I.; Dimitrijevic, E.; Lebrun, M.-E.; Bédard, A.-C.; Séguin, C.; Beauchemin, A. M. *J. Am. Chem. Soc.* **2008**, *130*, 17893. (c) Bourgeois, J.; Dion, I.; Cebrowski, P. H.; Loiseau, F.; Bédard, A.-C.; Beauchemin, A. M. *J. Am. Chem. Soc.* **2009**, *131*, 874. (d) Moran, J.; Pfeiffer, J. Y.; Gorelsky, S. I.; Beauchemin, A. M. *Org. Lett.* **2009**, *11*, 1895.

¹²³ For examples, see ref. 118d,e,f,h,i,j.

research will not be discussed in this chapter, as the focus will be made on organocatalytic transformations, which relate more closely to the chemistry that will be presented.

As mentioned, the tethering catalysis reactions developed so far were employed for hydrolysis of simple functional groups. The original work of Commeyras¹²⁴ *et al.* on the hydrolysis of α -aminonitriles using acetone as catalyst is an illustrative example (Scheme 4.1). In this reaction, the amine moiety of an α -aminonitrile reacts with acetone to transiently generate a hemiaminal, which can be deprotonated. The alcoholate portion of this hemiaminal then undergoes an intramolecular addition onto the nitrile moiety. Opening of the resulting intermediate followed by hydrolysis regenerates the acetone catalyst and yields the corresponding amide.

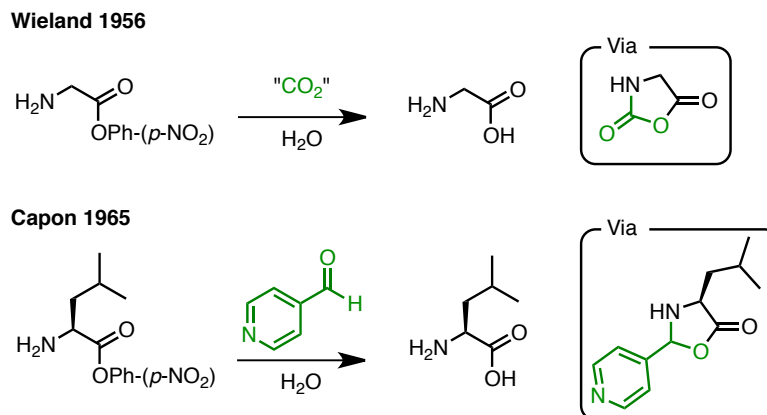
¹²⁴ (a) Pascal, R.; Taillades, J.; Commeyras, A. *Tetrahedron* **1978**, *34*, 2275. (b) Pascal, R.; Taillades, J.; Commeyras, A. *Bull. Soc. Chim. Fr.* **1978**, 177. (c) Pascal, R.; Taillades, J.; Commeyras, A. *Tetrahedron* **1980**, *36*, 2999. (d) Sola, R.; Brugidou, J.; Taillades, J.; Commeyras, A. *Tetrahedron Lett.* **1983**, *24*, 1501. (e) Sola, R.; Brugidou, J.; Taillades, J.; Commeyras, A. *New J. Chem.* **1984**, *8*, 459. (f) Sola, R.; Taillades, J.; Brugidou, J.; Commeyras, A. *New J. Chem.* **1989**, *13*, 881. (g) Taillades, J.; Beuzelin, I.; Gabrel, L.; Tabacik, V.; Bied, C.; Commeyras, A. *Orig. Life Evol. Biosph.* **1996**, *28*, 61. For discussion and representative experimental procedures, see: (h) Pascal, R.; Marnier, M. L.; Rousset, A.; Commeyras, A.; Taillades, J.; Mion, L. Process for the Chemical Catalytic Hydrolysis of an α -Aminonitrile or of One of the Salts Thereof. U.S. Patent 4,243,814, Jan 6, 1981. For kinetic resolution using chiral ketones, see: (i) Tadros, Z.; Lagriffoul, P. H.; Mion, L.; Taillades, J.; Commeyras, A. *J. Chem. Soc., Chem. Commun.* **1991**, 1373. (j) Taillades, J.; Garrel, L.; Lagriffoul, P.-H.; Commeyras, A. *Bull. Soc. Chim. Fr.* **1992**, *129*, 191. (k) Lagriffoul, P.-H.; Tadros, Z.; Taillades, J.; Commeyras, A. *J. Chem. Soc. Perkin Trans. 2* **1992**, 1279. (l) Taillades, J.; Garrel, L.; Guillen, F.; Collet, H.; Commeyras, A. *Bull. Soc. Chim. Fr.* **1995**, *132*, 119. (m) Taillades, J.; Garrel, L.; Guillen, F.; Collet, H.; Commeyras, A. *React. Polym.* **1995**, *24*, 261.

Commeyras 1978**Scheme 4.1** Organocatalyzed Nitrile Hydration

Several related reactions building on temporary intramolecularity were also developed. Prior to the work of Commeyras on acetone-catalyzed nitrile hydration, CO₂¹²⁵ and aldehyde¹²⁶ promoted ester hydrolysis was also discovered (Scheme 4.2). Wieland was able to employ bicarbonate as a carbon dioxide precursor.

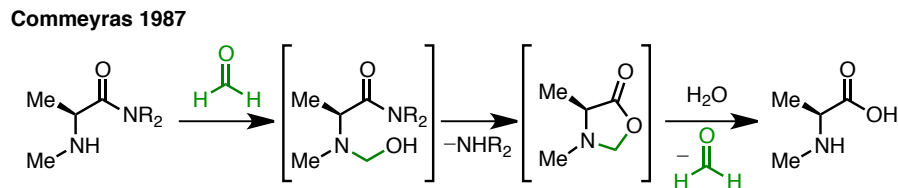
¹²⁵ (a) Wieland, V. T.; Lambert, R.; Lang, H. U.; Schramm, G. *Justus Liebigs Ann. Chem.* **1956**, 597, 181. (b) Wieland, V. T.; Jaenicke, F. *Justus Liebigs Ann. Chem.* **1956**, 599, 125.

¹²⁶ (a) Capon, B.; Capon, R. *J. Chem. Soc., Chem. Commun.* **1965**, 20, 502. (b) Hay, R. W.; Main, L. *Aust. J. Chem.* **1968**, 21, 155.



Scheme 4.2 Carbonyl-Catalyzed Ester Hydrolysis

This mode of catalysis has later been applied to more difficult α -aminoamide hydrolysis reaction. Commeyras showed that simple formaldehyde was an efficient catalyst for this transformation.¹²⁷ As summarized in Scheme 4.3, the proposed mechanism is very similar to the one of the nitrile hydrolysis reaction discussed previously.

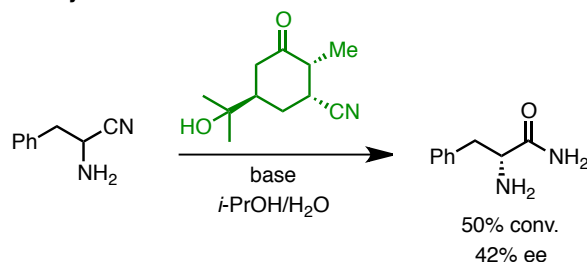


Scheme 4.3 Formaldehyde-Catalyzed Amide Hydrolysis

At the beginning of the 90's, Commeyras established the first enantioselective nitrile hydration reaction using chiral ketone catalysts (Scheme 4.4). This type of kinetic resolution reaction was found to achieve enantioselectivities as high as 42% ee. Although this value is modest, it validates an important and promising concept in organocatalysis: enantioselectivity can be induced through a chiral tethering catalyst.

¹²⁷ Pascal, R.; Lasperas, M.; Taillades, J.; Commeyras, A. *New. J. Chem.* **1987**, *11*, 235.

Commeyras 1991



Scheme 4.4 Ketone-Catalyzed Enantioselective Nitrile Hydrolysis

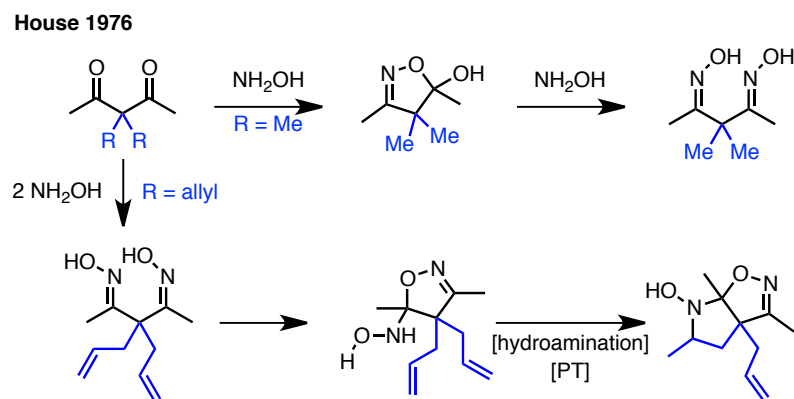
Common to all the hydrolysis reactions mentioned so far is the use of *stoichiometric* amounts of a carbonyl catalyst, even though turnover should occur according to the proposed mechanisms. This highlights the underdevelopment and opportunities associated with tethering catalysis: simple systems achieving high catalytic efficiency (catalyst turnover number and rates) remains to be established. In addition, highly stereoselective variants and the application of this strategy to complex reactions has scarcely been studied.

4.1.2 Cope-Type Hydroamination of Alkenes as a Mean for C–N Bond Formation

House, in 1976, reported the first observation of an intramolecular Cope-type hydroamination product.¹²⁸ While attempting to make 1,3-dioxime from 3,3-disubstituted 2,4-pentanediones and hydroxylamine, he noticed that when using allyl or propargyl substituents at the 3-position of his substrate, the product obtained was not the desired dioxime, but rather the bicyclic hydroamination product (Scheme 4.5). Due to absence of net change in oxidation level and the observation that trace amounts of oxidant promote the reaction, a radical chain mechanism was originally proposed for this transformation.

¹²⁸ (a) House, H. O.; Manning, D. T.; Melillo, D. G.; Lee, L. F.; Haynes, O. R.; Wilkes, B.; E. *J. Org. Chem.* **1976**, *41*, 855. (b) House, H. O.; Lee, L. F. *J. Org. Chem.* **1976**, *41*, 863.

Independently, Oppolzer also made the same observation in 1978 while studying the chemistry of nitrono compounds.¹²⁹



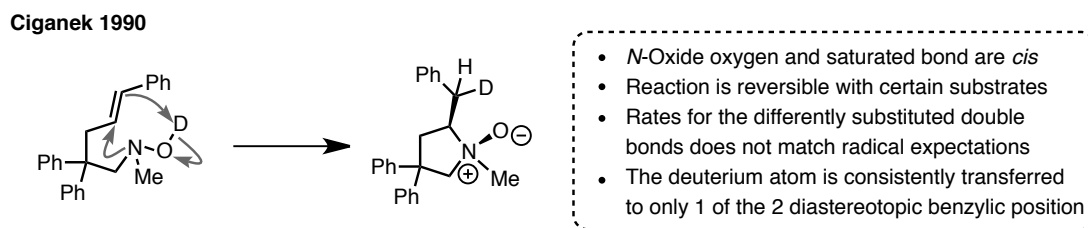
Scheme 4.5 House Alkene Hydroamination Product

In 1990, Ciganek further explored the scope and mechanism of this particular transformation.¹³⁰ He thereby established that the reaction did not proceed via a chain radical mechanism, but rather via a reverse Cope elimination pathway. To demonstrate this, Ciganek synthesized various substrates with different substitutions on the alkene portion. He also made a deuterated hydroxylamine to explore the fate of the hydrogen atom transfer. As summarized in Scheme 4.6, the results obtained are consistent with a concerted reverse Cope elimination. The following observations all agree with this mechanism: 1) after hydroamination, the oxygen of the *N*-oxide and the resulting saturated bond are always in a *cis* relationship, 2) with certain substrates, the reaction proved to be reversible at room temperature, 3) The rates observed for different substitutions on the double bond are inconsistent with a radical-based mechanism (cyclization of an internally substituted alkene is fast whereas it is slow with a terminally disubstituted compound), 4) when using a

¹²⁹ (a) Oppolzer, W.; Siles, S.; Snowden, R. L.; Bakker, B. H.; Petrzilka, M. *Tetrahedron Lett.* **1979**, 4391. (b) Oppolzer, W.; Siles, S.; Snowden, R. L.; Bakker, B. H.; Petrzilka, M. *Tetrahedron* **1985**, *17*, 3497.

¹³⁰ Ciganek, E. *J. Org. Chem.* **1990**, *55*, 3007.

deuterated substrate, deuterium incorporation on the product occurred at only one of the two diastereotopic positions, which can only be explained by a concerted mechanism.¹³¹



Scheme 4.6 Ciganek Mechanistic Proposal¹³⁰

These observations were later confirmed by Oppolzer in a report where he utilized this Cope-type hydroamination reaction for the synthesis of two natural products : (\pm)- α -Lycorane and (+)-Trianthine.¹³² In this report, an intramolecular hydroamination was executed on an alkene that was methyl,phenyl-disubstituted at the terminal position. The X-ray crystal structure of the product obtained confirmed that the hydroamination occurred in a suprafacial manner, which also supports the retro-Cope elimination mechanism.

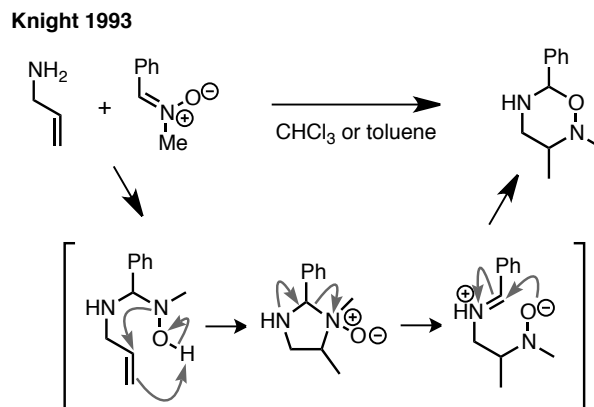
Also relevant to the chemistry that will be discussed in this chapter is the work of Knight on the addition of allylic nucleophiles to nitrones. The first report on this type of chemistry was published in 1993 and regarded the addition of allylamines to nitrones.¹³³ This would trigger a one-pot sequence featuring intramolecular Cope-type hydroamination, amination opening and ring closure (Scheme 4.7). The products of this sequence were essentially cyclized vicinal diamines.¹³⁴

¹³¹ For a following report with extended scope and mechanistic investigations, see: (a) Ciganek, E.; Read, J. Jr. *M. J. Org. Chem.* **1995**, *60*, 5795. (b) Ciganek, E. *J. Org. Chem.* **1995**, *60*, 5803.

¹³² Oppolzer, W.; Spivey, A. C.; Bochet, C. G. *J. Am. Chem. Soc.* **1994**, *116*, 3139.

¹³³ Gravestock, M. B.; Knight, D. W.; Thornton, S. R. *J. Chem. Soc., Chem. Commun.* **1993**, 169.

¹³⁴ For other reports on the synthesis of vicinal diamines, see: (a) Bell, K. E.; Coogan, M. P.; Gravestock, M. B.; Knight, D. W.; Thornton, S. R. *Tetrahedron Lett.* **1997**, *38*, 8545. (b) Gravestock, M. B.; Knight, D. W.; Malik, K. M. A.; Thornton, S. R. *J. Chem. Soc., Perkin, Trans. 1* **2000**, 3292.



Scheme 4.7 Knight's Synthesis of Vicinal Diamines

This strategy was later developed for the use of other allylic nucleophiles such as thiols and lithiated sulfoxides.¹³⁵

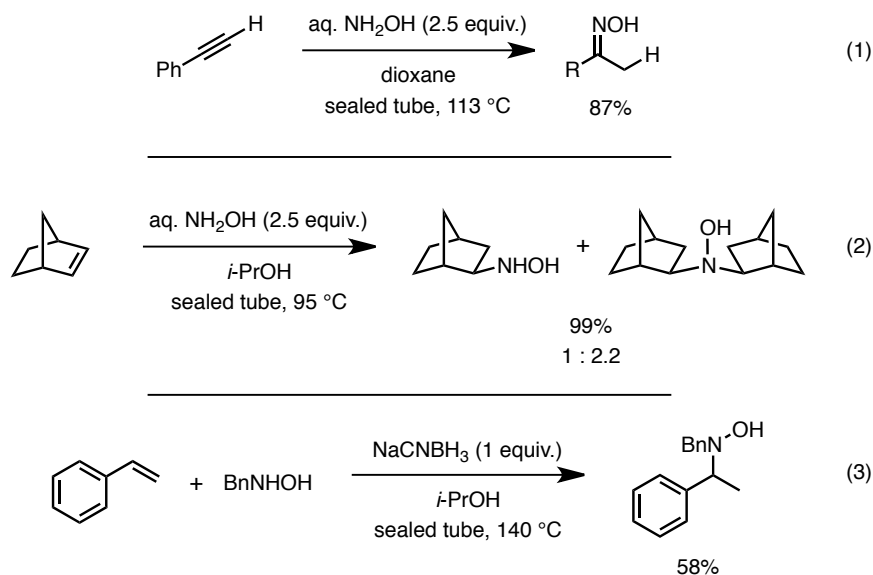
While these examples of intramolecular Cope-type hydroamination proved valuable for the synthesis of a variety of saturated heterocycles, the application of this strategy in the context of an intermolecular hydroamination has been much less forthcoming. Indeed, fundamental thermodynamic factors have hampered its use in synthesis. Nevertheless, our group showed in 2008 that aqueous hydroxylamine could react with different strained alkenes (or styrenes) and alkynes to form alkylhydroxylamines and oximes respectively (Scheme 4.8, Eqs. 1 and 2), albeit affording mixtures of regioisomers.¹³⁶ The conditions required to effect this transformation were however more forcing than for the related intramolecular reaction. A typical alkene hydroamination would be run at relatively high temperature (95-140 °C) in a sealed tube using *i*-PrOH as solvent. The use of this specific solvent has a substantial impact on the reaction outcome. In a subsequent full account on this

¹³⁵ (a) Coogan, M. P.; Gravestock, M. B.; Knight, D. W.; Thornton, S. R. *Tetrahedron Lett.* **1997**, *38*, 8549. (b) Hanrahan, J. R.; Knight, D. W. *Chem. Commun.* **1998**, 2231. (c) Knight, D. W.; Leese, M. P.; De Kimpe, N. *Tetrahedron Lett.* **2001**, 2597.

¹³⁶ Beauchemin, A. M.; Moran, J.; Lebrun, M.-E.; Séguin, C.; Dimitrijevic, E.; Zhang, L.; Gorelsky, S. I. *Angew. Chem., Int. Ed.* **2008**, *47*, 1410.

intermolecular reactivity,¹³⁷ it was found that using NaCNBH₃ as an additive also had a positive impact on the yields obtained when using alkylhydroxylamines as starting materials (Scheme 4.8, Eq 3). The presence of this reductive agent presumably prevents the decomposition of the alkylhydroxylamine starting material.

Beauchemin 2008



Scheme 4.8 Intermolecular Cope-Type Hydroamination

Although these examples of intermolecular, metal- and acid-free hydroamination seemed very promising, the conditions developed thus far did not allow for: 1) reaction of unbiased alkenes, 2) general high regioselectivity, 3) equimolar ratio of starting materials, 4) enantioselective reactivity and 5) low temperature reactivity.¹³⁸

¹³⁷ Moran, J.; Gorelsky, S. I.; Dimitrijevic, E.; Lebrun, M. E.; Bédard, A. C.; Séguin, C.; Beauchemin, A. M. *J. Am. Chem. Soc.* **2008**, *130*, 17893.

¹³⁸ For other reports from our group on intermolecular Cope-Type hydroamination, see: (a) Bourgeois, J.; Dion, I.; Cebrowski, P. H.; Loiseau, F.; Bédard, A. C.; Beauchemin, A. M. *J. Am. Chem. Soc.* **2009**, *131*, 874. (b) Roveda, J.-G.; Clavette, C.; Hunt, A. D.; Whipp, C. J.; Gorelsky, S. I.; Beauchemin, A. M. *J. Am. Chem. Soc.* **2009**, *131*, 8740. (c) Moran, J.; Pfeiffer, J. Y.; Gorelsky, S. I.; Beauchemin, A. M. *Org. Lett.* **2009**, *11*, 1895. (d) Loiseau, F.; Clavette, C.; Raymond, M.; Roveda, J.-G.; Burrell, A.; Beauchemin, A. M. *Chem. Commun.* **2011**, 562.

4.1.3 Merging Tethering Organocatalysis with Cope-Type Hydroamination

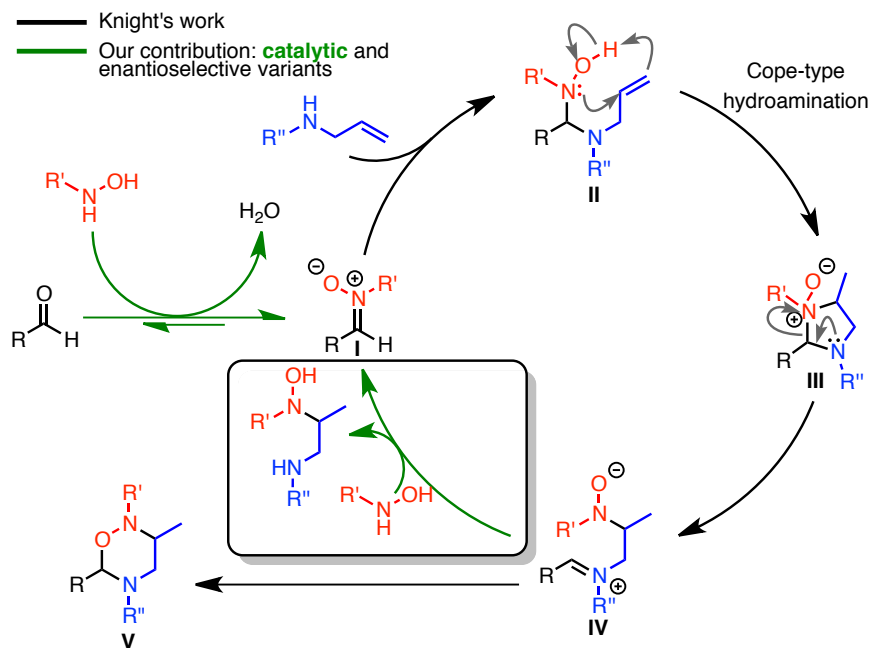
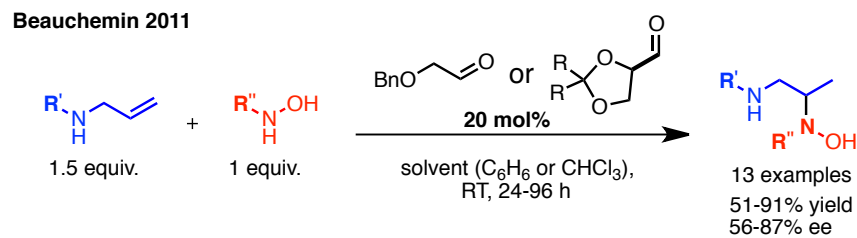
Reactivity

To address the intermolecular hydroamination limitations mentioned above, we were recently inspired by the work of Knight^{133,134} (Scheme 4.7) on the synthesis of diamines from nitrones and allylamines to advance the concept of tethering organocatalysis, which we believe, has the potential to solve many of the aforementioned issues. In fact, our group recently disclosed that simple aldehydes can act *solely*¹³⁹ as tethering catalysts to allow a formal intermolecular Cope-type hydroamination to proceed «intramolecularly» via the key formation of a mixed aminal (Scheme 4.9).¹⁴⁰ As opposed to more traditional tethering strategies,¹⁴¹ this catalytic method does not require additional synthetic steps for the installation and cleavage of the tether. It also allows the hydroamination to proceed at room temperature with a minimal excess of one of the reaction components. Additionally, it gives the possibility to form enantioenriched molecules through efficient transfer of stereochemical information using a chiral aldehyde catalyst.

¹³⁹ For selected examples of tethering *and* substrate activation catalysis, see: (a) Bedford, R. B. ; Coles, S. J. ; Hursthouse, M. B. ; Limmert, M. E. *Angew. Chem., Int. Ed.* **2003**, *42*, 112. (b) Lightburn, T. E. ; Dombrowski, M. T. ; Tan, K. L. *J. Am. Chem. Soc.* **2008**, *130*, 9210. (c) Grünanger, C. U. ; Breit, B. *Angew. Chem., Int. Ed.* **2008**, *47*, 7346. (d) Sun, X., Worthy, A. D. ; Tan, K. L. *Angew. Chem., Int. Ed.* **2011**, *50*, 8167. For a perspective, see : (e) Tan, K. L. *ACS Catalysis* **2011**, *1*, 877.

¹⁴⁰; MacDonald, M. J.; Schipper, D. J.; Ng, P.; Moran, J.; Beauchemin, A. M. *J. Am. Chem. Soc.* **2011**, *133*, 20100.

¹⁴¹ For reviews on temporary tether strategies, see: (a) Diederich, F. S. ; Stang, P. J. *Templated Organic Synthesis*; Wiley-VCH: Chichester, 2000. (b) Gauthier Jr, D. R. ; Zandi, K. S. ; Shea, K. J. *Tetrahedron* **1998**, *54*, 2289. (c) Bols, M. ; Skrydstrup, T. *Chem. Rev.* **1995**, *95*, 1253. (d) Fensterbank, L. ; Malacria, M. ; Sieburt, S. *Synthesis* **1997**, 813.



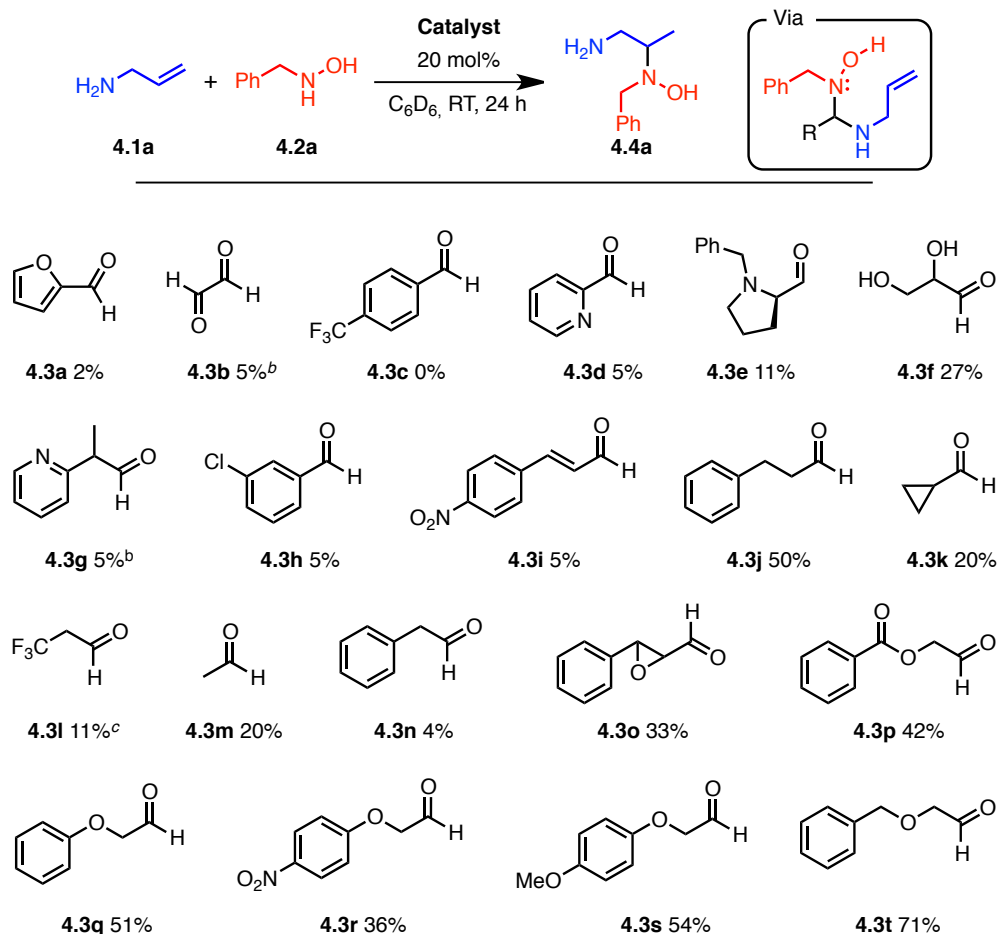
Scheme 4.9. Intermolecular Organocatalyzed Cope-Type Hydroamination

4.2 Results and Discussion

Given the lack of precedence for such complex catalytic tethering systems (Scheme 4.9) and our desire to achieve higher efficiency and enantioselectivity, we initiated mechanistic studies to probe the catalytic cycle of this transformation. This section will present a complete picture of this catalytic cycle, including information on the rate-determining step and catalyst inhibition pathways. A system that builds on this information to perform hydroamination reactions with higher catalytic efficiency than previously reported by using only 5 mol% of paraformaldehyde as pre-catalyst will also be presented.

4.2.1 Exploration of Different Competent Aldehyde Catalysts

Our interest in the development of catalytic tethering reactivity stems from ongoing efforts directed toward intermolecular Cope-type hydroamination reactions of alkenes. As discussed, strictly intermolecular reactivity is associated with multiple inherent limitations. Consequently, our efforts were naturally drawn to systems where preassociation or temporary intramolecularity could help to obtain increased reactivity. In our efforts to apply this concept to hydroamination, it was found that α -oxygenated aldehydes were essentially the only catalysts capable of providing a good yield of the desired vicinal diamine within 24 h at room temperature. Intrigued by the result of this preliminary aldehyde catalyst screening, a more thorough investigation of different aldehydes with specific properties was explored. To perform this screen, the reaction of allylamine **4.1a** with benzylhydroxylamine (**4.2a**) was studied as a hydroamination system. The results obtained are displayed in Table 4.1.

Table 4.1 Selected Examples of Aldehydes Tested for Catalytic Activity^a

^a Conditions: **4.1a** (1.5 equiv.), **4.2a** (1 equiv.), catalyst (20 mol%), C₆D₆, RT, 24 h. ^b Used as a 40% solution in water. ^c Used as the hydrate.

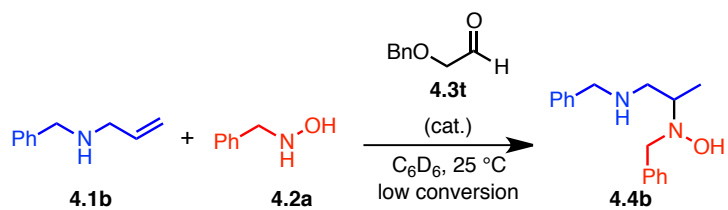
Useful information can be extracted from this study. First, it seems that aromatic or conjugated aldehydes are very inefficient at catalyzing the reaction. This could potentially be explained by the energetic price to pay to break the conjugation while trying to access the tetrahedral intermediate that can undergo hydroamination. Aliphatic aldehydes provided slightly better results with yields ranging from 11% to 50%. The best results were however obtained with α -oxygenated aldehydes. It seems like the inductive electron-withdrawing effect of the α -oxygen atom is crucial to obtain good yields. Aldehyde **4.3t**, which had been employed in the first communication of the group on the topic, still provided the best result

with a ^1H NMR yield of 71%. More electron-withdrawing substrates such as **4.3p**, **4.3q**, **4.3r** and **4.3s** were also synthesized and used as catalysts, but did not provide any improvement.

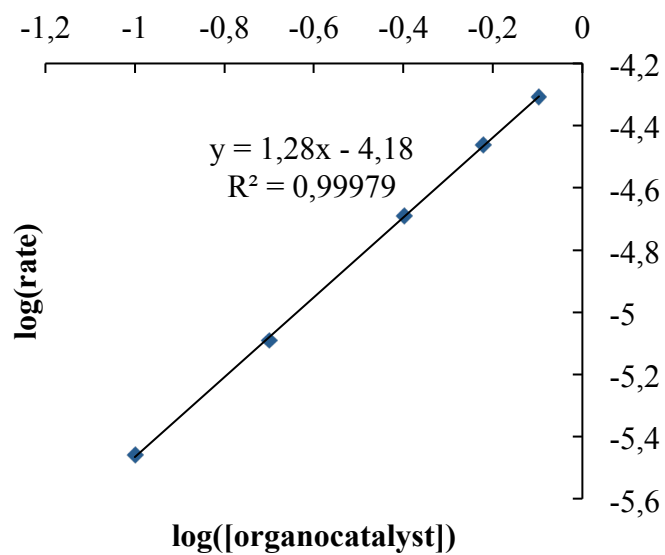
4.2.2 Kinetic Experiments

Although the prototypical catalytic cycle was based on literature precedents from the work of Knight,¹³³ the catalyst resting state and potential inhibition pathways were still unknown from this point. Further experiments were thus conducted to identify the rate-determining and kinetically significant steps of this process. To do so, the reaction of allylbenzylamine (1.5 equiv.) with benzylhydroxylamine using α -benzyloxyacetaldehyde (20 mol%) as catalyst was investigated. The typical reaction conditions employed (1 M in benzene, room temperature) are the result of a thorough optimization previously reported.¹⁴⁰

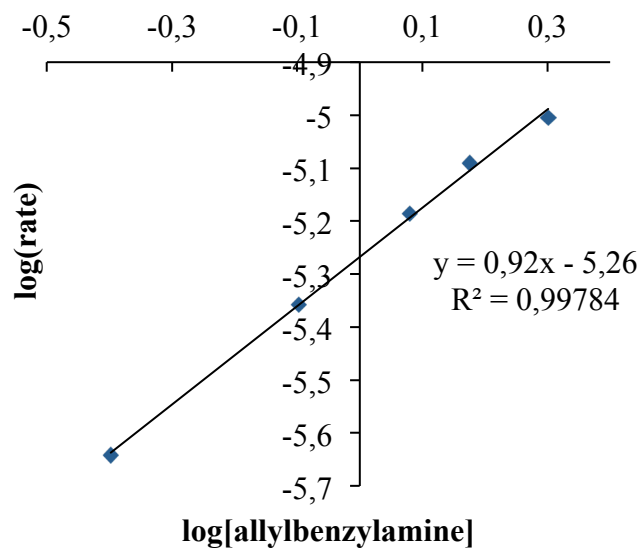
At the outset, the order of every component implicated in the reaction was evaluated (Figure 4.1). It was first determined from the linear log plot of initial rate versus the initial catalyst concentration that the reaction is approximately first order in aldehyde (Figure 4.1a). This is well in agreement with a catalytic cycle where only one molecule of aldehyde is involved prior to or at the rate-determining step. Then, drawing a log plot of the initial rate of the reaction versus the initial concentration of allylbenzylamine also gave a first order relationship (Figure 4.1b). This is again consistent with a single molecule of allylamine being involved before or at the rate-limiting step. Next, the order of benzylhydroxylamine was probed. Interestingly, an inverse order behavior was found for this reaction component (Figure 4.1c).



a)



b)



c)

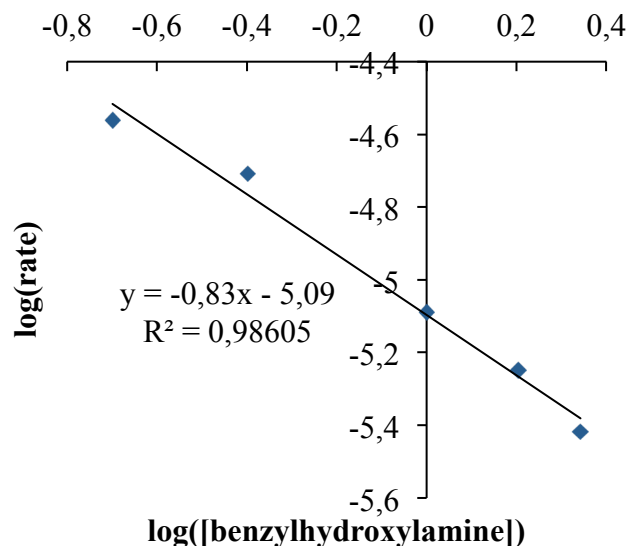


Figure 4.1 Log plot of the initial rate dependence on the concentration of the diverse reaction components showing (a) a first order dependence in organocatalyst (**4.3t**), (b) a first order dependence in allylbenzylamine (**4.1b**), and (c) an inverse order dependence in benzylhydroxylamine (**4.2a**).

To gain further insight into the reaction mechanism and explain this result, the reaction was conducted in a ^1H NMR probe using C_6D_6 as solvent (Figure 4.2). From this experiment, it was determined that nitron formation occurs rapidly upon addition of the reagents. The concentration of this intermediate can easily be monitored and it proved to be quite steady as the reaction proceeds, while still displaying a very slight increase over time. Of note, the product was formed at a constant rate for the 13 h period monitored (the ^1H NMR yield of product formation was 45% after 13 hours). This suggests that there is little to no product inhibition under the reaction conditions. This can also be well rationalized by the fact that the hydroxylamine becomes *N,N*-disubstituted as the alkene undergoes hydroamination. Thus, the product cannot interfere with nitron formation.

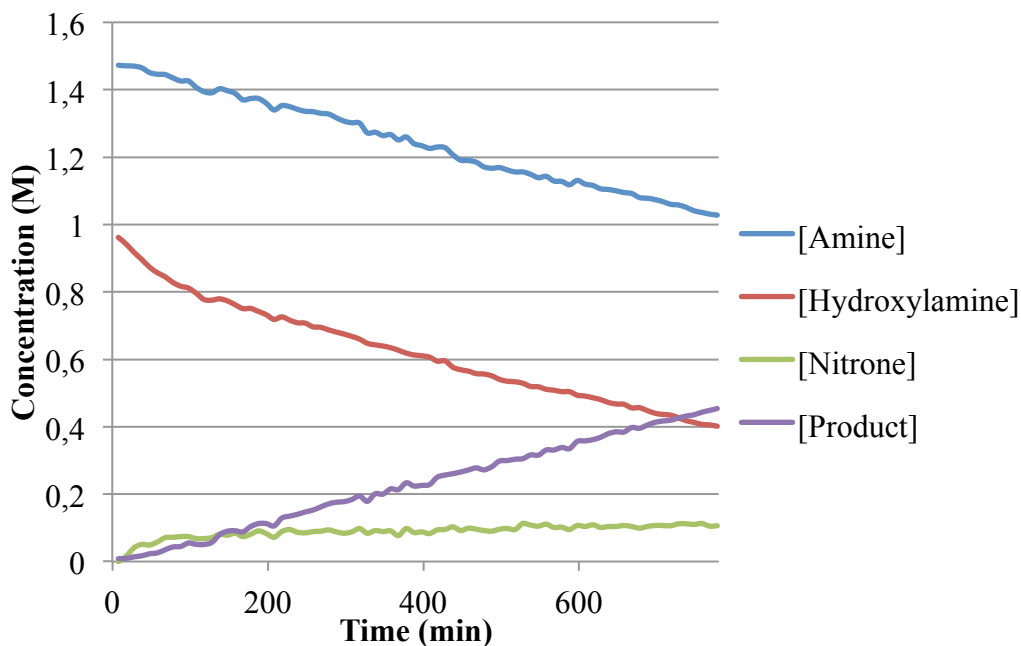
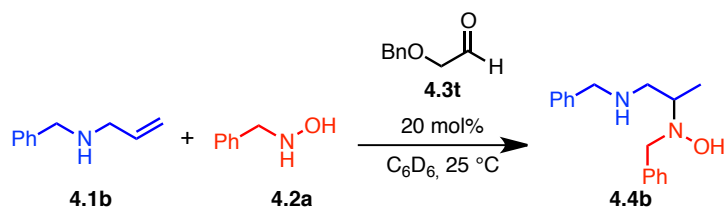


Figure 4.2 Reaction profile over 13 h period. Conditions: **4.1b** (0.75 mmol, 1.5 equiv.), **4.2a** (0.5 mmol, 1 equiv.), **4.3t** (0.1 mmol, 20 mol%) in C_6D_6 (1 M).

Taken together, these results are consistent with initial formation of nitrone **4.5a** (observed by 1H NMR) followed by the competitive addition of either benzylhydroxylamine or allylbenzylamine (Figure 4.3). The addition of benzylhydroxylamine affords an unreactive aminal (**4.6a**).¹⁴² This off-cycle pathway is (fortunately) reversible. On the other hand, the addition of allylbenzylamine leads to the formation of a key mixed aminal (**4.7a**) that can undergo the critical Cope-type hydroamination step. Of note, the addition of water to the reaction did not slow down the catalytic process. This rules out the competitive addition of water on the nitrone (or other intermediates) as a potential catalyst deactivation pathway(s).

¹⁴² For related hydroxylamine behavior, see: Turega, S. M.; Lorenz, C.; Sadownik, J. W.; Philp, D. *Chem. Commun.* **2008**, 4076.

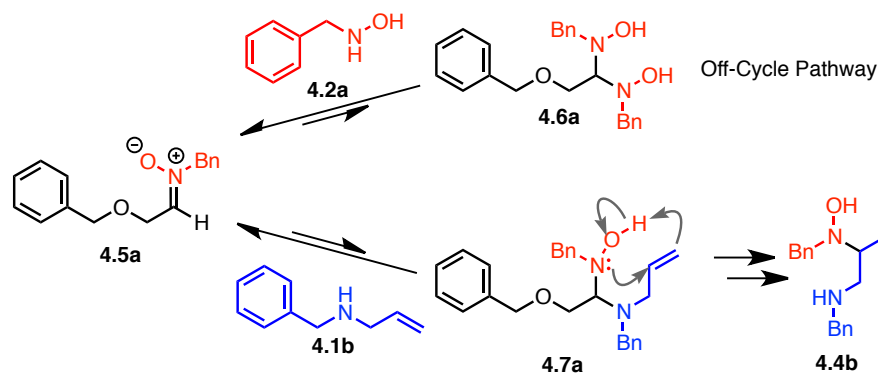
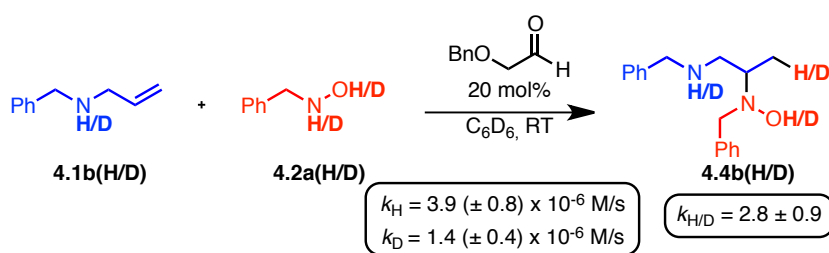


Figure 4.3 Competing 1,2-addition of **4.2a** and **4.1b** on **4.5a**, which explains the inverse order behavior in **4.2a**.

Deuterium kinetic isotope effect (DKIE) experiments were also conducted to probe the nature of the rate-determining step. All exchangeable protons of both starting materials were replaced by deuterium and the initial rate of the reaction was measured. As shown in Scheme 4.10, a primary DKIE of 2.8 ± 0.9 was obtained for this reaction. If we assume the proton transfer steps to have a low energy barrier, this result suggests that hydroamination is the rate-determining step of this catalytic process.



Scheme 4.10 DKIE Experiments

To corroborate this finding, the temperature dependence of the hydroamination reaction was monitored by ¹H NMR. The initial rate values were obtained at intervals of 10 °C between 25 and 55 °C. According to the Eyring plot generated with the data obtained (Figure 4.4), the ΔH^\ddagger of the reaction is 14.4 ± 0.9 kcal/mol and its ΔS^\ddagger value is -33 ± 3 e.u. These results are in good agreement with the values recently calculated by Krenske, Holmes,

Houk *et al.* for the intramolecular Cope-type hydroamination of alkenes through a 5-exo-trig type transition state.¹⁴³

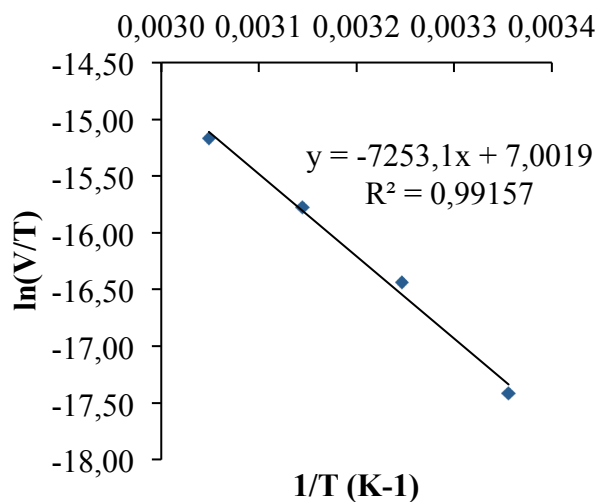
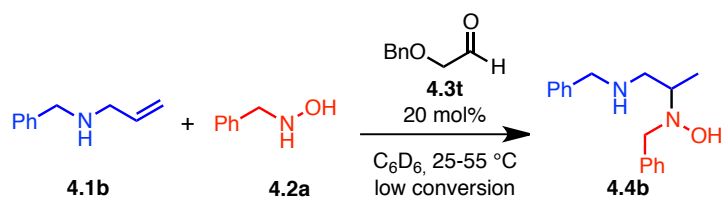
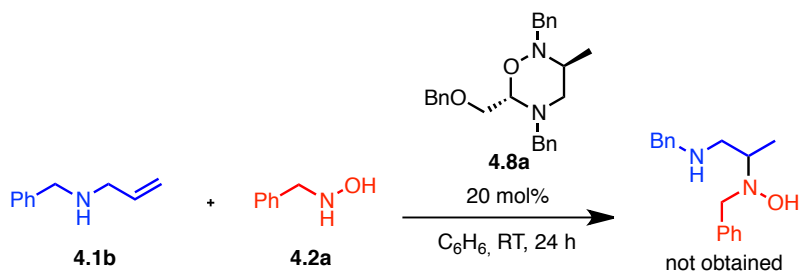


Figure 4.4 Eyring plot generated at intervals of 10 °C between 25 and 55 °C for the reaction of **4.1b** (0.75 mmol, 1.5 equiv.) and **4.2a** (0.5 mmol, 1 equiv.) in C_6D_6 (1 M) using **4.3t** (20 mol%) as catalyst.

Toward the turnover-enabling step of the originally proposed catalytic cycle (Scheme 4.9), two competing reactions can occur. The first one, which is desired, is a transimination providing the nitronc catalyst **I** and the hydroamination product. The second possibility is to generate adduct **V**, which results from a 6-endo-trig addition of the negatively charged oxygen onto the iminium ion in **IV**. The latter gives a 6-membered heterocycle (**V**) that has been extensively described by Knight. If the formation of this cyclized product is

¹⁴³ Krenske, E. H.; Davison, E. C.; Forbes, I. T.; Warner, J. A.; Smith, A. L.; Holmes, A. B.; Houk, K. N. *J. Am. Chem. Soc.* **2012**, *134*, 2434.

irreversible, this might represent an important source of catalyst inhibition. To test this, the cyclic compound **4.8a** has been synthesized according to Knight's procedure and utilized as a precatalyst for our hydroamination reaction (Scheme 4.11). Interestingly, no reaction occurred under these conditions. This observation suggests that this pathway (**IV** \rightarrow **V**) is irreversible and leads to catalyst inhibition.



Scheme 4.11 Confirmation of an Inhibition Pathway

Taking into account the results obtained herein, a more accurate catalytic cycle can now be drawn (Figure 4.5). The first step remains the fast reaction of the aldehyde precatalyst with benzyloxyamine to afford the nitron catalyst (**I**). According to the reaction monitored by 1H NMR, this nitron corresponds to the catalyst's resting state. From this point, either another molecule of benzyloxyamine or the allylamine can perform a 1,2-addition. The reaction of the later yields a mixed aminal (**II**) that can then undergo the rate-determining hydroamination. It is believed that the reason why only a limited number of aldehydes with very specific electronic properties are competent catalysts can be explained as follows. If the aldehyde is not inductively destabilized enough (i.e. aliphatic aldehydes) or very stable as is (i.e. aromatic aldehyde), the tetrahedral intermediate is present in a low concentration. Since the rate of the turnover-limiting step of the reaction is a function of the concentration of the mixed aminal **II**, a too stable aldehyde that disfavours the formation of aminals will be disadvantageous to the reaction. On the other hand, if the aldehyde is too

destabilized, it is believed that the aminal might be too stable and thus not easily returned to the nitron. As we showed that the formation of symmetrical aminal **VI** can compete with the mixed aminal **II**, a situation where the symmetrical aminal is formed and hardly returns to the nitron could be very detrimental to the reaction. It is thus important to have an aldehyde catalyst that favors preassociation while also allowing a good reversibility between the nitron and the aminal forms. In other words, an ideal catalyst would allow for a high and renewable concentration of mixed aminal **II**, which would be long-lived enough to undergo the slow hydroamination step.

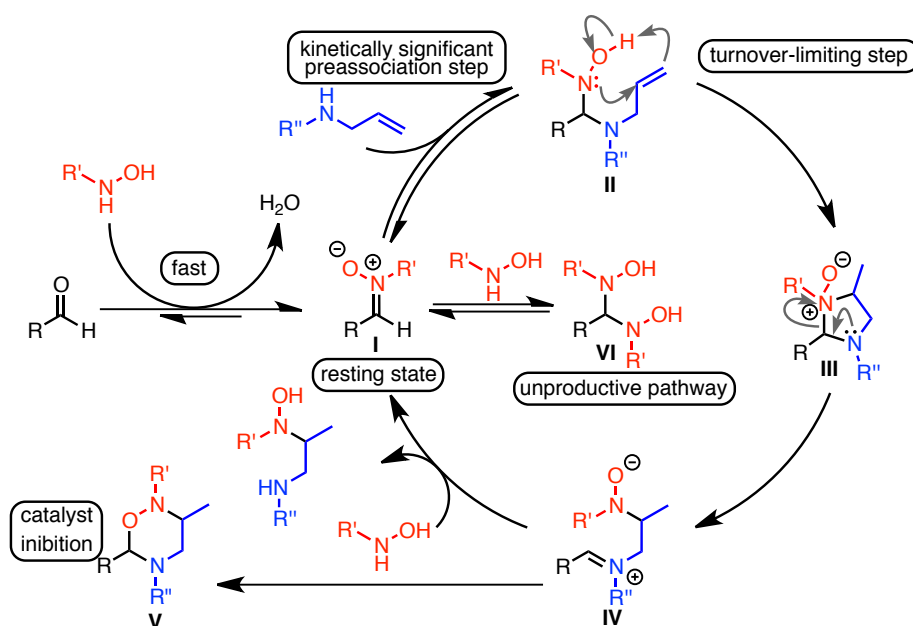


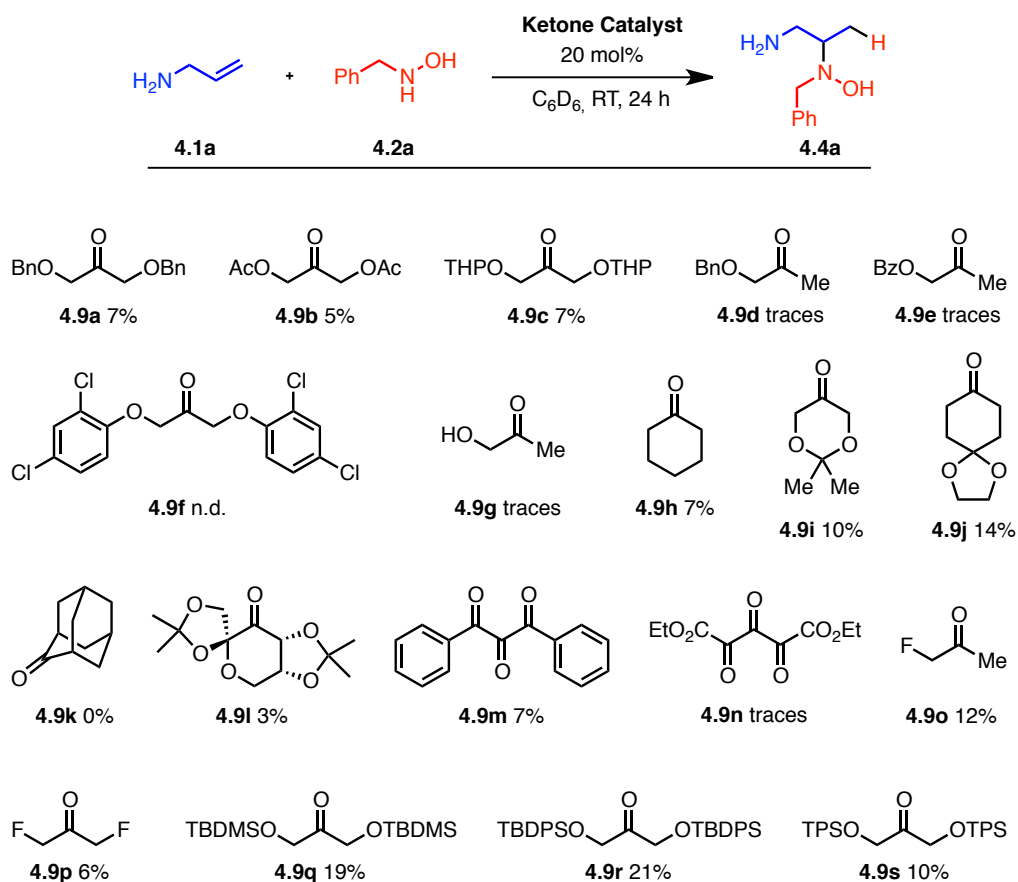
Figure 4.5 Proposed catalytic cycle.

4.2.3 Exploration of Ketone Catalysts

Having a better understanding of the operative catalytic cycle, we decided to reinvestigate the catalyst design in order to increase the speed of the reaction and hopefully

broaden its scope. It was initially thought that promoting hydroamination, the turnover-limiting step, would lead to increased reactivity. To do so, the possibility of using a ketone catalyst was explored. The rationale was to benefit from a Thorpe-Ingold effect that would favor the difficult cyclization: this is a common strategy for intramolecular hydroaminations and for Cope-type hydroaminations in particular.^{120,121}

Table 4.2 Screen of Ketone Catalysts

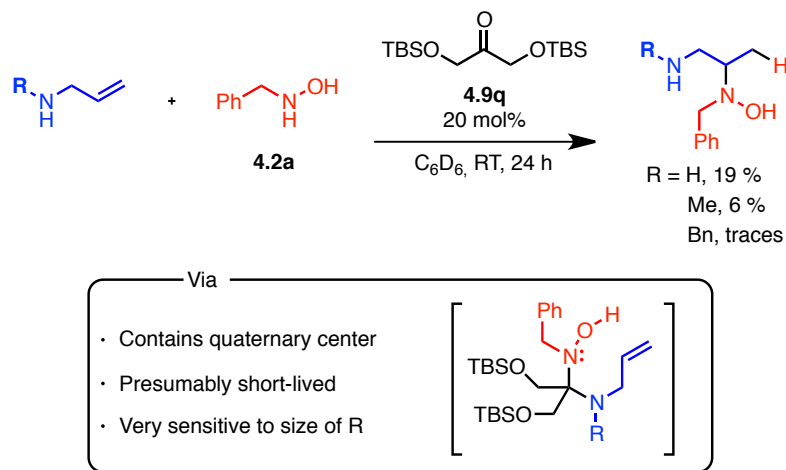


^a Conditions: **4.1a** (1.5 equiv.), **4.2a** (1 equiv.), catalyst (20 mol%), C₆D₆, RT, 24 h. ^b Used as a 40% solution in water. ^c Used as the hydrate.

Table 4.2 present the results of a ketone catalyst screening performed in the hope to find a more efficient catalyst than the aldehyde **4.3t** typically employed. A vast diversity of cyclic and acyclic inductively destabilized ketones was tested. To mimic the success obtained with the aldehyde catalysts, many α -oxygenated ketones were tried. Besides for the

silyl-protected α -oxygenated ketones, all such catalysts had very low activity providing yields in the range of traces to 7%. Similarly to the catalysts employed by Commeyras for the hydration of α -aminonitriles,^{124d,e} many cyclic ketones with different electronic properties were also tested. Again, only low yields were obtained. The best catalyst of this series, **4.9j**, gave a yield of 14%. Different types of electron-withdrawing groups were also investigated. Along these lines, triketones **4.9m** and **4.9n** gave low yields of 7% and traces of **4.4a**. 1-Fluoroacetone gave an interesting yield of 12% while 1,3-difluoroacetone only gave 6% product. The best results of this screening were obtained with silyl-protected α -oxygenated ketones. Indeed, using **4.9r**, a yield as high as 21% can be obtained, which is significantly better than all other types of ketones screened.

Given the interesting results obtained with the silyl-protected dihydroxyacetones, more experiments were conducted to evaluate the scope of this modest reactivity. Different allylamines were thus employed in the hydroamination reaction (Scheme 4.12).



Scheme 4.12 Steric Effects Using Ketone

In contrast to the results obtained with aldehyde **4.3t**, the ketone catalyst seemed to be considerably more sensitive to steric factors. Hydroamination of a primary allylamine with

benzylhydroxylamine using ketone **4.9q** provided a ^1H NMR yield of 19% over 24 hours. The use of methylallylamine (6%) and benzylallylamine (traces) gave much lower yields. This data suggests that the added steric hindrance present in the mixed aminal (increasing with $\text{R} = \text{H} < \text{Me} < \text{Bn}$) leads to an unfavorable preassociation equilibrium (**I** \rightleftharpoons **II**), and that this negative effect is more important than the probable acceleration of the Cope-type hydroamination step (**II** \rightleftharpoons **III**). As such, this observation is related to the concept of tether strain recently discussed by Krenske, Holmes, Houk *et al.* in related systems.¹⁴³

4.2.4 Bifunctional Organocatalysts

Even though low yields were obtained with ketone catalysts, the intriguing activity of silyl-protected 1,3-dihydroxyketones relative to the other ketones tested lead us to question whether another mode of activation could be present within the same catalyst. Indeed, we believe that this increased reactivity might be due to an internal Lewis acid activation of the nitron. Figure 4.6 illustrates this interaction.

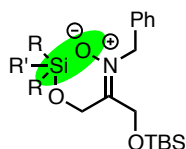
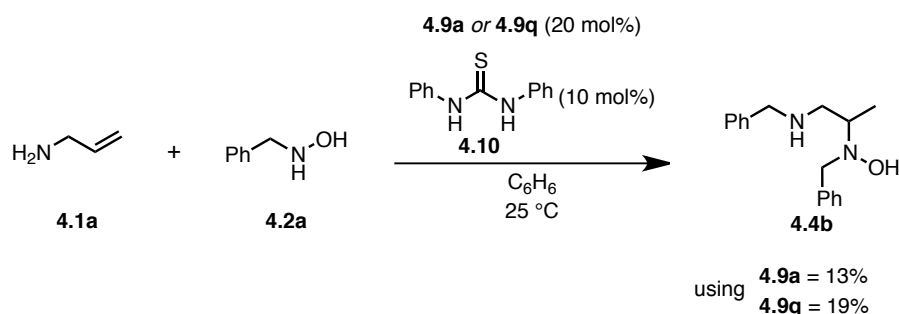


Figure 4.6 Possible Lewis acid activation of the nitron intermediate

In order to mimic this effect with other ketone catalysts that do not possess a built-in Lewis acid, an external hydrogen bonding organocatalyst was introduced as an additive in a reaction using ketone **4.9a** as a catalyst. The same experiment was also run with ketone **4.9q** as a control. It was thought that it might be possible to achieve the same kind of nitron

activation using a thiourea. This had been shown previously in the literature in the context of 1,2-additions of cyanide onto nitrones.¹⁴⁴ Scheme 4.13 summarizes the results obtained.



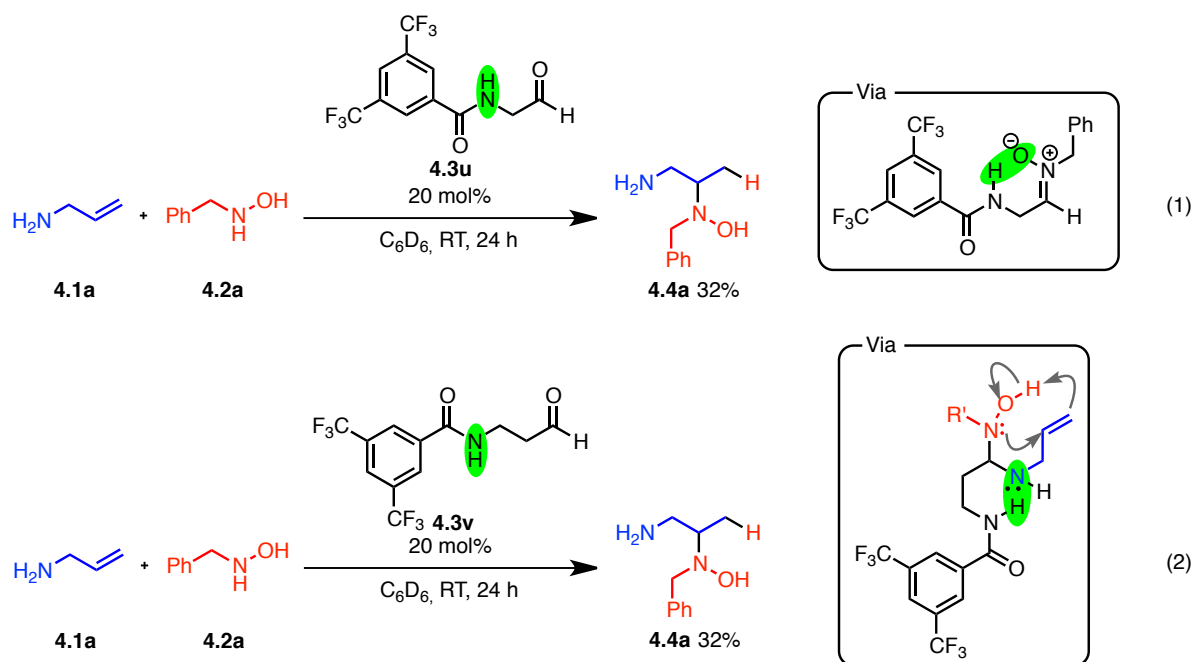
Scheme 4.13 Effect of Thiourea Co-Catalyst.

Interestingly, a 2-fold increase in yield was obtained when using **4.9a** as catalyst in conjunction with the thiourea **4.10** additive. Not only the yield is higher, but also the crude reaction mixture is much cleaner relative to the same reaction ran without thiourea. Increasing the co-catalyst loading to 20 mol% or using other ketones did not lead to any yield improvement beyond what can be obtained with ketone **4.4q** or **4.4r**. In the case where ketone **4.4q** was used with 10 mol% **4.10**, no change in the reaction outcome was provided by the hydrogen bond donor catalyst. This suggests that the beneficial impact of the thiourea co-catalyst might come from the same interaction as the silyl group has with the ketone **4.4q**.

Considering the high sensitivity of ketone catalysts toward steric factors, we wondered if a similar type of internal activation would be possible with aldehydes. The idea was to combine the good efficiency of aldehydes with an added Lewis acid activation. With that mindset, the first aldehyde tested was *tert*-butyldimethylsilyloxyacetaldehyde, which should provide a very similar activation as our best ketones. A low yield of 18% was obtained using this catalyst. Of note, there was no more benzyloxyamine (**4.2a**) present

¹⁴⁴ Okino, T.; Hoashi, Y.; Takemoto, Y. *Tetrahedron Lett.* **2003**, *44*, 2817.

in the reaction mixture after 24 h. The reason for decomposition of **4.2a** remains unclear. We thus synthesized a few other aldehydes with an internal hydrogen bond donor. We believed this could potentially activate the nitron or other intermediates of the catalytic cycle, similarly to the silicon protecting group or the thiourea co-catalyst. The structures synthesized are outlined in Scheme 4.14. In Eq. 1, aldehyde **4.3u** has a hydrogen bond donor on the nitrogen *alpha* to the carbonyl. It is thus believed that this configuration can activate the nitron via electrostatic interactions with the negatively charged oxygen, similarly to what we speculated with the silyl-protected 1,3-dihydroxyketones. The moderate yield of 32% obtained using **4.3u** cannot however allow us to conclude that such interactions are actually present. In Eq. 2, a very similar aldehyde was employed, but this time with a hydrogen bond donor that is at the *beta* position relative to the carbonyl. In this case, it was believed that an interaction with the most basic nitrogen of the mixed aminal could induce an easier hydroamination event by reducing the alkene electronic density through inductive effects. Again, a moderate yield of 36% was obtained using aldehyde **4.3v**. Consequently, we cannot confirm that this result, which is still better than the majority of aldehydes tested in Table 4.1, is due to the activation we propose. A further investigation of the possibility to use bifunctional organocatalysts should nevertheless be carried out. A better-engineered catalyst has the potential to address certain limitations of our current method. It could indeed allow for 1) faster reaction rates, 2) greater enantioselectivities through more rigid transition states, 3) broader scope that would include internal alkenes and 4) lower catalyst loadings.

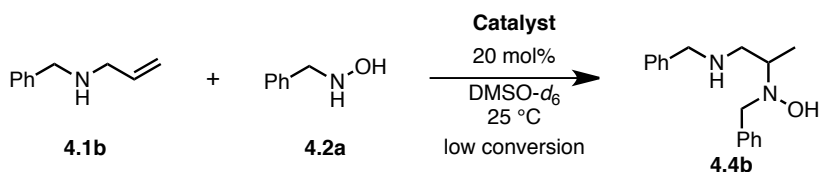


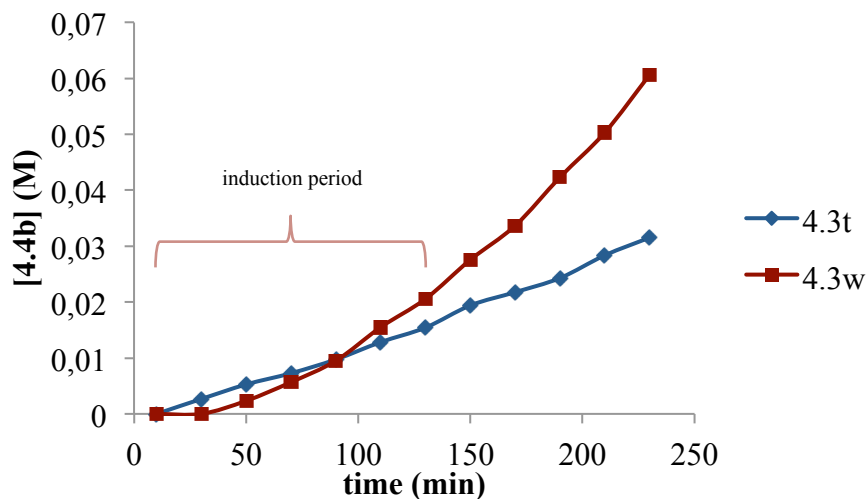
Scheme 4.14 Attempts at Internal Lewis Acid Activation

4.2.5 Formaldehyde as a More Active Catalyst

Taking the results with the ketone catalysts into account, we aimed at improving the reaction rate by favouring a high concentration of mixed aminal **II** in the reaction medium instead of increasing the rate of hydroamination. To do so, we hypothesized that using an even smaller electron-poor aldehyde would make for a more stable and long-lived mixed aminal. In accordance to the work of Commeyras *et al.* with aminoamide hydrolysis reactions¹²⁷ as well as the work of Knight on aldehyde-promoted hydroaminations of allylamine,^{133,134} we hypothesized that formaldehyde could accomplish this task. Pertinent to this idea is the fact that nitrones made from formaldehyde gave the highest rates and the broader hydroamination scope for the stoichiometric experiments performed by Knight *et al.*^{134a} Due to their instability, *in situ* generation of these nitrones from aqueous formaldehyde, benzylhydroxylamine hydrochloride and potassium carbonate was performed.

Despite the broad scope of this method, the rates were drastically diminished. To avoid such negative impact on reactivity we reasoned that, under specific conditions, paraformaldehyde could depolymerize and consequently be used as pre-catalyst. Perhaps not surprisingly, initial attempts performed by Melissa J. MacDonald (graduate student) with paraformaldehyde in C₆H₆ and CHCl₃ (i.e. original reaction conditions) resulted in low conversion. However, it was established by Valérie Lemieux (honour student) that polar solvents were superior and the use of either *t*-BuOH or DMSO led to high yields of the desired hydroamination products, with slightly better results using the *t*-BuOH. In order to compare the performance of α -benzyloxyacetaldehyde (**4.3t**) and formaldehyde (**4.3w**), the reaction rates of both catalytic systems were determined in DMSO-*d*₆. Interestingly, a three-fold rate increase at low conversion was observed using the formaldehyde-derived catalyst (Figure 4.7). Of note, the reaction where paraformaldehyde was used as a pre-catalyst required an induction time. This is likely due to the slow depolymerization of this reaction component.





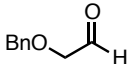
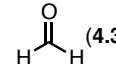
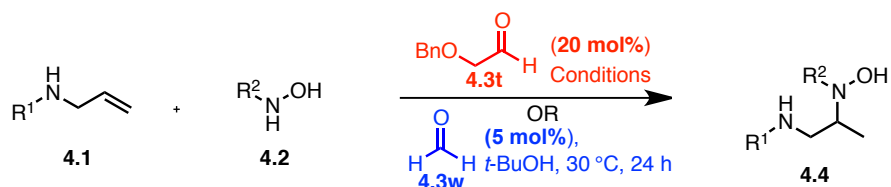
Catalyst	V_0	rel. rate
 (4.3t)	$2.38 \times 10^{-6} \text{ M/s}$	1
 (4.3w)	$6.91 \times 10^{-6} \text{ M/s}^b$	2.9

Figure 4.7 Initial rate comparison in DMSO- d_6 using **4.1b** (1.5 equiv.), **4.2a** (1 equiv.), catalyst **4.3t** or **4.3w** (20 mol%), DMSO- d_6 (1 M), 25 °C. ^b Value obtained after induction period.

Encouraged by this result, we next sought to determine if this improved reactivity would translate into improved catalytic activity. Gratifyingly, it was found that the catalyst loading in "formaldehyde" could be reduced to 5 mol% while still displaying increased yields compared to reactions using 20 mol% of α -benzyloxy-acetaldehyde (**3j**). Melissa J. MacDonald established the scope of the reaction using this more convenient catalyst. As shown in Table 2, isolated yields for alkene hydroamination using diverse secondary allylamines are significantly higher. *N*-Methyl, *N*-allyl and *N*-benzyl allylamines provided quantitative, 92% and 85% yields respectively (entries 1-3). Using various other starting materials also gave yield increases compared to the first generation conditions, albeit using 10 mol% of catalyst (entry 4-6). These results not only make for a more efficient alkene

hydroamination method, but also for a much more practical approach to vicinal diamines given that paraformaldehyde is inexpensive and readily available.

Table 4.3 Comparative Reaction Scope for the Formaldehyde-Catalyzed Cope-Type Hydroamination^{a,b}



Entry	Product	Conditions using 4.3t	Yield using 4.3t	Yield using 4.3w
1	 4.4b	C ₆ H ₆ , RT, 24 h	75%	85%
2	 4.4c	C ₆ H ₆ , RT, 24 h	72%	>98%
3	 4.4d	C ₆ H ₆ , RT, 24 h	69%	92%
4	 4.4e	CHCl ₃ , 60°C, 96 h	56%	66% ^c
5	 4.4f	CHCl ₃ , RT, 24 h	61%	74% ^c
6	 4.4g	CHCl ₃ , RT, 24 h	51%	80% ^c

^aResults obtained by Melissa J. MacDonald ^bConditions: **4.3t** catalyzed (red): Allylamine (1.5 equiv.), hydroxylamine (1 equiv.), **4.3t** (20 mol%), C₆H₆ or CHCl₃ (1 M), 24-96 h. **4.3w** catalyzed (blue): Allylamine (2 equiv.), hydroxylamine (1 equiv.), **4.3w** (5 mol%), *t*-BuOH (1 M), 30 °C, 24 h. ^cUsing 10 mol% **4.3w**.

The early development of an efficient tethering organocatalytic system operating at 5 mol% despite the presence of two different catalyst inhibition pathways suggests that this concept will be applicable to other reactions. Efforts along this path and the development of

a highly enantioselective variant of this tethered hydroamination reactivity are currently ongoing in our research group.

4.3 Summary and Outlook

In conclusion, the reaction mechanism of the recently developed aldehyde-catalyzed intermolecular Cope-type hydroaminations was investigated. Key observations that should help the development of tethering catalysis through temporary intramolecularity were made. As expected, the reaction was determined to be approximately first order in both the aldehyde catalyst (α -benzyloxyacetaldehyde) and the allylic amine. However, the reaction displays an inverse order behavior in benzyloxyamine, which reveals a significant off-cycle pathway leading to an unproductive symmetrical tether. This highlights the importance of an aldehyde catalyst that ensures reversible aminal formation. Kinetic isotope effect experiments ($k_H/k_D = 2.8 \pm 0.9$) suggest that hydroamination is the turnover-limiting step of this catalytic cycle. Generation of an Eyring plot revealed the important thermodynamic parameters associated with this slow step ($\Delta H^\ddagger = 14.4 \pm 0.9$ kcal/mol and $\Delta S^\ddagger = -33 \pm 3$ e.u.). It was also shown that while ketone catalysts are not very effective, the interesting results obtained with silyl-protected 1,3-dihydroxyacetone opened the door to the possibility of engineering bifunctional tethering organocatalysts. Finally, the overall mechanistic information obtained enabled the elaboration of a more accurate catalytic cycle and the development of a more efficient catalytic system for alkene hydroamination. Indeed, the use of 5 to 10 mol% of paraformaldehyde, a destabilized aldehyde known to hydrate or polymerize readily, proved more effective than the use of 20 mol% of α -

benzyloxyacetaldehyde, leading to high yields of intermolecular hydroamination products within 24 hours at 30 °C in *t*-BuOH.

Supporting Information

5.1 General Methods

^1H and ^{13}C spectra were recorded in CDCl_3 , C_6D_6 , Acetone- d_6 or DMSO- d_6 solutions on a Bruker AVANCE 300 MHz, a Bruker AVANCE 400 MHz, a Bruker AVANCE 500 MHz or a Variant INOVA 500 MHz. The chemical shifts are reported in parts per million (ppm) relative to the corresponding *protio*-solvent signal. High-resolution mass spectra were obtained by EI on a Kratos Concept IIIH. GCMS analyses were performed using an Agilent 5975C Series GC/MSD system. Infrared analyses were performed on an ABB Bomem Arid-Zone and the spectra were obtained as neat films on a sodium chloride window. Microwave reactions were performed on a *CEM Discover* microwave.

5.2 Rhodium(III)-Catalyzed Oxidative Synthesis of Isoquinolines

General Information

All rhodium-catalyzed isoquinoline formations were carried out without any particular precaution to exclude moisture or oxygen. Et_2O was dried and purified via an MBraun SP series solvent purification system. THF was freshly distilled from Na/benzophenone before each use. $[\text{Cp}^*\text{Rh}(\text{MeCN})_3][\text{SbF}_6]_2$ was made from $[\text{Cp}^*\text{RhCl}_2]_2$ (bought from Strem) following a literature procedure¹⁴⁵ and stored in a dessicator. All other reagents were used as is from commercial sources. Unless otherwise noted below, all other compounds have been reported in the literature or are commercially available.

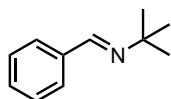
¹⁴⁵ White, C.; Thompson S. J.; Maitlis P. M. *J. Chem. Soc., Dalton Trans.* **1977**, 1654.

5.2.1 SYNTHESIS OF BENZALDIMINES

General procedure for the preparation of the *tert*-butylimines (A)

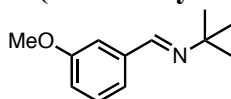
In an 8 mL screw-capped vial, the aldehyde (6 mmol, 1 eq.) was mixed with *tert*-butylamine (28.8 mmol, 4.8 eq.). The vial was sealed and the mixture was heated to 100°C for 4 hours. It was then cooled down to room temperature, diluted with Et₂O and dried over MgSO₄. After filtration, volatiles were evaporated under reduced pressure. The purification was carried out by Kugelrohr distillation. Unless otherwise mentioned, reactions following this general procedure were done on the same scale.

N-benzilidene-*tert*-butylamine (2.1a)



The reaction was carried out following general procedure A using 20 mmol (1 eq.) of the aldehyde and 96 mmol (4.8 eq.) of *tert*-butylamine to afford 2.62 g (81 %) of the desired compound. This product can also be purchased from commercial sources (CAS : 6852-58-0). ¹H NMR (400MHz, CDCl₃, 293K, TMS): δ 8.28 (1H, s), 7.78-7.70 (2H, m), 7.44-7.35 (3H, m), 1.30 (9H, s)

N-(3-methoxybenzilidene)-*tert*-butylamine (2.1b)



The reaction was carried out following general procedure A using 20 mmol (1 eq.) of 3-anisaldehyde and 96 mmol (4.8 eq.) of *tert*-Butylamine to afford 3.28 g (86 %) of the desired compound.

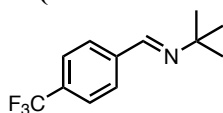
¹H NMR (400MHz, CDCl₃, 293K, TMS): δ 8.23 (1H, s), 7.36-7.33 (1H, m), 7.32-7.23 (2H, m), 6.96-6.89 (1H, m), 3.83 (3H, s), 1.29 (9H, s)

¹³C NMR (100MHz, CDCl₃, 293K, TMS): δ 159.9, 154.9, 138.7, 129.4, 121.0, 116.7, 111.7, 57.2, 55.3, 29.7

IR (ν_{max}/cm⁻¹): 2968, 2835, 1645, 1600, 1583, 1464, 1432, 1285, 1265, 1214, 1153, 1042, 781, 691

HRMS calculated for C₁₂H₁₇NO (M⁺): 191.1310; Found 191.1302

N-(4-trifluoromethylbenzilidene)-*tert*-butylamine (2.1c)



The desired compound (1.06 g, 77%) was obtained from 4-(trifluoromethyl)benzaldehyde and *tert*-butylamine following the general procedure A.

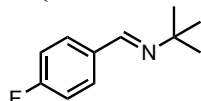
¹H NMR (400MHz, CDCl₃, 293K, TMS): δ 8.29 (1H, s), 7.85 (2H, d, *J* = 8.0 Hz), 7.64 (2H, d, *J* = 8.2 Hz), 1.31 (9H, s)

¹³C NMR (100MHz, CDCl₃, 293K, TMS): δ 153.6, 140.4, 131.82 (q, *J_F* = 32.3 Hz), 128.2, 125.5 (q, *J_F* = 3.8 Hz), 124.1 (q, *J_F* = 272.1 Hz), 57.8, 29.6

IR (ν_{max}/cm⁻¹): 2971, 2904, 1645, 1414, 1325, 1308, 1167, 1130, 1065, 836

HRMS calculated for C₁₂H₁₄F₃N (M⁺): 229.1078; Found 229.1059

N-(4-fluorobenzilidene)-*tert*-butylamine (2.1d)



The desired compound was obtained in 99% yield (1.07 g) from 4-fluorobenzaldehyde and *tert*-butylamine following general procedure A. The product was deemed pure after evaporation of the volatiles. No need for Kugelrohr distillation.

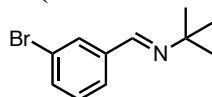
¹H NMR (400MHz, CDCl₃, 293K, TMS): δ 8.23 (1H, s), 7.77-7.70 (2H, m), 7.11-7.03 (2H, m), 1.29 (9H, s)

¹³C NMR (100MHz, CDCl₃, 293K, TMS): δ 164.0 (d, *J* = 249.7 Hz), 153.7, 133.5 (d, *J_F* = 3.0 Hz), 129.7 (d, *J_F* = 8.5 Hz), 115.5 (d, *J_F* = 21.8 Hz), 57.2, 29.7

IR (ν_{max}/cm⁻¹): 2969, 1644, 1605, 1511, 1219, 1151, 835

HRMS calculated for C₁₁H₁₄FN (M⁺): 179.1110; Found 179.1106

N-(3-bromobenzilidene)-*tert*-butylamine (2.1e)



The desired compound (1.17 g, 81 %) was obtained from 3-bromobenzaldehyde and *tert*-butylamine following the general procedure A.

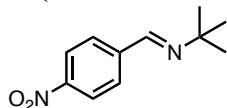
¹H NMR (400MHz, CDCl₃, 293K, TMS): δ 8.19 (1H, s), 7.94 (1H, br t, *J* = 1.7 Hz), 7.61 (1H, ddd, *J* = 7.7, 1.2, 1.2 Hz), 7.50 (1H, ddd, *J* = 8.0, 2.1, 1.1 Hz), 7.25 (1H, dd, *J* = 7.7, 7.7 Hz), 1.28 (9H, s)

¹³C NMR (100MHz, CDCl₃, 293K, TMS): δ 153.5, 139.2, 133.0, 130.4, 130.0, 126.8, 122.9, 57.5, 29.6

IR (ν_{max}/cm⁻¹): 2968, 1643, 1570, 1472, 1368, 1194, 778, 684

HRMS calculated for C₁₁H₁₄NBr (M⁺): 239.0310; Found : 239.0324

N-(4-nitrobenzilidene)-*tert*-butylamine (2.1f)



The desired compound (1.19 g, 96 %) was obtained from 4-nitrobenzaldehyde and *tert*-butylamine following general procedure A. The product was pure after evaporation of the volatiles.

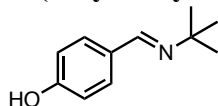
¹H NMR (400MHz, CDCl₃, 293K, TMS): δ 8.33 (1H, s), 8.28-8.23 (2H, m), 7.94-7.90 (2H, m), 1.32 (9H, s)

¹³C NMR (100MHz, CDCl₃, 293K, TMS): δ 152.9, 148.8, 142.7, 128.6, 123.8, 58.2, 29.5

IR (ν_{max}/cm⁻¹): 2970, 1600, 1532, 1346, 1203, 853, 836, 749

HRMS calculated for C₁₁H₁₄N₂O₂ (M⁺): 206.1055; Found 206.1070

N-(4-hydroxybenzylidene)-*tert*-butylamine (2.1g)



The desired compound (692 mg, 58%) was obtained from 4-hydroxybenzaldehyde and *tert*-butylamine following the general procedure A.

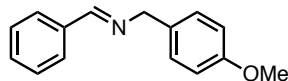
¹H NMR (400MHz, CDCl₃, 293K, TMS): δ 8.17 (1H, s), 7.53-7.47 (2H, m), 6.66-6.61 (2H, m), 1.32 (9H, s)

¹³C NMR (100MHz, DMSO-d₆, 293K, TMS): δ 159.4, 152.3, 129.3, 128.0, 115.2, 56.3, 29.7

IR (ν_{max}/cm⁻¹): 2971, 1637, 1593, 1216, 1445, 1281, 1169, 828

HRMS calculated for C₁₁H₁₅NO (M⁺): 177.1154; Found 177.1161

(*E*)-*N*-benzylidene-1-(4-methoxyphenyl)methanamine (2.1h)



Flame dried 4Å molecular sieves (15 g) were added to a solution of 4-methoxybenzylamine (14.6 mmol, 1.48 mL, 1 eq.) in CH₂Cl₂ (75 mL) under Ar. After stirring for 5 min, benzaldehyde (14.6 mmol, 2.0 g, 1 eq.) was added. The reaction mixture was stirred overnight at room temperature. It was then filtered over celite and evaporated under reduced pressure to afford the desired product as a clear oil (3.13 g, 95%).

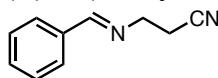
¹H NMR (400MHz, CDCl₃, 293K, TMS): δ 8.35 (1H, br t, *J* = 1.3 Hz), 7.79-7.73 (2H, m), 7.42-7.36 (3H, m), 7.26-7.22 (2H, m), 6.90-6.85 (2H, m), 4.75 (2H, s), 3.77 (3H, s),

¹³C NMR (100MHz, DMSO-d₆, 293K, TMS): δ 161.5, 158.7, 136.2, 131.3, 130.7, 129.2, 128.5, 128.2, 113.9, 64.5, 55.2

IR (ν_{max}/cm⁻¹): 2835, 1644, 1611, 1511, 1247, 1174, 1036, 817, 694

HRMS calculated for C₁₅H₁₅NO (M⁺): 225.1154; Found 225.1138

(*E*)-3-(benzylideneamino)propanenitrile (2.1i)

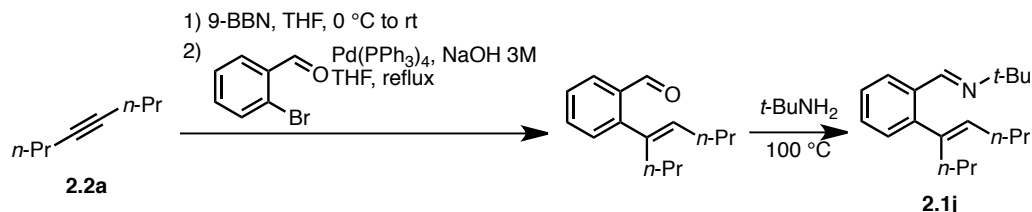


In a seal tube, 3-(Dimethylamino)propionitrile was added to a mixture of benzaldehyde (6.0 mmol, 610 μL, 1 equiv.) and MgSO₄ (1.0 g) in MeOH (2 mL). The tube was sealed and

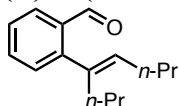
heated at 100 °C for 2h. The resulting mixture was filtered and evaporated under reduced pressure to afford **2.1i** as a clear yellow oil. Spectral data is consistent with literature.¹⁴⁶

¹H-NMR (400 MHz; CDCl₃, 293K, TMS): δ 8.36 (s, 1H), 7.75 (dd, *J* = 7.7, 1.7 Hz, 2H), 7.46-7.40 (m, 3H), 3.85 (td, *J* = 6.7, 1.3 Hz, 2H), 2.77 (t, *J* = 6.7 Hz, 2H).

Preparation of (*E*)-2-methyl-*N*-(2-((*E*)-oct-4-en-4-yl)benzylidene)propan-2-amine (**2.1j**)



(*E*)-2-(oct-4-en-4-yl)benzaldehyde



To a flame microwave tube under Ar were combined 4-octyne (2.1 mmol, 308 μL, 2.1 eq.) and 0.5 mL of THF. The solution was cooled to 0 °C and a 0.5 M solution of 9-BBN in THF (1.1 mmol, 2.2 mL, 1.1 eq.) was added dropwise. The mixture was stirred at 0 °C for 2 hours, allowed to warm to room temperature and stirred for a further 4 hours. Pd(PPh₃)₄ (0.05 mmol, 58 mg, 5 mol%), 2-bromobenzaldehyde (1 mmol, 116 μL, 1eq.) THF (2 mL) and aqueous NaOH (3 mmol, 1mL of a 3M solution, 3 eq.) were added and the reaction mixture was subjected to microwave heating (Power = 300W, temp = 125 °C, Max pressure = 250 psi, hold time = 8 min). The reaction mixture was cooled down to room temperature, brine and Et₂O were added and the aqueous layer was extracted 3 times with Et₂O. The combined organic layers were dried over MgSO₄, filtered and evaporated under reduced pressure. The crude product was purified by flash column chromatography using 1.5% EtOAc in pet. ether to afford 29.9 mg (14 %) of the desired product.

¹H NMR (400MHz, CDCl₃, 293K, TMS): δ 10.16 (1H, d, *J* = 0.7 Hz), 9.04 (1H, dd, *J* = 7.8, 1.2 Hz), 7.52 (1H, ddd, *J* = 7.5, 7.5, 1.5 Hz), 7.38-7.29 (2H, m), 5.31 (1H, t, *J* = 7.3 Hz), 2.50-2.44 (2H, m), 2.24 (2H, dt, *J* = 7.3, 7.3 Hz), 1.48 (2H, tq, *J* = 7.4, 7.4 Hz), 1.39-1.28 (2H, m), 0.97 (3H, t, *J* = 7.3 Hz), 0.89 (3H, t, *J* = 7.3 Hz)

¹³C NMR (100MHz, CDCl₃, 293K, TMS): δ 192.7, 148.9, 136.7, 135.2, 134.3, 133.2, 129.2, 127.5, 126.8, 34.6, 30.6, 22.9, 21.3, 14.2, 14.0

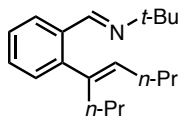
IR (ν_{max}/cm⁻¹): 2960, 2931, 2871, 1695, 1597, 1464, 1194, 763

HRMS calculated for C₁₅H₂₀O (M⁺): 216.1514; Found 216.1515

R_f: 0.35 with 3% EtOAc in pet. ether.

(*E*)-2-methyl-*N*-(2-((*E*)-oct-4-en-4-yl)benzylidene)propan-2-amine (**2.1j**)

¹⁴⁶ Huang, J.-M.; Zhang, J.-F.; Dong, Y.; Gong, W. *J. Org. Chem.* **2011**, *76*, 3511.



The desired compound was obtained in 99% yield (157 mg) from (*E*)-2-(oct-4-en-4-yl)benzaldehyde (0.587 mmol, 127 mg, 1 eq.) and *tert*-butylamine (2.82 mmol, 296 μ L, 4.8 eq.) following general procedure A. The product was pure after evaporation of the volatiles.

^1H NMR (400MHz, CDCl_3 , 293K, TMS): δ 8.45 (1H, s), 7.94 (1H, dd, $J = 7.6, 1.6$ Hz), 7.34-7.23 (2H, m), 7.17-7.14 (1H, m), 5.28 (1H, t, $J = 7.3$ Hz), 2.41-2.35 (2H, m), 2.19 (2H, dt, $J = 7.3, 7.3$ Hz), 1.46 (2H, tq, $J = 7.4$ Hz), 1.35-1.23 (11H, m), 0.97 (3H, t, $J = 7.3$ Hz), 0.87 (3H, t, $J = 7.3$ Hz)

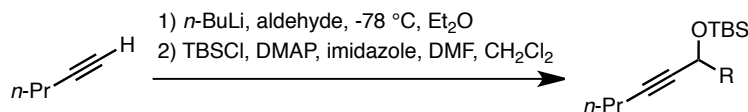
^{13}C NMR (100MHz, CDCl_3 , 293K, TMS): δ 155.6, 145.5, 138.3, 134.8, 132.6, 129.3, 128.6, 126.7, 126.5, 57.3, 34.5, 30.5, 29.8, 23.0, 21.2, 14.1, 14.0

IR ($\nu_{\text{max}}/\text{cm}^{-1}$): 2961, 2931, 2872, 1695, 1637, 1464, 1196, 760

HRMS calculated for $\text{C}_{19}\text{H}_{29}\text{N}$ (M^+): 271.2300; Found 271.2329

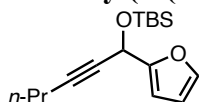
5.2.2 SYNTHESIS OF UNSYMMETRICAL ALKYNES

General procedure for the preparation of alkynes with silyl-protected alkynyl alcohols (B)



In a flame dried round-bottomed flask under Ar, 2.5 M *n*-BuLi in hexane (6.3 mmol, 2.52 mL, 1.05 eq.) was added dropwise at -78 $^{\circ}\text{C}$ to a solution of 1-pentyne (6.0 mmol, 592 μ L, 1.0 eq.) in dry Et_2O (60 mL). The reaction mixture was allowed to stir 30 min at -78 $^{\circ}\text{C}$. The aldehyde (6.3 mmol, 1.05 eq.) was then slowly added and the stirring was continued for 10 min at -78 $^{\circ}\text{C}$. The reaction mixture was then slowly warmed to room temperature and was stirred for a further 2 hours. Water was then added and the aqueous layer was extracted three times with Et_2O . The combined organic layers were dried over MgSO_4 , filtered and evaporated under reduced pressure. The crude product obtained was then diluted in dry CH_2Cl_2 (18 mL) and cooled to 0 $^{\circ}\text{C}$. 1H-imidazole (7.2 mmol, 490 mg, 1.2 eq.), DMAP (0.12 mmol, 15 mg, 0.02 eq.) and DMF (180 μ L) followed by TBSCl (7.2 mmol, 1.09 g, 1.2 eq) were added to the solution under Ar. The mixture was then warmed to room temperature and stirred for 4 hours. It was then diluted with CH_2Cl_2 and washed with water and brine. The organic phase was dried over MgSO_4 , filtered and evaporated under reduced pressure. The residue was then purified by flash column chromatography on silica gel (see below for specific eluent composition). Unless otherwise mentioned, reactions following this general procedure were done on the same scale.

tert-butyl(1-(furan-2-yl)hex-2-ynoxy)dimethylsilane (2.2b)



Following the general procedure B, the desired compound was obtained as a clear oil in 83% (1.40 g) yield after flash column chromatography on silica gel using 3% EtOAc in pet. ether.

¹H NMR (400MHz, CDCl₃, 293K, TMS): δ 7.36-7.36 (1H, m), 6.38-6.36 (1H, m), 6.33-6.30 (1H, m), 5.47-5.50 (1H, m), 2.23 (2H, td, *J* = 7.1, 2.1 Hz), 1.61-1.51 (2H, m), 1.00 (3H, t, *J* = 7.3 Hz), 0.92 (9H, s), 0.14 (6H, s)

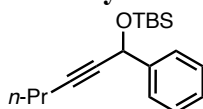
¹³C NMR (100MHz, CDCl₃, 293K, TMS): δ 154.4, 142.2, 110.1, 106.8, 85.7, 78.5, 59.2, 25.8, 21.9, 20.8, 18.4, 13.5, -4.7, -4.8

IR (*v*_{max}/cm⁻¹): 2961, 2931, 2858, 1473, 1464, 1252, 1138, 1056, 839, 777, 736

HRMS calculated for C₁₂H₁₇O₂Si ((M⁺ - *t*-Bu)): 221.0998; Found 221.0986

R_f: 0.17 with EtOAc 2% in pet. ether.

tert-butyl dimethyl(1-phenylhex-2-ynoxy)silane (2.2c)



Following the general procedure B, the desired compound was obtained as a clear oil in 86% (1.49 g) yield after flash column chromatography on silica gel using 4% Et₂O in pet. ether.

¹H NMR (400MHz, CDCl₃, 293K, TMS): δ 7.52-7.47 (2H, m), 7.37-7.30 (2H, m), 7.29-7.23 (1H, m), 5.52-5.48 (1H, m), 2.23-2.18 (2H, m), 1.50-1.49 (2H, m), 0.98 (3H, t, *J* = 7.3 Hz), 0.94 (9H, s), 0.17 (3H, s), 0.15 (3H, s)

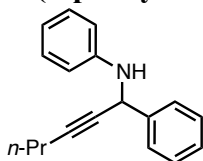
¹³C NMR (100MHz, CDCl₃, 293K, TMS): δ 142.4, 128.2, 127.4, 126.1, 86.2, 81.2, 65.0, 25.9, 22.0, 20.8, 18.4, 13.5, -4.4, -4.9

IR (*v*_{max}/cm⁻¹): 2959, 2931, 2858, 1473, 1252, 1137, 1062, 837, 778, 696

HRMS calculated for C₁₄H₁₉OSi ((M⁺ - *t*-Bu)): 231.1205; Found 231.1197

R_f: 0.24 with EtOAc 2% in pet. ether.

***N*-(1-phenylhex-2-ynyl)aniline (2.2d)**



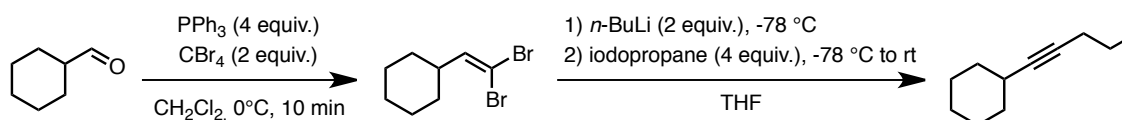
Following a literature procedure¹⁴⁷, a mixture of benzaldehyde (4 mmol, 407 μL, 1 eq.), and aniline (4.8 mmol, 437 μL, 1.2 eq.) was heated at 60 °C for about 2 hours. Then, RuCl₃•3H₂O (0.12 mmol, 30 mg, 3 mol%), CuBr (1.2 mmol, 172 mg, 30 mol%) and 1-pentyne (4.8 mmol, 473 μL, 1.2 eq.) were added into the mixture under Ar. The mixture was

¹⁴⁷ Li, C.-J.; Wei, C. *Chem. Commun.* **2002**, 268.

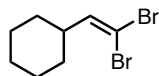
stirred at room temperature for 10 min and then at 40 °C for 16 hours. The mixture was diluted with Et₂O and washed once with water and twice with a 2 M aqueous solution of NH₄OH. The organic layer was dried over MgSO₄, filtered and evaporated under reduced pressure. The purification was carried out by flash column chromatography using 4% Et₂O in pet. ether as eluent to afford 150 mg (15%) of the desired product. Characterization data corresponds to the literature values¹⁴⁸.

¹H NMR (400MHz, CDCl₃, 293K, TMS): δ 7.61-7.55 (2H, m), 7.41-7.26 (3H, m), 7.22-7.14 (2H, m), 6.79-6.68 (3H, m), 5.25 (1H, br s), 4.04 (1H, br s), 2.19 (2H, td, *J* = 7.1, 2.1 Hz), 1.52 (2H, qt, *J* = 7.4, 7.4 Hz), 0.94 (3H, t, *J* = 7.3 Hz)

Procedure for the preparation of pent-1-ynylcyclohexane (2.2e)



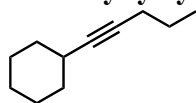
(2,2-dibromovinyl)cyclohexane



In a round-bottomed flask under Ar, PPh₃ (32 mmol, 8.39 g, 4 eq.) was added portionwise over 5 min to a solution of CBr₄ (16 mmol, 5.31 g, 2 eq.) in CH₂Cl₂ (30 mL). The resulting mixture was stirred at 0 °C for 30 min. Cyclohexanecarboxaldehyde (8 mmol, 969 μL, 1 eq.) was then added and the mixture was stirred at 0 °C for 10 min. A mixture of 1:1 water : brine was added and the layers were separated. The aqueous layer was extracted with CH₂Cl₂ and the combined organic layers were dried over MgSO₄. The volume of solvent was then doubled with pet. ether and the mixture was filtered. The filtrate was then evaporated under reduced pressure. The white solid obtained was dissolved in a minimum amount of CH₂Cl₂. Pet. ether was then added until no more white solid formation is observed. The mixture was filtered and the filtrate was evaporated under reduced pressure. The purification was carried out by flash column chromatography using 100% pet. ether as eluent. The product obtained is a clear oil (1.41 g, 66%). Spectral data is consistent with literature values¹⁴⁹.

¹H NMR (400MHz, CDCl₃, 293K, TMS): δ 6.23 (1H, d, *J* = 9.1 Hz), 2.33-2.22 (1H, m), 1.77-1.59 (5H, m), 1.37-1.05 (5H, m)

Pent-1-ynylcyclohexane (2.2e)



In a flame dried round-bottomed flask under argon, 2.5 M *n*BuLi (7.05 mmol, 2.8 mL, 2.1 eq.) was added dropwise at -78 °C to a solution of the dibromoalkene (3.36 mmol, 900 mg, 1

¹⁴⁸ Yadav, J. S.; Reddy, B. V. S.; Naveenkumar, V.; Rao, R. S.; Nagaiah, K. *New J. Chem.* **2004**, 335.

¹⁴⁹ Trost, B. M.; Livingston, R. C. *J. Am. Chem. Soc.* **2008**, *130*, 11970-11978.

eq.) in THF (17 mL). The mixture stirred at -78 °C for 1 hour. Iodopropane (13.44 mmol, 1.31 mL, 4 eq.) was added at -78°C and the mixture was warmed to room temperature. Stirring was continued overnight. Water and pet. ether were added to the mixture and the layers were separated. The aqueous layer was extracted three times with pet. ether. The combined organic fractions were dried over MgSO₄, filtered and evaporated under reduced pressure. The purification was carried out by flash column chromatography using pet. ether as eluent. The product obtained is a colorless oil (304 mg, 60%).

¹H NMR (400MHz, CDCl₃, 293K, TMS): δ 2.37-2.27 (1H, m), 2.17-2.10 (2H, m), 1.82-1.63 (4H, m), 1.56-1.20 (8H, m), 0.97 (3H, t, *J* = 7.3 Hz)

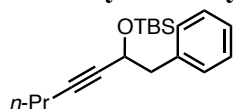
¹³C NMR (100MHz, CDCl₃, 293K, TMS): δ 84.8, 79.9, 33.2, 29.2, 26.0, 25.0, 22.6, 20.8, 13.4

IR (ν_{max}/cm⁻¹): 2931, 2854, 1449, 889

HRMS calculated for C₁₁H₁₈ (M⁺): 150.1409; Found 150.1407

R_f: 0,52 with 100% pet. ether

tert-butyldimethyl(1-phenylhept-3-yn-2-yloxy)silane (2.2f)



Following the general procedure B, the title compound was obtained as a clear oil in 17% (250 mg) yield after flash column chromatography on silica gel using 2.5% Et₂O in pet. ether.

¹H NMR (400MHz, CDCl₃, 293K, TMS): δ 7.29-7.17 (5H, m), 4.46 (1H, ddt, *J* = 7.8, 5.9, 2.0 Hz), 2.98-2.87 (2H, m), 2.16 (2H, td, *J* = 7.0, 2.0 Hz), 1.55-1.45 (2H, m), 0.95 (3H, t, *J* = 7.3 Hz), 0.83 (9H, s), -0.06 (3H, s), -0.07 (3H, s)

¹³C NMR (100MHz, CDCl₃, 293K, TMS): δ 138.1, 129.9, 128.0, 126.4, 85.1, 81.6, 64.6, 45.7, 25.8, 22.1, 20.8, 18.3, 13.5, -5.0, -5.2

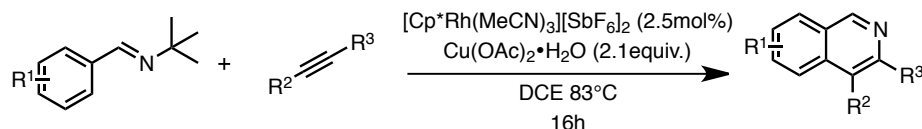
IR (ν_{max}/cm⁻¹): 2958, 2934, 2857, 1472, 1254, 1083, 835, 778

HRMS calculated for C₁₅H₂₁OSi ((M⁺ - *t*-Bu)): 245.1362; Found 245.1349

R_f: 0.21 with 2.5% Et₂O in pet. ether.

5.2.3 SYNTHESIS OF ISOQUINOLINES

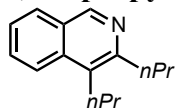
General procedure for the formation of isoquinolines (C)



To a 16x150mm test tube equipped with a stir bar was added [Cp^{*}Rh(MeCN)₃][SbF₆]₂ (6.2 mg, 0.0075 mmol, 2.5 mol%) and Cu(OAc)₂·H₂O (125.4 mg, 0.63mmol, 2.1 eq.). If the imine (0.36 mmol, 1.2 eq.) was a solid, it was also added at this point. DCE was then added followed by the alkyne and the imine, if it is a liquid. The tube

was then sealed with a rubber septum and pierced with a syringe needle to avoid excessive pressure. It was then placed in a preheated oil bath and heated at reflux for 16 hours while maintaining constant stirring. The reaction mixture was then cooled to room temperature before being diluted with Et₂O. An aqueous solution of ammonium hydroxide 2M was added and the aqueous phase was extracted with Et₂O. The combined organic layers were dried over MgSO₄, filtered and evaporated under reduced pressure. The purification was carried out by flash column chromatography on silica gel (see below for specific eluent composition).

3,4-dipropylisoquinoline (2.3a)



Following the general procedure C, the desired compound was obtained as a yellow oil after flash column chromatography on silica gel using 15% EtOAc in pet. ether.

¹H NMR (400MHz, CDCl₃, 293K, TMS): δ 9.08 (1H, s), 7.97 (1H, dd, *J* = 8.6, 0.6), 7.91 (1H, d, *J* = 8.1 Hz), 7.63-7.70 (1H, m), 7.48-7.53 (1H, m), 2.92-3.05 (4H, m), 1.77-1.87 (2H, m), 1.64-1.74 (2H, m), 1.10 (3H, t, *J* = 7.4 Hz), 1.05 (3H, t, *J* = 7.4 Hz)

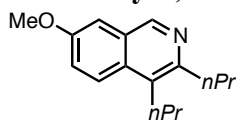
¹³C NMR (100MHz, CDCl₃, 293K, TMS): δ 153.0, 150.1, 135.4, 129.9, 128.2, 128.0, 127.2, 125.6, 123.0, 37.3, 29.9, 24.1, 23.6, 14.6, 14.3

IR (ν_{max}/cm⁻¹): 2960, 2930, 2871, 1622, 1575, 1465, 1458, 1376, 1248, 749

HRMS calculated for C₁₅H₁₉N (M⁺): 213.1518; Found 213.1522

R_f: 0.15 with 10% EtOAc in pet. ether

7-methoxy-3,4-dipropylisoquinoline (2.3b)



Following the general procedure C, the desired compound was obtained as a yellow oil after flash column chromatography on silica gel using 50% EtOAc in pet. ether.

¹H NMR (400MHz, CDCl₃, 293K, TMS): δ 8.98 (1H, s), 7.87 (1H, d, *J* = 9.3 Hz), 7.32 (1H, dd, *J* = 9.3, 2.7 Hz), 7.17 (1H, d, *J* = 2.6 Hz), 3.93 (3H, s), 2.88-3.01 (4H, m), 1.75-1.86 (2H, m), 1.61-1.72 (2H, m), 1.08 (3H, t, *J* = 7.4 Hz), 1.04 (3H, t, *J* = 7.4 Hz)

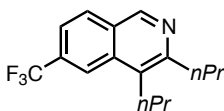
¹³C NMR (100MHz, CDCl₃, 293K, TMS): δ 157.3, 151.2, 148.7, 131.0, 128.4, 128.2, 124.8, 122.9, 105.2, 55.4, 37.1, 29.9, 24.2, 23.7, 14.6, 14.3

IR (ν_{max}/cm⁻¹): 2959, 2931, 2871, 1629, 1579, 1502, 1465, 1418, 1385, 1212, 1163, 1033, 828

HRMS calculated for C₁₆H₂₁NO (M⁺): 243.1623; Found 243.1610

R_f: 0.27 with 50% EtOAc in pet. ether

3,4-dipropyl-6-(trifluoromethyl)isoquinoline (2.3c)



Following the general procedure C, the desired compound was obtained as a yellow oil after flash column chromatography on silica gel using 15% EtOAc in pet. ether.

¹H NMR (400MHz, CDCl₃, 293K, TMS): δ 9.16 (1H, s), 8.25 (1H, m), 8.04 (1H, d, *J* = 8.5 Hz), 7.69 (1H, dd, *J* = 8.5, 1.2 Hz), 3.09-2.95 (4H, m), 1.89-1.77 (2H, m), 1.75-1.64 (2H, m), 1.11 (3H, t, *J* = 7.4), 1.05 (3H, t, *J* = 7.4 Hz),

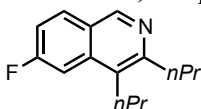
¹³C NMR (100MHz, CDCl₃, 293K, TMS): δ 154.7, 150.0, 134.5, 131.5 (q, *J* = 32.2 Hz), 129.4, 128.9, 127.9, 124.1 (q, *J* = 272.7 Hz), 121.4 (q, *J* = 3.1 Hz), 120.9 (q, *J* = 4.6 Hz), 37.3, 29.8, 24.3, 23.5, 14.5, 14.3,

IR (ν_{max}/cm⁻¹): 2969, 2874, 1584, 1369, 1308, 1281, 1185, 1160, 1130, 1071, 895

HRMS calculated for C₁₆H₁₈F₃N (M⁺): 281.1391; Found 281.1372

R_f: 0.38 with 20% EtOAc in pet. ether

6-fluoro-3,4-dipropylisoquinoline (2.3d)



Following the general procedure C, the desired compound was obtained as a yellow oil after flash column chromatography on silica gel using 20% EtOAc in pet. ether.

¹H NMR (400MHz, CDCl₃, 293K, TMS): δ 9.04 (1H, s), 7.92 (1H, dd, *J* = 8.9, 5.9 Hz), 7.54 (1H, dd, *J* = 11.2, 2.3 Hz), 7.31-7.24 (1H, m), 2.97-2.91 (4H, m), 1.86-1.75 (2H, m), 1.72-1.61 (2H, m), 1.10 (3H, t, *J* = 7.3 Hz), 1.04 (3H, t, *J* = 7.3 Hz)

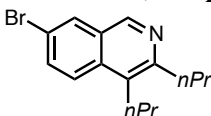
¹³C NMR (100MHz, CDCl₃, 293K, TMS): δ 163.4 (d, *J* = 250.2 Hz), 153.9, 149.7, 137.0 (d, *J* = 9.5 Hz), 131.1 (d, *J* = 9.9 Hz), 127.7 (d, *J* = 5.6 Hz), 124.5, 116.1 (d, *J* = 25.7 Hz), 106.9 (d, *J* = 21.7), 37.4, 30.1, 23.8, 23.5, 14.6, 14.3

IR (ν_{max}/cm⁻¹): 2961, 2932, 2872, 1630, 1578, 1501, 1434, 1245, 1226, 1194, 861

HRMS calculated for C₁₅H₁₈FN (M⁺): 231.1423; Found 231.1416

R_f: 0.26 with 20% EtOAc in pet. ether

7-bromo-3,4-dipropylisoquinoline (2.3e)

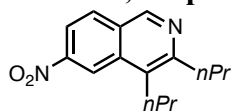


Following the general procedure C, the desired compound was obtained as a yellow solid after flash column chromatography on silica gel using 10% EtOAc in pet. ether.

¹H NMR (400MHz, CDCl₃, 293K, TMS): δ 9.00 (1H, s), 8.06 (1H, d, *J* = 2.0 Hz), 7.84 (1H, d, *J* = 9.1 Hz), 7.72 (1H, dd, *J* = 9.1, 2.1 Hz), 3.02-2.90 (4H, m), 1.86-1.75 (2H, m), 1.72-1.60 (2H, m), 1.09 (3H, t, *J* = 7.3 Hz), 1.04 (3H, t, *J* = 7.3 Hz)

¹³C NMR (100MHz, CDCl₃, 293K, TMS): δ 153.6, 149.0, 133.9, 133.3, 130.1, 128.3, 128.2, 125.1, 119.3, 37.3, 29.8, 24.1, 23.4, 14.6, 14.3
IR (ν_{max}/cm⁻¹): 2960, 2930, 2871, 1571, 1470, 1087, 904 824
HRMS calculated for C₁₅H₁₈BrN (M⁺): 291.0623; Found 291.0591
R_f: 0.46 with 15% EtOAc in pet. ether
Melting Point : 37-39 °C

6-nitro-3,4-dipropylisoquinoline (2.3f)



Following the general procedure C, the desired compound was obtained as a yellow oil after flash column chromatography on silica gel using 20% EtOAc in pet. ether.

¹H NMR (400MHz, CDCl₃, 293K, TMS): δ 9.22 (1H, s), 8.93-8.90 (1H, m), 8.27 (1H, dd, *J* = 8.9, 2.1 Hz), 8.08 (1H, d, *J* = 8.9 Hz), 3.13-3.06 (2H, m), 3.03-2.97 (2H, m), 1.89-1.79 (2H, m), 1.78-1.66 (2H, m), 1.14 (3H, t, *J* = 7.3 Hz), 1.06 (3H, t, *J* = 7.3 Hz)

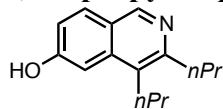
¹³C NMR (100MHz, CDCl₃, 293K, TMS): δ 155.6, 150.0, 148.4, 134.7, 130.2, 130.0, 128.6, 120.0, 119.1, 37.3, 29.9, 24.5, 23.4, 14.5, 14.3

IR (ν_{max}/cm⁻¹): 2967, 2936, 2874, 1576, 1533, 1424, 1345, 740

HRMS calculated for C₁₅H₁₈N₂O₂ (M⁺): 258.1368; Found 258.1374

R_f: 0.23 with 20% EtOAc in pet. ether

3,4-dipropylisoquinolin-6-ol (2.3g)



Following the general procedure C, the desired compound was obtained as a yellow solid after flash column chromatography on silica gel using 10% *i*PrOH in toluene.

¹H NMR (400MHz, CDCl₃, 293K, TMS): δ 8.92 (1H, s), 7.81 (1H, d, *J* = 8.8 Hz), 7.28 (1H, d, *J* = 2.0 Hz), 7.19 (1H, dd, *J* = 8.8, 2.2 Hz), 2.96-2.90 (2H, m), 2.89-2.82 (2H, m), 1.84-1.73 (2H, m), 1.67-1.56 (2H, m), 1.03-0.94 (6H, m)

¹³C NMR (100MHz, CDCl₃, 293K, TMS): δ 161.3, 150.9, 147.8, 138.4, 130.5, 127.9, 122.2, 119.9, 105.3, 36.3, 30.1, 23.9, 23.5, 14.5, 14.3

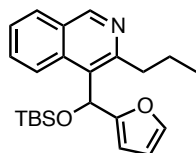
IR (ν_{max}/cm⁻¹): 2959, 2928, 2877, 1617, 1458, 1438, 1396, 1240, 1144, 851, 727

HRMS calculated for C₁₅H₁₉NO (M⁺): 229.1467; Found 229.1444

R_f: 0.24 with 10% *i*PrOH in toluene

Melting Point : decomposes at 152 °C

4-((*tert*-butyldimethylsilyloxy)(furan-2-yl)methyl)-3-propylisoquinoline (2.3h)



Following the general procedure C, the title compound was obtained as a yellow solid after flash column chromatography on silica gel using 10% EtOAc in pet. ether.

¹H NMR (400MHz, CDCl₃, 293K, TMS): δ 9.15 (1H, s), 8.54 (1H, d, *J* = 8.5 Hz), 7.91-7.88 (1H, m), 7.58-7.53 (1H, m), 7.51-7.46 (1H, m), 7.55 (1H, ddd, *J* = 8.6, 6.8, 1.5 Hz), 7.49 (1H, ddd, *J* = 8.0, 6.8, 1.2 Hz), 7.32-7.30 (1H, m), 6.52 (1H, s), 6.27-6.24 (1H, m), 6.03-6.01 (1H, m), 3.06-3.00 (2H, m), 1.85-1.71 (2H, m), 1.01 (3H, t, *J* = 7.3 Hz), 0.85 (9H, s), 0.16 (3H, s), -0.16 (3H, s)

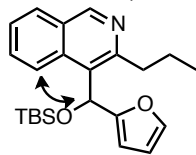
¹³C NMR (100MHz, CDCl₃, 293K, TMS): δ 156.2, 152.6, 152.3, 141.9, 135.1, 129.3, 128.0, 127.7, 126.8, 126.4, 125.0, 110.2, 107.0, 67.6, 38.0, 25.7, 23.6, 18.2, 14.4, -4.9, -4.9

IR (ν_{max}/cm⁻¹): 2957, 2930, 2857, 1624, 1578, 1472, 1253, 1145, 1071, 1044, 1005, 939, 839, 778, 748

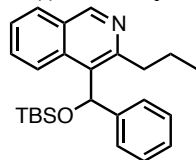
HRMS calculated for C₂₃H₃₁NO₂Si (M⁺): 381.2124; Found 381.2106

R_f: 0.20 with 10% EtOAc in pet. ether

NOESY (400MHz, CDCl₃, 293K, TMS)



4-((*tert*-butyldimethylsilyloxy)(phenyl)methyl)-3-propylisoquinoline (2.3i)



Following the general procedure C, the desired compound was obtained as a yellow solid after flash column chromatography on silica gel using 10% EtOAc in pet. ether.

¹H NMR (400MHz, CDCl₃, 293K, TMS): δ 9.17 (1H, s), 8.18-8.13 (1H, m), 7.91-7.85 (1H, m), 7.48-7.41 (2H, m), 7.33-7.24 (4H, m), 7.23-7.17 (1H, m), 6.61 (1H, s), 3.06 (2H, t, *J* = 8.2 Hz), 1.90-1.66 (2H, m), 1.01 (3H, t, *J* = 7.3 Hz), 0.88 (9H, s), 0.16 (3H, s), -0.38 (3H, s)

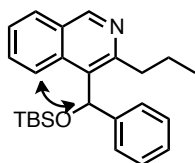
¹³C NMR (100MHz, CDCl₃, 293K, TMS): δ 152.3, 144.5, 134.8, 129.4, 129.0, 128.1, 128.0, 127.8, 126.6, 125.9, 125.6, 71.3, 37.8, 25.8, 23.5, 18.3, 14.5, -4.7, -5.0 (2 carbons missing due to overlapping)

IR (ν_{max}/cm⁻¹): 2957, 2929, 2857, 1622, 1579, 1493, 1472, 1252, 1099, 1066, 854, 835, 776, 750, 708

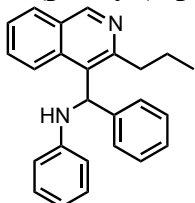
HRMS calculated for C₂₅H₃₃NOSi (M⁺): 391.2331; Found 391.2308

R_f: 0.19 with 10% EtOAc in pet. ether

NOESY (400MHz, CDCl₃, 293K, TMS)



***N*-(phenyl(3-propylisoquinolin-4-yl)methyl)aniline (2.3j)**



Following the general procedure C, the title compound was obtained as a yellow solid after flash column chromatography on silica gel using 30% EtOAc in pet. ether.

¹H NMR (400MHz, CDCl₃, 293K, TMS): δ 9.18 (1H, s), 7.99-7.91 (2H, m), 7.53-7.44 (2H, m), 7.36-7.15 (7H, m), 6.79-6.73 (1H, m), 6.66-6.62 (2H, m), 6.31-6.27 (1H, br d, *J* = 3 Hz), 4.43-4.37 (1H, br d), 3.17-3.00 (2H, m), 1.84-1.51 (2H, m), 0.91 (3H, t, *J* = 7.3 Hz)

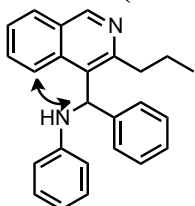
¹³C NMR (100MHz, CDCl₃, 293K, TMS): δ 154.1, 152.2, 148.2, 142.7, 134.2, 130.4, 129.4, 128.6, 128.5, 128.5, 128.3, 126.7, 126.6, 126.1, 124.5, 118.0, 113.1, 57.3, 38.8, 23.8, 14.3

IR (ν_{max}/cm⁻¹): 3062, 3028, 2958, 2935, 2871, 1602, 1501, 1449, 1311, 1251, 905, 750, 724, 694

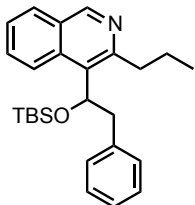
HRMS calculated for C₂₅H₂₄N₂ (M⁺): 352.1940; Found 352.1921

R_f: 0.33 with 30% EtOAc in pet. ether

NOESY (400MHz, CDCl₃, 293K, TMS)



4-(1-(*tert*-butyldimethylsilyloxy)-2-phenylethyl)-3-propylisoquinoline (2.3k)



Following the general procedure C, the title compound was obtained as a yellow solid after flash column chromatography on silica gel using 12% EtOAc in pet. ether

¹H NMR (400MHz, CDCl₃, 293K, TMS): δ 9.10 (1H, s), 8.98-8.93 (1H, m), 7.92 (1H, d, *J* = 8.2 Hz), 7.67 (1H, ddd, *J* = 8.6, 6.8, 1.4 Hz), 7.54 (1H, ddd, *J* = 8.0, 6.9, 1.0), 7.32-7.17 (5H, m), 5.51 (1H, dd, *J* = 9.2, 4.6 Hz), 3.46 (1H, dd, *J* = 13.5, 9.2 Hz), 3.08 (1H, dd, *J* =

13.5, 4.5 Hz), 2.92-2.78 (2H, m), 1.88-1.59 (2H, m), 1.06 (3H, t, $J = 7.3$ Hz), 0.69 (9H, s), -0.26 (3H, s), -0.45 (3H, s)

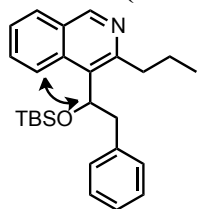
^{13}C NMR (100MHz, CDCl_3 , 293K, TMS): δ 151.8, 151.1, 139.0, 134.7, 129.7, 129.3, 129.1, 128.2, 128.2, 128.1, 126.8, 126.4, 125.9, 74.1, 45.3, 37.6, 25.7, 23.3, 18.0, 14.6, -5.1, -5.5

IR ($\nu_{\text{max}}/\text{cm}^{-1}$): 2957, 2928, 2856, 1576, 1472, 1251, 1080, 937, 835, 777, 752, 698

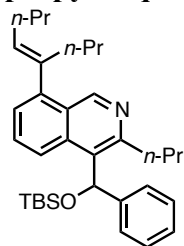
HRMS calculated for $\text{C}_{26}\text{H}_{35}\text{NOSi}$ ($(\text{M}^+ - t\text{-Bu})$): 348.1784; Found 348.1787

R_f : 0.21 with 10% EtOAc in pet. ether.

NOESY (400MHz, CDCl_3 , 293K, TMS)



(*E*)-4-((*tert*-butyldimethylsilyloxy)(phenyl)methyl)-8-(oct-4-en-4-yl)-3-propylisoquinoline (2.31)



Following the general procedure C, the desired compound was obtained as a yellow oil after flash column chromatography on silica gel using 4% EtOAc in pet. ether.

^1H NMR (400MHz, CDCl_3 , 293K, TMS): δ 9.36 (1H, d, $J = 0.7$ Hz), 8.04 (1H, br d, $J = 8.7$ Hz), 7.40-7.24 (5H, m), 7.23-7.14 (2H, m), 6.62 (1H, s), 5.49 (1H, t, $J = 7.3$ Hz), 3.03 (2H, t, $J = 8.3$ Hz), 2.51 (2H, t, $J = 7.5$ Hz), 2.27 (2H, td, $J = 7.3$ Hz), 1.91-1.69 (2H, m), 1.51 (2H, tq, $J = 7.3, 7.3$ Hz), 1.35-1.23 (2H, m), 1.00 (6H, t, $J = 7.3$ Hz), 0.90-0.84 (12H, m), 0.15 (3H, s), -0.39 (3H, s)

^{13}C NMR (100MHz, CDCl_3 , 293K, TMS): δ 151.0, 144.7, 143.8, 138.0, 135.1, 132.7, 128.8, 128.8, 128.1, 126.6, 126.4, 125.7, 125.4, 71.3, 37.8, 35.0, 30.5, 25.9, 23.5, 23.0, 21.6, 18.3, 14.6, 14.1, 14.1 (2 ^{13}C missing even after extensive scanning)

IR ($\nu_{\text{max}}/\text{cm}^{-1}$): 2958, 2931, 2871, 1670, 1452, 1264

HRMS calculated for $\text{C}_{33}\text{H}_{47}\text{NOSi}$ ($(\text{M} - t\text{-BDMS})^+$): 386.2484; Found 386.2430

R_f : 0.53 with 10% EtOAc in pet. ether.

5.3 Rhodium(III)-Catalyzed Redox-Neutral Synthesis of Nitrogen-Containing Heterocycles

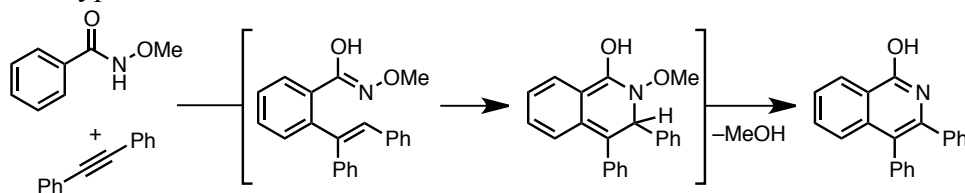
General Information

All rhodium-catalyzed isoquinolone formations were carried out without any particular precautions to extrude moisture or oxygen. Toluene was dried and purified via an MBraun SP series solvent purification system. $[\text{Cp}^*\text{RhCl}_2]_2$ was prepared from $\text{RhCl}_3 \cdot x\text{H}_2\text{O}$ (bought from Pressure Chemicals) following a literature procedure¹⁵⁰ and stored in a desiccator. $[\text{Cp}^*\text{RhCl}_2]_2$ could alternatively be bought from Strem Chemicals. All other reagents were used as is from commercial sources. Unless otherwise noted below, all other compounds have been reported in the literature or are commercially available.

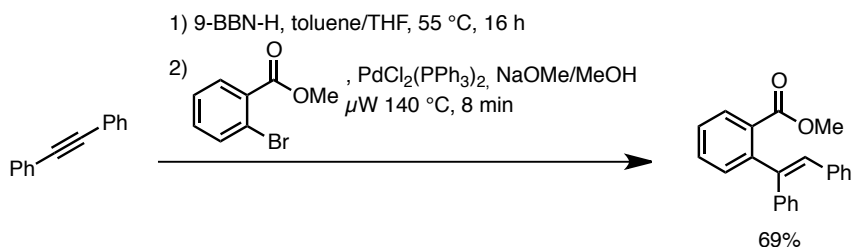
5.3.1 MECHANISTIC EXPERIMENTS OF SECTION 3.2.2

Electrocyclization Experiment

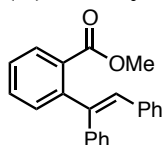
Mechanistic Hypothesis:



Preparation of the starting material



(E)-Methyl 2-(1,2-diphenylvinyl)benzoate



In a flame dried microwave tube under Ar was added diphenylacetylene (2.10 mmol, 374 mg, 1.05 equiv.). A 0.5M solution of 9-BBN-H (2.10 mmol, 4.2 mL, 1.05 equiv.) in THF

¹⁵⁰ Fujita, K.-I.; Takahashi, Y.; Owaki, M.; Yamamoto, K.; Yamaguchi, R. *Org. Lett.* **2004**, *6*, 2785.

was then added via syringe and the resulting mixture was allowed to stir at 55°C for 16h. Then, methyl-2-bromobenzoate (2.00 mmol, 281 μ L, 1 equiv.) was added, followed by PdCl₂(PPh₃) (0.10 mmol, 70.2 mg, 0.05 equiv.), and MeONa (6.00 mmol, 324 mg, 3 equiv.) in MeOH (2mL). The tube was sealed and heated in the microwave at 140°C (300W, hold time 8 min). The mixture was diluted with ether and washed with sat. NH₄Cl. The organic phase was dried over MgSO₄, filtered and evaporated under reduced pressure. The resulting mixture was purified by flash column chromatography using 2% EtOAc in pet. ether. The product obtained is a white solid (431 mg, 69%).

¹H NMR (400 MHz, CDCl₃, 293K, TMS): δ 7.69 (1H, ddd, J = 7.6, 1.4, 0.5 Hz), 7.44 (1H, td, J = 7.5, 1.5 Hz), 7.37-7.33 (2H, m), 7.22-7.10 (10H, m), 6.63 (1H, s), 3.59 (3H, s)

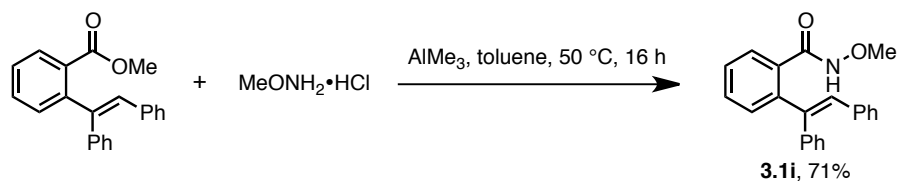
¹³C NMR (100 MHz, CDCl₃, 293K, TMS): δ 169.2, 144.5, 142.2, 139.8, 137.4, 131.9, 130.9, 130.9, 130.4, 129.6, 129.5, 129.4, 128.0, 128.0, 127.3, 127.3, 126.9, 52.0

IR (v_{max}/cm⁻¹): 3062, 3025, 2951, 1727, 1290, 1257, 1124, 1084, 698

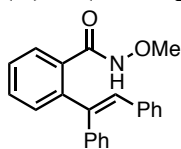
HRMS calculated for C₂₂H₁₈O₂ (M⁺): 314.1307; Found 314.1329

R_f: 0.25 with 5% EtOAc in pet. ether

Melting Point: 60-62 °C



(E)-2-(1,2-Diphenylvinyl)-N-methoxybenzamide (3.1i)



Under Ar, a 2.0M solution of AlMe₃ in toluene (4.45 mmol, 2.23 mL, 7 equiv.) was added dropwise to a suspension of methoxyamine hydrochloride (4.45 mmol, 370 mg, 7 equiv.) in dry toluene. The resulting mixture was stirred at rt for 1 hour. Then, (*E*)-Methyl 2-(1,2-diphenylvinyl)benzoate (0.64 mmol, 200 mg, 1 equiv.) in a minimum amount of toluene was added to the mixture via syringe after which the reaction was stirred at 50°C for 16h. The reaction mixture was carefully quenched with a 10% solution of HCl. It was then diluted with CH₂Cl₂ and water. The aqueous phase was washed three time with CH₂Cl₂. The combined organic fractions were dried over MgSO₄, filtered and evaporated under reduced pressure. The purification was performed by flash column chromatography using 40% EtOAc in pet. ether. The product obtained is a white solid (149.2 mg, 71%).

¹H NMR (400 MHz, CDCl₃, 293K, TMS): δ 8.34 (1H, br s), 7.51-7.38 (2H, m), 7.38-7.29 (2H, m), 7.25-7.06 (10H, m), 6.78 (1H, s), 3.50 (3H, s)

¹³C NMR (100 MHz, CDCl₃, 293K, TMS): δ 167.4, 143.1, 141.1, 139.4, 136.9, 132.9, 131.1, 131.0, 130.5, 129.4, 128.6, 128.3, 128.1, 127.7, 127.7, 127.2, 64.4 (1 signal missing due to overlap)

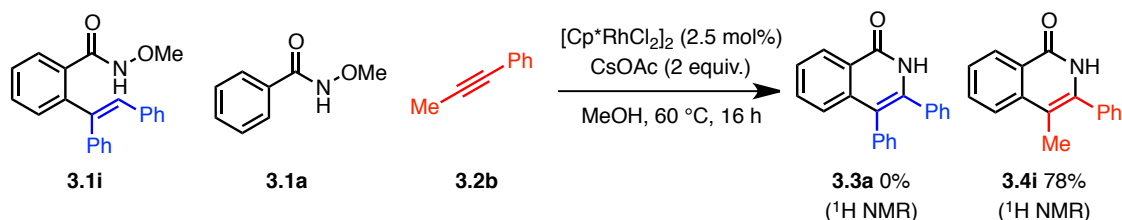
IR (v_{max}/cm⁻¹): 3186, 1657, 1492, 1442, 761, 724, 697

HRMS calculated for C₂₂H₁₉NO₂ (M⁺): 329.1416; Found 329.1395

R_f: 0.27 with 40% EtOAc in pet. ether

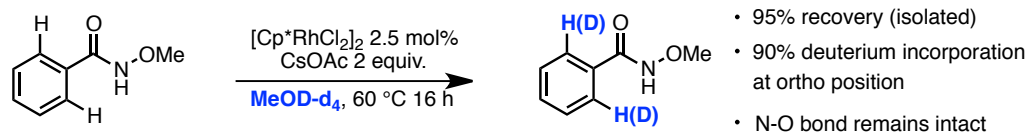
Melting Point: 119-122 °C

Electrocyclization Experimental Refutation

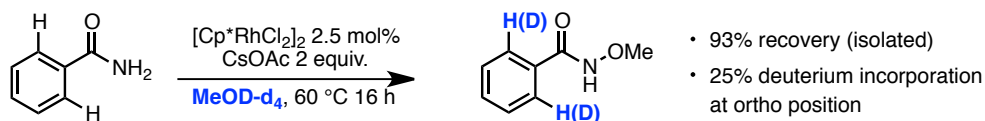


Without any particular precautions to extrude oxygen or moisture, **S2** (33 mg, 0.10 mmol, 0.5 equiv.), **1a** (30 mg, 0.20 mmol, 1 equiv.), **2b** (28 uL, 0.22 mmol, 1.1 equiv.), $[\text{Cp}^*\text{RhCl}_2]_2$ (3.1 mg, 0.005 mmol, 2.5 mol%) and CsOAc (77 mg, 0.40 mmol, 2 equiv.) were weighed in a 13x100 mm test tube equipped with a stir bar. MeOH (1 mL) was added and the mixture was stirred at 60°C for 16h after which the reaction mixture was diluted with CH₂Cl₂ and internal standard (1,3,5-trimethoxybenzene, 11.2 mg, 0.07 mmol, 0.33 equiv.) was added. After stirring the solution, an aliquot was evaporated under a flow of nitrogen and chloroform was added. ¹H NMR spectra of the unpurified mixture revealed that none of the **1a** product was formed, suggesting that isoquinolones are not formed via a hydroarylation/electrocyclization pathway.

Ortho Deuteration Experiments (Scheme 3.15, eq. 1, 2)

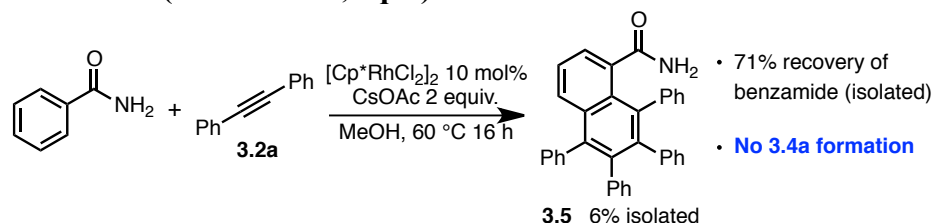


Without any particular precautions to extrude oxygen or moisture, **1a** (30 mg, 0.20 mmol, 1 equiv.), $[\text{Cp}^*\text{RhCl}_2]_2$ (3.1 mg, 0.005 mmol, 2.5 mol%) and CsOAc (77 mg, 0.40 mmol, 2 equiv.) were weighed in a 13x100 mm test tube equipped with a stir bar. MeOH (1 mL) was added and the mixture was stirred at 60°C for 16h after which, the reaction mixture was diluted with CH₂Cl₂ and transferred in a round bottom flask. Silica was added to the flask and volatiles were evaporated under reduced pressure. The purification was performed by flash column chromatography on silica gel using 55% EtOAc in pet. ether. Found 90% deuterium incorporation at the *ortho* position of the hydroxamic acid.



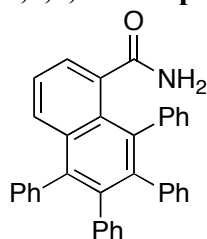
Without any particular precautions to extrude oxygen or moisture, benzamide (24 mg, 0.20 mmol, 1 equiv.), $[\text{Cp}^*\text{RhCl}_2]_2$ (3.1 mg, 0.005 mmol, 2.5 mol%) and CsOAc (77 mg, 0.40 mmol, 2 equiv.) were weighted in a 13x100 mm test tube equipped with a stir bar. MeOH (1 mL) was added and the mixture was stirred at 60°C for 16h after which the reaction mixture was diluted with CH_2Cl_2 and transferred in a round bottom flask. Silica was added to the flask and volatiles were evaporated under reduced pressure. The purification was performed by flash column chromatography on silica gel using 70% EtOAc in pet. ether. Found 25% deuterium incorporation at the *ortho* position of the hydroxamic acid.

Benzamide Reaction (Scheme 3.15, eq. 3)



Without any particular precautions to extrude oxygen or moisture, benzamide (24 mg, 0.20 mmol, 1 equiv.), **2a** (71 mg, 0.40 mmol, 2 equiv.), $[\text{Cp}^*\text{RhCl}_2]_2$ (12.4 mg, 0.02 mmol, 10 mol%) and CsOAc (77 mg, 0.40 mmol, 2 equiv.) were weighted in a 13x100 mm test tube equipped with a stir bar. MeOH (1 mL) was added and the mixture was stirred at 60°C for 16a after which the reaction mixture was diluted with CH_2Cl_2 and transferred in a round bottom flask. Silica was added to the flask and volatiles were evaporated under reduced pressure. The purification was performed by flash column chromatography on silica gel using 20% acetone in toluene. Recovered 71% of the starting benzamide and isolated 5.8 mg (6%) of **5**. No formation of **4a** was observed.

5,6,7,8-Tetraphenyl-1-naphthamide (3.5)



^1H NMR (400 MHz, CDCl_3 , 293 K, TMS): δ 7.69 (1H, dd, $J = 8.5, 1.2$ Hz), 7.57 (1H, dd, $J = 6.9, 1.2$ Hz), 7.35 (1H, dd, $J = 8.5, 7.0$ Hz), 7.24-7.09 (10H, m), 6.85-6.72 (10H, m), 5.23 (1H, br s), 4.94 (1H, br s)

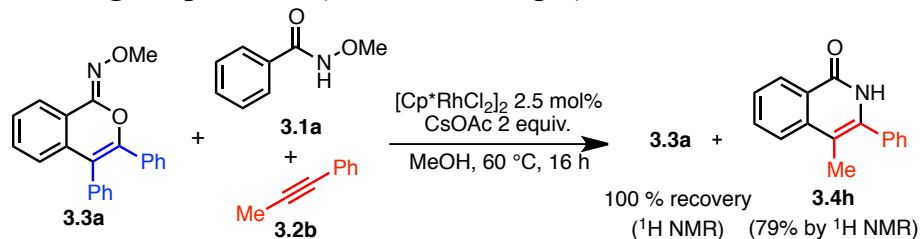
^{13}C NMR (100 MHz, CDCl_3 , 293 K, TMS): δ 172.7, 141.2, 140.2, 140.2, 140.1, 139.7, 139.4, 138.9, 137.3, 135.5, 133.5, 132.8, 131.1, 131.0, 129.7, 128.7, 127.6, 126.8, 126.7, 126.6, 126.5, 125.4, 125.3, 124.6

IR ($\nu_{\text{max}}/\text{cm}^{-1}$): 3057, 1656, 1601, 1439, 1365, 1137, 1109

HRMS (EI): calculated for $\text{C}_{35}\text{H}_{25}\text{NO}$ (M^+): 475.1936; Found 475.1991

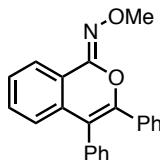
R_f: 0.24 with acetone 20% in toluene

N-O Bond Cleavage Experiment (Scheme 3.15, eq. 4)



Without any particular precautions to extrude oxygen or moisture, **3.3a** (28.4 mg, 0.09 mmol, 0.43 equiv.), **3.1a** (30 mg, 0.20 mmol, 1 equiv.), **3.2b** (28 μL , 0.22 mmol, 1.1 equiv.), $[\text{Cp}^*\text{RhCl}_2]_2$ (3.1 mg, 0.005 mmol, 2.5 mol%) and CsOAc (77 mg, 0.40 mmol, 2 equiv.) were weighted in a 13x100 mm test tube equipped with a stir bar. MeOH (1 mL) was added and the mixture was stirred at 60°C for 16h after which the reaction mixture was diluted with CH_2Cl_2 and an internal standard (1,3,5-trimethoxybenzene, 11.2 mg, 0.067 mmol, 0.33 equiv.) was added. The solution was stirred and an aliquot was evaporated under a flow of nitrogen. Chloroform was added and a $^1\text{H NMR}$ spectra of the unpurified mixture was taken which indicated 100% recovery of **3.3a**.

2-Methoxy-3,4-diphenylisoquinolin-1(2H)-one (**3.3a**)



In an 8 mL test tube *N*-methoxybenzamide (1.00 mmol, 151.2 mg, 1 eq.) was combined with 1,2-diphenylethyne (1.10 mmol, 196.0 mg, 1.1 eq.), $\text{Cp}^*\text{Rh}(\text{MeCN})_3 \cdot 2\text{SbF}_6$ (0.05 mmol, 41.6 mg, 0.05 eq), and $\text{Cu}(\text{OAc})_2 \cdot \text{H}_2\text{O}$ (0.40 mmol, 79.6 mg, 0.4 eq) in DMF (0.2 M, 5 mL). No special precautions were taken to exclude moisture. The tube was capped and heated for 16 hrs at 40°C with an oxygen balloon. The reaction mixture was diluted with ether and extracted twice from an aqueous solution of ammonium chloride. The organic phase was dried over Mg_2SO_4 , filtered and concentrated. The crude was dry-loaded onto silica and purified by chromatography with a gradient of 0% to 3% Et_2O in pet. ether. The desired product was a pale yellow solid obtained in 43% yield (140 mg).

$^1\text{HNMR}$ (400 MHz, CDCl_3 , 293K, TMS): δ 8.06-8.04 (m, 1H), 7.38-7.28 (m, 7H), 7.23-7.15 (m, 5H), 6.94-6.92 (m, 1H), 4.01 (s, 3H)

$^{13}\text{CNMR}$ (100 MHz, CDCl_3 , 293K, TMS): δ 148.6, 148.2, 134.9, 133.4, 133.1, 131.3, 130.8, 128.9, 128.6, 127.8, 127.8, 127.7, 124.8, 123.8, 120.9, 115.4, 62.7 (one signal missing due to overlap)

IR (neat, $\nu_{\text{max}}/\text{cm}^{-1}$): 3055, 2941, 2898, 2824, 1643, 1616, 1600, 1479, 1452, 1338, 1201, 1092, 1050, 907, 761, 698

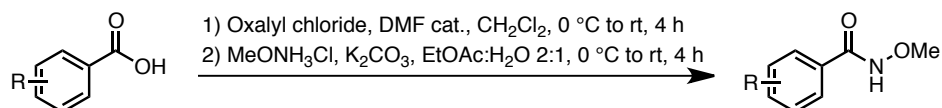
HRMS calculated for $\text{C}_{22}\text{H}_{17}\text{NO}_2$ (M^+): 327.1259; Found 327.1264

MP 166-168°C

R_f : 0.30 with 4% Et_2O in pet. ether

5.3.2 SYNTHESIS OF *O*-METHYL HYDROXAMATES

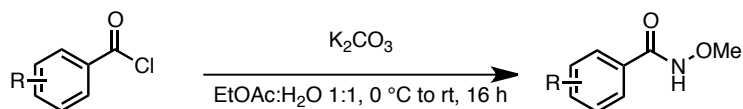
General Procedure D



1) To a solution of the carboxylic acid (1 equiv.) in CH₂Cl₂ (0.3 M) at 0°C under Ar was added dropwise oxalyl chloride (1.2 equiv.) followed by a catalytic amount of DMF (2 drops). The reaction was allowed to stir at rt until completion (typically 4h). The solvent was then removed under reduce pressure to afford the corresponding crude acid chloride.

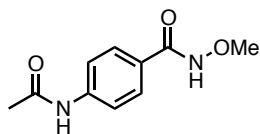
2) Methoxyamine hydrochloride (1.1 equiv.) was added to a biphasic mixture of K₂CO₃ (2 equiv.) in a 2:1 mixture of EtOAc:H₂O (0.2 M). The resulting solution was cooled to 0°C followed by dropwise addition of the unpurified acid chloride dissolved in a minimum amount of EtOAc. The flask containing the acid chloride was then rinsed with additional EtOAc. The reaction was allowed to stir for 4h while reaching rt. Afterwards, the phases were separated and the aqueous phase was extracted twice with EtOAc. The combined organic layers were dried over MgSO₄, filtered, and evaporated under reduced pressure. The residue was purified by flash column chromatography on silica gel (see below for specific eluent composition).

General Procedure E



In a 25 mL round-bottom flask, *o*-methylhydroxylamine (2.25 mmol, 1.5 equiv.) and potassium carbonate (3.00 mmol, 2.0 eq.) were combined in a 2:1 mixture of EtOAc:H₂O (0.12 M). The flask was capped and the mixture was cooled in an ice bath with NaCl. No special precautions were taken to exclude moisture or oxygen. The acid chloride (1.50 mmol, 1.0 equiv.) was added dropwise and the reaction was stirred to rt over 16h. The reaction mixture was then diluted with EtOAc and washed twice with water and brine. The organic layers were dried over Mg₂SO₄, filtered and concentrated. The products were obtained as pure solids without need for purification

4-Acetamido-*N*-methoxybenzamide (3.1b)



The desired compound was a pale orange/yellow solid obtained in 64% yield (201 mg) from 4-acetamidobenzoic acid (1.50 mmol, 269 mg, 1 equiv.) following general procedure D. The product was pure after work-up.

¹H NMR (400 MHz, DMSO-d₆, 293K, TMS): δ 11.62 (1H, s), 10.18 (1H, s), 7.71-7.64 (4H, m), 3.69 (3H, s), 2.07 (3H, s)

¹³C NMR (100 MHz, DMSO-d₆, 293K, TMS): δ 168.8, 163.8, 142.3, 127.9, 126.4, 118.2, 63.2, 24.1

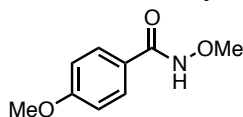
IR (nujol mull, ν_{max}/cm⁻¹): 3189, 3126, 1673, 1657, 1600, 1539, 1412, 1301, 852, 758

HRMS calculated for C₁₀H₁₂N₂O₃ (M⁺): 208.0848; Found 208.0857

Melting Point: 223-226°C

R_f: 0.14 with 50% EtOAc in pet. ether

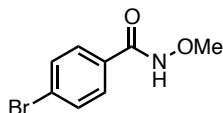
N, 4-Dimethoxybenzamide (3.1c)



The desired compound was an off-white solid obtained in 82% yield (149 mg) from 4-methoxybenzoyl chloride (1.00 mmol, 138 μl, 1 equiv.) following general procedure E. The product was pure after work-up. Spectral data was consistent with that previously reported.¹⁵¹

¹H NMR (400 MHz, CDCl₃, 293K, TMS): δ 8.64 (1H, s), 7.71 (2H, d, *J* = 8.7 Hz), 6.92 (2H, d, *J* = 8.7 Hz), 3.88 (3H, s), 3.85 (3H, s)

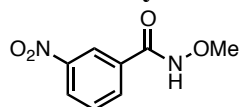
4-Bromo-N-methoxybenzamide (3.1d)



The desired compound was a white solid obtained in 96% yield (330 mg) from 4-bromobenzoic acid (1.50 mmol, 302 mg, 1 equiv.) following general procedure D. The product was pure after work-up. Spectral data was consistent with that previously reported.¹⁵²

¹H NMR (400 MHz, CDCl₃, 293K, TMS): δ 9.46 (1H, s), 7.64-7.61 (2H, m), 7.57-7.53 (2H, m), 3.84 (3H, s)

N-Methoxy-3-nitrobenzamide (3.1e)



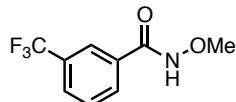
¹⁵¹ Miyata, O.; Koizumi, T.; Asai, H.; Iba, R.; Naito, T. *Tetrahedron* **2004**, *60*, 3893.

¹⁵² Wang, G.-W.; Yuan, T.-T. *J. Org. Chem.* **2010**, *75*, 476.

The desired compound was an off-white solid obtained in 78% yield (153 mg) from 3-nitrobenzoyl chloride (1.00 mmol, 185.6 mg, 1 eq.) following general procedure E. The product was pure after work-up. Spectral data was consistent with that previously reported.¹⁵³

¹H NMR (400 MHz, Acetone-d₆, 293K): δ 11.19 (1H, s), 8.63 (1H, t, *J* = 1.9 Hz), 8.41 (1H, d, *J* = 7.4 Hz), 8.25 (1H, ddd, *J* = 7.8, 1.5, 1.1 Hz), 7.81 (1H, t, *J* = 8.0 Hz), 3.84 (3H, s)

3-(Trifluoromethyl)-*N*-methoxybenzamide (3.1f)



The desired compound was an off-white solid obtained in 93% yield (306 mg) from 3-(trifluoromethyl)benzoic acid (1.50 mmol, 285 mg, 1 equiv.) following general procedure D. The product was pure after work-up.

¹H NMR (400 MHz, DMSO-d₆, 293K, TMS): δ 12.03 (1H, s), 8.08-8.06 (2H, m), 7.94 (1H, d, *J* = 7.7 Hz), 7.75 (1H, t, *J* = 7.7 Hz), 3.75 (3H, s)

¹³C NMR (100 MHz, DMSO-d₆, 293K, TMS): δ 162.4, 133.2, 131.1, 129.9, 129.3 (q, *J*_F = 31.9 Hz), 128.2 (q, *J*_F = 3.2), 123.9 (q, *J*_F = 270.6 Hz), 123.6 (q, *J*_F = 3.3 Hz), 63.3

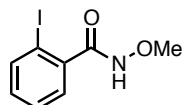
IR (nujol mull, ν_{max}/cm⁻¹): 3166, 1657, 1590, 1523, 1335, 1284, 942, 912, 818, 785, 691

HRMS calculated for C₉H₈NO₂F₃ (M⁺): 219.0507; Found 219.0494

Melting Point: 120-122°C

R_f: 0.50 with 50% EtOAc in pet. ether

2-Iodo-*N*-methoxybenzamide (3.1g)



The desired compound was a fluffy, off-white solid obtained in 85% yield (355 mg) from 2-iodobenzoic acid (1.50 mmol, 372 mg, 1 equiv.) following general procedure D. The product was pure after work-up.

¹H NMR (400 MHz, CDCl₃, 293K, TMS): δ 8.68 (1H, s), 7.85 (1H, d, *J* = 8.0 Hz), 7.40-7.34 (2H, m), 7.15-7.11 (1H, m), 3.92 (3H, s)

¹³C NMR (100 MHz, CDCl₃, 293K, TMS): δ 166.9, 139.9, 138.6, 131.8, 128.7, 128.2, 93.0, 64.6

IR (neat, ν_{max}/cm⁻¹): 3169, 2971, 2938, 2817, 1653, 1586, 1512, 1459, 1301, 1053, 1013, 942, 889, 751, 687

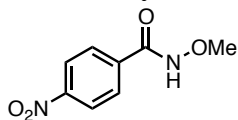
HRMS calculated for C₈H₈NO₂I (M⁺): 276.9600; Found 276.9594

Melting Point: 97-100°C

R_f: 0.36 with 50% EtOAc in pet. ether

¹⁵³ McCarthy, D. G.; Hegarty, A. F.; *J. Chem. Soc. Perkin II* **1976**, 1080.

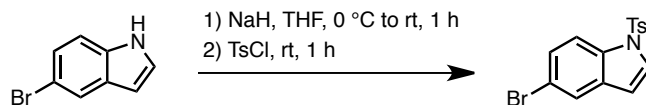
N-Methoxy-4-nitrobenzamide (3.1h)



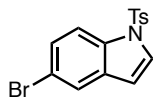
The desired compound was an off-white solid obtained in 67% yield (130.8 mg) from 4-nitrobenzoyl chloride (1.00 mmol, 186 mg, 1 equiv.) following general procedure E. The product was pure after work-up. Spectral data was consistent with that previously reported.¹⁵⁴

¹H NMR (400MHz, DMSO-d₆, 293K, TMS): δ 12.09 (1H, s), 8.32 (2H, d, J = 8.8 Hz), 7.99 (2H, d, J = 8.8 Hz), 3.75 (3H, s)

5.3.3 SYNTHESIS OF UNSYMMETRICAL ALKYNES

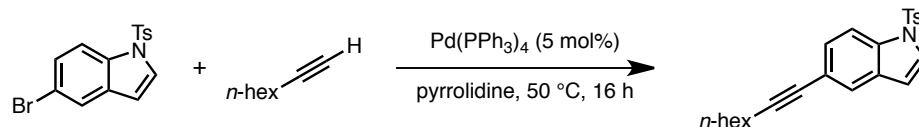


5-Bromo-1-tosyl-1H-indole



NaH (60% suspension in paraffin) (210 mg, 5.30 mmol, 1.05 equiv.) was added to a stirred solution of 5-bromoindole (980 mg, 5.00 mmol, 1 equiv.) in anhydrous THF (10 mL, 0.5 M) at 0 °C over a 5 min period. After stirring at rt for 1h, tosyl chloride (1.0 g, 5.30 mmol, 1.05 equiv.) was added slowly. The reaction mixture was stirred for an additional 1h at rt after which it was poured into 50 mL of 5% aq. NaHCO₃ and extracted with ether (3 x 30 mL). The combined organic layers were washed with brine, dried with MgSO₄ and concentrated. Two recrystallizations from ethanol afforded the desired compound in 59% yield. Spectral data was consistent with previously reported data.¹⁵⁵

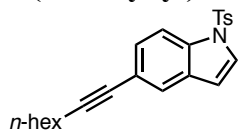
¹H NMR (400 MHz, CDCl₃, 293 K): δ 7.86 (1H, d, J = 8.8 Hz), 7.74 (2H, d, J = 8.4 Hz), 7.66 (1H, d, J = 1.8 Hz), 7.56 (1H, d, J = 3.7 Hz), 7.40 (1H, dd, J = 8.8, 1.9 Hz), 7.23 (2H, d, J = 8.1 Hz), 6.59 (1H, d, J = 3.6 Hz), 2.35 (3H, s).



¹⁵⁴ Miyata, O.; Koizumi, T.; Asai, H.; Iba, R.; Naito, T. *Tetrahedron* **2004**, *60*, 3893.

¹⁵⁵ Fresneda, P. M.; Molina, P.; Bleda, J. A. *Tetrahedron*, **2001**, *57*, 2355.

5-(Oct-1-ynyl)-1-tosyl-1H-indole (2e)



In a dried test tube a mixture of 1-octyne (80 μ L, 0.80 mmol, 1.2 equiv.), 5-Bromo-1-tosyl-1H-indole (245 mg, 0.70 mmol, 1 equiv.) and Pd(PPh₃)₄ (40 mg, 0.04 mmol, 5 mol%) in pyrrolidine (1.8 mL, 0.40 M) under Ar was stirred at 50 °C overnight. Afterwards, the pyrrolidine was evaporated and the residue was purified by column chromatography (10 cm x 3 cm) with 10% ether in hexanes to give 73% of the desired product.

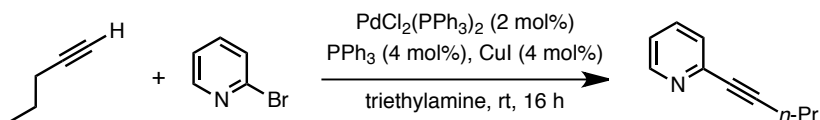
¹H NMR (400 MHz, CDCl₃, 293 K): δ 7.89 (1H, d, J = 8.6 Hz), 7.73 (2H, d, J = 8.4 Hz), 7.56 (1H, d, J = 1.0 Hz), 7.54 (1H, d, J = 3.7 Hz), 7.33 (1H, dd, J = 8.6 Hz, 1.5 Hz), 7.21 (2H, d, J = 8.0 Hz), 6.59 (1H, dd, J = 3.7, 0.7 Hz), 2.39 (2H, t, J = 7.1 Hz), 2.33 (3H, s), 1.63 – 1.56 (2H, m), 1.48 – 1.41 (2H, m), 1.34 – 1.30 (4H, m), 0.90 (3H, t, J = 7.2 Hz).

¹³C NMR (100 MHz, CDCl₃, 293 K): δ 145.1 (C), 135.2 (C), 133.9 (C), 130.7 (C), 129.9 (CH), 128.1 (CH), 127.1 (CH), 127.8 (CH), 124.6 (CH), 119.2 (C), 113.4 (CH), 108.9 (CH), 89.6 (C), 80.5 (C), 31.4 (CH₂), 28.8 (CH₂), 28.6 (CH₂), 22.6 (CH₃), 21.6 (CH₂), 19.4 (CH₂), 14.1 (CH₃).

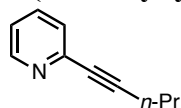
FTIR: 2930, 1457, 1375, 1175, 670 cm⁻¹.

HRMS (EI): calculated for C₂₃H₂₅NO₂S (M⁺): 379.1606; found for C₂₃H₂₅NO₂S (M⁺) 379.1616.

R_f: 0.48 with ether 20% in hexanes



2-(Pent-1-ynyl)pyridine (2c)



CuI (38 mg, 0.2 mmol, 4 mol%), PdCl₂(PPh₃)₂ (70 mg, 0.10 mmol, 2 mol%), PPh₃ (53 mg, 0.20 mmol, 4 mol%) and Et₃N (15 mL) were placed in a round bottom flask under Ar with a stir bar. 2-bromopyridine was added and the resulting mixture was stirred at 25°C for 30 min. The alkyne was added and the reaction was stirred under Ar at 25°C for 16h. Afterwards, sat. NH₄Cl was added and the aqueous phase was extracted three times with ether. The combined organic fraction was dried over MgSO₄, filtered and evaporated under reduced pressure. The purification was performed by flash column chromatography using 12 % EtOAc in pet. ether. The product obtained is a yellow oil (679 mg, 94%). Spectral data was consistent with previously reported data.¹⁵⁶

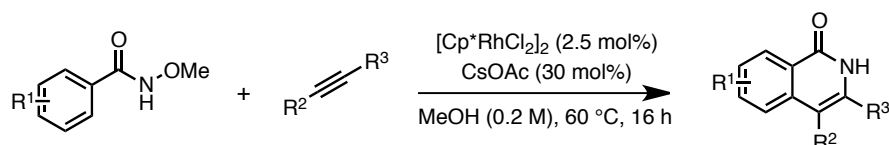
¹H NMR (400 MHz, CDCl₃, 293 K): δ 8.54 (1H, ddd, J = 4.9, 1.8, 0.9 Hz), 7.61 (1H, td, J =

¹⁵⁶ Siebeneicher, H.; Doye, S. *Eur. J. Org. Chem.* **2002**, 1213.

7.7, 1.8 Hz), 7.37 (1H, dt, $J = 7.8, 1.0$ Hz), 7.18 (1H, ddd, $J = 7.6, 4.9, 1.2$ Hz), 2.42 (2H, t, $J = 7.1$ Hz), 1.67 (2H, sext, $J = 7.3$ Hz), 1.06 (3H, d, $J = 7.4$ Hz)

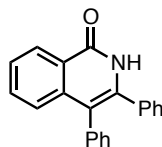
5.3.4 SYNTHESIS OF SUBSTITUTED ISOQUINOLONES

General Procedure F



Without any particular precautions to extrude oxygen or moisture, the hydroxamic acid (1 equiv.), the alkyne (if solid) (1.1 equiv.), $[\text{Cp}^*\text{RhCl}_2]_2$ (2.5 mol%) and CsOAc (30 mol%) were weighted in a 13x100 mm test tube equipped with a stir bar. MeOH was added followed immediately by the alkyne (if liquid) and the mixture was stirred at 60°C for 16 hours. Afterwards, the reaction mixture was diluted with CH_2Cl_2 and transferred in a round bottom flask. Silica was added to the flask and volatiles were evaporated under reduced pressure. The purification was performed by flash column chromatography on silica gel. (see below for specific eluent composition).

3,4-Diphenylisoquinolin-1(2H)-one (3.4a)



3.4a was an off-white solid obtained in 90% yield (80.6 mg) from **3.1a** (0.30 mmol, 45 mg, 1 equiv.) following general procedure F. The product was isolated by column chromatography using 40% EtOAc in pet. ether.

^1H NMR (400 MHz, DMSO- d_6 , 293K, TMS): δ 11.56 (1H, s), 8.33 (1H, dd, $J = 8.0, 1.1$ Hz), 7.64 (1H, ddd, $J = 8.3, 7.0, 1.4$ Hz), 7.54-7.50 (1H, m), 7.30-7.22 (8H, m), 7.17-7.15 (3H, m)

^{13}C NMR (100 MHz, DMSO- d_6 , 293K, TMS): δ 161.7, 138.6, 138.1, 135.8, 134.6, 132.5, 131.7, 129.8, 128.2, 128.2, 127.7, 127.1, 126.8, 126.3, 125.0, 124.9, 115.4

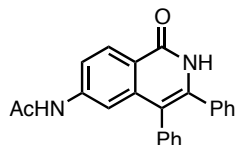
IR ($\nu_{\text{max}}/\text{cm}^{-1}$): 2928, 1647, 694, 557

HRMS calculated for $\text{C}_{21}\text{H}_{15}\text{NO}$ (M^+): 297.1154; Found 297.1167

R_f : 0.45 with EtOAc 50% in pet. ether

Melting Point: 242-246 °C

N-(1,2-Dihydro-1-oxo-3,4-diphenylisoquinolin-6-yl)acetamide (3.4b)



The desired compound was an off-white solid obtained in 73% yield (52.1 mg) from **3.1b** (0.20 mmol, 42 mg, 1 equiv.) following general procedure F. The product was isolated by column chromatography using 75% CH₂Cl₂ in 23% pet. ether and 2% MeOH.

¹H NMR (400 MHz, DMSO-d₆, 293K, TMS): δ 11.36 (1H, s), 10.19 (1H, s), 8.23 (1H, d, *J* = 8.7 Hz), 7.86 (1H, dd, *J* = 8.8, 2.0 Hz), 7.39 (1H, d, *J* = 1.9 Hz), 7.29-7.25 (3H, m), 7.21-7.19 (5H, m), 7.14-7.12 (2H, m), 2.00 (3H, s)

¹³C NMR (100 MHz, DMSO-d₆, 293K, TMS): δ 168.8, 161.3, 143.0, 139.2, 138.9, 136.0, 134.7, 131.7, 129.8, 128.2, 128.1, 127.9, 127.6, 127.0, 120.4, 117.9, 115.4, 113.3, 24.1

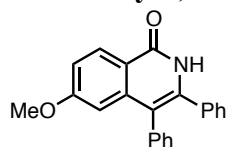
IR (nujol mull, ν_{max}/cm⁻¹): 3283, 3199, 1687, 1647, 1610, 1583, 1543, 1408, 889, 761, 694

HRMS calculated for C₂₃H₁₈N₂O₂ (M⁺): 354.1368; Found 354.1396

Melting Point: decomposes above 300°C

R_f: 0.20 with 75% CH₂Cl₂, 23% pet. ether and 2% MeOH

6-Methoxy-3,4-diphenylisoquinolin-1(2H)-one (3.4c)



The desired compound was a pale orange solid obtained in 88% yield (52.0 mg) from **3.1c** (0.20 mmol, 36 mg, 1 equiv.) following general procedure F. The product was isolated by column chromatography using 2% isopropanol in toluene.

¹H NMR (300 MHz, DMSO-d₆, 303K, TMS): δ 11.36 (1H, s), 8.25 (1H, d, *J* = 8.8 Hz), 7.30-7.13 (11H, m), 6.51 (1H, d, *J* = 2.0 Hz), 3.67 (3H, s)

¹³C NMR (75 MHz, DMSO-d₆, 303K, TMS): δ 162.3, 161.4, 140.1, 139.2, 135.9, 134.6, 131.7, 129.8, 129.1, 128.2, 128.2, 127.7, 127.1, 118.9, 115.1, 114.5, 107.2, 55.2

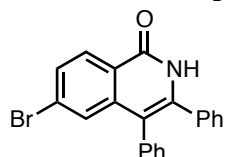
IR (nujol mull, ν_{max}/cm⁻¹): 3129, 1647, 1613, 1278, 868, 781

HRMS calculated for C₂₂H₁₇NO₂ (M⁺): 327.1259; Found 327.1251

Melting Point: decomposes above 225°C

R_f: 0.20 with 75% CH₂Cl₂, 23% pet. ether and 2% MeOH

6-Bromo-3,4-diphenylisoquinolin-1(2H)-one (3.4d)



The desired compound was a tan-coloured solid obtained in 88% yield (66.3 mg) from **3.1d** (0.20 mmol, 46 mg, 1 equiv.) following general procedure F. The product was isolated by column chromatography using 50% Et₂O in pet. ether then 75% Et₂O in pet. ether.

¹H NMR (400 MHz, DMSO-d₆, 293K, TMS): δ 11.73 (1H, s), 8.23 (1H, d, *J* = 8.5 Hz), 7.68 (1H, dd, *J* = 8.5, 1.9 Hz), 7.35-7.29 (3H, m), 7.25-7.21 (6H, m), 7.18-7.15 (2H, m)

¹³C NMR (75 MHz, DMSO-d₆, 303K, TMS): δ 161.2, 140.3, 139.9, 135.1, 134.2, 131.6, 129.8, 129.3, 129.2, 128.4, 127.7, 127.4, 126.9, 126.8, 123.9, 114.4 (one peak missing due to overlap)

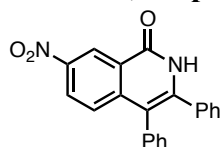
IR (nujol mull, ν_{max}/cm⁻¹): 3169, 1653, 1613, 1593, 885, 771, 706, 573

HRMS calculated for C₂₁H₁₄BrNO (M⁺): 375.0259; Found 375.0272

Melting Point : decomposes above 250°C

R_f: 0.20 with 50% Et₂O in pet. ether

7-Nitro-3,4-diphenylisoquinolin-1(2H)-one (3.4e)



The desired compound was a yellow solid obtained in 85% yield (58.3 mg) from **3.1e** (0.20 mmol, 39 mg, 1 equiv.) following general procedure F. The mixture was filtered, washing with methanol and then a minimal amount of cold chloroform. The precipitate was collected from the filter paper. Due to poor solubility, the product was spun for 10 minutes at 120°C in the NMR machine, after which the probe was cooled to run the spectra.

¹H NMR (300 MHz, DMSO-d₆, 303K, TMS): δ 12.07 (1H, s), 9.00-8.99 (1H, m), 8.39 (1H, ddd, *J* = 9.1, 2.6, 1.9 Hz), 7.34-7.25 (9H, m), 7.19-7.16 (2H, m)

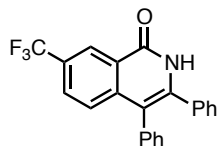
¹³C NMR (75 MHz, DMSO-d₆, 303K, TMS): δ 161.0, 144.8, 143.2, 142.7, 134.9, 133.8, 131.6, 129.7, 128.8, 128.5, 127.8, 127.5, 126.8, 126.4, 124.7, 122.7, 115.3

IR (nujol mull, ν_{max}/cm⁻¹): 3152, 1670, 1640, 1610, 1566, 828, 768, 694

HRMS calculated for C₂₁H₁₄N₂O₃ (M⁺): 342.1004; Found 342.1004

Melting Point: decomposes above 300°C

7-(Trifluoromethyl)-3,4-diphenylisoquinolin-1(2H)-one (3.4f)



The desired compound was an off-white solid obtained in 76% yield (55.4 mg) from **3.1f** (0.20 mmol, 43 mg, 1 equiv.) following general procedure F. The product was isolated by column chromatography using 40% Et₂O in pet. ether.

¹H NMR (400 MHz, CDCl₃, 293K, TMS): δ 10.27 (1H, s), 8.70 (1H, m), 7.75 (1H, dd, *J* = 8.6, 1.7 Hz), 7.47 (1H, d, *J* = 8.6 Hz), 7.35-7.26 (8H, m), 7.19-7.16 (2H, m)

¹³C NMR (100 MHz, CDCl₃, 293K, TMS): δ 162.6, 141.1, 139.9, 135.1, 134.3, 131.7, 129.4, 129.1, 128.6, 128.6, 128.6, 128.5, 128.3 (q, *J*_F = 33.0 Hz), 128.3, 127.6, 126.5, 125.2 (q, *J*_F = 4.2 Hz), 124.8, 123.9 (q, *J*_F = 270.2 Hz), 116.8

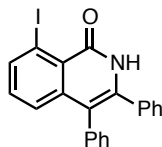
IR (neat, ν_{max}/cm⁻¹): 3156, 2921, 1660, 1620, 1549, 1496, 1325, 1147, 1127, 1066, 838, 728, 701

HRMS calculated for C₂₂H₁₄F₃NO (M⁺): 365.1027; Found 365.1005

Melting Point: decomposes above 225°C

R_f: 0.46 with 50% Et₂O in pet. ether

8-Iodo-3,4-diphenylisoquinolin-1(2H)-one (3.4g)



The desired compound was an off-white solid obtained in 48% yield (41.0 mg) from **3.1g** (0.20 mmol, 55 mg, 1 equiv.) following general procedure F. The mixture was filtered, washing with methanol and then a minimal amount of cold chloroform. The precipitate was collected from the filter paper. Due to poor solubility, the product was spun for 10 minutes at 120°C in the NMR machine, after which the probe was cooled to run the spectra.

¹H NMR (300 MHz, DMSO-d₆, 303K, TMS): δ 11.57 (1H, s), 8.10 (1H, d, *J* = 7.5 Hz), 7.30-7.19 (9H, m), 7.14-7.09 (3H, m)

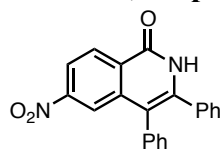
¹³C NMR (75 MHz, DMSO-d₆, 303K, TMS): δ 159.8, 140.5, 140.3, 139.2, 135.9, 134.1, 132.9, 131.8, 129.7, 128.4, 127.7, 127.2, 125.8, 123.2, 115.3, 94.1 (one peak missing due to overlap)

IR (nujol mull, ν_{max}/cm⁻¹): 3152, 1647, 1586, 1301, 560

HRMS calculated for C₂₁H₁₄INO (M⁺): 423.0120; Found 423.0118

Melting Point: decomposes above 250°C

6-Nitro-3,4-diphenylisoquinolin-1(2H)-one (3.4h)



The desired compound was a yellow solid obtained in 89% yield (60.7 mg) from **3.1h** (0.20 mmol, 39 mg, 1 equiv.) following general procedure F. The product was isolated by column chromatography using 50% Et₂O in pet. ether.

¹H NMR (400 MHz, CDCl₃, 293K, TMS): δ 10.15 (1H, s), 8.58-8.56 (1H, m), 8.23-8.20 (2H, m), 7.38-7.26 (8H, m), 7.19-7.17 (2H, m)

¹³C NMR (100 MHz, CDCl₃, 293K, TMS): δ 161.7, 150.6, 139.7, 139.5, 134.3, 134.1, 131.6, 129.6, 129.2, 129.2, 128.9, 128.6, 128.5, 128.1, 121.2, 120.1, 117.1

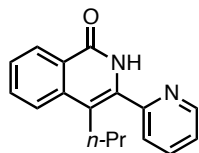
IR (neat, ν_{max}/cm⁻¹): 3173, 3032, 2924, 2857, 1657, 1620, 1533, 1345, 902, 835, 795, 744, 701

HRMS calculated for C₂₁H₁₄N₂O₃ (M⁺): 342.1004; Found 342.1021

Melting Point: 251-252 °C

R_f: 0.17 with 50% Et₂O in pet. ether

4-Propyl-3-(pyridin-2-yl)isoquinolin-1(2H)-one (3.4i)



The desired compound was an off-white solid obtained in 57% yield (45.5 mg) from **3.1a** (0.30 mmol, 45 mg, 1 equiv.) following general procedure F, but heating the reaction mixture at 100 °C in a sealed tube for 48 hours instead of heating it at 60°C for 16 hours. The purification was performed by flash column chromatography using 80-90% EtOAc in pet. ether.

¹H NMR (400 MHz, CDCl₃, 293K, TMS): δ 9.71 (1H, s), 8.75 (1H, ddd, *J* = 4.8, 1.8, 1.0 Hz), 8.50 (1H, ddd, *J* = 8.0, 1.5, 0.5 Hz), 7.85 (1H, td, *J* = 7.8, 1.8 Hz), 7.82 (1H, d, *J* = 8.8 Hz), 7.74 (1H, ddd, *J* = 8.3, 6.9, 1.4 Hz), 7.63 (1H, dt, *J* = 8.0, 1.0 Hz), 7.54 (1H, ddd, *J* = 8.0, 7.0, 1.1 Hz), 7.37 (1H, ddd, *J* = 7.6, 4.8, 1.1 Hz), 2.89-2.85 (2H, m), 1.83-1.73 (2H, m), 1.04 (3H, t, *J* = 7.4 Hz)

¹³C NMR (100 MHz, CDCl₃, 293K, TMS): δ 161.9, 152.07, 149.8, 138.1, 136.7, 134.2, 132.5, 128.0, 126.9, 126.6, 124.1, 124.0, 123.5, 115.6, 29.4, 23.7, 14.2

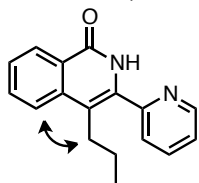
IR (ν_{max}/cm⁻¹): 2958, 1660, 1479, 767

HRMS calculated for C₁₇H₁₆N₂O (M⁺): 264.1263; Found 264.1283

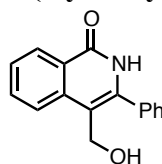
R_f: 0.15 with EtOAc 50% in pet. ether

Melting Point: decomposes at 156-162 °C

NOESY (400 MHz, CDCl₃, 293K, TMS)



4-(Hydroxymethyl)-3-phenylisoquinolin-1(2H)-one (3.4j)



The desired compound was a yellow solid obtained in 55% yield (60.7 mg) from **3.1a** (0.30 mmol, 45 mg, 1 equiv.) following general procedure F. The purification was performed by flash column chromatography using 5% isopropanol in toluene.

¹H NMR (400 MHz, CDCl₃, 293K, TMS): δ 8.78 (1H, br s), 8.44 (1H, dd, *J* = 8.1, 1.2 Hz), 8.01 (1H, d, *J* = 8.2 Hz), 7.77 (1H, ddd, *J* = 8.3, 7.1, 1.4 Hz), 7.56-7.51 (6H, m), 4.74 (2H, s)
¹³C NMR (100 MHz, CDCl₃, 293K, TMS): δ 162.4, 139.8, 137.6, 134.2, 133.3, 129.9, 129.0, 128.8, 127.9, 126.9, 125.6, 124.0, 112.5, 58.6

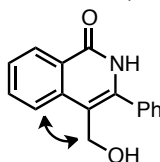
IR (ν_{max}/cm⁻¹): 1650, 1345, 758, 691

HRMS calculated for C₁₆H₁₃NO (M⁺): 251.0946; Found 251.0967

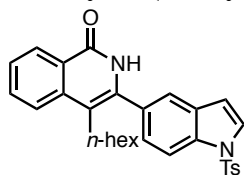
R_f: 0.15 with isopropanol 5% in toluene

Melting Point: Turns black over 280 °C

NOESY (400 MHz, CDCl₃, 293K, TMS); COSY (400 MHz, CDCl₃, 293K, TMS)



4-Hexyl-3-(1-tosyl-1*H*-indol-5-yl)isoquinolin-1(2*H*)-one (3.4k)



The desired compound was an off-white solid obtained in 80% yield (120.1 mg) from **3.1a** (0.3- mmol, 45 mg, 1 equiv.) following general procedure F. The purification was performed by flash column chromatography using 3% isopropanol in toluene.

¹H NMR (400 MHz, CDCl₃, 293K, TMS): δ 8.82 (1H, br s), 8.42 (1H, d, *J* = 7.9 Hz), 8.09 (1H, d, *J* = 8.6 Hz), 7.82 (2H, d, *J* = 8.4 Hz), 7.75-7.73 (2H, m), 7.67 (1H, d, *J* = 3.7 Hz), 7.60 (1H, d, *J* = 1.2 Hz), 7.49 (1H, ddd, *J* = 8.1, 5.4, 2.7 Hz), 7.37 (1H, dd, *J* = 8.5, 1.6 Hz), 7.28 (2H, d, *J* = 8.0 Hz), 6.71 (1H, dd, *J* = 3.7, 0.6 Hz), 2.60 (2H, t, *J* = 8.0 Hz), 2.36 (3H, s), 1.59-1.52 (m, 2H), 1.26-1.11 (m, 6H), 0.80-0.75 (3H, t, *J* = 7.0 Hz).

¹³C NMR (100 MHz, CDCl₃, 293K, TMS): δ 162.1, 145.3, 138.0, 136.7, 135.2, 134.8, 132.7, 130.9, 130.7, 130.1, 128.0, 127.6, 126.91, 126.3, 125.4, 123.8, 122.1, 114.7, 113.8, 109.0, 31.4, 30.5, 29.3, 27.3, 22.5, 21.7, 14.0 (1 signal missing due to overlap)

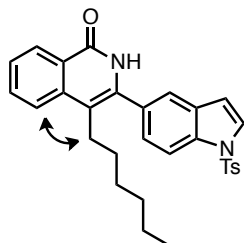
IR (ν_{max}/cm⁻¹): 2928, 2861, 1647, 1374, 1175, 1131, 667, 587

HRMS calculated for C₁₆H₁₃NO (M⁺): 498.1977; Found 498.2001

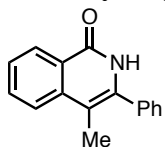
R_f: 0.30 with isopropanol 5% in toluène

Melting Point : 169-171 °C

NOESY (400 MHz, CDCl₃, 293K, TMS)



4-Methyl-3-phenylisoquinolin-1(2H)-one (3.4l)



The desired compound was an off-white solid obtained in 61% yield (28.7 mg) from **3.1a** (0.20 mmol, 30 mg, 1 eq.) following general procedure F. The purification was performed by flash column chromatography using 3% isopropanol in toluene.

¹H NMR (400 MHz, CDCl₃, 293K, TMS): δ 9.61 (1H, br s), 8.42 (1H, d, *J* = 7.96 Hz), 7.76-7.72 (2H, m), 7.75-7.43 (6H, m), 2.26 (3H, s)

¹³C NMR (100 MHz, CDCl₃, 293K, TMS): δ 162.6, 138.8, 136.8, 135.3, 132.7, 129.3, 129.0, 128.7, 127.7, 126.3, 125.4, 123.6, 109.1, 13.9

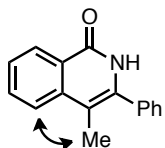
IR (ν_{max}/cm⁻¹): 1653, 761, 701

HRMS calculated for C₁₆H₁₃NO (M⁺): 235.0997; Found 235.1019

R_f: 0.29 with EtOAc 50% in pet. ether

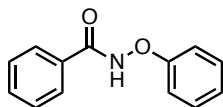
Melting Point: decomposes at 200-204 °C

NOESY (400 MHz, CDCl₃, 293K, TMS); COSY (400 MHz, CDCl₃, 293K, TMS)



5.3.5 PREPARATION OF THE SUBSTRATES BEARING DIFFERENT INTERNAL OXIDANTS

N-phenoxybenzamide (3.1k)



To a solution of 2 parts EtOAc in one part H₂O containing Na₂CO₃ (2 equiv.) was added *O*-phenylhydroxylamine hydrochloride (1 equiv.) (prepared following a literature procedure¹⁵⁷). The mixture was cooled to 0°C and benzoyl chloride (1 equiv.) was added dropwise to the mixture. It was then allowed to stir at 0°C for 2 hours. The reaction was then quenched with sat. NaHCO₃ and more EtOAc was added. The organic layer was washed twice with sat. NaHCO₃. It was then dried over MgSO₄, filtered and evaporated under reduced pressure. The purification was made by flash column chromatography using 20% EtOAc in pet. ether as eluent. The product obtained is a white solid (207 mg, 94%).

¹⁵⁷ Petrassi, H. M.; Sharpless, K. B.; Kelly, J. W.; *Org. Lett.* **2001**, *3*, 139.

¹H-NMR (400 MHz; DMSO-d₆, 293K): δ 12.48 (s, 1H), 7.90-7.87 (m, 2H), 7.62 (t, *J* = 7.4 Hz, 1H), 7.55-7.51 (m, 2H), 7.38-7.32 (m, 2H), 7.10 (d, *J* = 8.1 Hz, 2H), 7.04 (tt, *J* = 7.3, 0.9 Hz, 1H).

¹³C NMR (100 MHz, DMSO-d₆, 293K): δ 164.9, 159.6, 132.1, 131.4, 129.5, 128.7, 127.3, 122.4, 113.0

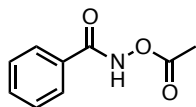
IR (ν_{max}/cm⁻¹): 3186, 1660, 1591, 1489, 1200

HRMS calculated for C₁₃H₁₁N₁O₂ (M⁺): 213.0790; Found 213.0797

R_f: 0.62 with 50% EtOAc in pet. ether

Melting Point: 131-133 °C

N-acetoxybenzamide (3.1l)

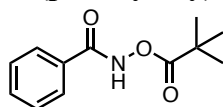


Benzohydroxamic acid (411 mg, 3 mmol, 1 equiv.), CH₂Cl₂ (9 mL) and NaOH 2M were charged in a round bottom flask. Ac₂O (312 μL, 3.3 mmol, 1.1 equiv.) was added via syringe. After stirring at room temperature for 3 h, the organic layer was separated and the aqueous layer was extracted with CH₂Cl₂. The combined organic fractions were washed with brine, dried with MgSO₄, filtered and evaporated under reduced pressure to afford the desired product as a white solid (514 mg, 96%).

¹H NMR (400 MHz, CDCl₃, 293K, TMS): δ 9.45 (br s, 1H), 7.84-7.81 (m, 2H), 7.61-7.56 (m, 1H), 7.50-7.45 (m, 2H), 2.31 (s, 3H).

Spectral data matched the one previously reported.¹⁵⁸

N-(pivaloyloxy)benzamide (3.1m)



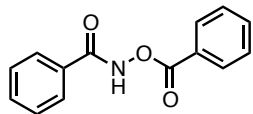
Pivalic anhydride (18.3 mmol, 3.70 mL, 1 equiv.) was added to a suspension of benzohydroxamic acid (21.9 mmol, 3.0 g, 1.2 equiv.) in dichloromethane (100 mL). The resulting mixture was allowed to stir at room temperature for 16 hours. It was then transferred to a separatory funnel and washed with sat. NaHCO₃. The organic layer was dried over MgSO₄, filtered and evaporated under reduced pressure. The purification was made by flash chromatography using 15% ethyl acetate in pet. ether as eluent. The product obtained is a white solid (3.28 g, 81%).

¹H NMR (400 MHz, CDCl₃, 293K, TMS): 9.58 (br s, 1H), 7.81-7.79 (m, 2H), 7.56-7.52 (m, 1H), 7.45-7.41 (m, 2H), 1.35 (s, 9H).

Spectral data was consistent with that previously reported.¹⁵⁸

N-(benzyloxy)benzamide (3.1n)

¹⁵⁸ Zhang, Z.; Yu, Y.; Liebeskind, L. S. *Org. Lett.* **2008**, *10*, 3005.



Benzohydroxamic acid (1.00 g, 7.29 mmol, 1 equiv.) and sodium *tert*-Butoxide (701 mg, 7.29 mmol, 1 equiv.) were stirred together at room temperature in diethyl ether (30 mL) for 30 min. Benzoyl chloride (850 μ L, 7.29 mmol, 1 equiv.) was then added dropwise and the reaction mixture was allowed to stir at room temperature for 16 h. It was then diluted with EtOAc and washed with water and sat. NaHCO₃. The organic fraction containing the product in the solid form was diluted with acetone to dissolve it almost completely. The organic phase was dried over MgSO₄, filtered and evaporated under reduced pressure to afford the desired product as a white solid (1.24 g, 70%) in an analytically pure form.

¹H NMR (400 MHz, DMSO-*d*₆, 293K): δ 12.64 (s, 1H), 8.10-8.08 (m, 2H), 7.89-7.86 (m, 2H), 7.78 (tt, *J* = 7.5, 1.5 Hz, 1H), 7.66-7.61 (m, 3H), 7.57-7.53 (m, 2H).

¹³C NMR (100 MHz, DMSO-*d*₆, 293K): δ 164.8, 164.4, 134.4, 132.4, 131.0, 129.5, 129.2, 128.7, 127.4, 126.9

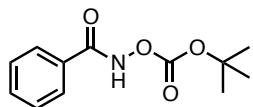
IR (v_{max}/cm⁻¹): 3193, 1767, 1653, 1239

HRMS calculated for C₁₄H₁₁N₁O₃ (M⁺): 241.0739; Found 241.0700

R_f: 0.63 with 50% EtOAc in pet. ether

Melting Point: 154-157°C

N-(*tert*-butoxycarbonyloxy)benzamide (3.1o)



Boc₂O (5.5 mmol, 1.26 mL, 1.1 equiv.) was added to a suspension of benzohydroxamic acid (5 mmol, 686 mg, 1 equiv.) in CH₂Cl₂ (20 mL). As seen by TLC, the conversion was low after 2h stirring at room temperature. NaOtBu (0.25 mmol, 24 mg, 0.05 equiv.) was added and the reaction mixture was allowed to stir for 16 hours at room temperature. More CH₂Cl₂ was added and the reaction mixture was washed twice with sat. NaHCO₃ after which the organic phase was dried over MgSO₄, filtered and evaporated under reduced pressure. The purification was made by flash column chromatography using 10-30% EtOAc in pet. ether as eluent.

¹H-NMR (400 MHz; CDCl₃, 293K, TMS): δ 9.27 (s, 1H), 7.82-7.80 (m, 2H), 7.57-7.53 (m, 1H), 7.46-7.42 (m, 2H), 1.55 (s, 9H).

¹³C NMR (100 MHz, CDCl₃, 293K, TMS): δ 166.8, 152.8, 132.7, 130.7, 128.8, 127.5, 86.0, 27.6

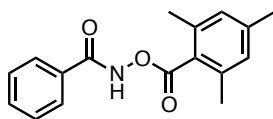
IR (v_{max}/cm⁻¹): 3216, 1988, 1787, 1667, 1246, 1150

HRMS calculated for C₇H₇NO₂ ((M-CO₂*t*-Bu)⁺): 137.0477; Found 137.0470

R_f: 0.56 with 50% EtOAc in pet. ether

Melting Point: 112-115 °C with gas evolution

N-(2,4,6-trimethylbenzoyloxy)benzamide (3.1p)



Benzoyl chloride (0.92 mmol, 107 μ L, 1 equiv.) was added dropwise at 0 °C to a biphasic solution of *O*-mesitylhydroxylamine hydrochloride (prepared according to a literature procedure,¹⁵⁹ 0.92 mmol, 200 mg, 1 equiv.) and Na₂CO₃ (1.84 mmol, 195 mg, 2 equiv.) in a 2:1 EtOAc:H₂O mixture (4.5 mL). The resulting mixture was allowed to reach room temperature and it was stirred for 16 hours. More EtOAc was added and the organic phase was washed with sat. NaHCO₃ after which it was dried over MgSO₄, filtered and evaporated under reduced pressure. The purification was made by flash column chromatography using 15% EtOAc in pet. ether as eluent. The product obtained is a white solid (208 mg, 80%).

¹H-NMR (400 MHz; CDCl₃, 293K, TMS): δ 9.65 (d, *J* = 0.2, 1H), 7.89 (dd, *J* = 8.3, 1.3, 2H), 7.61-7.56 (m, 1H), 7.48 (t, *J* = 7.6, 2H), 6.91 (d, *J* = 0.5, 2H), 2.43 (s, 6H), 2.31 (s, 3H)

¹³C NMR (100 MHz, CDCl₃, 293K, TMS): δ 168.5, 166.6, 141.0, 136.9, 132.8, 130.8, 128.9, 128.7, 127.6, 126.5, 21.3, 20.1

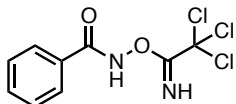
IR (v_{max}/cm⁻¹): 3196, 1772, 1653, 1506, 1237

HRMS found only the 2,4,6-trimethylbenzoic acid mass, C₁₀H₁₂O₂ (M⁺) calculated: 164.0837; Found 164.0850

R_f: 0.63 with 50% EtOAc in pet. ether

Melting Point: 151-152 °C

N-(2,2,2-trichloro-1-iminoethoxy)benzamide (3.1q)



Triethylamine (3.3 mmol, 460 μ L, 1.1 equiv.) was added to a suspension of benzohydroxamic acid (3 mmol, 411 mg, 1 equiv) in CH₂Cl₂ (10 mL) under Ar atmosphere. Trichloroacetonitrile (3.3 mmol, 330 μ L, 1.1 equiv.) was then added and the reaction was stirred for 2 hours at room temperature. More CH₂Cl₂ was added and the reaction mixture was washed with sat. NaHCO₃. The aqueous phase was then extracted twice with CH₂Cl₂. The organic phase was dried over MgSO₄, filtered and evaporated under reduced pressure. The purification was made by flash column chromatography using 10% EtOAc in pet. ether as eluent. The product obtained is a beige solid (45 mg, 5%).

¹H-NMR (400 MHz; CDCl₃, 293K, TMS): δ 9.82 (br s, 1H), 8.64 (br s, 1H), 7.54-7.51 (m, 2H), 7.40-7.35 (m, 2H), 7.19 (tt, *J* = 7.4, 1.3 Hz, 1H).

¹³C NMR (100 MHz, CDCl₃, 293K, TMS): δ

IR (v_{max}/cm⁻¹): 3314, 1707, 1537, 1499, 1449, 1231

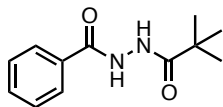
HRMS calculated for C₉H₇N₂O₂Cl₃ (M⁺): 279.9573; Found 279.9616

R_f: 0.25 with 10% EtOAc in pet. ether

Melting Point: 157-161 °C

¹⁵⁹ Carpino, L. A. *J. Am. Chem. Soc.* **1960**, *82*, 3133.

N'-pivaloylbenzohydrazide (3.1r)



Pivalic anhydride (8.1 mmol, 1.6 mL, 1.1 equiv.) was added to a mixture of benzhydrazide (1.0 g, 7.3 mmol, 1 equiv.) in CH₂Cl₂ (50 mL). The reaction was allowed to stir at room temperature for 16 hours. The mixture was then washed 3 times with sat. NH₄Cl and 3 times with NaHCO₃ after which the organic fraction was dried over MgSO₄, filtered and evaporated under reduced pressure. The purification was made by flash column chromatography using 50% EtOAc in pet. ether as eluent. The product obtained is a white solid (1.31 g, 81%).

¹H-NMR (400 MHz; DMSO-d₆, 293K, TMS): δ 10.20 (s, 1H), 9.54 (s, 1H), 7.89-7.87 (m, 2H), 7.59-7.54 (m, 1H), 7.51-7.47 (m, 2H), 1.19 (s, 9H).

¹³C NMR (100 MHz, DMSO-d₆, 293K, TMS): δ 176.9, 165.6, 132.8, 131.7, 128.4, 127.4, 37.6, 27.3

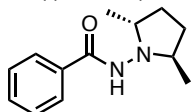
IR (ν_{max}/cm⁻¹): 3263, 1651, 1526, 1486

HRMS calculated for C₁₂H₁₆N₂O₂ (M⁺): 220.1212; Found 220.1197

R_f: 0.53 with 80% EtOAc in pet. ether

Melting Point: 187-189 °C

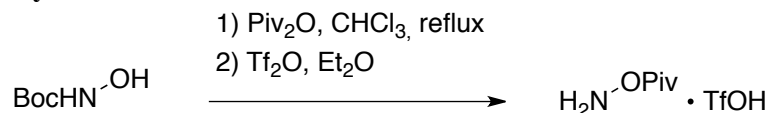
N-((2*R*,5*R*)-2,5-dimethylpyrrolidin-1-yl)benzamide (3.1s)



1k was prepared according to a literature procedure¹⁶⁰ and obtained as a generous gift from Christian Clavette.

5.3.6 ISOQUINOLONE SCOPE SUBSTRATES

O-pivaloylhydroxyamine triflic acid



Pivalic anhydride (3.66 mL, 18.02 mmol, 1.2 equiv.) was added to a solution of *tert*-Butyl hydroxycarbamate (2.00 g, 15.02 mmol, 1 equiv.) in chloroform (40 mL). The reaction mixture was refluxed for 16 hours. The mixture was then quenched with sat. NaHCO₃ and

¹⁶⁰ Roveda, J. G.; Clavette, C.; Hunt, A. D.; Gorelsky, S. I.; Whipp, C. J.; Beauchemin, A. M. *J. Am. Chem. Soc.* **2009**, *131*, 8740-8741.

diluted with CH₂Cl₂. The organic phase was washed 3 times with sat. NaHCO₃ after which it was dried over MgSO₄, filtered and evaporated under reduced pressure. The white solid obtained (3.53g, 16.23 mmol) was dissolved in diethylether (40 mL) and triflic acid (1.44 mL, 16.23 mmol, 1 equiv.) was added dropwise at 0°C. The reaction was allowed to reach rt and it was diluted with pet. ether (40 mL) to precipitate the product. The mixture was filtrated to obtain the desired product as a white solid (2.85 g, 71% over 2 steps).

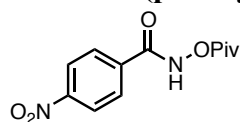
¹H NMR (400 MHz; DMSO-d₆, 293K): δ 1.18 (s, 9H)

¹³C NMR (100 MHz, DMSO-d₆, 293K): δ 174.9, 120.8 (q, *J* = 322.2 Hz, 1C), 38.0, 26.6.

¹⁹F NMR (377 MHz, DMSO-d₆, 293K): δ -77.8

HRMS calculated for C₁₃H₁₇NO₃ (M⁺): 235.1208; Not found. Found only PivOH: calculated for C₅O₂H₁₀ (M⁺): 102.0681; Found 102.0640

4-nitro-*N*-(pivaloyloxy)benzamide (3.1t)



To a solution of 2 parts EtOAc in one part H₂O containing Na₂CO₃ (212 mg, 2.0 mmol, 2 equiv.) was added *O*-pivaloylhydroxyamine triflic acid (267 mg, 1 mmol, 1 equiv.). The mixture was cooled to 0°C and 4-nitrobenzoyl chloride (186 mg, 1 mmol, 1 equiv.) was added to the mixture. It was then allowed to stir at 0°C for 2 hours. The reaction was then quenched with sat. NaHCO₃ and more EtOAc was added. The organic layer was washed twice with sat. NaHCO₃. It was then dried over MgSO₄, filtered and evaporated under reduced pressure. The purification was made by flash column chromatography using 25% EtOAc in pet. ether as eluent. The product obtained is a white solid (86 mg, 32%).

¹H-NMR (400 MHz; CDCl₃, 293K, TMS): δ 9.50 (br s, 1H), 8.31 (d, *J* = 9.0 Hz, 2H), 7.99 (d, *J* = 8.9 Hz, 2H), 1.37 (s, 9H).

¹³C NMR (100 MHz, CDCl₃, 293K, TMS): δ 176.8, 164.5, 150.2, 136.4, 128.8, 124.0, 38.51, 27.0

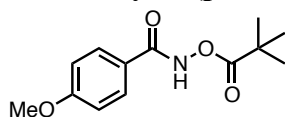
IR (ν_{max}/cm⁻¹): 3320, 2971, 1752, 1700, 1534, 1087

GC-MSD mass: calculated for C₈H₆N₂O₅ (M⁺-(*t*-Bu)): 210.0; Found = 210.1

R_f: 0.33 with 20% EtOAc in pet. ether

Melting Point: 110-112 °C

4-methoxy-*N*-(pivaloyloxy)benzamide (3.1u)



To a solution of 2 parts EtOAc in one part H₂O containing Na₂CO₃ (424 mg, 4.0 mmol, 2 equiv.) was added *O*-pivaloylhydroxyamine triflic acid (534 mg, 2 mmol, 1 equiv.). The mixture was cooled to 0°C and 4-methoxybenzoyl chloride (270 μL, 1 mmol, 1 equiv.) was added to the mixture. It was then allowed to stir at 0°C for 2 hours. The reaction was then quenched with sat. NaHCO₃ and more EtOAc was added. The organic layer was washed

twice with sat. NaHCO₃. It was then dried over MgSO₄, filtered and evaporated under reduced pressure. The purification was made by flash column chromatography using 25% EtOAc in pet. ether as eluent. The product obtained is a white solid (403 mg, 80%).

¹H-NMR (400 MHz; CDCl₃, 293K, TMS): δ 9.36 (br s, 1H), 7.79 (d, *J* = 8.9 Hz, 2H), 6.93 (d, *J* = 8.9 Hz, 2H), 3.85 (s, 3H), 1.36 (s, 9H).

¹³C NMR (100 MHz, CDCl₃, 293K, TMS): δ 177.3, 166.7, 163.1, 129.4, 123.0, 114.0, 55.4, 38.5, 27.0

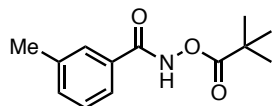
IR (ν_{max}/cm⁻¹): 3243, 2978, 1774, 1653, 1606, 1496, 1261, 1072, 1029

GC-MSD mass: calculated for C₉H₉NO₃ (M⁺-(*t*-Bu)): 251.2; Found = 251.1

R_f: 0.27 with 20% EtOAc in pet. ether

Melting Point: 138-140 °C

3-methyl-*N*-(pivaloyloxy)benzamide (3.1v)



Oxalyl chloride (102 μL, 1.2 mmol, 1.2 equiv.) was added to a solution of 3-toluic acid in dichloromethane. 2 drops of DMF were added and the reaction was stirred at room temperature for 3 h. Then, volatiles were removed under reduced pressure to afford the crude 3-toluic acid chloride.

To a solution of 2 parts EtOAc in one part H₂O containing Na₂CO₃ (424 mg, 4.0 mmol, 2 equiv.) was added *O*-pivaloylhydroxyamine triflic acid (534 mg, 2 mmol, 1 equiv.). The mixture was cooled to 0°C and 3-toluic acid chloride was added to the mixture. It was then allowed to stir at 0°C for 2 hours. The reaction was then quenched with sat. NaHCO₃ and more EtOAc was added. The organic layer was washed twice with sat. NaHCO₃. It was then dried over MgSO₄, filtered and evaporated under reduced pressure. The purification was made by flash column chromatography using 25% EtOAc in pet. ether as eluent. The product obtained is a white solid (403 mg, 80%).

¹H-NMR (400 MHz; CDCl₃, 293K, TMS): δ 9.64 (s, 1H), 7.61-7.57 (m, 2H), 7.34-7.27 (m, 2H), 2.36 (s, 3H), 1.34 (s, 9H).

¹³C NMR (100 MHz, CDCl₃, 293K, TMS): δ 177.0, 166.9, 138.6, 133.4, 130.8, 128.6, 128.1, 124.5, 38.4, 27.0, 21.3

IR (ν_{max}/cm⁻¹): 3213, 2982, 1781, 1657, 1479, 1078

HRMS calculated for C₁₃H₁₇NO₃ (M⁺): 235.1208; Found 235.1140

R_f: 0.46 with 20% EtOAc in pet. ether

Melting Point: 80-82 °C

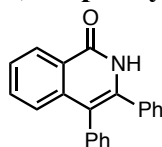
5.3.7 SYNTHESIS OF DISUBSTITUTED ISOQUINOLONES FROM *N*-(OPiv)

BENZAMIDES

General Procedure G

Without any particular precautions to extrude oxygen or moisture, the pivaloyl-protected hydroxamic acid (**3.1**) (1 equiv.), the alkyne (if solid) (1.1 equiv.), $[\text{Cp}^*\text{RhCl}_2]_2$ (0.5 mol%) and CsOAc (2 equiv.) were weighted in a 13x100 mm test tube equipped with a stir bar. MeOH (0.2 M) was then added (followed immediately by the alkyne if it is a liquid). The reaction was stirred at room temperature for 16 hours. Afterwards, it was diluted with CH_2Cl_2 and transferred to a round bottom flask. Silica was added to the flask and volatiles were evaporated under reduced pressure. The purification was performed by flash column chromatography on silica gel (see below for specific eluents).

3,4-diphenylisoquinolin-1(2H)-one (**3.4a**)



3.4a is an off-white solid obtained in 96% yield (80.6 mg) from **3.1m** (4.52 mmol, 1.00 g, 1 equiv.) following general procedure G. The product was isolated by column chromatography using 40% EtOAc in pet. ether.

^1H NMR (400 MHz, DMSO- d_6 , 293K, TMS): δ 11.56 (1H, s), 8.33 (1H, dd, $J = 8.0, 1.1$ Hz), 7.64 (1H, ddd, $J = 8.3, 7.0, 1.4$ Hz), 7.54-7.50 (1H, m), 7.30-7.22 (8H, m), 7.17-7.15 (3H, m)

^{13}C NMR (100 MHz, DMSO- d_6 , 293K, TMS): δ 161.7, 138.6, 138.1, 135.8, 134.6, 132.5, 131.7, 129.8, 128.2, 128.2, 127.7, 127.1, 126.8, 126.3, 125.0, 124.9, 115.4

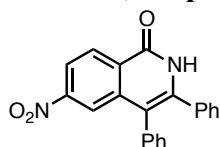
IR ($\nu_{\text{max}}/\text{cm}^{-1}$): 2928, 1647, 694, 557

HRMS calculated for $\text{C}_{21}\text{H}_{15}\text{NO}$ (M^+): 297.1154; Found 297.1167

R_f : 0.45 with EtOAc 50% in pet. ether

Melting Point: 242-246 °C

6-nitro-3,4-diphenylisoquinolin-1(2H)-one (**3.4g**)



The desired compound is a yellow solid obtained in 90% yield (62.0 mg) from **3.1t** (0.20 mmol, 45 mg, 1 equiv.) following general procedure G. The product was isolated by column chromatography using 50% Et₂O in pet. ether.

^1H NMR (400 MHz, CDCl_3 , 293K, TMS): δ 10.15 (1H, s), 8.58-8.56 (1H, m), 8.23-8.20 (2H, m), 7.38-7.26 (8H, m), 7.19-7.17 (2H, m)

^{13}C NMR (100 MHz, CDCl_3 , 293K, TMS): δ 161.7, 150.6, 139.7, 139.5, 134.3, 134.1, 131.6, 129.6, 129.2, 129.2, 128.9, 128.6, 128.5, 128.1, 121.2, 120.1, 117.1

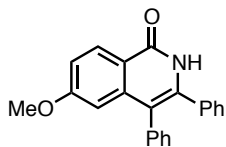
IR (neat, $\nu_{\text{max}}/\text{cm}^{-1}$): 3173, 3032, 2924, 2857, 1657, 1620, 1533, 1345, 902, 835, 795, 744, 701

HRMS calculated for $C_{21}H_{14}N_2O_3$ (M^+): 342.1004; Found 342.1021

Melting Point: 251-252 °C

R_f: 0.17 with 50% Et₂O in pet. ether

6-methoxy-3,4-diphenylisoquinolin-1(2H)-one (3.4c)



The desired compound is a pale orange solid obtained in 89% yield (87.4 mg) from **3.1u** (0.30 mmol, 75 mg, 1 equiv.) following general procedure G. The product was isolated by column chromatography using 2% isopropanol in toluene.

¹H NMR (300 MHz, DMSO-*d*₆, 303K, TMS): δ 11.36 (1H, s), 8.25 (1H, d, *J* = 8.8 Hz), 7.30-7.13 (11H, m), 6.51 (1H, d, *J* = 2.0 Hz), 3.67 (3H, s)

¹³C NMR (75 MHz, DMSO-*d*₆, 303K, TMS): δ 162.3, 161.4, 140.1, 139.2, 135.9, 134.6, 131.7, 129.8, 129.1, 128.2, 128.2, 127.7, 127.1, 118.9, 115.1, 114.5, 107.2, 55.2

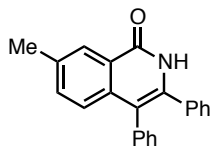
IR (nujol mull, ν_{max}/cm⁻¹): 3129, 1647, 1613, 1278, 868, 781

HRMS calculated for $C_{22}H_{17}NO_2$ (M^+): 327.1259; Found 327.1251

Melting Point: decomposes above 225°C

R_f: 0.20 with 75% CH₂Cl₂, 23% pet. ether and 2% MeOH

7-methyl-3,4-diphenylisoquinolin-1(2H)-one (3.4m)



The desired compound is a pale orange solid obtained in 92% yield (86.4 mg) from **3.1v** (0.30 mmol, 71 mg, 1 equiv.) following general procedure G. The product was isolated by column chromatography using 2% isopropanol in dichloromethane.

¹H NMR (300 MHz, DMSO-*d*₆, 303K, TMS): δ 11.46 (s, 1H), 8.12 (dd, *J* = 1.2, 0.6 Hz, 1H), 7.47 (ddd, *J* = 8.4, 2.0, 0.5 Hz, 1H), 7.32-7.21 (m, 8H), 7.14-7.12 (m, 2H), 7.06 (d, *J* = 8.3 Hz, 1H), 2.45 (s, 3H)

¹³C NMR (75 MHz, DMSO-*d*₆, 303K, TMS): δ 161.6, 137.5, 136.0, 135.8, 134.6, 133.8, 131.7, 129.8, 128.2, 128.1, 127.7, 127.0, 126.4, 125.0, 115.4, 20.9 (2 signals missing due to overlap)

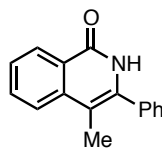
IR (ν_{max}/cm⁻¹): 2925, 1646, 1616, 1492, 1345

HRMS calculated for $C_{22}H_{17}NO$ (M^+): 311.1310; Found 311.1308

Melting Point: decomposes above 270°C

R_f: 0.38 with 3% isopropanol in dichloromethane

4-methyl-3-phenylisoquinolin-1(2H)-one (3.4l)



The desired compound was an off-white solid obtained in 92% yield (65.1mg) from **3.1m** (0.30 mmol, 66 mg, 1 eq.) following general procedure G. The purification was performed by flash column chromatography using 3% isopropanol in toluene.

¹H NMR (400 MHz, CDCl₃, 293K, TMS): δ 9.61 (1H, br s), 8.42 (1H, d, *J* = 7.96 Hz), 7.76-7.72 (2H, m), 7.75-7.43 (6H, m), 2.26 (3H, s)

¹³C NMR (100 MHz, CDCl₃, 293K, TMS): δ 162.6, 138.8, 136.8, 135.3, 132.7, 129.3, 129.0, 128.7, 127.7, 126.3, 125.4, 123.6, 109.1, 13.9

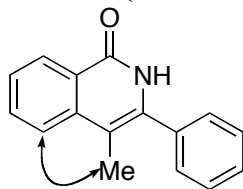
IR (ν_{max}/cm⁻¹): 1653, 761, 701

HRMS calculated for C₁₆H₁₃NO (M⁺): 235.0997; Found 235.1019

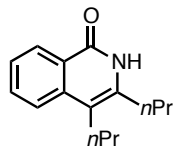
R_f: 0.29 with EtOAc 50% in pet. ether

Melting Point: decomposes at 200-204 °C

NOESY (400 MHz, CDCl₃, 293K, TMS); COSY (400 MHz, CDCl₃, 293K, TMS)



3,4-dipropylyisoquinolin-1(2H)-one (3.4n)



The desired compound was an off-white solid obtained in 70% yield (47.9 mg) from **3.1m** (0.30 mmol, 66 mg, 1 eq.) following general procedure G. The purification was performed by flash column chromatography using 5 to 10% acetone in dichloromethane.

¹H NMR (400 MHz, CDCl₃, 293K, TMS): δ 11.38 (s, 1H), 8.46 (d, *J* = 7.9 Hz, 1H), 7.67 (dd, *J* = 4.5, 1.1 Hz, 2H), 7.46-7.42 (m, 1H), 2.72-2.67 (m, 4H), 1.76 (sextet, *J* = 7.6 Hz, 2H), 1.66-1.54 (m, 2H), 1.08-1.03 (m, 6H).

¹³C NMR (100 MHz, CDCl₃, 293K, TMS): δ 163.8, 138.5, 138.3, 132.3, 127.7, 125.3, 125.1, 123.0, 113.0, 33.0, 28.6, 23.6, 22.8, 14.4, 14.0

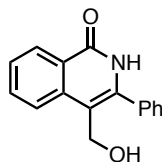
IR (ν_{max}/cm⁻¹): 2955, 2874, 1660, 1633

HRMS calculated for C₁₅H₁₉NO (M⁺): 229.1467; Found 229.1452

R_f: 0.54 with 40% ethyl acetate in pet. ether

Melting Point: decomposes at 176-180 °C

4-(hydroxymethyl)-3-phenylisoquinolin-1(2H)-one (3.4j)



The desired compound was an off-white solid obtained in 99% yield (74.8 mg) from **3.1m** (0.30 mmol, 66 mg, 1 equiv.) following general procedure G. The purification was performed by flash column chromatography using 5% isopropanol in toluene.

¹H NMR (400 MHz, CDCl₃, 293K, TMS): δ 8.78 (1H, br s), 8.44 (1H, dd, *J* = 8.1, 1.2 Hz), 8.01 (1H, d, *J* = 8.2 Hz), 7.77 (1H, ddd, *J* = 8.3, 7.1, 1.4 Hz), 7.56-7.51 (6H, m), 4.74 (2H, s)

¹³C NMR (100 MHz, CDCl₃, 293K, TMS): δ 162.4, 139.8, 137.6, 134.2, 133.3, 129.9, 129.0, 128.8, 127.9, 126.9, 125.6, 124.0, 112.5, 58.6

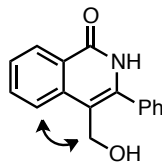
IR (ν_{max}/cm⁻¹): 1650, 1345, 758, 691

HRMS calculated for C₁₆H₁₃NO (M⁺): 251.0946; Found 251.0967

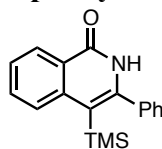
R_f: 0.15 with isopropanol 5% in toluene

Melting Point: Turns black over 280 °C

NOESY (400 MHz, CDCl₃, 293K, TMS); COSY (400 MHz, CDCl₃, 293K, TMS)



3-phenyl-4-(trimethylsilyl)isoquinolin-1(2H)-one (**3.4o**)



The desired compound was an off-white solid obtained in 55% yield (74.8 mg) from **3.1m** (0.30 mmol, 66 mg, 1 equiv.) following general procedure G. The purification was performed by flash column chromatography using 5% acetone in pet. ether.

¹H NMR (400 MHz, CDCl₃, 293K, TMS): δ 7.80 (dt, *J* = 7.5, 0.9 Hz, 1H), 7.60 (s, 1H), 7.44-7.34 (m, 4H), 7.19-7.15 (m, 1H), 7.12-7.10 (m, 2H), 6.12 (d, *J* = 8.0 Hz, 1H), 0.25 (s, 9H).

¹³C NMR (100 MHz, CDCl₃, 293K, TMS): δ 168.3, 140.7, 139.7, 136.6, 131.9, 130.2, 129.0, 128.9, 128.3, 126.7, 125.1, 124.6, 123.0, 0.4

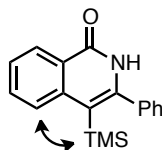
IR (ν_{max}/cm⁻¹): 3223, 1701, 1613, 849

HRMS calculated for C₁₈H₁₉NOSi (M⁺): 293.1236; Found 293.1241

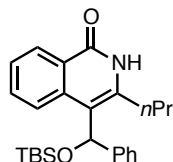
R_f: 0.76 with 50% EtOAc in pet. ether.

Melting Point: 202-208 °C

NOESY (300 MHz, CDCl₃, 293K, TMS)



4-((*tert*-butyldimethylsilyloxy)(phenyl)methyl)-3-propylisoquinolin-1(2*H*)-one (3.4p)



The desired compound was an off-white solid obtained in 83% yield (102.8 mg) from **3.1m** (0.30 mmol, 66 mg, 1 equiv.) following general procedure G. The corresponding alkyne was prepared according to a literature procedure.¹⁶¹ The purification was performed by flash column chromatography using 10% ethyl acetate in pet. ether.

¹H NMR (300 MHz, CDCl₃, 293K, TMS): δ 11.84 (s, 1H), 8.41 (dd, *J* = 7.9, 1.4 Hz, 1H), 7.87-7.84 (m, 1H), 7.45-7.18 (m, 7H), 6.31 (s, 1H), 2.94-2.73 (m, 2H), 1.78-1.74 (m, 2H), 1.07 (t, *J* = 7.2 Hz, 3H), 0.91 (s, 9H), 0.19 (s, 3H), -0.22 (s, 3H).

¹³C NMR (100 MHz, CDCl₃, 293K, TMS): δ 164.5, 144.5, 140.1, 137.1, 131.6, 128.2, 127.0, 126.6, 125.6, 125.5, 125.5, 114.7, 70.4, 33.3, 25.8, 23.1, 18.3, 14.3, 4.5, 4.9

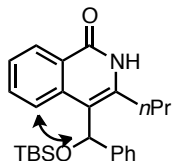
IR (ν_{max}/cm⁻¹):

HRMS calculated for C₂₅H₃₃NO₂Si (M⁺): 407.2281; Found: 407.2283

R_f: 0.82 with 40% EtOAc in pet. ether.

Melting Point: 154-160 °C

NOESY (300 MHz, CDCl₃, 293K, TMS)



5.3.8 SYNTHESIS OF MONOSUBSTITUTED ISOQUINOLONONES

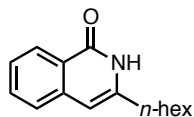
General Procedure H

Without any particular precautions to extrude oxygen or moisture, the pivaloyl-protected hydroxamic acid (**3.1**) (1 equiv.), the alkyne (if solid) (1.1 equiv.), [Cp**Rh*Cl₂]₂ (2.5 mol%) and CsOAc (2 equiv.) were weighted in a 13x100 mm test tube equipped with a stir bar. MeOH (0.2 M) was then added (followed immediately by the alkyne if it is a liquid). The reaction was stirred at room temperature for 16 hours. Afterwards, it was diluted with CH₂Cl₂ and transferred to a round bottom flask. Silica was added to the flask and volatiles

¹⁶¹ Guimond, N.; Fagnou, K. *J. Am. Chem. Soc.* **2009**, *131*, 12050.

were evaporated under reduced pressure. The purification was performed by flash column chromatography on silica gel (see below for specific eluents).

3-hexylisoquinolin-1(2H)-one (3.4q)



The desired compound is an off-white solid obtained in 92% yield (63.2 mg) from **3.1m** (0.30 mmol, 66 mg, 1 equiv.) following general procedure G. The purification was performed by flash column chromatography using 2% isopropanol in dichloromethane.

¹H-NMR (400 MHz; CDCl₃, 293K, TMS): δ 11.51 (d, *J* = 0.4 Hz, 1H), 8.39 (dt, *J* = 8.1, 0.6 Hz, 1H), 7.61 (ddd, *J* = 8.1, 7.0, 1.3 Hz, 1H), 7.47 (d, *J* = 7.9 Hz, 1H), 7.42 (ddd, *J* = 8.1, 7.0, 1.1 Hz, 1H), 6.32 (s, 1H), 2.65 (t, *J* = 7.7 Hz, 2H), 1.76 (dt, *J* = 15.3, 7.6 Hz, 2H), 1.44-1.29 (m, 6H), 0.90-0.87 (m, 3H).

¹³C NMR (100 MHz, CDCl₃, 293K, TMS): δ 164.8, 142.3, 138.7, 132.5, 127.2, 125.6, 124.4, 103.8, 33.4, 31.5, 28.8, 28.3, 22.6, 14.1 (one signal missing due to overlap)

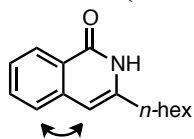
IR (ν_{max}/cm⁻¹): 2928, 2854, 1662, 1635

HRMS calculated for C₁₅H₁₉NO (M⁺): 229.1467; Found 229.1458

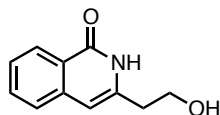
R_f: 0.66 with 40% EtOAc in pet. ether

Melting Point: 114-117 °C

NOESY (300 MHz, CDCl₃, 293K, TMS)



3-(2-hydroxyethyl)isoquinolin-1(2H)-one (3.4r)



The desired compound is an off-white solid obtained in 92% yield (63.2 mg) from **3.1m** (0.30 mmol, 66 mg, 1 equiv.) following general procedure H. The reaction was run at 60 °C instead of room temperature. The purification was performed by flash column chromatography using 2% isopropanol in dichloromethane.

¹H-NMR (400 MHz; DMSO-*d*₆, 293K, TMS): δ 11.17 (s, 1H), 8.13 (dd, *J* = 7.5, 0.5 Hz, 1H), 7.63 (ddd, *J* = 8.0, 7.0, 1.2 Hz, 1H), 7.54 (d, *J* = 7.7 Hz, 1H), 7.41-7.37 (m, 1H), 6.36 (s, 1H), 4.77 (t, *J* = 5.3 Hz, 1H), 3.70 (q, *J* = 5.9 Hz, 2H), 2.64 (t, *J* = 6.5 Hz, 2H).

¹³C NMR (100 MHz, CDCl₃, 293K, TMS): δ 163.0, 140.8, 138.7, 132.8, 127.0, 126.2, 125.9, 124.9, 103.7, 60.0, 36.5

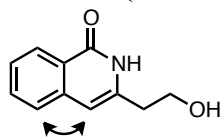
IR (ν_{max}/cm⁻¹): 3387, 2941, 1666, 1643, 1553, 1049

HRMS calculated for C₁₁H₁₁NO₂ (M⁺): 189.0790; Found 189.0790

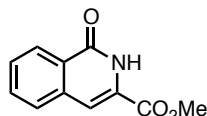
R_f: 0.32 with 20% isopropanol in toluene

Melting Point: 172-175 °C

NOESY (300 MHz, CDCl₃, 293K, TMS)



Methyl 1-oxo-1,2-dihydroisoquinoline-3-carboxylate (3.4s)



The desired compound is an off-white solid obtained in 49% yield (29.7 mg) from **3.1m** (0.30 mmol, 66 mg, 1 equiv.) following general procedure H. The reaction was run at 60 °C instead of room temperature. The purification was performed by flash column chromatography using 45% ethyl acetate in pet. ether.

¹H-NMR (400 MHz; CDCl₃, 293K, TMS): δ 9.26 (s, 1H), 8.46 (dt, *J* = 8.0, 0.6 Hz, 1H), 7.76-7.61 (m, 3H), 7.39 (s, 1H), 4.00 (s, 3H).

¹³C NMR (100 MHz, CDCl₃, 293K, TMS): δ 162.2, 161.8, 136.0, 133.1, 129.5, 128.3, 128.2, 128.0, 127.7, 111.4, 53.2

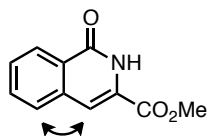
IR (ν_{max}/cm⁻¹): 2928, 1731, 1663, 1301

HRMS calculated for C₁₁H₉NO₃ (M⁺): 203.0582; Found 203.0574

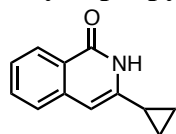
R_f: 0.33 with 50% ethyl acetate in pet. ether

Melting Point: 148-153 °C

NOESY (300 MHz, CDCl₃, 293K, TMS)



3-cyclopropylisoquinolin-1(2H)-one (3.4t)



The desired compound is an off-white solid obtained in 95% yield (52.6 mg) from **3.1m** (0.30 mmol, 66 mg, 1 equiv.) following general procedure H. The purification was performed by flash column chromatography using 15% isopropanol in toluene. (contains 3% of the other regioisomer)

¹H-NMR (400 MHz; CDCl₃, 293K, TMS): δ 11.11 (s, 1H), 8.37 (dt, *J* = 8.1, 0.7 Hz, 1H), 7.60 (ddd, *J* = 8.1, 7.0, 1.3 Hz, 1H), 7.45-7.37 (m, 2H), 6.21 (s, 1H), 1.99-1.92 (m, 1H), 1.07-1.02 (m, 2H), 0.95-0.91 (m, 2H).

¹³C NMR (100 MHz, CDCl₃, 293K, TMS): δ 164.4, 143.5, 138.7, 132.5, 127.3, 125.6, 124.4, 101.4, 13.5, 7.4 (1 signal missing due to overlap)

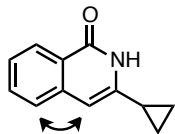
IR (ν_{max}/cm⁻¹): 2998, 1643, 1553, 1479

HRMS calculated for C₁₂H₁₁NO (M⁺): 185.0841; Found 185.0862

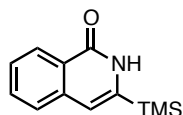
R_f: 0.49 with 50% EtOAc in pet. ether

Melting Point: 151-164 °C

NOESY (300 MHz, CDCl₃, 293K, TMS)



3-(trimethylsilyl)isoquinolin-1(2H)-one (3.4u)



The desired compound is an off-white solid obtained in 75% yield (49.2 mg) from **3.1m** (0.30 mmol, 66 mg, 1 equiv.) following general procedure H. The purification was performed by flash column chromatography using 7% ethyl acetate in dichloromethane.

¹H-NMR (400 MHz; CDCl₃, 293K, TMS): δ 10.63 (s, 1H), 8.40 (dt, *J* = 8.0, 0.6 Hz, 1H), 7.65 (ddd, *J* = 8.1, 7.0, 1.3 Hz, 1H), 7.54-7.47 (m, 2H), 6.65 (s, 1H), 0.41 (s, 9H).

¹³C NMR (100 MHz, CDCl₃, 293K, TMS): δ 164.2, 143.4, 137.5, 132.4, 127.2, 126.8, 126.2, 126.0, 113.4, 2.2

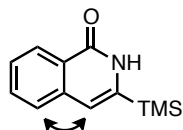
IR (ν_{max}/cm⁻¹): 3127, 3028, 2955, 2901, 1653, 1617, 1254

HRMS calculated for C₁₂H₁₅NOSi (M⁺): 217.0923; Found 217.0901

R_f: 0.76 with 50% EtOAc in pet. ether

Melting Point: 154-158 °C

NOESY (300 MHz, CDCl₃, 293K, TMS);

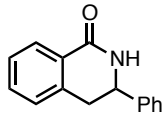


5.3.9 SYNTHESIS OF 3,4-DIHYDROISOQUINOLONES

General procedure I

Without any particular precautions to extrude oxygen or moisture, the pivaloyl-protected hydroxamic acid (**1**)(1 equiv.), [Cp**Rh*Cl₂]₂ (0.5 mol%) and CsOAc (2 equiv.) were weighted in a 13x100 mm test tube equipped with a stir bar. MeOH (0.2 M) was then added followed immediately by the alkene (1.1 equiv.). The reaction was stirred at room temperature for 16 hours. Afterwards, it was diluted with CH₂Cl₂ and transferred to a round bottom flask. Silica was added to the flask and volatiles were evaporated under reduced pressure. The purification was performed by flash column chromatography on silica gel (see below for specific eluents). Then, the resulting compound was dissolved in MeCN and washed with pet. ether to remove residual pivalic acid that seems to stick to these molecules.

3-phenylisoquinolin-1(2*H*)-one (3.9a)

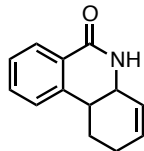


The desired compound is an off-white solid obtained in 90% yield (60.3 mg) from **3.1m** (0.30 mmol, 66 mg, 1 equiv.) following general procedure I. The purification was performed by flash column chromatography using 30% ethyl acetate in pet. ether.

¹H-NMR (400 MHz; CDCl₃, 293K, TMS): δ 8.12 (dd, *J* = 7.7, 1.2 Hz, 1H), 7.46 (td, *J* = 7.5, 1.5 Hz, 1H), 7.41-7.34 (m, 6H), 7.18 (d, *J* = 7.5 Hz, 1H), 6.13 (s, 1H), 4.86 (ddd, *J* = 10.9, 4.9, 1.1 Hz, 1H), 3.23-3.09 (m, 2H).

Spectral data matched the one previously reported.¹⁶²

1,2,4a,5-tetrahydrophenanthridin-6(10*bH*)-one (3.9b)



The desired compound is an off-white solid obtained in 77% yield (46.2 mg) from **3.1m** (0.30 mmol, 66 mg, 1 equiv.) following general procedure I. The purification was performed by flash column chromatography using 3% isopropanol in toluene.

¹H-NMR (400 MHz; CDCl₃, 293K, TMS): δ 8.08 (dd, *J* = 7.7, 1.4 Hz, 1H), 7.49 (td, *J* = 7.5, 1.5 Hz, 1H), 7.36 (td, *J* = 7.6, 1.2 Hz, 1H), 7.27-7.24 (m, 1H), 6.06-6.01 (m, 2H), 5.80 (ddt, *J* = 9.8, 4.8, 2.4 Hz, 1H), 4.29-4.27 (m, 1H), 2.97-2.92 (m, 1H), 2.25-2.19 (m, 2H), 2.04-1.93 (m, 1H), 1.73-1.67 (m, 1H).

¹³C NMR (100 MHz, CDCl₃, 293K, TMS): δ 165.0, 142.8, 132.5, 132.3, 128.0, 127.5, 127.2, 127.1, 124.4, 48.0, 37.8, 25.2, 25.0.

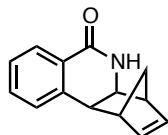
IR (ν_{max}/cm⁻¹): 3206, 2931, 1668, 1466, 1398

HRMS calculated for C₁₃H₁₃NO (M⁺): 199.0997; Found 199.0984

R_f: 0.36 with 50% EtOAc in pet. ether

Melting Point: 141-148 °C

3.9c



¹⁶² Koltunov, K. Y.; Prakash, G. K. S.; Rasul, G.; Olah, G. A. *J. Org. Chem.* **2002**, *67*, 8943.

The desired compound is a white solid obtained in 91% yield (288.2 mg) from **3.1m** (1.50 mmol, 332 mg, 1 equiv.) following general procedure I. The purification was performed by flash column chromatography using 50% ethyl acetate in pet. ether.

¹H-NMR (400 MHz; CDCl₃, 293K, TMS): δ 8.14 (dd, *J* = 8.1, 1.4 Hz, 1H), 7.51-7.47 (m, 1H), 7.33-7.29 (m, 2H), 6.75 (s, 1H), 6.39 (dt, *J* = 4.3, 2.3 Hz, 1H), 6.14 (td, *J* = 3.5, 2.1 Hz, 1H), 3.73 (d, *J* = 8.8 Hz, 1H), 3.09 (d, *J* = 8.8 Hz, 1H), 2.92 (t, *J* = 1.8 Hz, 2H), 1.64 (d, *J* = 9.4 Hz, 1H), 1.47 (dt, *J* = 9.4, 1.6 Hz, 1H).

¹³C NMR (100 MHz, CDCl₃, 293K, TMS): δ 164.2, 140.0, 139.3, 134.8, 132.4, 128.4, 127.7, 126.4, 126.1, 54.2, 52.9, 52.2, 42.7, 39.3.

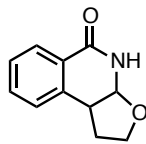
IR (ν_{max}/cm⁻¹): 2941, 1673, 1459, 1335

HRMS calculated for C₉H₇NO (M⁺-cyclopentadiene): 145.0528; Found 145.0539

R_f: 0.38 with 50% EtOAc in pet. ether

Melting Point: melts with gas formation at 190 °C

1,2,3a,4-tetrahydrofuro[2,3-*c*]isoquinolin-5(9*bH*)-one (3.9d)



The desired compound is an off-white solid obtained in 77% yield (43.8 mg) from **3.1m** (0.3 mmol, 66 mg, 1 equiv.) following general procedure I. The purification was performed by flash column chromatography using 8% isopropanol in toluene.

¹H-NMR (400 MHz; CDCl₃, 293K, TMS): δ 8.16 (dd, *J* = 7.6, 1.4 Hz, 1H), 7.57 (td, *J* = 7.4, 1.5 Hz, 1H), 7.52-7.46 (m, 2H), 7.38 (s, 1H), 4.83 (d, *J* = 4.4 Hz, 1H), 4.35 (t, *J* = 4.5 Hz, 1H), 4.09-3.99 (m, 2H), 2.43 (dtd, *J* = 13.2, 8.9, 5.6 Hz, 1H), 2.24 (dddd, *J* = 13.1, 7.0, 3.9, 2.2 Hz, 1H).

¹³C NMR (100 MHz, CDCl₃, 293K, TMS): δ 164.8, 135.3, 132.6, 129.3, 129.0, 127.9, 127.4, 75.2, 66.7, 54.2, 34.9

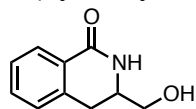
IR (ν_{max}/cm⁻¹): 3213, 2885, 1669, 1606, 1583, 1409, 1334, 1045, 760

HRMS calculated for C₁₁H₁₁NO₂ (M⁺): 189.0790; Found 189.0785

R_f: 0.10 with 50% EtOAc in pet. ether

Melting Point: 132-138 °C

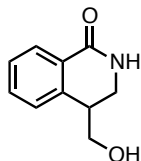
3-(hydroxymethyl)-3,4-dihydroisoquinolin-1(2*H*)-one (3.9e-regio 1)



The desired compound is an off-white solid obtained in 37% yield (19.9 mg) from **3.1m** (0.3 mmol, 66 mg, 1 equiv.) following general procedure I. The purification was performed by flash column chromatography using 15% isopropanol in toluene.

¹H-NMR (400 MHz; DMSO-*d*₆, 293K, TMS): δ 7.83 (dd, *J* = 7.7, 1.1 Hz, 1H), 7.75 (s, 1H), 7.46 (td, *J* = 7.5, 1.4 Hz, 1H), 7.34-7.28 (m, 2H), 4.92 (s, 1H), 3.59-3.41 (m, 2H), 2.99 (dd, *J* = 16.0, 5.1 Hz, 1H), 2.86 (dd, *J* = 15.9, 8.1 Hz, 1H). Spectral data is consistent with that previously reported.¹⁶³

4-(hydroxymethyl)-3,4-dihydroisoquinolin-1(2*H*)-one (3.9e-regio 2)



The desired compound is an off-white solid obtained in 48% yield (25.5 mg) from **3.1m** (0.3 mmol, 66 mg, 1 equiv.) following general procedure I. The purification was performed by flash column chromatography using 15% isopropanol in toluene.

¹H-NMR (400 MHz; CDCl₃, 293K, TMS): δ 8.04 (d, *J* = 7.4 Hz, 1H), 7.46 (td, *J* = 7.5, 1.1 Hz, 1H), 7.35 (td, *J* = 7.6, 1.0 Hz, 1H), 7.28-7.23 (m, 1H), 6.50 (s, 1H), 3.78-3.67 (m, 4H), 3.05-3.01 (m, 1H), 2.57 (s, 1H).

¹³C NMR (100 MHz, DMSO-*d*₆, 293K, TMS): δ 164.5, 140.5, 132.2, 129.5, 128.3, 127.5, 127.4, 62.3. (2 signals missing due to overlap with DMSO signal)

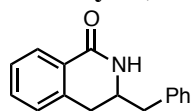
IR (ν_{max}/cm⁻¹): 3307, 2931, 2874, 1657, 1479

HRMS calculated for C₁₀H₁₁NO₂ (M⁺): 177.0790; Found 177.0781

R_f: 0.12 with 50% EtOAc in pet. ether

Melting Point: 120-127°C

3-benzyl-3,4-dihydroisoquinolin-1(2*H*)-one (3.9f-regio 1)



The desired compound is an off-white solid obtained in 57% yield (40.6 mg) from **3.1m** (0.3 mmol, 66 mg, 1 equiv.) following general procedure I. The purification was performed by flash column chromatography using 2.5% isopropanol in toluene.

¹H-NMR (400 MHz; CDCl₃, 293K, TMS): δ 8.09 (dd, *J* = 7.5, 1.5 Hz, 1H), 7.41 (td, *J* = 7.4, 1.6 Hz, 1H), 7.36 (td, *J* = 7.5, 1.4 Hz, 1H), 7.29 (ddd, *J* = 7.9, 6.4, 1.4 Hz, 2H), 7.23-7.20 (m, 1H), 7.14-7.11 (m, 2H), 7.08 (dd, *J* = 7.2, 0.9 Hz, 1H), 6.30 (s, 1H), 3.58 (ddd, *J* = 12.5, 4.3, 0.9 Hz, 1H), 3.28 (ddd, *J* = 12.5, 4.7, 2.9 Hz, 1H), 3.11-3.06 (m, 1H), 3.00-2.87 (m, 2H).

¹³C NMR (100 MHz, DMSO-*d*₆, 293K, TMS): δ 166.1, 142.4, 139.1, 132.2, 129.1, 128.6, 128.3, 128.1, 127.3, 127.1, 126.6, 43.0, 40.0, 39.8

IR (ν_{max}/cm⁻¹): 3210, 3069, 3025, 2925, 1669, 1476, 1335.

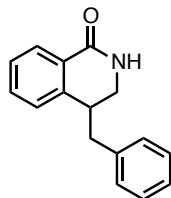
HRMS calculated for C₁₆H₁₅NO (M⁺): 237.1154; Found 237.1166

¹⁶³ Grunewald, G. L.; Caldwell, T. M.; Li, Q.; Dahanukar, V. H.; McNeil, B.; Criscione, K. R. *J. Med. Chem.*, **1999**, *42*, 4351.

R_f: 0.27 with 50% EtOAc in pet. ether

Melting Point: 120-122°C

4-benzyl-3,4-dihydroisoquinolin-1(2H)-one (3.9f-regio 2)



The desired compound is an off-white solid obtained in 28% yield (19.9 mg) from **3.1m** (0.3 mmol, 66 mg, 1 equiv.) following general procedure I. The purification was performed by flash column chromatography using 2.5% isopropanol in toluene.

¹H-NMR (400 MHz; CDCl₃, 293K, TMS): δ 8.06 (dd, *J* = 7.7, 1.1 Hz, 1H), 7.45 (td, *J* = 7.5, 1.4 Hz, 1H), 7.37-7.32 (m, 3H), 7.29-7.25 (m, 1H), 7.20 (dt, *J* = 7.0, 2.4 Hz, 3H), 6.06 (s, 1H), 3.99-3.91 (m, 1H), 3.03-2.80 (m, 4H).

¹³C NMR (100 MHz, DMSO-*d*₆, 293K, TMS): δ 166.1, 137.7, 136.6, 132.4, 129.2, 129.0, 128.6, 128.0, 127.5, 127.2, 52.5, 41.8, 34.2. (1 signal missing due to overlap)

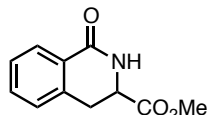
IR (ν_{max}/cm⁻¹): 3203, 2928, 1669, 1606, 1466, 1345

HRMS calculated for C₁₆H₁₅NO (M⁺): 237.1154; Found 237.1152

R_f: 0.39 with 50% EtOAc in pet. ether

Melting Point: 142-147°C

methyl 1-oxo-1,2,3,4-tetrahydroisoquinoline-3-carboxylate (3.9g)



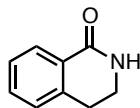
The desired compound was obtained as a 4.5:1 mixture of regioisomers that were inseparable by flash chromatography in 95% yield (19.9 mg) from **3.1m** (0.3 mmol, 66 mg, 1 equiv.) following general procedure I, but with the use of 2.5 mol% [Cp**RhCl*₂]₂. The purification was performed by flash column chromatography using 5% isopropanol in toluene.

¹H-NMR (400 MHz; CDCl₃, 293K, TMS): δ 8.10-8.07 (m, 1H), 7.51-7.46 (m, 1H), 7.41-7.37 (m, 1H), 7.25 (d, *J* = 7.9 Hz, 1H), 6.39 (s, 1H), 4.42 (ddd, *J* = 10.2, 5.1, 1.9 Hz, 1H), 3.81 (s, 3H), 3.36-3.31 (m, 1H), 3.22 (dd, *J* = 15.6, 10.2 Hz, 1H).

Spectral data of the major regioisomer match the data previously reported.¹⁶⁴

3,4-dihydroisoquinolin-1(2H)-one (3.9h)

¹⁶⁴ Janin, Y. L.; Roulland, E.; Beurdeley-Thomas, A.; Decaudin, D.; Monneret, C.; Poupon, M.-F. *J. Chem. Soc., Perkin Trans. 1*, **2002**, 529.

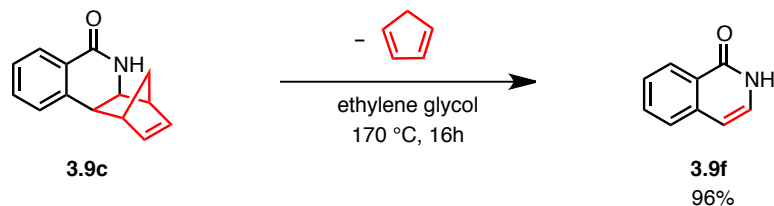


Without any particular precautions to extrude oxygen or moisture, the pivaloyl-protected hydroxamic acid (**3.1m**) (1 equiv.), [Cp*RhCl₂]₂ (0.5 mol%) and CsOAc (2 equiv.) were weighed in a 13x100 mm test tube equipped with a stir bar. MeOH (0.2 M) was then added and ethylene was bubbled through the reaction mixture for about 3 min. The needle was pulled out of the solvent and the vial was sealed under an ethylene atmosphere (balloon). The reaction was stirred at room temperature for 16 hours. Afterwards, it was diluted with CH₂Cl₂ and transferred to a round bottom flask. Silica was added to the flask and volatiles were evaporated under reduced pressure. The purification was performed by flash column chromatography on silica gel. The desired compound was obtained in 98% yield (43.1 mg) from **3.1m** (0.3 mmol, 66 mg, 1 equiv.). The purification was performed by flash column chromatography using 4% isopropanol in dichloromethane.

¹H-NMR (400 MHz; CDCl₃, 293K, TMS): δ 8.08-8.06 (m, 1H), 7.45 (td, *J* = 7.5, 1.5, 1H), 7.38-7.34 (m, 1H), 7.23-7.21 (m, 1H), 6.38 (s, 1H), 3.58 (td, *J* = 6.6, 2.9, 2H), 3.01 (t, *J* = 6.6, 2H)

Spectral data match the one previously reported.¹⁶⁵

Retro Diels-Alder Reaction



3.9c (0.30 mmol, 63.4 mg) was dissolved in ethylene glycol (0.3M) and heated for 16h at 170 °C. The resulting mixture was then cooled down to room temperature and diluted with dichloromethane and brine. The aqueous phase was extracted with dichloromethane and the combined organic fractions were washed with more brine. The organic fraction was dried over MgSO₄, filtered and evaporated under reduced pressure to afford **3.9f** as a white solid. The compound was analytically pure without any further purification necessary.

¹H-NMR (400 MHz; CDCl₃, 293K, TMS): δ 10.69 (br s, 1H), 8.43 (dt, *J* = 8.1, 0.7 Hz, 1H), 7.68 (ddd, *J* = 8.0, 7.0, 1.3 Hz, 1H), 7.57 (d, *J* = 7.9 Hz, 1H), 7.52 (ddd, *J* = 8.1, 7.1, 1.1 Hz, 1H), 7.15 (dd, *J* = 7.2, 0.3 Hz, 1H), 6.56 (d, *J* = 7.1 Hz, 1H).

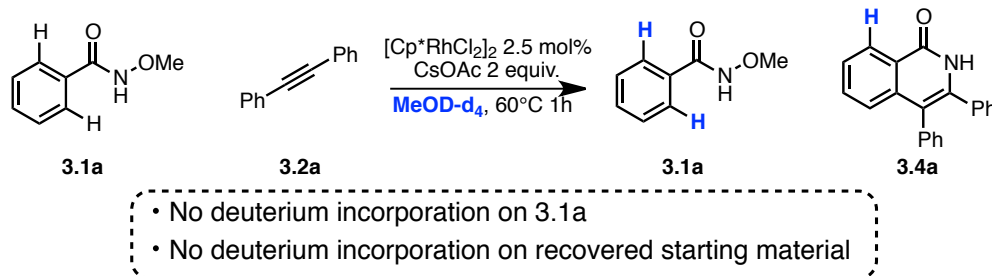
Spectral data is consistent with that previously reported.¹⁶⁶

5.3.10 MECHANISTIC EXPERIMENTS

¹⁶⁵ Ren, W.; Yamane, M. *J. Org. Chem.* **2009**, *74*, 8332.

¹⁶⁶ Lu, W.-D.; Lin, C.-F.; Wang, C.-J.; Wang, S.-J.; Wu, M.-J. *Tetrahedron*, **2002**, *58*, 7315.

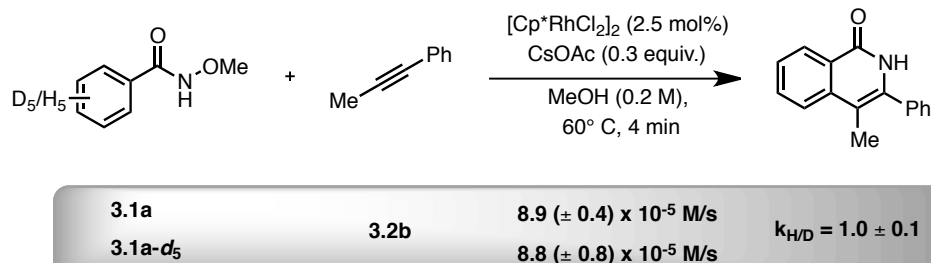
Irreversibility of alkyne insertion



Without any particular precautions to extrude oxygen or moisture, **3.1a** (60 mg, 0.40 mmol, 1 equiv.), **3.2a** (78.4 mg, 0.44 mmol, 1.1 equiv.) $[\text{Cp}^*\text{RhCl}_2]_2$ (6.2 mg, 0.025 mmol, 2.5 mol%) and CsOAc (153 mg, 0.80 mmol, 2 equiv.) were weighed in a 13x100 mm test tube equipped with a stir bar. MeOH (1 mL) was added and the mixture was stirred at 60°C for 5 h after which the reaction mixture was diluted with CH_2Cl_2 and transferred to a round bottom flask. Silica was added to the flask and volatiles were evaporated under reduced pressure. The purification was performed by flash column chromatography on silica gel using 40% EtOAc in pet. ether. Both **3.1a** and **3.4a** were isolated and no deuterium incorporation was found.

KIE experiments

With 3.1a/3.1a D-5 as substrate

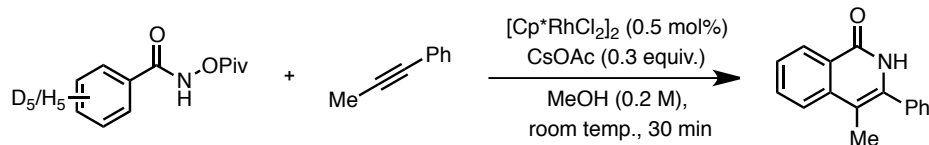


Without any particular precautions to extrude oxygen or moisture, **3.1a** (78 mg, 0.50 mmol, 1 equiv.), **3.2b** (69 μL , 0.55 mmol, 1.1 equiv.), CsOAc (29 mg, 0.15 mmol, 0.3 equiv.) and the internal standard trimethoxybenzene (28 mg, 0.167 mmol, 0.33 equiv.), were weighed in a 10 mL round bottom flask equipped with a stir bar. MeOH (2.5 mL, 0.2M) was added and the mixture was stirred at 60 °C for 5 min. $[\text{Cp}^*\text{RhCl}_2]_2$ (6.2 mg, 0.025 mmol, 2.5 mol%) was then added in one portion and timing was started. An aliquot of 0.5 mL was taken every minute for 4 minutes and immediately quenched in a mixture of TFA (30 μL) and chloroform (1 mL). Volatiles were removed under a flow of air and ^1H NMR was taken. The yield was found by integrating the methyl peak of the isoquinolone.

	[3.1a]			
time (sec)	H-5 run 1	H-5 run 2	D-5 run 1	D-5 run 2
60	0,0162	0,0156	0,0168	0,0144
120	0,0236	0,022	0,0244	0,0206
180	0,0292	0,0274	0,0294	0,025

240 0,033 0,0308 0,0342 0,029

With 3.1m/3.1m D-5 as substrate

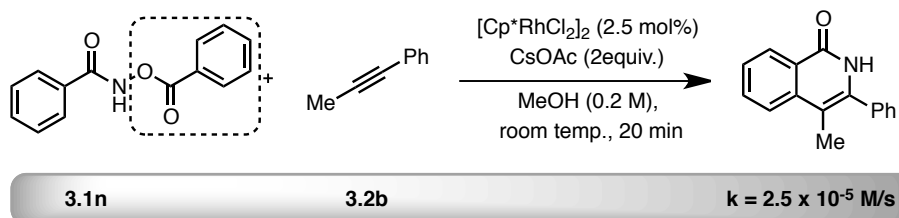
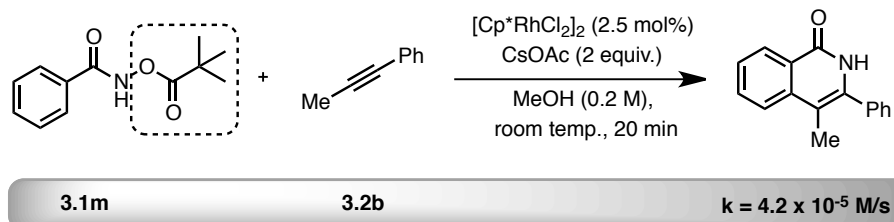


3.1m		4.8 (± 0.2) x 10⁻⁵ M/s	k_{H/D} = 15 ± 1
3.1m-d₅	3.2b	0.33 (± 0.01) x 10⁻⁵ M/s	

Without any particular precautions to extrude oxygen or moisture, **3.1m** (155 mg, 0.70 mmol, 1 equiv.), **3.2b** (96.4 μL, 0.77 mmol, 1.1 equiv.), CsOAc (153 mg, 0.80 mmol, 2 equiv.) and trimethoxybenzene (39 mg, 0.233 mmol, 0.33 equiv.), the internal standard, were weighed in a 10 mL round bottom flask equipped with a stir bar. MeOH (3.5 mL, 0.2M) was added and the mixture was stirred at rt for 2 min. $[\text{Cp}^*\text{RhCl}_2]_2$ (2.2 mg, 0.005 mmol, 0.5 mol%) was then added in one portion and timing was started. An aliquot of 0.5 mL was taken every 5 minutes for 30 minutes and immediately quenched in a mixture of TFA (30 μL) and dichloromethane (1 mL). Volatiles were removed under a flow of air and ¹H NMR was taken. The yield was found by integrating the methyl peak of the isoquinolone.

[3.1m]				
time (sec)	H-5 run 1	H-5 run 2	D-5 run 1	D-5 run 2
300	0,008	0,01	0,00086	0,00092
600	0,02	0,022	0,00172	0,0018
900	0,032	0,034	0,00268	0,00284
1200	0,046	0,048	0,00368	0,00364
1500	0,06	0,066	0,00432	0,00486
1800	0,078	0,084	0,00568	0,00604

Rate with different internal oxidants



$$k_{\text{OPiv/OBz}} = 1.7$$

Rate with substrate **3.1m** was calculated in the KIE experiment, see above.

Rate with substrate **3.1n**

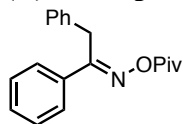
Without any particular precautions to extrude oxygen or moisture, **3.1n** (169 mg, 0.70 mmol, 1 equiv.), **3.2b** (96.4 μL , 0.77 mmol, 1.1 equiv.), CsOAc (153 mg, 0.80 mmol, 2 equiv.) and trimethoxybenzene (39 mg, 0.233 mmol, 0.33 equiv.), the internal standard, were weighed in a 10 mL round bottom flask equipped with a stir bar. MeOH (3.5 mL, 0.2M) was added and the mixture was stirred at rt for 2 min. $[\text{Cp}^*\text{RhCl}_2]_2$ (2.2 mg, 0.005 mmol, 0.5 mol%) was then added in one portion and timing was started. An aliquot of 0.5 mL was taken every 5 minutes for 20 minutes and immediately quenched in a mixture of TFA (30 μL) and dichloromethane (1 mL). Volatiles were removed under a flow of air and ^1H NMR was taken. The yield was found by integrating the methyl peak of the isoquinolone.

time (sec)	[3.1n]
300	0,007
600	0,0146
900	0,022
1200	0,0296

5.3.11 ISOQUINOLINE SYNTHESIS RELATED EXPERIMENTS

Preparation of the starting materials

(*E*)-1,2-diphenylethanone *O*-pivaloyl oxime (**3.10c**)



Pivalic anhydride (2.23 mL, 11 mmol, 1.3 equiv.) was added to a solution of (*E*)-1,2-diphenylethanone oxime (1.75 g, 8.3 mmol, 1 equiv.) in dichloromethane (30 mL). The reaction mixture was allowed to stir for 16 h at room temperature after which it was diluted with more dichloromethane and washed with sat. NaHCO₃. The organic layer was dried over MgSO₄, filtered and evaporated under reduced pressure. The purification was made by flash column chromatography using EtOAc 7.5% in pet. ether as eluent. The product obtained is a white solid (1.72g, 70%)

¹H-NMR (400 MHz; CDCl₃, 293K, TMS): δ 7.76-7.74 (m, 2H), 7.40-7.32 (m, 3H), 7.28-7.24 (m, 2H), 7.21-7.16 (m, 3H), 4.23 (s, 2H), 1.23 (s, 9H).

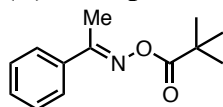
¹³C NMR (100 MHz, CDCl₃, 293K, TMS): δ 174.9, 164.1, 135.3, 134.2, 130.5, 128.8, 128.6, 128.0, 127.5, 126.7, 38.7, 34.5, 27.1

IR (ν_{max}/cm⁻¹): 2978, 1757, 1445, 1115

HRMS calculated for C₁₉H₂₁NO₂ (M⁺): 295.1572; Found 295.1583

R_f: 0.33 with 10% EtOAc in pet. ether

(*E*)-acetophenone *O*-pivaloyl oxime (**3.10d**)



Pivalic anhydride (2.23 mL, 11 mmol, 1.1 equiv.) was added to a solution of acetophenone oxime (1.35 g, 10 mmol, 1 equiv.) in dichloromethane (30 mL). The reaction mixture was allowed to stir for 16 h at room temperature after which it was diluted with more dichloromethane and washed with sat. NaHCO₃. The organic layer was dried over MgSO₄, filtered and evaporated under reduced pressure. The purification was made by flash column chromatography using 10% EtOAc in pet. ether to afford **3.10d** as a white solid (2.09 g, 95%).

¹H-NMR (300 MHz; CDCl₃, 293K, TMS): δ 7.76-7.73 (m, 2H), 7.42-7.38 (m, 3H), 2.37 (s, 3H), 1.33 (s, 9H)

¹³C NMR (75 MHz, CDCl₃, 293K, TMS): δ 175.0, 163.1, 134.9, 130.5, 128.5, 127.0, 38.8, 27.3, 14.3

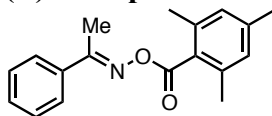
IR (ν_{max}/cm⁻¹): 2974, 1760, 1309, 1114

HRMS calculated for C₁₃H₁₇NO₂ (M⁺): 219.1259; Found 219.1248

R_f: 0.48 with 10% EtOAc in pet. ether

Melting Point: 60-62°C

(*E*)-acetophenone *O*-2,4,6-trimethylbenzoyl oxime (**3.10e**)



Acetophenone oxime (2.00 g, 14.8 mmol, 1 equiv.) and NaOtBu (1.42 g, 14.8 mmol, 1 equiv.) were stirred together at room temperature for 30 min. Then, the mixture was cooled down to 0 °C and mesityl chloride (2.47 mL, 14.8 mmol, 1 equiv.) was added dropwise. It was then brought back to room temperature and stirred until completion as judge by TLC. The reaction was then quenched with sat. NaHCO₃ and the organic phase was washed three

times with sat. NaHCO₃ after which it was dried over MgSO₄, filtered and evaporated under reduced pressure. The purification was made by flash column chromatography using 7% ethyl acetate in pet. ether to afford a white solid (2.94 g, 71%).

¹H-NMR (300 MHz; CDCl₃, 293K, TMS): δ 7.82-7.79 (m, 2H), 7.46-7.42 (m, 3H), 6.91 (s, 2H), 2.40-2.38 (m, 9H), 2.32 (s, 3H).

¹³C NMR (100 MHz, DMSO-d₆, 293K, TMS): δ 167.35, 163.3, 139.8, 135.7, 134.8, 130.6, 129.4, 128.6, 128.4, 127.1, 21.2, 19.9, 14.6

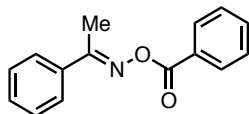
IR (ν_{max}/cm⁻¹): 2922, 1756, 1612, 1240, 1163, 1048

GC-MSD mass: calculated for C₈H₆N₂O₅ (M⁺-(*t*-Bu)): 210.0; Found = 210.1

R_f: 0.55 with 10% EtOAc in pet. ether

Melting Point: 82-85°C

(*E*)-acetophenone *O*-benzoyl oxime (3.10f)



Acetophenone oxime (270 mg, 2.0 mmol, 1 equiv.) and NaO*t*Bu (211 mg, 2.2 mmol, 1.1 equiv.) were stirred together at room temperature in Et₂O (10 mL) for 30 min. Then, the mixture was cooled down to 0 °C and benzoyl chloride (232 μL, 2.0 mmol, 1 equiv.) was added dropwise. It was then brought back to room temperature and stirred until completion as judge by TLC. The reaction was then quenched with sat. NaHCO₃ and the organic phase was washed three times with sat. NaHCO₃ after which it was dried over MgSO₄, filtered and evaporated under reduced pressure. The purification was made by flash column chromatography using 15% Et₂O in pet. ether to afford a white solid (327 mg, 68%).

¹H-NMR (300 MHz; CDCl₃, 293K, TMS): δ 8.16-8.13 (m, 2H), 7.85-7.81 (m, 2H), 7.64-7.60 (m, 1H), 7.52-7.41 (m, 5H), 2.54 (s, 3H).

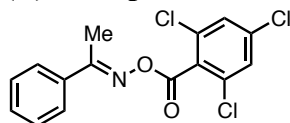
¹³C NMR (100 MHz, CDCl₃, 293K, TMS): δ 163.8, 163.6, 134.9, 133.3, 130.7, 129.7, 129.2, 128.6, 128.6, 127.1, 14.7

IR (ν_{max}/cm⁻¹): 1744, 1314, 1248, 1060

HRMS calculated for C₁₅H₁₃NO₂ (M⁺): 239.0946; Found 239.0927

R_f: 0.35 with 20% Et₂O in pet. ether

(*E*)-acetophenone *O*-(2,4,6-trichlorobenzoyl) oxime (3.10g)



Acetophenone oxime (250 mg, 1.85 mmol, 1 equiv.) and NaO*t*Bu (178 mg, 1.85 mmol, 1 equiv.) were stirred together at room temperature in Et₂O (10 mL) for 30 min. Then, the mixture was cooled down to 0 °C and 2,4,6-trichlorobenzoyl chloride (289 μL, 1.85 mmol, 1 equiv.) was added dropwise. It was then brought back to room temperature and stirred until completion as judge by TLC. The reaction was then quenched with sat. NaHCO₃ and the organic phase was washed three times with sat. NaHCO₃ after which it was dried over MgSO₄, filtered and evaporated under reduced pressure. The purification was made by flash column chromatography using 10% Et₂O in pet. ether to afford a white solid (592 mg, 93%).

¹H-NMR (300 MHz; CDCl₃, 293K, TMS): δ 7.76-7.74 (m, 2H), 7.48-7.39 (m, 5H), 2.43 (s, 3H).

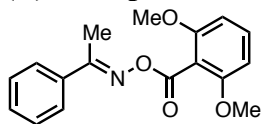
¹³C NMR (100 MHz, CDCl₃, 293K, TMS): δ 164.7, 162.0, 136.6, 134.1, 133.1, 131.1, 131.0, 128.6, 128.1, 127.1, 14.8

IR (ν_{max}/cm⁻¹): 1765, 1578, 1246, 1108

HRMS found the mass for the 2,4,6-trichlorobenzoyl fragment (calculated for C₇H₂Cl₃O (M⁺): 206.9171, found: 206.9167) and the acetophenone imine fragment (calculated for C₈H₈N (M⁺): 118.0657; found 118.0645)

R_f: 0.56 with 10% EtOAc in pet. ether

(E)-acetophenone O-(2,6-dimethoxybenzoyl) oxime (3.10h)



Acetophenone oxime (270 mg, 2.0 mmol, 1 equiv.) and NaOtBu (211 mg, 2.2 mmol, 1.1 equiv.) were stirred together at room temperature in Et₂O (10 mL) for 30 min. Then, the mixture was cooled down to 0 °C and 2,6-dimethoxybenzoyl chloride (prepared from the corresponding carboxylic acid using oxalyl chloride, 2.0 mmol, 1 equiv.) was added dropwise. It was then brought back to room temperature for 16 h. The reaction was then quenched with sat. NaHCO₃ and the organic phase was washed three times with sat. NaHCO₃ after which it was dried over MgSO₄, filtered and evaporated under reduced pressure. The purification was made by flash column chromatography using 25% EtOAc in pet. ether to afford a white solid (273 mg, 46%).

¹H-NMR (400 MHz; CDCl₃, 293K, TMS): δ 7.80-7.77 (m, 2H), 7.44-7.37 (m, 3H), 7.33 (t, *J* = 8.4 Hz, 1H), 6.59 (d, *J* = 8.4 Hz, 2H), 3.83 (s, 6H), 2.39 (s, 3H).

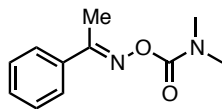
¹³C NMR (100 MHz, CDCl₃, 293K, TMS): δ 164.1, 163.8, 157.9, 135.0, 131.6, 130.6, 128.5, 127.3, 111.5, 104.0, 56.1, 14.7

IR (ν_{max}/cm⁻¹): 1761, 1596, 1476, 1257, 1113, 1049

HRMS found the mass for the 2,6-dimethoxybenzoyl fragment (calculated for C₉H₉CO₃ (M⁺): 165.0552, found: 165.0548) and the acetophenone imine fragment (calculated for C₈H₈N (M⁺): 118.0657; found 118.0645)

R_f: 0.23 with 20% EtOAc in pet. ether

(E)-acetophenone O-dimethylcarbamoyl oxime (3.10i)



Acetophenone oxime (250 mg, 1.85 mmol, 1 equiv.) and NaOtBu (178 mg, 1.85 mmol, 1 equiv.) were stirred together at room temperature in CH₂Cl₂ (10 mL) for 30 min. Then, the mixture was cooled down to 0 °C and dimethylcarbamoyl chloride (171 μL, 1.85 mmol, 1 equiv.) was added dropwise. It was then brought back to room temperature and stirred until completion as judge by TLC. The reaction was then quenched with sat. NaHCO₃ and the organic phase was washed three times with sat. NaHCO₃ after which it was dried over MgSO₄, filtered and evaporated under reduced pressure. The purification was made by flash

column chromatography using 50% EtOAc in pet. ether to afford a white solid (225 mg, 59%).

¹H-NMR (400 MHz; CDCl₃, 293K, TMS): δ 7.77-7.74 (m, 2H), 7.42-7.36 (m, 3H), 3.04 (s, 6H), 2.37 (s, 3H).

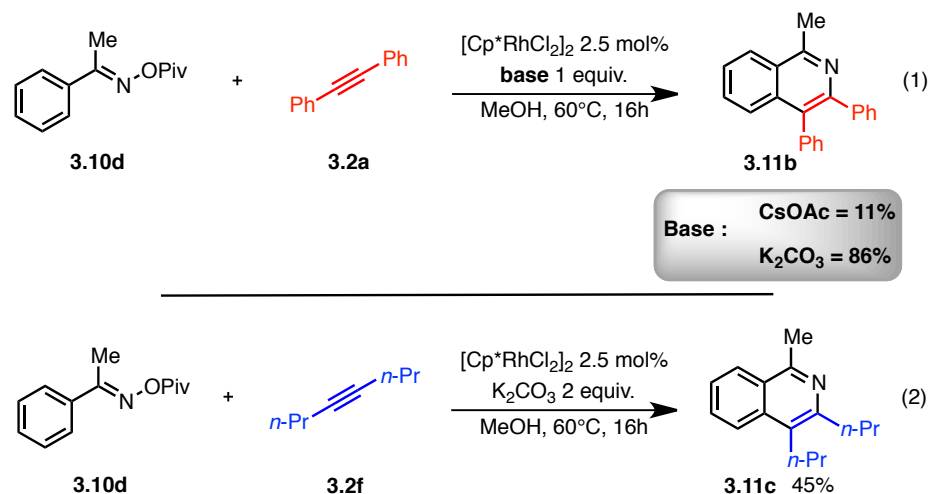
¹³C NMR (100 MHz, CDCl₃, 293K, TMS): δ 160.8, 154.9, 135.2, 130.2, 128.5, 127.0, 36.9, 14.3

IR (ν_{max}/cm⁻¹): 1737, 1382, 1157

HRMS calculated for C₁₁H₁₄N₂O₂ (M⁺): 206.1055; Found 206.1046

R_f: 0.32 with 50% EtOAc in pet. ether

Base effect in isoquinoline synthesis



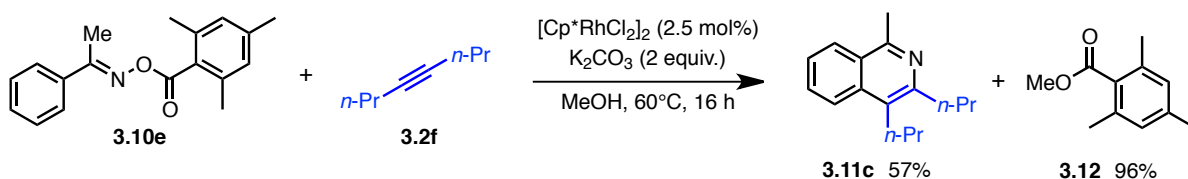
Scheme 3.24, eq 1

3.10d (44 mg, 0.20 mmol, 1 equiv.), **3.2a** (39 mg, 0.22 mmol, 1.1 equiv.) [Cp*RhCl₂]₂ and the base (0.2 mmol, 1 equiv.) were weighed in a 13 x 100 mm test tube. MeOH (1 mL) was added and the reaction mixture was stirred in an oil bath at 60 °C for 16h. The reaction was cooled down and diluted with dichloromethane. Next, trimethoxybenzene (11.2 mg, 0.066 mmol, 0.33 equiv.) was added as internal standard. Volatiles of an aliquot were then evaporated and the resulting mixture was analyzed by ¹H NMR.

Scheme 3.24, eq 2

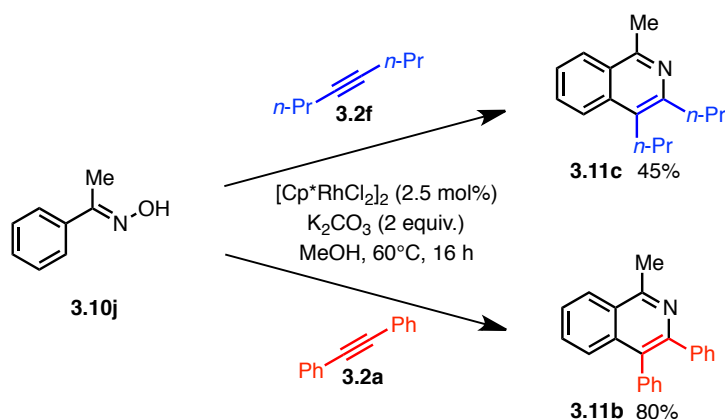
3.10d (44 mg, 0.20 mmol, 1 equiv.), **3.2f** (32 μL, 0.22 mmol, 1.1 equiv.) [Cp*RhCl₂]₂ and K₂CO₃ (28 mg, 0.2 mmol, 1 equiv.) were weighed in a 13 x 100 mm test tube. MeOH (1 mL) was added and the reaction mixture was stirred in an oil bath at 60 °C for 16h. The reaction was cooled down and diluted with dichloromethane. Next, trimethoxybenzene (11.2 mg, 0.066 mmol, 0.33 equiv.) was added as internal standard. Volatiles of an aliquot were then evaporated and the resulting mixture was analyzed by ¹H NMR.

Observation of a methyl ester side product



Scheme 3.25

3.10e (56 mg, 0.20 mmol, 1 equiv.), **3.2f** (32 μL , 0.22 mmol, 1.1 equiv.) $[\text{Cp}^*\text{RhCl}_2]_2$ and K_2CO_3 (28 mg, 0.2 mmol, 1 equiv.) were weighed in a 13 x 100 mm test tube. MeOH (1 mL) was added and the reaction mixture was stirred in an oil bath at 60 °C for 16h. The reaction was cooled down and diluted with dichloromethane. Next, trimethoxybenzene (11.2 mg, 0.066 mmol, 0.33 equiv.) was added as internal standard. Volatiles of an aliquot were then evaporated and the resulting mixture was analyzed by ^1H NMR.



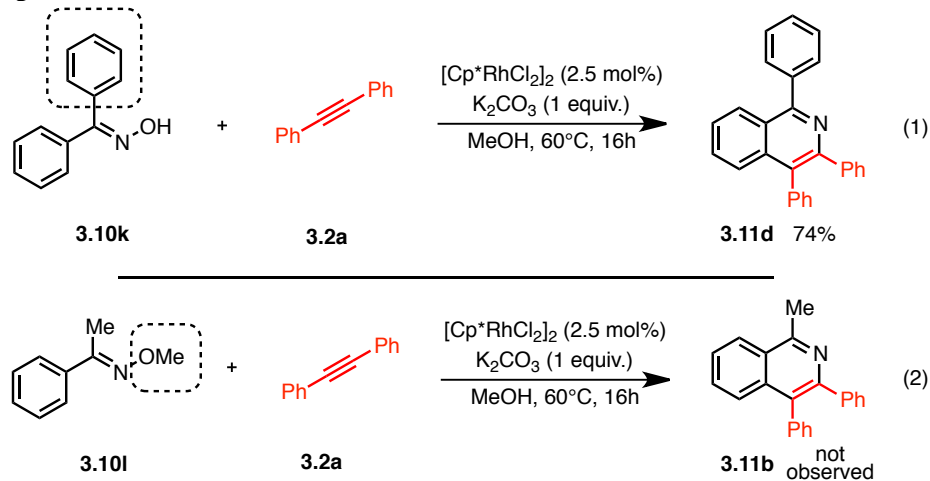
Scheme 3.26 top equation

3.10j (27 mg, 0.20 mmol, 1 equiv.), **3.2f** (39 mg, 0.22 mmol, 1.1 equiv.) $[\text{Cp}^*\text{RhCl}_2]_2$ and K_2CO_3 (28 mg, 0.2 mmol, 1 equiv.) were weighed in a 13 x 100 mm test tube. MeOH (1 mL) was added and the reaction mixture was stirred in an oil bath at 60 °C for 16h. The reaction was cooled down and diluted with dichloromethane. Next, trimethoxybenzene (11.2 mg, 0.066 mmol, 0.33 equiv.) was added as internal standard. Volatiles of an aliquot were then evaporated and the resulting mixture was analyzed by ^1H NMR.

Scheme 3.26 bottom equation

3.10j (27 mg, 0.20 mmol, 1 equiv.), **3.2a** (32 μL , 0.22 mmol, 1.1 equiv.) $[\text{Cp}^*\text{RhCl}_2]_2$ and K_2CO_3 (28 mg, 0.2 mmol, 1 equiv.) were weighed in a 13 x 100 mm test tube. MeOH (1 mL) was added and the reaction mixture was stirred in an oil bath at 60 °C for 16h. The reaction was cooled down and diluted with dichloromethane. Next, trimethoxybenzene (11.2 mg, 0.066 mmol, 0.33 equiv.) was added as internal standard. Volatiles of an aliquot were then evaporated and the resulting mixture was analyzed by ^1H NMR.

Control experiments



Scheme 3.27 eq 1

3.10k (39 mg, 0.20 mmol, 1 equiv.), **3.2a** (39 mg, 0.22 mmol, 1.1 equiv.) [Cp*RhCl₂]₂ and K₂CO₃ (28 mg, 0.2 mmol, 1 equiv.) were weighed in a 13 x 100 mm test tube. MeOH (1 mL) was added and the reaction mixture was stirred in an oil bath at 60 °C for 16h. The reaction was cooled down and diluted with dichloromethane. Next, trimethoxybenzene (11.2 mg, 0.066 mmol, 0.33 equiv.) was added as internal standard. Volatiles of an aliquot were then evaporated and the resulting mixture was analyzed by ¹H NMR.

Scheme 3.27, eq 2

3.10l (30 mg, 0.20 mmol, 1 equiv.), **3.2a** (39 mg, 0.22 mmol, 1.1 equiv.) [Cp*RhCl₂]₂ and K₂CO₃ (28 mg, 0.2 mmol, 1 equiv.) were weighed in a 13 x 100 mm test tube. MeOH (1 mL) was added and the reaction mixture was stirred in an oil bath at 60 °C for 16h. The reaction was cooled down and diluted with dichloromethane. Next, trimethoxybenzene (11.2 mg, 0.066 mmol, 0.33 equiv.) was added as internal standard. Volatiles of an aliquot were then evaporated and the resulting mixture was analyzed by ¹H NMR.

5.3.12 DFT CALCULATIONS

All density functional calculations were performed at the B3LYP¹⁶⁷/TZVP¹⁶⁸ level (DZVP¹⁶⁹ for Rh) using the Gaussian 03 package.¹⁷⁰ Spin-restricted treatment was used for

¹⁶⁷ (a) Becke, A. D. *J. Chem. Phys.* **1993**, *98*, 5648; (b) Lee, C.; Yang, W.; Parr, R. G. *Phys. Rev. B* **1988**, *37*, 785.

¹⁶⁸ Schafer, A.; Huber, C.; Ahlrichs, R. *J. Chem. Phys.* **1994**, *100*, 5829.

¹⁶⁹ Godbout, N.; Salahub, D. R.; Andzelm, J.; Wimmer, E. *Can. J. Chem.* **1992**, *70*, 560.

¹⁷⁰ Gaussian 03, Revision C.02, M. J. Frisch, G. W. Trucks, H. B. Schlegel, G. E. Scuseria, M. A. Robb, J. R. Cheeseman, J. A. Montgomery, Jr., T. Vreven, K. N. Kudin, J. C. Burant, J. M. Millam, S. S. Iyengar, J. Tomasi, V. Barone, B. Mennucci, M. Cossi, G. Scalmani, N. Rega, G. A. Petersson, H. Nakatsuji, M. Hada, M.

all closed-shell species. Tight SCF convergence criteria were used for all calculations. The converged wave functions were tested to confirm that they corresponded to ground-state surfaces. The second-order derivative of the energy with respect to nuclear positions was evaluated to determine the nature of the stationary points. Gibbs free energy of species was evaluated at 298 K and 1 atm using the harmonic oscillator approximation and unscaled vibrational frequencies. Intrinsic reaction coordinate (IRC)¹⁷¹ calculations were used to confirm the reaction pathways through the corresponding transition states (TSs) for all reaction steps.

Solvent effects were evaluated at the single-point calculations of the solvation energies using the gas-phase geometries. Solvation energies in methanol were calculated using the PCM model^{172,173,174} with the united atom topological model (UAHF). Gibbs free energies in the solution were estimated by addition of the solvation energies ΔG_{solv} to gas-phase Gibbs free energies.

Table S1. Electronic and Gibbs free energies (a.u.) at 298K in the gas-phase, and solvation energies in methanol (kcal mol⁻¹).

	E (a.u.)	G (a.u.)	ΔG_{solv}
[Rh(Cp)(OAc) ₂]	-5338.421910	-5338.280229	-15.2
[Rh(Cp)(OAc)] ⁺	-5109.585916	-5109.487983	-60.6
[Rh(Cp)(OAc)(MeOH)] ⁺	-5225.398238	-5225.252295	-53.7
[Rh(Cp)(OAc)(C ₂ H ₂)] ⁺	-5186.981631	-5186.857753	-52.8
MeOH	-115.770989	-115.742706	-6.2
AcOH	-229.178653	-229.144517	-1.5
AcO ⁻	-228.611690	-228.591421	-36.4
C ₂ H ₂	-77.362338	-77.354297	-1.1
Reactant	-628.994060	-628.866895	-8.4
C ₉ H ₇ NO (final product)	-477.334616	-477.226869	-10.4

Table S2. Relative Gibbs free energies (kcal mol⁻¹) at 298K in the gas-phase and in methanol (Schemes 8-9).

	$\Delta G_{\text{gas-phase}}$	$\Delta G_{\text{methanol}}$
[Rh(Cp)(OAc) ₂]	0.0	0.0
[Rh(Cp)(OAc)] ⁺	126.0	8.8
[Rh(Cp)(OAc)(MeOH)] ⁺	112.5	8.4

Ehara, K. Toyota, R. Fukuda, J. Hasegawa, M. Ishida, T. Nakajima, Y. Honda, O. Kitao, H. Nakai, M. Klene, X. Li, J. E. Knox, H. P. Hratchian, J. B. Cross, V. Bakken, C. Adamo, J. Jaramillo, R. Gomperts, R. E. Stratmann, O. Yazyev, A. J. Austin, R. Cammi, C. Pomelli, J. W. Ochterski, P. Y. Ayala, K. Morokuma, G. A. Voth, P. Salvador, J. J. Dannenberg, V. G. Zakrzewski, S. Dapprich, A. D. Daniels, M. C. Strain, O. Farkas, D. K. Malick, A. D. Rabuck, K. Raghavachari, J. B. Foresman, J. V. Ortiz, Q. Cui, A. G. Baboul, S. Clifford, J. Cioslowski, B. B. Stefanov, G. Liu, A. Liashenko, P. Piskorz, I. Komaromi, R. L. Martin, D. J. Fox, T. Keith, M. A. Al-Laham, C. Y. Peng, A. Nanayakkara, M. Challacombe, P. M. W. Gill, B. Johnson, W. Chen, M. W. Wong, C. Gonzalez, and J. A. Pople, Gaussian, Inc., Wallingford CT, 2004.

¹⁷¹ (a) Gonzalez, C.; Schlegel, H. B. *J. Chem. Phys.* **1989**, *90*, 2154; (b) Gonzalez, C.; Schlegel, H. B. *J. Phys. Chem.* **1990**, *94*, 5523.

¹⁷² Cancès, M. T.; Mennucci, B.; Tomasi, J. *J. Chem. Phys.* **1997**, *107*, 3032.

¹⁷³ Cossi, M.; Barone, V.; Mennucci, B.; Tomasi, J. *Chem. Phys. Lett.* **1998**, *286*, 253.

¹⁷⁴ Mennucci, B.; Tomasi, J. *J. Chem. Phys.* **1997**, *106*, 5151.

[Rh(Cp)(OAc)(C ₂ H ₂)] ⁺	116.3	8.0
II	4.9	7.9
TS from II to III	19.0	20.5
TS from II to III, cationic form	127.5	34.7
III	-0.2	4.9
IV	2.5	-4.3
V	4.3	-1.3
TS from V to VI	18.9	11.4
VI	-8.6	-13.8
TS from VI to VII	6.1	-0.2
VII	-19.8	-24.0
TS from VII to VIII	-19.1	-23.2
VIII	-86.1	-91.0

Optimized atomic coordinates (Å)

Reactant

C	3.977538	-0.632747	0.238949
C	3.049957	-1.448444	-0.401096
C	1.746283	-1.005264	-0.593572
C	1.363892	0.262573	-0.144637
C	2.304182	1.083365	0.483291
C	3.602955	0.634663	0.678345
H	4.992384	-0.980583	0.388301
H	3.343011	-2.427550	-0.759150
H	1.039477	-1.633828	-1.119976
H	1.999323	2.069264	0.808763
H	4.325275	1.273642	1.171053
C	-0.021048	0.808990	-0.314514
O	-0.278390	1.991448	-0.336795
N	-0.981945	-0.188684	-0.492307
H	-0.941153	-1.011705	0.105961
O	-2.306743	0.297500	-0.518592
C	-3.156533	-0.431713	0.256545
O	-2.791209	-1.378052	0.908615
C	-4.558313	0.088451	0.142061
H	-5.139082	-0.603748	-0.471123
H	-5.004839	0.112181	1.135134
H	-4.583525	1.076706	-0.310884

Entry I (Scheme 8)

Rh	-0.277402	-0.361067	-0.045496
C	-2.172551	0.103729	0.966593
H	-2.212404	0.778047	1.804947

C	-2.304595	0.479418	-0.404492
H	-2.408661	1.492389	-0.753579
C	-2.139419	-0.682766	-1.197865
H	-2.141237	-0.720414	-2.275524
C	-1.953722	-1.807640	-0.315433
H	-1.798323	-2.831045	-0.616278
C	-1.987522	-1.319024	1.009574
H	-1.825422	-1.904240	1.901291
C	2.046447	-1.344058	0.065922
O	1.427663	-1.289378	-1.038425
O	1.421653	-1.008688	1.121128
C	3.485634	-1.755646	0.126781
H	4.103506	-0.863478	0.001342
H	3.714483	-2.200003	1.094174
H	3.716124	-2.449306	-0.680380
O	0.884207	1.333119	-0.291085
C	0.444456	2.521621	0.011293
O	-0.680702	2.798050	0.413094
C	1.510687	3.594328	-0.171009
H	2.255611	3.493112	0.621144
H	2.024555	3.467577	-1.123845
H	1.055828	4.580773	-0.111848

Entry II (Scheme 8)

Rh	-0.674953	-0.823255	-0.357941
N	-0.212940	0.979776	0.616181
C	-0.059762	-2.476680	-1.783849
H	0.142812	-3.479823	-1.442938
C	-1.307167	-1.978382	-2.194594
H	-2.232593	-2.531127	-2.229620
C	-1.152721	-0.574167	-2.489832
H	-1.922808	0.106942	-2.810693
C	0.214803	-0.239687	-2.299098
H	0.626987	0.749881	-2.405639
C	0.891635	-1.393242	-1.817833
H	1.933139	-1.453236	-1.547781
O	-2.439966	-0.886155	0.883093
O	-0.587432	-1.752380	1.629355
C	-1.796689	-1.428908	1.834275
C	-2.441155	-1.643431	3.169356
H	-3.515069	-1.782850	3.055594
H	-1.993199	-2.497738	3.674458
H	-2.272466	-0.753442	3.780293
O	-1.325050	1.852264	0.794723
C	0.957069	1.694498	0.565888
C	2.213922	0.865311	0.549822
C	2.359031	-0.307051	1.295271

C	3.300294	1.348929	-0.184176
C	3.570770	-0.992362	1.288961
H	1.529865	-0.676866	1.882790
C	4.502787	0.652639	-0.203229
H	3.191374	2.281634	-0.722991
C	4.641235	-0.521079	0.534372
H	3.679457	-1.892790	1.881785
H	5.336779	1.032329	-0.781270
H	5.582908	-1.057009	0.531264
O	1.020919	2.918161	0.580828
C	-1.744921	2.546349	-0.298024
O	-1.363951	2.354463	-1.424555
C	-2.761966	3.572208	0.121978
H	-3.412172	3.183436	0.904582
H	-2.227558	4.435554	0.524160
H	-3.343137	3.882647	-0.743194

Transition state from II to III (CMD IS, one imaginary frequency at $944i\text{ cm}^{-1}$)

Rh	0.029663	-0.825669	-0.427882
N	-0.870766	0.801000	0.474712
C	0.509085	-0.525465	-2.589535
H	1.075188	0.322504	-2.938621
C	1.047371	-1.807802	-2.212761
H	2.089539	-2.081991	-2.209359
C	-0.028617	-2.626211	-1.823933
H	0.047402	-3.631775	-1.441000
C	-1.247858	-1.878602	-1.974095
H	-2.242052	-2.239204	-1.766888
C	-0.905859	-0.596009	-2.479415
H	-1.590362	0.222035	-2.640453
O	-0.414554	-1.924348	1.335139
O	1.240523	-0.963338	2.488607
C	0.258535	-1.746363	2.393639
C	-0.163144	-2.517179	3.622503
H	0.716295	-2.875103	4.156246
H	-0.701483	-1.835570	4.284652
H	-0.817414	-3.344123	3.357078
O	-2.231078	0.844278	0.828729
C	-0.200819	1.969578	0.647220
C	1.254775	1.742825	0.352249
C	1.732342	0.418626	0.295878
C	2.099593	2.819906	0.118919
C	3.079512	0.208102	-0.041801
H	1.397220	-0.335434	1.295067
C	3.432070	2.587741	-0.207852
H	1.698070	3.823493	0.187725
C	3.923006	1.283921	-0.289702

H	3.478965	-0.799685	-0.053898
H	4.093735	3.424392	-0.398340
H	4.965472	1.112256	-0.530479
O	-0.674867	3.042942	0.993810
C	-3.078907	1.378180	-0.103504
C	-4.435756	1.577257	0.514192
H	-4.669525	0.782779	1.221532
H	-4.423547	2.522124	1.061951
H	-5.187103	1.631375	-0.270190
O	-2.772754	1.640339	-1.235698

Transition state from II to III (CMD TS, cationic form, one imaginary frequency at $801i \text{ cm}^{-1}$)

Rh	-0.125815	-0.874977	-0.186049
N	-0.628657	1.228988	-0.175792
C	0.719500	-1.819436	-2.032551
H	1.624025	-1.473120	-2.505502
C	0.636144	-2.798610	-0.977475
H	1.462024	-3.333010	-0.536834
C	-0.737240	-2.980333	-0.664561
H	-1.124616	-3.622497	0.111260
C	-1.504699	-2.094542	-1.469375
H	-2.575726	-1.982022	-1.462475
C	-0.593055	-1.391702	-2.327661
H	-0.875011	-0.628699	-3.035114
O	-0.963531	-0.981290	1.740935
O	0.819148	-0.074656	2.733052
C	-0.323510	-0.589821	2.775515
C	-0.992983	-0.784211	4.111904
H	-0.461158	-1.568238	4.654838
H	-0.910220	0.131650	4.696216
H	-2.034296	-1.070539	3.991761
O	-1.868406	1.857346	0.077712
C	0.355330	2.076585	-0.155373
C	1.699662	1.506033	-0.178799
C	1.820602	0.180624	0.303947
C	2.795258	2.216050	-0.657252
C	3.087795	-0.414359	0.257449
H	1.235328	-0.047244	1.410730
C	4.040546	1.594086	-0.688907
H	2.679143	3.235222	-1.002402
C	4.185503	0.284275	-0.236978
H	3.229182	-1.408354	0.663986
H	4.900818	2.135842	-1.060439
H	5.161731	-0.184239	-0.249994
C	-2.918900	1.461836	-0.757069
C	-4.202495	2.037648	-0.245473

H	-4.597811	1.374152	0.527775
H	-4.057634	3.020008	0.201138
H	-4.917880	2.089961	-1.062503
O	-2.755449	0.755234	-1.704662
O	0.222901	3.389320	-0.100113
H	-0.717676	3.629807	-0.059112

Entry III (Scheme 8)

Rh	0.005950	-0.926006	-0.222065
N	-0.735043	0.893838	0.583442
C	-1.129240	-1.254925	-2.079729
H	-1.511018	-0.420972	-2.643811
C	0.135096	-1.898689	-2.246363
H	0.913104	-1.590875	-2.925598
C	0.223139	-2.929963	-1.288811
H	1.063601	-3.587145	-1.131714
C	-1.058372	-3.022183	-0.614139
H	-1.302768	-3.726094	0.166004
C	-1.884148	-2.021582	-1.110007
H	-2.889032	-1.799641	-0.790662
O	1.026275	-1.403812	1.677348
O	0.500397	0.418845	2.874299
C	1.087717	-0.733457	2.714996
C	1.873248	-1.210238	3.901917
H	2.723562	-0.542680	4.055593
H	1.254619	-1.163589	4.798668
H	2.229175	-2.223385	3.736839
O	-2.081786	1.053131	1.031516
C	-0.223095	2.061347	-0.001046
C	1.137082	1.761824	-0.526680
C	1.489754	0.419013	-0.667186
C	2.033948	2.780077	-0.847569
C	2.771259	0.095149	-1.101167
H	0.003203	0.678738	2.006413
C	3.308470	2.452500	-1.291071
H	1.717328	3.810636	-0.739342
C	3.675964	1.113052	-1.408612
H	3.080614	-0.938515	-1.201361
H	4.015772	3.233525	-1.541328
H	4.673974	0.855318	-1.745126
O	-0.775986	3.142019	-0.014134
C	-3.040436	1.244968	0.074523
C	-4.333687	1.636256	0.737143
H	-4.448193	1.156172	1.707841
H	-4.318320	2.717053	0.894093
H	-5.165259	1.387957	0.081357
O	-2.864278	1.115817	-1.106058

Entry IV (Scheme 8)

Rh	0.201943	-0.772777	-0.052913
N	0.452393	1.192161	0.127546
C	0.618803	-2.345912	1.397913
H	0.304711	-2.255246	2.425518
C	-0.136060	-2.943375	0.338812
H	-1.136611	-3.332854	0.420445
C	0.637220	-2.850549	-0.832394
H	0.341350	-3.168200	-1.819512
C	1.936971	-2.307231	-0.477792
H	2.732443	-2.090293	-1.172617
C	1.934853	-2.025500	0.881817
H	2.734267	-1.572686	1.445825
O	1.647386	1.849358	0.493830
C	-0.642734	2.055302	0.233069
C	-1.895170	1.261263	0.060604
C	-1.759357	-0.123021	-0.074750
C	-3.138709	1.880160	0.025871
C	-2.907518	-0.887795	-0.257099
C	-4.282062	1.105443	-0.150625
H	-3.193940	2.956970	0.134094
C	-4.162947	-0.272516	-0.294550
H	-2.853071	-1.962526	-0.380716
H	-5.258255	1.573623	-0.178168
H	-5.049891	-0.879463	-0.437541
O	-0.578146	3.253571	0.410477
C	2.705724	1.669200	-0.349588
C	3.841337	2.554377	0.091784
H	3.642093	3.574367	-0.243807
H	3.923795	2.575524	1.177854
H	4.767072	2.204516	-0.358646
O	2.716976	0.920451	-1.289669

Entry V (Scheme 8)

Rh	0.002444	-0.892819	0.274657
N	-0.705644	1.042961	0.079458
C	0.559685	-2.478049	-1.282602
H	1.551754	-2.483765	-1.702917
C	0.137276	-3.169262	-0.124348
H	0.737073	-3.838505	0.472030
C	-1.269561	-2.907639	0.061699
H	-1.881471	-3.309547	0.853944
C	-1.682772	-2.023356	-0.937155
H	-2.664908	-1.599593	-1.066284
C	-0.538638	-1.702953	-1.751664
H	-0.545798	-1.047370	-2.606871

O	-1.989224	1.401701	0.560458
C	0.153643	2.103147	0.009231
C	1.537428	1.572363	-0.172111
C	1.731628	0.199070	-0.046980
C	2.613459	2.422523	-0.418942
C	3.015526	-0.326872	-0.146155
C	3.893532	1.896722	-0.538347
H	2.422796	3.486155	-0.499909
C	4.092380	0.524863	-0.400845
H	3.198829	-1.388691	-0.028787
H	4.735371	2.550219	-0.731497
H	5.090463	0.110335	-0.487048
O	-0.148035	3.285667	0.071024
C	-0.328002	-0.440200	2.450823
H	-1.248266	0.011438	2.747360
C	0.813745	-0.880947	2.379193
H	1.809579	-1.182462	2.613764
C	-2.978685	1.419986	-0.384635
O	-2.859129	1.019024	-1.509622
C	-4.224164	2.018904	0.214427
H	-5.078391	1.781405	-0.414894
H	-4.385974	1.662781	1.231541
H	-4.099295	3.102826	0.259367

Transition state from V to VI (TS2, one imaginary frequency at $380i\text{ cm}^{-1}$)

Rh	-0.060777	-0.916792	0.293012
N	-0.704531	1.054919	0.152706
C	0.231177	-2.319227	-1.556600
H	1.037879	-2.169014	-2.255815
C	0.293343	-3.102465	-0.357746
H	1.133863	-3.692474	-0.027810
C	-0.980937	-3.043476	0.273679
H	-1.255739	-3.544706	1.188310
C	-1.797930	-2.164100	-0.473983
H	-2.822770	-1.905281	-0.265207
C	-1.039790	-1.725642	-1.621060
H	-1.394190	-1.026108	-2.360790
O	-1.999513	1.445102	0.574189
C	0.175800	2.089313	0.126394
C	1.554391	1.537045	-0.069806
C	1.801398	0.198081	0.251395
C	2.565759	2.324660	-0.613694
C	3.056328	-0.356964	-0.018633
C	3.812592	1.772066	-0.876034
H	2.344043	3.361295	-0.836689
C	4.050992	0.426323	-0.591152
H	3.265958	-1.387694	0.242882

H	4.597632	2.381470	-1.306383
H	5.020576	-0.009382	-0.802025
O	-0.081275	3.283778	0.201371
C	0.008632	-0.504892	2.329724
H	-0.754611	-0.560577	3.081248
C	1.235795	-0.328202	2.080685
H	2.214098	-0.301728	2.519419
C	-2.948781	1.454643	-0.404617
O	-2.788607	1.049158	-1.524601
C	-4.218805	2.052049	0.143884
H	-5.050499	1.793928	-0.507287
H	-4.407246	1.713869	1.162332
H	-4.106937	3.138017	0.171059

Entry VI (Scheme 8)

Rh	-0.002187	0.766219	0.202848
N	0.886895	-1.072996	-0.171271
C	-0.079053	2.515785	-1.469093
H	-0.591157	2.432968	-2.414907
C	-0.691702	2.928618	-0.216594
H	-1.716487	3.242457	-0.093264
C	0.293844	2.920145	0.783175
H	0.164444	3.213131	1.812261
C	1.481848	2.358998	0.202584
H	2.435082	2.241236	0.692276
C	1.244945	2.195910	-1.221122
H	1.957208	1.777148	-1.912789
O	2.138545	-1.518307	0.332228
C	-0.056015	-2.042423	-0.117685
C	-1.424503	-1.382697	-0.275044
C	-2.087779	-0.808581	0.840927
C	-2.110310	-1.518121	-1.494858
C	-3.429396	-0.411814	0.691102
C	-3.423128	-1.106688	-1.618358
H	-1.600304	-1.983304	-2.329318
C	-4.088339	-0.561109	-0.514704
H	-3.946697	0.007199	1.546097
H	-3.942667	-1.224526	-2.561286
H	-5.124491	-0.257582	-0.604489
O	0.074220	-3.248688	-0.009251
C	-0.266308	0.076917	2.098182
H	0.388003	0.296810	2.933907
C	-1.379780	-0.638336	2.144678
H	-1.807474	-1.071889	3.046279
C	3.226522	-1.071884	-0.343431
O	3.203279	-0.293123	-1.261295
C	4.464718	-1.708841	0.236231

H	5.340924	-1.155192	-0.092492
H	4.417781	-1.744501	1.324013
H	4.534261	-2.737182	-0.124942

Transition state from VI to VII (TS3, one imaginary frequency at 375i cm⁻¹)

Rh	-0.597136	-0.987519	0.217956
N	-0.163660	1.089044	0.474637
C	-1.166101	-2.401143	-1.599750
H	-0.438552	-2.739928	-2.319783
C	-1.444217	-3.028068	-0.321441
H	-0.999330	-3.946413	0.030526
C	-2.489916	-2.316921	0.316894
H	-2.954828	-2.566486	1.256613
C	-2.726138	-1.155267	-0.459541
H	-3.448334	-0.382363	-0.251343
C	-1.930650	-1.246917	-1.676694
H	-1.916582	-0.504283	-2.457536
O	-1.212206	1.965596	0.843380
C	0.968079	1.764478	0.078572
C	2.133498	0.855058	-0.093799
C	2.293042	-0.329897	0.664089
C	3.127542	1.245192	-0.992332
C	3.465514	-1.082749	0.469116
C	4.261592	0.473509	-1.188830
H	2.983380	2.173252	-1.530192
C	4.426815	-0.697387	-0.449215
H	3.614415	-1.981309	1.056696
H	5.016197	0.783971	-1.900323
H	5.315112	-1.303536	-0.580813
O	1.021145	2.973172	-0.101848
C	0.083120	-0.418120	1.958551
H	-0.442034	-0.358130	2.905669
C	1.392669	-0.720804	1.758098
H	1.872007	-1.287326	2.555400
C	-1.965108	2.448313	-0.196883
O	-1.899039	2.051546	-1.326760
C	-2.869744	3.536677	0.313951
H	-3.703982	3.664946	-0.371868
H	-3.225743	3.320446	1.320471
H	-2.294145	4.463946	0.353102

Entry VII (Scheme 8)

Rh	1.266292	-0.557734	-0.179009
N	-0.023380	1.140038	-0.157296
C	0.927157	-2.284618	1.499732
H	0.443891	-2.101009	2.446104
C	0.250139	-2.491565	0.230541

H	-0.817349	-2.598358	0.109758
C	1.229920	-2.769931	-0.769084
H	1.044654	-3.049319	-1.793074
C	2.477465	-2.470633	-0.186903
H	3.436063	-2.528544	-0.679670
C	2.284254	-2.245840	1.242750
H	3.069358	-2.038253	1.952865
O	0.747598	2.408719	-0.018038
C	-1.086454	1.142941	0.861832
C	-2.325401	0.531455	0.418830
C	-2.546668	0.189728	-0.947406
C	-3.350335	0.353525	1.368265
C	-3.817308	-0.326810	-1.298593
C	-4.570906	-0.161227	0.995394
H	-3.150983	0.634169	2.394282
C	-4.800480	-0.499951	-0.352771
H	-4.004542	-0.588618	-2.333497
H	-5.351776	-0.303933	1.731281
H	-5.762881	-0.901486	-0.647390
O	-0.841915	1.622052	1.947390
C	-0.284808	0.833550	-1.518881
C	-1.523514	0.398386	-1.905471
H	0.474962	1.158419	-2.211216
H	-1.696042	0.180148	-2.950104
C	2.073968	2.253318	-0.110145
C	2.800758	3.541346	0.123489
H	2.385495	4.336947	-0.495049
H	2.675973	3.833007	1.168412
H	3.855599	3.399636	-0.096570
O	2.613240	1.184591	-0.347993

Transition state from VII to VIII (TS4, one imaginary frequency at $106i\text{ cm}^{-1}$)

Rh	1.294092	-0.530468	-0.213901
N	-0.060623	1.079266	-0.140764
C	1.045803	-2.271254	1.461429
H	0.566257	-2.108560	2.413460
C	0.365019	-2.505603	0.200856
H	-0.698154	-2.657356	0.090771
C	1.345588	-2.737827	-0.811128
H	1.160924	-3.022451	-1.833802
C	2.586535	-2.392545	-0.240615
H	3.540916	-2.408953	-0.744407
C	2.398808	-2.176099	1.189456
H	3.181817	-1.937015	1.891895
O	0.686570	2.415220	0.060917
C	-1.099567	1.008698	0.899131
C	-2.359340	0.446649	0.442320

C	-2.618807	0.217416	-0.938357
C	-3.358968	0.195532	1.401253
C	-3.898621	-0.263514	-1.298800
C	-4.592071	-0.283306	1.019245
H	-3.131364	0.390185	2.441181
C	-4.858791	-0.510614	-0.344227
H	-4.113805	-0.439004	-2.346404
H	-5.354129	-0.482982	1.761641
H	-5.830461	-0.884109	-0.645020
O	-0.826029	1.391104	2.015450
C	-0.368649	0.895380	-1.508969
C	-1.612548	0.495741	-1.901101
H	0.400603	1.213912	-2.193776
H	-1.808057	0.355667	-2.955137
C	2.004086	2.301067	-0.073249
C	2.715674	3.588914	0.216849
H	2.234828	4.422813	-0.293544
H	2.666325	3.781318	1.290810
H	3.754309	3.499061	-0.091324
O	2.571372	1.261412	-0.383865

Entry VIII (Scheme 8)

Rh	-1.308134	-0.365376	0.123539
N	0.674687	0.247879	0.081940
C	-1.492363	-2.346467	-0.810071
H	-0.818282	-2.630512	-1.600543
C	-1.258715	-2.539522	0.567836
H	-0.382536	-2.995341	0.994735
C	-2.349853	-1.933794	1.277989
H	-2.441571	-1.870978	2.351372
C	-3.275666	-1.403689	0.332540
H	-4.168422	-0.841474	0.544514
C	-2.743342	-1.634949	-0.957276
H	-3.178692	-1.292845	-1.881983
O	-3.944817	1.346466	-0.608296
C	1.681385	-0.706092	-0.129632
C	3.080894	-0.237392	-0.090337
C	3.378997	1.126313	0.117843
C	4.119013	-1.160890	-0.271294
C	4.727870	1.530556	0.139996
C	5.437346	-0.745825	-0.243931
H	3.859633	-2.198713	-0.432481
C	5.739221	0.607521	-0.038008
H	4.962747	2.576737	0.298111
H	6.236518	-1.463280	-0.382903
H	6.773199	0.931150	-0.018869
O	1.408469	-1.888415	-0.344587

C	1.011621	1.566221	0.268682
C	2.285739	2.030146	0.293948
H	0.168141	2.228181	0.396605
H	2.467875	3.084901	0.452643
C	-3.018017	2.055775	-0.243791
C	-3.154546	3.565581	-0.138471
H	-4.172394	3.865945	-0.376190
H	-2.892692	3.895972	0.868047
H	-2.458617	4.044998	-0.829508
O	-1.817299	1.633330	0.081315

Final product

C	1.713809	1.315538	-0.000013
C	0.363221	0.919365	-0.000022
C	0.068067	-0.465043	-0.000018
C	1.103585	-1.407269	0.000004
C	2.421994	-0.994450	0.000024
C	2.723938	0.373976	0.000018
H	1.953220	2.372482	-0.000022
H	0.840126	-2.456887	-0.000002
H	3.221118	-1.724952	0.000041
H	3.758296	0.696367	0.000039
C	-1.326859	-0.938431	-0.000004
O	-1.678860	-2.108845	-0.000047
N	-2.274078	0.083090	0.000064
H	-3.233682	-0.232114	0.000090
C	-0.716539	1.870287	-0.000036
C	-1.990086	1.428474	0.000020
H	-0.510041	2.931106	-0.000073
H	-2.846402	2.088444	0.000012

5.4 Mechanistic Investigations on Cope-Type Hydroamination Through Tethering Organocatalysis

General Information

All reagents were used as is from commercial sources. Unless otherwise noted below, all other compounds have been reported in the literature or are commercially available. The benzene used for aldehyde screening was degassed and stored over 4Å molecular sieves. Due to the instability of the α -benzyloxyacetaldehyde, a 1M solution in benzene was prepared according to a modified procedure from the literature¹⁷⁵ and used for all the experiments performed in benzene.

¹⁷⁵ Pollex, A.; Millet, A.; Müller, J.; Hiersemann, M.; Abraham, L. *J. Org. Chem.* **2005**, *70*, 5579.

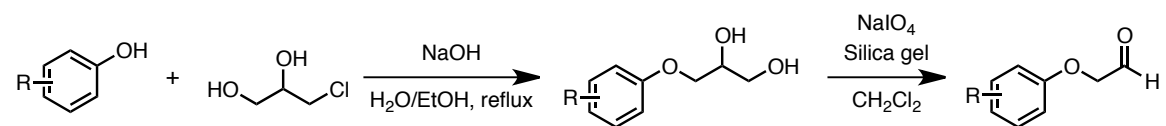
5.4.1 ALDEHYDE SCREENING

General procedure

N-Benzylhydroxylamine (0.0616 g, 0.500 mmol, 1.00 equiv.), and the aldehyde if solid (0.100 mmol, 0.20 equiv.) were weighted in a 13x100 mm test tube. The tube was sealed with a rubber septum and flushed with argon. Benzene (0.5 mL, 1M) was then added via syringe followed by the aldehyde if liquid and allylamine (0.056 mL, 0.75 mmol, 1.50 equiv.). The mixture was allowed to stir for 24 h at room temperature under argon before 1,3,5-trimethoxybenzene (0.0280 g, 0.167 mmol, 0.33 equiv.) was added. The mixture was diluted with dichloromethane (~ 2 mL) and an aliquot was taken apart. Volatiles of this aliquot were evaporated under a flow of air and the resulting mixture was then dissolved in CDCl₃. An ¹H NMR was taken and the yield calculated using the internal standard peak. Yields for different aldehydes are shown in Table 4.1 (Chapter 4).

Preparation of non-commercial aldehydes

Phenoxyacetaldehydes preparation



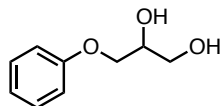
General procedure J

A solution of NaOH (2.50 g, 62.5 mmol, 1.25 equiv.) in H₂O (10 mL) was added to a solution of the appropriate phenol (50.0 mmol, 1.00 equiv.) in EtOH (30 mL). The resulting mixture was heated under reflux for 10 min. Then, a solution of 3-chloro-1,2-propanediol (60.0 mmol, 5.00 mL, 1.20 equiv.) in EtOH (5 mL) was slowly added and the mixture was further heated under reflux until completion as judge by TLC (16 h). EtOH was then removed under reduced pressure and Et₂O was added, along with more water. The aqueous phase was extracted twice with Et₂O and the combined organic layers were dried over MgSO₄, filtered and evaporated under reduced pressure. The purification was made by recrystallization. See below for specific conditions.

General procedure K

A 0.65M solution of NaIO₄ (20.0 mL, 13.0 mmol, 1.30 equiv.) in water was added to a vigorously stirred suspension of silica gel (20.0 g) in CH₂Cl₂ (140 mL). A solution of the diol (10.0 mmol, 1.00 equiv.) in CH₂Cl₂ (20 mL) was then added and the resulting mixture was allowed to stir at room temperature for 2 h after which it was filtered over a small plug of silica (washing with CH₂Cl₂) and the volatiles were evaporated under reduced pressure. The products obtained after this step were analytically pure.

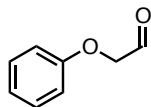
3-Phenoxy-1,2-propanediol



The compound was prepared according to general procedure J using phenol as starting material. The resulting solid was recrystallized using a 1:1 mixture of Et₂O in hexanes. After using 100 mL of the hot solvent, the mixture was still cloudy. Hot Et₂O was added until the mixture became clear. It was then allowed to stand at room temperature for 5 min and then at 0 °C until complete crystallization. The product obtained is a white solid (7.7 g, 92%). Spectral data is consistent with literature.¹⁷⁶

¹H-NMR (400 MHz; CDCl₃, 293K): δ 7.24 (dd, *J* = 8.6, 7.4 Hz, 2H), 6.94 (t, *J* = 7.4 Hz, 1H), 6.87 (d, *J* = 7.9 Hz, 2H), 4.10-4.06 (m, 1H), 3.96 (d, *J* = 5.4 Hz, 2H), 3.80-3.67 (m, 3H), 3.43-3.38 (br s, 1H).

2-Phenoxyacetaldehyde (4.3q)



The compound was prepared following the general procedure K using 3-phenoxy-1,2-propanediol (1.68 g, 10.0 mmol). 2-Phenoxyacetaldehyde was obtained as a clear oil (904 mg, 71%).

¹H-NMR (400 MHz; CDCl₃, 293K): δ 9.87 (t, *J* = 1.1 Hz, 1H), 7.35-7.30 (m, 2H), 7.02 (tt, *J* = 7.4, 1.0 Hz, 1H), 6.92-6.89 (m, 2H), 4.58 (d, *J* = 1.1 Hz, 2H).

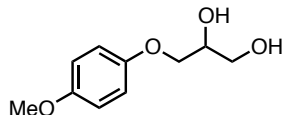
¹³C NMR (100 MHz, CDCl₃, 293K): δ 199.4, 157.6, 129.7, 121.9, 114.5, 72.6

IR (ν_{max}/cm⁻¹): 1740, 1600, 1496, 1247, 1055

HRMS calculated for C₈H₈O₂ (M⁺): 136.0524; Found 136.0529

R_f: 0.26 with 20% EtOAc in pet. ether

2-(4-Methoxyphenoxy)-1,2-propanediol



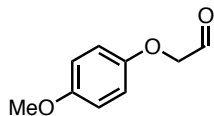
The compound was prepared according to general procedure J using 4-methoxyphenol as starting material. EtOAc was used in place of Et₂O in the work up. The resulting solid was recrystallized using a 1:1 mixture of Et₂O in hexanes. After using 100 mL of the hot solvent, the mixture was still cloudy. Hot Et₂O was added until the mixture became clear. It was then allowed to stand at room temperature for 5 min and then at 0°C until complete crystallization. The product obtained is a white solid (9.40 g, 95%). Spectral data is consistent with literature.¹⁷⁷

¹H-NMR (400 MHz; CDCl₃, 293K): δ 6.85-6.80 (m, 4H), 4.09-4.05 (m, 1H), 4.02-3.95 (m, 2H), 3.83-3.80 (m, 1H), 3.75-3.71 (m, 4H), 2.60-2.59 (m, 1H), 2.03-2.00 (m, 1H).

2-(4-Methoxyphenoxy)acetaldehyde (4.3s)

¹⁷⁶ Huang, K.; Wang, H.; Stepanenko, V.; Jesús, M. D. Torruellas, C.; Correa, W.; Ortiz-Marciales, M. *J. Org. Chem.* **2011**, *76*, 1883.

¹⁷⁷ Iwashita, M.; Makide, K.; Nonomura, T.; Misumi, Y.; Otani, Y.; Ishida, M.; Taguchi, T.; Tsujimoto, M.; Aoki, J.; Arai, H.; Ohwada T. *J. Med. Chem.* **2009**, *52*, 5837.



The compound was prepared following the general procedure K using 3-(4-methoxyphenoxy)-1,2-propanediol (1.98 g, 10.0 mmol). The product was obtained as an orange solid (1.23 g, 74%).

¹H-NMR (400 MHz; CDCl₃, 293K): δ 9.86 (t, *J* = 1.1 Hz, 1H), 6.85 (s, 4H), 4.53 (d, *J* = 1.1 Hz, 2H), 3.78 (s, 3H).

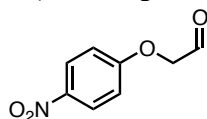
¹³C NMR (100 MHz, CDCl₃, 293K): δ 199.6, 154.6, 151.8, 115.6, 114.8, 73.5, 55.7

δ IR (ν_{max}/cm⁻¹): 2836, 1738, 1509, 1234, 1033, 827

HRMS calculated for C₉H₁₀O₃ (M⁺): 166.0630; Found 166.0629

R_f: 0.23 with 20% EtOAc in pet. ether

2-(4-Nitrophenoxy)acetaldehyde (4.3r)



A solution of NaOH (0.500 g, 12.5 mmol, 1.25 equiv.) in H₂O (2 mL) was added to a solution of the appropriate phenol (10.0 mmol, 1.00 equiv.) in EtOH (6 mL). The resulting mixture was heated under reflux for 10 min. Then, a solution of 3-chloro-1,2-propanediol (12.0 mmol, 1.00 mL, 1.20 equiv.) in EtOH (1 mL) was slowly added and the mixture was further heated under reflux until completion as judge by TLC (16 h). EtOH was then removed under reduced pressure and Et₂O was added, along with more water. The aqueous phase was extracted 2x with Et₂O and the combined organic layers were dried over MgSO₄, filtered and evaporated under reduced pressure to afford the crude diol.

A 0.65M solution of NaIO₄ (20.0 mL, 13.0 mmol, 1.3 equiv.) in water was added to a vigorously stirred suspension of silica gel (20.0 g) in CH₂Cl₂ (140 mL). A solution of the crude diol in CH₂Cl₂ (20 mL) was then added and the resulting mixture was allowed to stir at room temperature for 2 h after which it was filtered over a small plug of silica (washing with CH₂Cl₂) and the volatiles were evaporated under reduced pressure. S5 was obtained as an analytically pure white solid (1.40 g, 77%).

¹H-NMR (400 MHz; CDCl₃, 293K): δ 9.87 (s, 1H), 8.23 (d, *J* = 9.3 Hz, 2H), 6.99 (d, *J* = 9.3 Hz, 2H), 4.75 (s, 2H).

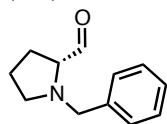
¹³C NMR (100 MHz, CDCl₃, 293K): δ 196.8, 162.3, 142.3, 126.1, 114.7, 72.8

IR (ν_{max}/cm⁻¹): 1751, 1710, 1609, 1591, 1499, 1333, 1279, 1115, 848, 752

HRMS calculated for C₈H₇NO₄ (M⁺): 181.0375; Found 181.0368

R_f: 0.31 with 50% EtOAc in pet. ether

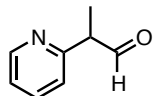
(2R)-1-Benzylpyrrolidine-2-carbaldehyde (4.3e)



To a -40°C solution of DMSO (533 μL , 7.5 mmol, 1.5 equiv.) in CH_2Cl_2 (25 mL) was added oxalyl chloride (635 μL , 7.5 mmol, 1.5 equiv.) over 10 min. The resulting mixture was stirred at -40°C for 20 min. *N*-Benzyl-L-prolinol (886 μL , 5.0 mmol, 1.0 equiv.) was then added and the mixture was stirred for 15 min after which Et_3N (2.09 mL, 15.0 mmol, 3 equiv.) was added. The slurry was allowed to stir for 30 min at -40°C before being allowed to warm to room temperature. Water was added and the aqueous phase was extracted twice with CH_2Cl_2 . The combined organic layers were dried over MgSO_4 , filtered and evaporated under reduced pressure. The resulting oil was then triturated with Et_2O and filtered over celite to remove leftover $\text{Et}_3\text{N}\cdot\text{HCl}$ salt. The resulting oil was purified by Kugelrohr distillation. Product was collected at 140°C under 0.15 mmHg (0.645 g, 68%). Spectral data is consistent with literature.¹⁷⁸

$^1\text{H-NMR}$ (400 MHz; CDCl_3 , 293K): δ 9.30 (d, $J = 4.0$ Hz, 1H), 7.34-7.26 (m, 5H), 3.75 (d, $J = 12.9$ Hz, 1H), 3.67 (d, $J = 12.9$ Hz, 1H), 3.14-3.09 (m, 1H), 3.01-2.96 (m, 1H), 2.40 (m, 1H), 2.03-1.83 (m, 4H).

2-(Pyridin-2-yl)propanal (4.3d)



To a flame dried round bottom flask was added 2-ethylpyridine (1.14 mL, 10.0 mmol, 1 equiv.) and dry diethyl ether (40 mL). The mixture was cooled at -78°C and *n*-BuLi (2.5 M solution in hexane, 4.80 mL, 12.0 mmol, 1.10 equiv.) was added dropwise. The cooling bath was then removed and the reaction mixture was allowed to warm to room temperature. It was stirred at this temperature for 30 min after which it was cooled again to -78°C . DMF (3.90 mL, 50.0 mmol, 5.00 equiv.) was then added and the reaction mixture stirred at -78°C for 30 min before being brought to room temperature. It was allowed to stir at room temperature for 30 min before being quenched with sat. NH_4Cl . The aqueous phase was extracted 3 times with Et_2O . The combined organic layers were dried over MgSO_4 , filtered and evaporated under reduced pressure. The purification was made by flash column chromatography using 10% EtOAc in pet. ether as eluent. The product obtained (0.305 g, 23%) is a mixture of the desired aldehyde and the enol form which matches the results previously reported.¹⁷⁹

Aldehyde form:

$^1\text{H NMR}$ (400 MHz, CDCl_3 , 293K, TMS): δ 9.86 (d, $J = 1.4$ Hz, 1H), 8.63-8.61 (m, 1H), 7.72-7.68 (m, 1H), 7.24-7.20 (m, 2H), 3.82 (qd, $J = 7.1, 1.3$ Hz, 1H), 1.51 (d, $J = 7.1$ Hz, 3H).

Enol form:

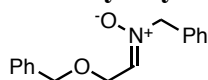
$^1\text{H NMR}$ (400 MHz, CDCl_3 , 293K, TMS): δ 8.36-8.34 (m, 1H), 7.73-7.69 (m, 1H), 7.06 (m, 3H), 1.88 (d, $J = 1.2$ Hz, 3H).

¹⁷⁸ Thai, K.; Wang, L.; Dudding, T.; Bilodeau, F.; Gravel, M. *Org. Lett.* **2010**, *12*, 5708.

¹⁷⁹ Settambolo, R.; Pucci, S.; Bertozzi, S.; Raffaello, L. *J. Organomet. Chem.* **1995**, *489*, C50.

5.4.2 MOLECULES FOR MECHANISTIC EXPERIMENTS

C-Benzylloxymethane-*N*-benzylnitron



N-Benzylhydroxylamine (271 mg, 2.2 mmol, 1.1 equiv.) was added to a mixture of 2-benzyloxyacetaldehyde (300 mg, 2.0 mmol, 1 equiv.) in CHCl₃ (5 mL). After stirring for 3 hours TLC shows complete conversion. The solvent was evaporated under reduced pressure and the purification was made by flash column chromatography using 10 % *i*-PrOH in toluene as eluent. The product obtained is an off-white solid (0.510 g, 99%)

¹H-NMR (400 MHz; CDCl₃, 293K): δ 7.40-7.25 (m, 11H), 6.78 (t, *J* = 4.3 Hz, 1H), 4.84 (s, 2H), 4.52 (s, 2H), 4.46 (d, *J* = 4.3 Hz, 2H).

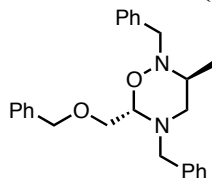
¹³C NMR (100 MHz, CDCl₃, 293K): δ 137.4, 137.1, 132.1, 129.6, 129.2, 129.0, 128.5, 128.0, 128.0, 73.8, 69.0, 66.1z

IR (ν_{max}/cm⁻¹): 3032, 1613, 1455, 1162, 1120, 908, 700

HRMS calculated for C₁₆H₁₇NO₂ (M⁺): 255.1259; Found 255.1220

R_f: 0.26 with 10% *i*-PrOH in toluene

Oxadiazinane (4.8a)



N-Allylbenzylamine (157 μL, 1.0 mmol, 1.0 equiv.) was added to a mixture of C-benzylloxymethane-*N*-benzylnitron (255 mg, 1.0 mmol, 1 equiv.) in CHCl₃ 0.75 mL. The mixture was heated at 50 °C in an oil bath under argon for 48 h. Volatiles were then evaporated under reduced pressure and the resulting mixture was purified by flash column chromatography using 8% EtOAc in pet. ether as eluent. The product was obtained as a clear oil (0.184 g, 46%).

¹H-NMR (400 MHz; CDCl₃, 293K): δ 7.48-7.20 (m, 15H), 4.80 (dd, *J* = 5.5, 3.6 Hz, 1H), 4.39 (d, *J* = 12.1 Hz, 1H), 4.36 (d, *J* = 12.1 Hz, 1H), 4.24 (d, *J* = 14.5 Hz, 1H), 3.93 (d, *J* = 13.7 Hz, 1H), 3.77 (d, *J* = 14.5 Hz, 1H), 3.70 (dd, *J* = 11.2, 3.6 Hz, 1H), 3.58-3.54 (m, 2H), 3.15-3.07 (m, 1H), 2.79 (dd, *J* = 12.9, 2.7 Hz, 1H), 2.59 (dd, *J* = 12.8, 10.6 Hz, 1H), 1.00 (d, *J* = 6.2 Hz, 3H).

¹³C NMR (100 MHz, CDCl₃, 293K): δ 138.8, 138.1, 138.0, 128.8, 128.7, 128.7, 128.2, 128.1, 128.0, 127.6, 127.4, 126.9, 126.7, 93.2, 72.9, 69.7, 58.9, 56.9, 54.5, 52.2, 16.2

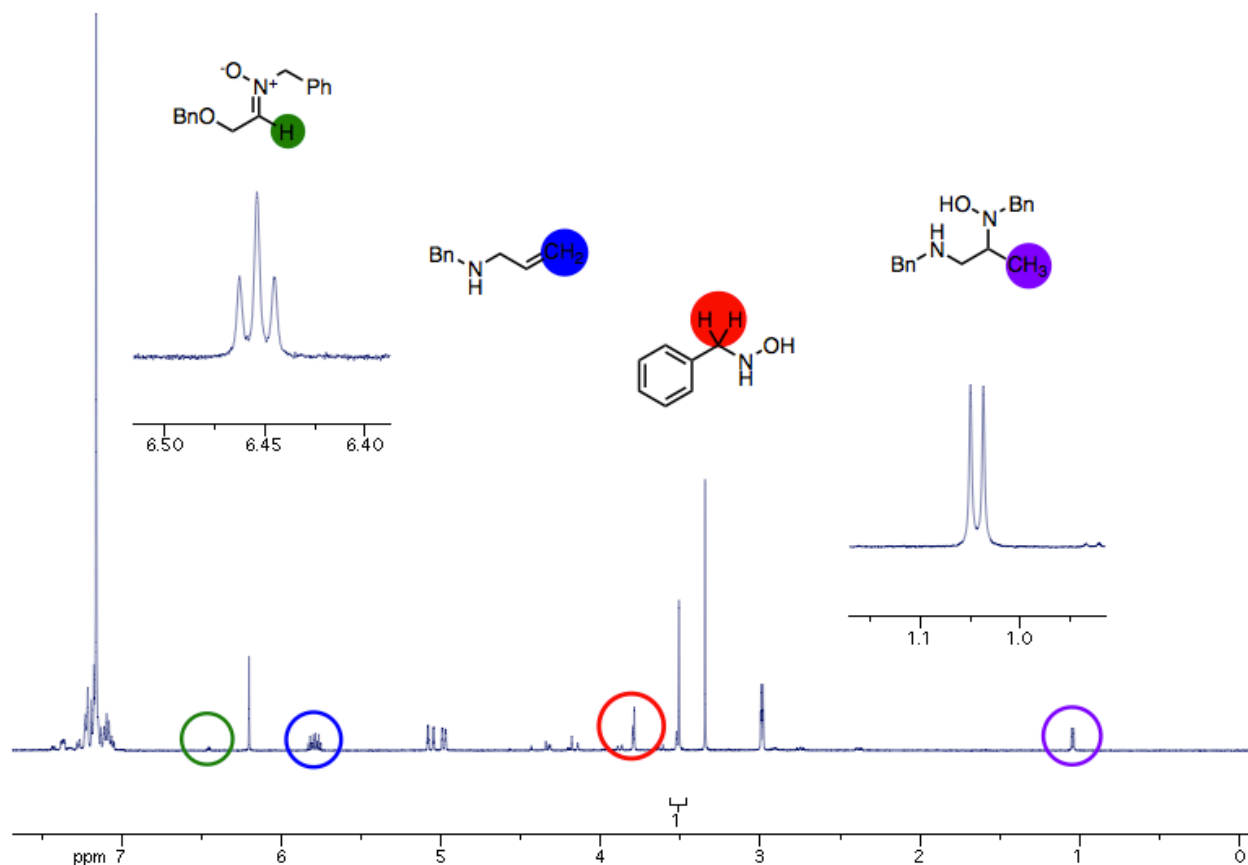
IR (ν_{max}/cm⁻¹): 3029, 2855, 1496, 1453, 1121, 1085, 736, 697

HRMS calculated for C₂₆H₃₀N₂O₂ (M⁺): 402.2307; Found 402.2304

R_f: 0.52 with 15% EtOAc in pet. ether

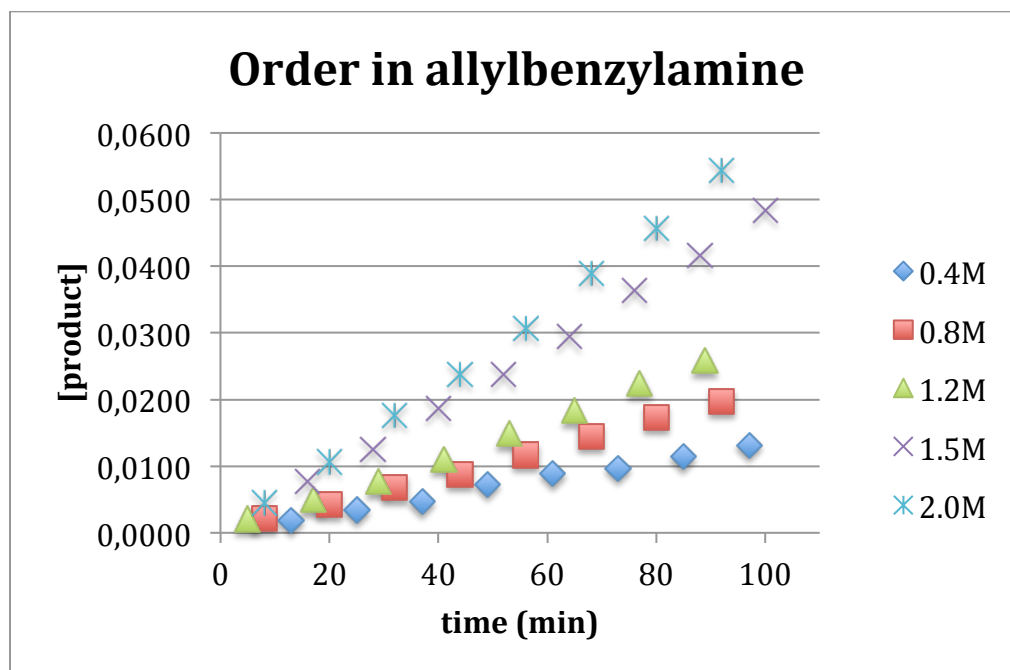
5.4.3 KINETIC EXPERIMENTS

Representative NMR spectra for data analysis



Order in *N*-allylbenzylamine.

N-Benzylhydroxylamine (0.0616 g, 0.500 mmol) and 1,3,5-trimethoxybenzene (the internal standard, 0.0280 mg, 0.167 mmol) were weighted in a 1-dram vial. The vial was capped with rubber septum and flushed with argon. C₆D₆ was then added. The amount of C₆D₆ added corresponds to 0.500 mL minus the amount of organocatalyst solution used. The aldehyde catalyst solution (1M in benzene, 0.100 mL, 0.100 mmol) was then added. The mixture was allowed to stir at room temperature for about 20 minutes (approximate time to form the nitron) after which allylbenzylamine (0.4M, 0.8M, 1.2M, 1.5M, 2.0M) is added neat via syringe. The resulting mixture was then transferred in an NMR tube via pipette and the tube was quickly flushed with argon. The NMR tube was taken to the spectrometer and heated to 298 K. Using a custom program made by our NMR professional, Dr. Glenn Facey, a 8 scan spectrum was acquired every 12 minutes for a period of 96 minutes. The time after which the first spectrum was acquired varied slightly from one experiment to another. The concentration of product formed was determined by integrating the product's peak ($\delta = 1.1$ ppm (d, 3H)) relative to the internal standard peak ($\delta = 6.08$ ppm).



[allylbenzylamine]	time (min)	[product] (M)	V_0
0.4 M	13	0.0019	2.28E-6 M/s
	25	0.0034	
	37	0.0047	
	49	0.0073	
	61	0.0089	
	73	0.0097	
	85	0.0114	
	97	0.0131	

[allylbenzylamine]	time (min)	[product] (M)	V_0
0.8 M	8	0.0021	4.39E-6 M/s
	20	0.0043	
	32	0.0068	
	44	0.0088	
	56	0.0117	
	68	0.0145	
	80	0.0174	
	92	0.0197	

[allylbenzylamine]	time (min)	[product] (M)	V_0
1.2 M	5	0.0021	6.51E-6 M/s

[allylbenzylamine]	time (min)	[product] (M)	V ₀
	17	0.0050	
	29	0.0077	
	41	0.0111	
	53	0.0148	
	65	0.0184	
	77	0.0225	
	89	0.0258	

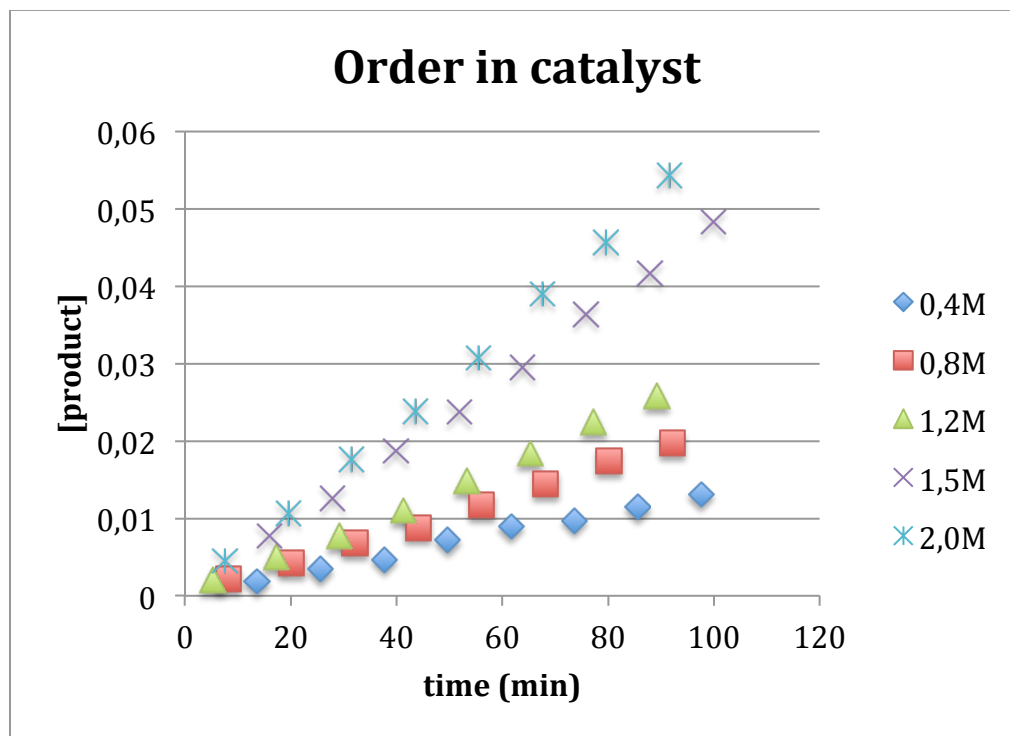
[allylbenzylamine]	time (min)	[product] (M)	V ₀
1.5 M	16	0.0077	8.12E-6 M/s
	28	0.0126	
	40	0.0187	
	52	0.0238	
	64	0.0295	
	76	0.0363	
	88	0.0417	
	100	0.0483	

[allylbenzylamine]	time (min)	[product] (M)	V ₀
2.0 M	8	0.0045	9,89E-6 M/s
	20	0.0106	
	32	0.0177	
	44	0.0238	
	56	0.0307	
	68	0.0390	
	80	0.0457	
	92	0.0543	

Order in catalyst (α -benzyloxyacetaldehyde)

N-Benzylhydroxylamine (0.0616 g, 0.500 mmol) and 1,3,5-trimethoxybenzene (the internal standard, 0.0280 g, 0.167 mmol) were weighted in a 1-dram vial. The vial was capped with a rubber septum and flushed with argon. C₆D₆ was then added. The amount of C₆D₆ added corresponds to 0.500 mL minus the amount of organocatalyst solution used. The aldehyde catalyst solution (1M in benzene, 0.1M, 0.2M, 0.4M, 0.6M, 0.8M) was then added. The mixture was allowed to stir at room temperature for about 20 minutes (approximate time to form the nitron) after which allylbenzylamine (117 μ L, 0.750 mmol) is added neat via syringe. The resulting mixture was then transferred in an NMR tube via pipette and the tube was quickly flushed with argon. The NMR tube was taken to the spectrometer and heated to

298 K. Using a custom program made by our NMR professional, Dr. Glenn Facey, a 8 scan spectrum was acquired every 12 minutes for a period of 96 minutes. The time after which the first spectrum was acquired varied slightly from one experiment to another. The concentration of product formed was determined by integrating the product's peak ($\delta = 1.1$ ppm (d, 3H)) relative to the internal standard peak ($\delta = 6.08$ ppm).



[catalyst]	time (min)	[product] (M)	V_0
0.1 M	5	0.0010	3.47E-6 M/s
	17	0.0032	
	29	0.0057	
	41	0.0074	
	53	0.0101	
	65	0.0123	
	77	0.0155	
	89	0.0182	

[catalyst]	time (min)	[product] (M)	V_0
0.2 M	16	0.0077	8.12E-6 M/s
	28	0.0126	
	40	0.0187	

[catalyst]	time (min)	[product] (M)	V_0
	52	0.0238	
	64	0.0295	
	76	0.0363	
	88	0.0417	
	100	0.0483	

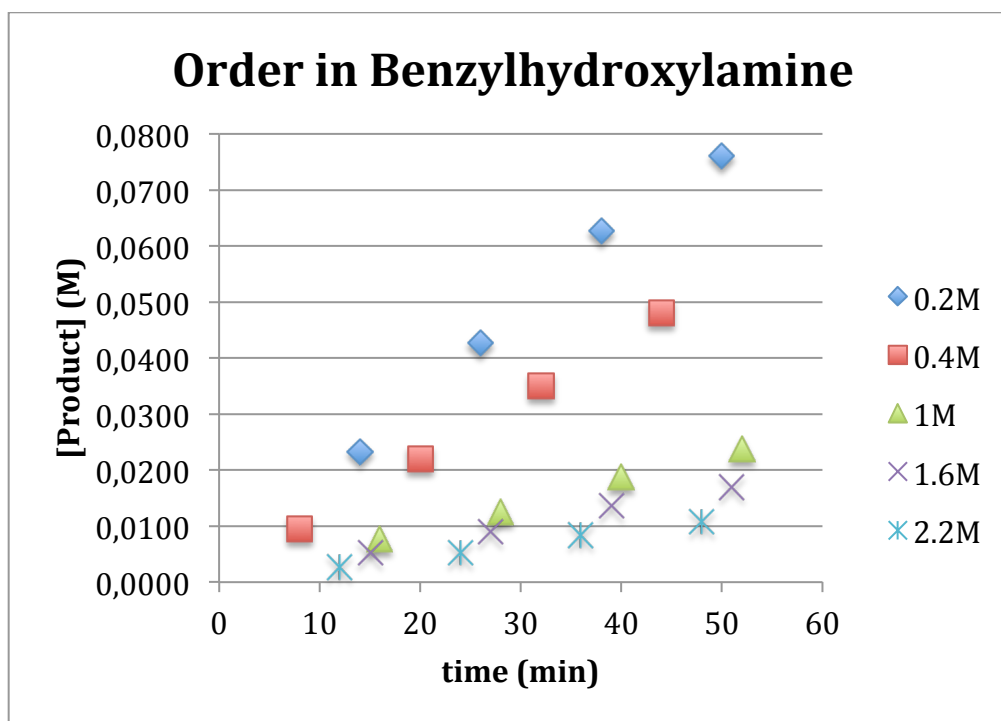
[catalyst]	time (min)	[product] (M)	V_0
0.4 M	14	0.0167	2.04E-5 M/s
	26	0.0298	
	38	0.0437	
	50	0.0633	
	62	0.0767	
	74	0.0910	
	86	0.1073	
	98	0.1240	

[catalyst]	time (min)	[product] (M)	V_0
0.6 M	14	0.0289	3.45E-5 M/s
	26	0.0533	
	38	0.0783	
	50	0.1037	
	62	0.1293	
	74	0.1533	
	86	0.1790	
	98	0.2017	

[catalyst]	time (min)	[product] (M)	V_0
0.8 M	13	0.0387	4.93E-5 M/s
	25	0.0770	
	37	0.1143	
	49	0.1533	
	61	0.1907	
	73	0.2267	
	85	0.2597	
	97	0.2923	

Order in *N*-benzylhydroxylamine

N-Benzylhydroxylamine (0.2M, 0.4M, 1M, 1.6M, 2.2M) and 1,3,5-trimethoxybenzene (the internal standard, 0.0280 g, 0.167 mmol) were weighted in a 1-dram vial. The vial was capped with a rubber septum and flushed with argon. C₆D₆ was then added. The amount of C₆D₆ added corresponds to 0.500 mL minus the amount of organocatalyst solution used. The aldehyde catalyst solution (1M in benzene, 0.100 mL, 0.100 mmol) was then added. The mixture was allowed to stir at room temperature for about 20 minutes (approximate time to form the nitrone) after which allylbenzylamine (0.117 mL, 0.750 mmol) is added neat via syringe. The resulting mixture was then transferred in an NMR tube via pipette and the tube was quickly flushed with argon. The NMR tube was taken to the spectrometer and heated to 298 K. Using a custom program made by our NMR professional, Dr. Glenn Facey, a 8 scan spectrum was acquired every 12 minutes for a period of 48 minutes. The time after which the first spectrum was acquired varied slightly from one experiment to another. The concentration of product formed was determined by integrating the product's peak ($\delta = 1.1$ ppm (d, 3H)) relative to the internal standard peak ($\delta = 6.08$ ppm).



[benzylhydroxylamine]	time (min)	[product] (M)	V_0
0.2 M	14	0.0232	2.74E-5 M/s
	26	0.0427	
	38	0.0627	
	50	0.0760	

[benzylhydroxylamine]	time (min)	[product] (M)	V_0
-----------------------	------------	---------------	-------

[benzylhydroxylamine]	time (min)	[product] (M)	V_0
0.4 M	8	0.0096	1.96E-5 M/s
	20	0.0219	
	32	0.0350	
	44	0.0480	

[benzylhydroxylamine]	time (min)	[product] (M)	V_0
1.0 M	16	0.0077	8.12E-6 M/s
	28	0.0126	
	40	0.0187	
	52	0.0238	

[benzylhydroxylamine]	time (min)	[product] (M)	V_0
1.6 M	15	0.0052	5.65E-6 M/s
	27	0.0089	
	39	0.0136	
	51	0.0170	

[benzylhydroxylamine]	time (min)	[product] (M)	V_0
2.2 M	12	0.0027	3.82E-6 M/s
	24	0.0052	
	36	0.0084	
	48	0.0108	

5.4.4 DEUTERIUM KINETIC ISOTOPE EFFECT (DKIE) EXPERIMENTS

Protocol for the determination of DKIE values

In a 13x100 mm test tube was added 1,3,5-trimethoxybenzene (the internal standard, 0.0280 g, 0.167 mmol, 0.333 equiv.) and *N*-benzylhydroxylamine (0.0616 g, 0.500 mmol, 1.00 equiv.). The test tube was sealed with a rubber septum and flushed with argon after which MeOD (0.5 mL) was added followed by allylbenzylamine (0.117 mL, 0.750 mmol, 1.50 equiv.). The mixture was allowed to stir for 20 min at room temperature under argon. Then, the tube was placed under high vacuum to evaporate MeOD. It is important to be careful at this point because the solution bumps readily. Once most of the MeOD was removed, the tube was refilled with argon and another portion of 0.5 mL MeOD was added. It was stirred for 20 min and then removed under high vacuum. This cycle was repeated until the mixture was allowed to stir 3 x 20 min in MeOD. After removal of the last portion of MeOD, C_6D_6

(0.4 mL) was added followed by a 1M solution of the catalyst in benzene (0.100 mL, 0.100 mmol, 0.20 equiv.). The mixture was then quickly transferred in a NMR tube and flushed with argon. The NMR tube was then taken to the spectrometer and heated to 298 K. Using a custom program made by our NMR professional, Dr. Glenn Facey, a 8 scan spectrum was acquired every 12 minutes for a period of 10 hours. The data was «batch processed» with *inmr* software for a faster reaction analysis. The concentration of product formed was determined by integrating the product's peak ($\delta = 1.1$ ppm (t, 2H)) relative to the internal standard peak ($\delta = 6.08$ ppm).

The exact same protocol was employed for the determination of the rate of the reaction with non-deuterated starting material except for the fact that MeOH was employed instead of MeOD. Also, the spectra were acquired over a period of 96 min instead of 10 hours. As opposed to the deuterated reaction, each spectrum was analyzed individually.

Run	V_0 H (M/s)	V_0 D (M/s)	KIE
1	3.12×10^{-6}	9.15×10^{-7}	3.40
2	3.76×10^{-6}	1.62×10^{-6}	2.32
3	4.98×10^{-6}	1.78×10^{-6}	2.80
Average	3.95×10^{-6}	1.43×10^{-6}	2.84
Std. Dev.	0.77×10^{-6}	0.37×10^{-6}	0.9 (from error propagation analysis)

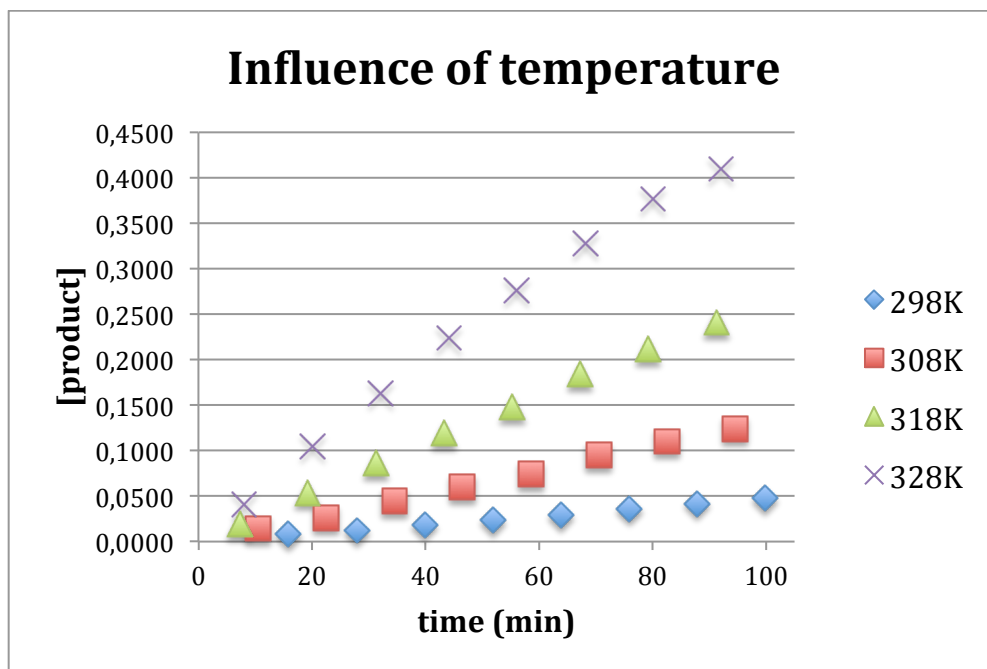
$$\text{KIE} = 2.8 \pm 0.9$$

5.4.5 EYRING PLOT

General procedure

N-Benzylhydroxylamine (0.0616 g, 0.500 mmol, 1.00 equiv.) and 1,3,5-trimethoxy-benzene (the internal standard, 0.0280 g, 0.167 mmol) were weighted in a 1 dram vial. The vial was capped with a rubber septum and flushed with argon. C_6D_6 (0.400 mL) was then added. The aldehyde catalyst solution (1M in benzene, 0.100 mL, 0.100 mmol, 0.20 equiv.) was then added. The mixture was allowed to stir at room temperature for about 20 minutes (approximate time to form the nitron) after which allylbenzylamine (0.117 mL, 0.750 mmol, 1.50 equiv.) was added neat via syringe. The resulting mixture was then transferred in an NMR tube via pipette and the tube was quickly flushed with argon. The NMR tube was taken to the spectrometer and heated to the desired temperature. Using a custom program made by our NMR professional, Dr. Glenn Facey, a 8 scan spectrum was acquired every 12 minutes for a period of 96 minutes. The time after which the first spectrum was acquired varied slightly from one experiment to another. The concentration of product formed was

determined by integrating the product's peak ($\delta = 1.1$ ppm (d, 3H)) relative to the internal standard peak ($\delta = 6.08$ ppm).



temperature (K)	time (min)	[product] (M)	V_0
298	16	0.0077	8.12E-6 M/s
	28	0.0126	
	40	0.0187	
	52	0.0238	
	64	0.0295	
	76	0.0363	
	88	0.0417	
	100	0.0483	

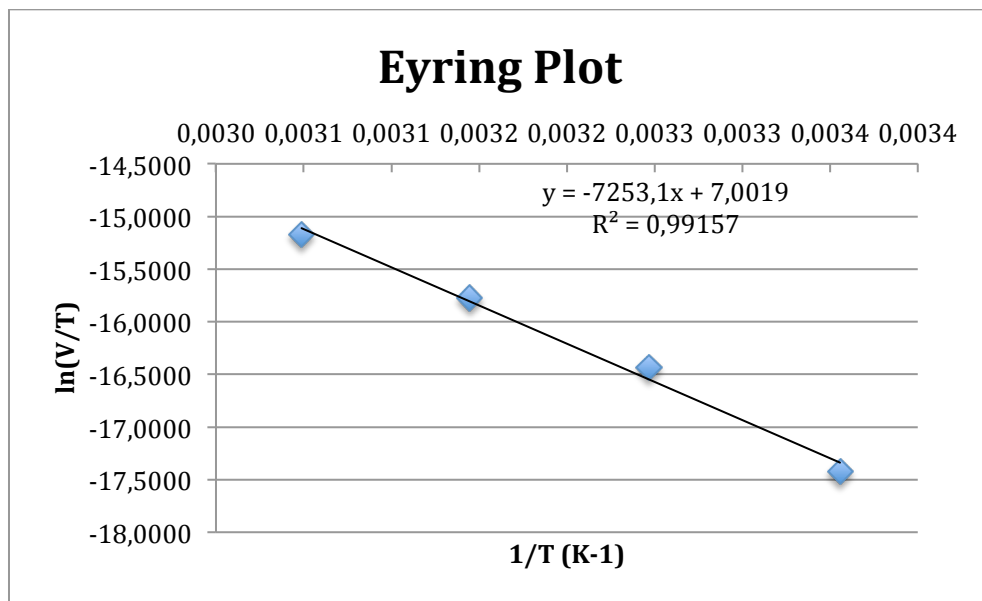
temperature (K)	time (min)	[product] (M)	V_0
308	11	0.0141	2,24E-5 M/s
	23	0.0261	
	35	0.0443	
	47	0.0600	
	59	0.0740	
	71	0.0950	
	83	0.1103	
	95	0.1240	

temperature (K)	time (min)	[product] (M)	V_0
318	7	0.0195	4.48E-5 M/s
	19	0.0540	
	31	0.0863	
	43	0.1193	
	55	0.1480	
	67	0.1837	
	79	0.2117	
	91	0.2407	

temperature (K)	time (min)	[product] (M)	V_0
328	8	0.0410	8.45E-5 M/s
	20	0.1047	
	32	0.1630	
	44	0.2243	
	56	0.2763	
	68	0.3277	
	80	0.3767	
	92	0.4100	

Eyring plot parameters:

T (K)	V_0	$1/T$ (K^{-1})	$\ln(V_0/(1/T))$
298	8.12E-6 M/s	0.0034	-17.4183
308	2.24E-5 M/s	0.0032	-16.4365
318	4.48E-5 M/s	0.0031	-15.7754
328	8.45E-5 M/s	0.0030	-15.1718



Plotting $1/T$ vs $\ln(V_0/T)$ and performing a least-squares linear regression analysis gives:

$$y = -(7253 \pm 472) x + (7.00 \pm 1.51), R^2 = 0.99157$$

From the Eyring equation, $\ln(V_0/T) = -\Delta H^\ddagger/(RT) + \Delta S^\ddagger/R + \ln(k_B/h)$:

$$-\Delta H^\ddagger/R = -7253 \pm 472 \text{ K}^{-1}; R = 1.98588 \text{ cal K}^{-1} \text{ mol}^{-1}$$

Therefore, $\Delta H^\ddagger = 14.4 \pm 0.9 \text{ kcal mol}^{-1}$

$$\Delta S^\ddagger/R + \ln(k_B/h) = 7.00 \pm 1.51; \ln(k_B/h) = 23.76$$

Therefore, $\Delta S^\ddagger = -33 \pm 3 \text{ e.u.}$

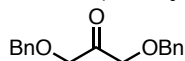
5.4.6 KETONE SCREENING

General procedure

N-Benzylhydroxylamine (0.0616 g, 0.500 mmol, 1.00 equiv.), and the ketone if solid (0.100 mmol, 0.20 equiv.) were weighted in a 13x100 mm test tube. The tube was sealed with a rubber septum and flushed with argon. Benzene (0.5 mL, 1M) was then added via syringe followed by the ketone if liquid and allylamine (0.056 mL, 0.75 mmol, 1.50 equiv.). The mixture was allowed to stir for 24 h at room temperature under argon before 1,3,5-trimethoxybenzene (0.0280 g, 0.167 mmol, 0.33 equiv.) was added. The mixture was diluted with dichloromethane (~ 2 mL) and an aliquot was taken apart. Volatiles of this aliquot were evaporated under a flow of air and the resulting mixture was then dissolved in CDCl₃. An ¹H NMR was taken and the yield calculated using the internal standard peak. Yields for different ketones are shown in Table 4.1 (Chapter 4).

Preparation of non-commercial ketones

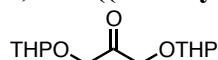
1,3-bis(benzyloxy)propan-2-one (4.9a)



A mixture of DMSO (2.5 mL, 35.2 mmol, 9.6 equiv.) and $\text{py}\cdot\text{SO}_3$ (2.51 g, 15.8 mmol, 4.3 equiv.) was pre-mixed for 10 min before being added at 0 °C to a mixture of 1,3-dibenzyloxy-2-propanol (1.00 g, 3.7 mmol, 1.0 equiv.) and triethylamine (2.5 mL, 18.0 mmol, 4.8 equiv.) in CH_2Cl_2 (5 mL). The mixture was allowed to stir at 0 °C for 1 h before being brought to room temperature. It was stirred for a further 2 h after which TLC analysis showed complete conversion. The mixture was diluted with Et_2O and washed 3x with 10% HCl and 2x with brine. The organic phase was then dried over MgSO_4 , filtered and evaporated under reduced pressure. The purification was made via flash column chromatography using 18% EtOAc in pet. ether as eluent. The product obtained is an off-white solid (864 mg, 87%). Spectral data is consistent with literature.¹⁸⁰

$^1\text{H-NMR}$ (400 MHz; CDCl_3 , 293K): δ 7.38-7.29 (m, 10H), 4.58 (s, 4H), 4.25 (s, 4H)

1,3-bis((tetrahydro-2H-pyran-2-yl)oxy)propan-2-one (4.9c)



$\text{TsOH}\cdot\text{H}_2\text{O}$ (53 mg, 0.3 mmol, 0.05 equiv.) was added to a suspension of dihydropyran (4.05 mL, 44.4 mmol, 8.00 equiv.) and dihydroxyacetone dimer (1.00 g, 5.6 mmol, 1.00 equiv.) in Et_2O (40 mL). The mixture was allowed to stir at room temperature for 16 h. The reaction mixture was then diluted with more Et_2O , washed 3x with sat. NaHCO_3 and 1x with brine. The organic phase was dried over MgSO_4 , filtered and evaporated under reduced pressure. The purification was made by flash column chromatography using 18% EtOAc in pet. ether as eluent. The product obtained is a clear oil (2.36 g, 82%).

$^1\text{H-NMR}$ (400 MHz; CDCl_3 , 293K): δ 4.61 (t, $J = 3.5$ Hz, 2H), 4.46-4.24 (m, 4H), 3.85-3.76 (m, 2H), 3.51-3.46 (m, 2H), 1.86-1.47 (m, 12H)

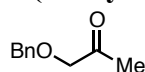
$^{13}\text{C NMR}$ (100 MHz, CDCl_3 , 293K): δ 206.0, 205.9, 98.9, 98.9, 70.8, 70.8, 62.4, 62.4, 30.3, 30.2, 25.3, 19.2, 19.2

IR ($\nu_{\text{max}}/\text{cm}^{-1}$): 2943, 2870, 1739, 1127, 1077, 1036

HRMS mass not found

R_f : 0.31 with 10% EtOAc in pet. ether

1-(benzyloxy)propan-2-one (4.9d)



(((2-methylallyl)oxy)methyl)benzene (prepared according to a literature procedure,¹⁸¹ 1.4 g, 8.5 mmol, 1.0 equiv.) was dissolved in CH_2Cl_2 . The flask was cooled at -78°C and a flow of O_3 was bubbled through the solution until a blue color persisted. O_3 bubbling was stopped

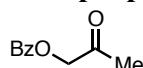
¹⁸⁰ hsu, L.-Y.; Wise, D. S.; Kucera, L. S.; Drach, J. C.; Townsend, L. B. *J. Org. Chem.* **1992**, *57*, 3354.

¹⁸¹ Blanc, A.; Toste, D. F. *Angew. Chem., Int. Ed.* **2006**, *45*, 2096.

and replace with argon until the blue color disappeared. The mixture was kept under argon and triphenylphosphine (2.7 g, 10.2 mmol, 1.2 equiv.) was added in one portion at -78 °C. The mixture was kept at this temperature for 1h before being allowed to reach room temperature. It was stirred for a further 3h after which the volatiles were removed under reduced pressure. The purification was then made via flash column chromatography using 15% EtOAc in pet. ether. The product obtained is a clear oil (801 mg, 57%). Spectral data is consistent with literature.¹⁸²

¹H-NMR (400 MHz; CDCl₃, 293K): δ 7.39-7.30 (m, 5H), 4.60 (s, 2H), 4.06 (s, 2H), 2.17 (s, 3H).

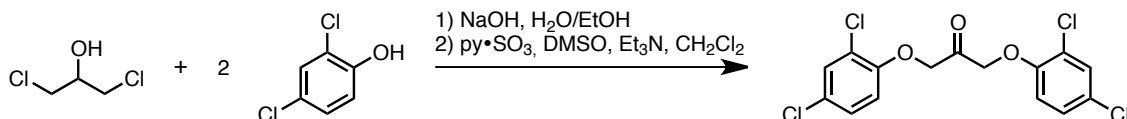
2-oxopropyl benzoate (4.9e)



Benzoyl chloride (2.44 mL, 21.9 mmol, 1.5 equiv.) was added dropwise to a solution of hydroxyacetone (1.00 mL, 14.6 mmol, 1.0 equiv.) dimethylaminopyridine (178 mg, 1.5 mmol, 0.1 equiv.) and triethylamine (4.07 mL, 29.2 mmol, 2.0 equiv.) in CH₂Cl₂ (25 mL) at 0 °C. The mixture became almost all solid while adding the benzoyl chloride. More CH₂Cl₂ was added in order to make the mixture more liquid and allow proper stirring. The mixture was stirred at room temperature for 16 h. It was then diluted with more CH₂Cl₂, washed 2x with 10% HCl and 2x with brine. The organic fraction was dried over MgSO₄, filtered and evaporated under reduced pressure. The purification was made via flash column chromatography using 15 % EtOAc in pet. ether as eluent to afford 4.9e (1.04g, 40%). Spectral data is consistent with literature.¹⁸³

¹H-NMR (400 MHz; CDCl₃, 293K): δ 8.11-8.09 (m, 2H), 7.60 (tt, *J* = 7.4, 1.6 Hz, 1H), 7.49-7.45 (m, 2H), 4.89 (s, 2H), 2.25 (s, 3H).

1,3-bis(2,4-dichlorophenoxy)propan-2-one (4.9f)



1) To a solution of 2,4-dichlorophenol (7.8 g, 48 mmol, 2.4 equiv.) in EtOH (30 mL), a solution of NaOH in H₂O was added and the mixture was refluxed for 10 min. Then, a solution of 1,3-dichloropropan-2-ol (1.9 mL, 20 mmol, 1 equiv.) was added and the resulting mixture was refluxed for 16 h. After being brought to room temperature, it was diluted with sat. NH₄Cl and EtOAc. The organic phase was washed 1x with NH₄Cl and 2x with brine after which it was dried over MgSO₄, filtered and evaporated under reduced pressure. The solid obtained (8.10 g, 106%) was relatively clean and employed for the next step without further purification.

2) A mixture of DMSO (1.9 mL, 26.2 mmol, 10.0 equiv.) and py•SO₃ (1.78 g, 11.2 mmol, 4.3 equiv.) was pre-mixed for 10 min before being added at 0 °C to a mixture of 1,3-bis(2,4-dichlorophenoxy)propan-2-ol (crude mixture, 1.00 g, 2.6 mmol, 1.0 equiv.) and triethylamine

¹⁸² Boger, D. L.; Palanki, M. S. *J. Am. Chem. Soc.* **1992**, *114*, 9318.

¹⁸³ Nguyen-Ba, N.; Brown, W.; Lee, N.; Zacharie, B. *Synthesis* **1998**, 759.

(1.78 mL, 12.8 mmol, 4.9 equiv.) in CH₂Cl₂ (5 mL). The mixture was allowed to stir at 0 °C for 1 h before being brought to room temperature. It was stirred for a further 2 h after which TLC analysis showed complete conversion. The mixture was diluted with Et₂O and washed 3x with 10% HCl and 2x with brine. The organic phase was then dried over MgSO₄, filtered and evaporated under reduced pressure. The purification was made via flash column chromatography using 15% acetone in pet. ether as eluent. The product obtained is a white solid (707 mg, 71%).

¹H-NMR (400 MHz; DMSO-d₆, 293K): δ 7.58 (d, *J* = 2.5 Hz, 2H), 7.36 (dd, *J* = 8.9, 2.5 Hz, 2H), 7.16 (d, *J* = 9.0 Hz, 2H), 5.21 (s, 4H)

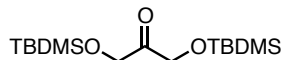
¹³C NMR (100 MHz, DMSO-d₆, 293K): δ 152.2, 129.3, 127.8, 124.9, 122.2, 115.0, 71.0

IR (ν_{max}/cm⁻¹): 1744, 1479, 1090, 802

HRMS calculated for C₁₅H₁₀Cl₄O₃ (M⁺): 377.9384; Found 377.9364

R_f: 0.26 with 15% acetone in pet. ether

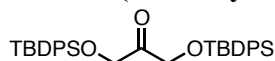
***O,O'*-bis(*tert*-butyldimethylsilyl)dihydroxyacetone (4.9q)**



TBDMSCl (3.53 g, 23.4 mmol, 3.9 equiv.) was slowly added at 0 °C to a stirred solution of dihydroxyacetone dimer (1.08 g, 6.0 mmol, 1.0 equiv.), imidazole (2.96 g, 46.9 mmol, 7.8 equiv.) and dimethylaminopyridine (122 mg, 1.0 mmol, 0.2 equiv.) in DMF (8 mL) under argon. The water/ice bath was removed after 10 min and the reaction mixture was allowed to stir at room temperature for 3 h. It was then diluted with Et₂O and washed 3x with sat. NH₄Cl. The organic phase was then dried over MgSO₄, filtered and evaporated under reduced pressure. The resulting clear oil was passed through a small plug of silica while washing with 10% Et₂O in pet. ether. Solvent was removed under reduced pressure to provide **4.9q** as a clear oil (2.81 g, 73%). Spectral data is consistent with literature.¹⁸⁴

¹H-NMR (400 MHz; CDCl₃, 293K): δ δ 4.42 (s, 4H), 0.92 (s, 18H), 0.09 (s, 12H).

***O,O'*-bis(*tert*-butyldiphenylsilyl)dihydroxyacetone (4.9r)**



TBDPSCl (3.04 mL g, 11.7 mmol, 3.9 equiv.) was slowly added at 0 °C to a stirred solution of dihydroxyacetone dimer (540 mg, 3.0 mmol, 1.0 equiv.), imidazole (1.48 g, 23.4 mmol, 7.8 equiv.) and dimethylaminopyridine (61 mg, 0.5 mmol, 0.2 equiv.) in DMF (5 mL) under argon. The water/ice bath was removed after 10 min and the reaction mixture was allowed to stir at room temperature for 3 h. It was then diluted with Et₂O and washed 3x with sat. NH₄Cl. The organic phase was then dried over MgSO₄, filtered and evaporated under reduced pressure. The resulting clear oil was passed through a small plug of silica while washing with 10% Et₂O in pet. ether. Solvent was removed under reduced pressure to provide **4.9r** as a white solid (2.70 g, 79%).

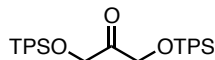
¹H-NMR (400 MHz; CDCl₃, 293K): δ 7.60-7.57 (m, 8H), 7.44-7.40 (m, 4H), 7.37-7.33 (m, 8H), 4.41 (s, 4H), 1.02 (s, 18H).

¹³C NMR (100 MHz, CDCl₃, 293K): δ 207.2, 135.4, 132.5, 129.9, 127.8, 68.5, 26.7, 19.2

¹⁸⁴ Ravindar, K.; Reddy, M. S.; Deslongchamps, P. *Org. Lett.* **2011**, *13*, 3178.

IR ($\nu_{\max}/\text{cm}^{-1}$): 2934, 2858, 1744, 1427, 1113, 1089, 701
HRMS calculated for $\text{C}_{31}\text{H}_{33}\text{O}_3\text{Si}_2$ ($\text{M}-t\text{Bu}^+$): 509.1968; Found 509.1995
R_f: 0.26 with 5% Et_2O in pet. ether

O,O'-bis(triphenylsilyl)dihydroxyacetone (4.9s)



Triphenylsilylchloride (6.9 g, 23.4 mmol, 3.9 equiv.) was added at 0 °C to a stirred solution of dihydroxyacetone dimer (1.1 g, 6.0 mmol, 1.0 equiv.) and pyridine (3.8 mL, 46.8 mmol, 7.8 equiv.) in DMF (8 mL). The water/ice bath was taken off after 10 min and the solution was allowed to stir at room temperature for 16 h. It was then diluted with Et_2O , washed 3x with sat. NH_4Cl and 1x with brine. The organic phase was then dried over MgSO_4 , filtered and evaporated under reduced pressure. The purification was made via flash column chromatography using 8% EtOAc in pet. ether as eluent. The cleanest fractions were collected and evaporated under reduced pressure. The resulting sticky solid was then recrystallized using a mixture of Et_2O and pet. ether. The crystallization was allowed to occur over a week-end in a freezer at -20 °C. The pure product was then collected by filtration (1.56 g, 17%)

¹H-NMR (400 MHz; CDCl_3 , 293K): δ 7.57-7.55 (m, 12H), 7.45-7.41 (m, 6H), 7.37-7.33 (m, 12H), 4.54 (s, 4H).

¹³C NMR (100 MHz, CDCl_3 , 293K): δ 206.7, 135.3, 133.0, 130.3, 128.0, 68.2

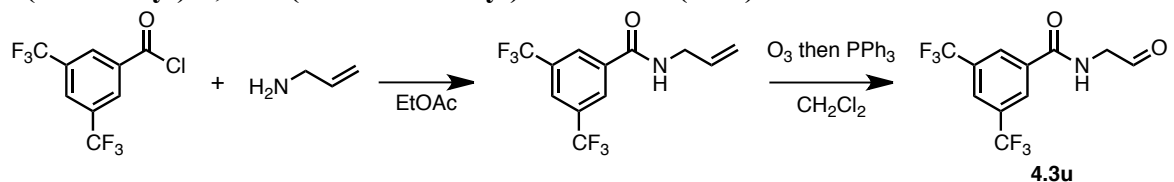
IR ($\nu_{\max}/\text{cm}^{-1}$): 3069, 1742, 1429, 1118, 712, 699

HRMS calculated for $\text{C}_{33}\text{H}_{29}\text{O}_3\text{Si}_2$ ($\text{M}-\text{Ph}^+$): 529.1655; Found 529.1637

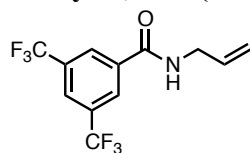
R_f: 0.45 with 10% EtOAc in pet. ether

5.4.7 "BIFUNCTIONAL" ORGANOCATALYSTS PREPARATION

N-(2-oxoethyl)-3,5-bis(trifluoromethyl)benzamide (4.3u)



N-allyl-3,5-bis(trifluoromethyl)benzamide



3,5-bis(trifluoromethyl)benzoyl chloride (700 μL , 3.9 mmol, 1 equiv.) was added to a mixture of allylamine (870 μL , 11.6 mmol, 3 equiv.) in EtOAc at 0 °C. After addition, the mixture was allowed to reach room temperature. It was then stirred for a further 2 h after which TLC showed complete conversion. The mixture was diluted with more EtOAc , washed 2x with 10% HCl , 1x with NaHCO_3 and 1x with brine. The organic phase was then dried over MgSO_4 , filtered and evaporated under reduced pressure. The resulting oil was the

filtered over a plug of silica while washing with 20% EtOAc in pet. ether. The solvent was evaporated to afford a clear oil that immediately solidified (1.09 g, 96%).

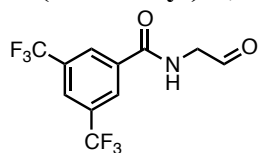
¹H-NMR (400 MHz; CDCl₃, 293K): δ 8.25 (s, 2H), 7.97 (s, 1H), 7.24 (s, 1H), 5.90 (ddt, *J* = 17.1, 10.3, 5.7 Hz, 1H), 5.24 (dq, *J* = 17.1, 1.4 Hz, 1H), 5.18 (dd, *J* = 10.2, 1.3 Hz, 1H), 4.08 (tt, *J* = 5.7, 1.4 Hz, 2H).

¹³C NMR (100 MHz, CDCl₃, 293K): δ 164.9, 136.5, 133.3, 132.2 (q, *J* = 33.9 Hz), 127.5, 125.1-124.9 (m), 123.0 (q, *J* = 272.9 Hz), 117.3, 42.9

IR (ν_{max}/cm⁻¹): 3297, 3089, 1652, 1559, 1277, 1134

HRMS calculated for C₁₂H₉F₆NO₂ (M⁺): 297.0588; Found 297.0577

N-(2-oxoethyl)-3,5-bis(trifluoromethyl)benzamide (4.3u)



N-allyl-3,5-bis(trifluoromethyl)benzamide (500 mg, 1.7 mmol, 1.0 equiv.) was dissolved in CH₂Cl₂. The flask was cooled at -78 °C and a flow of O₃ was bubbled through the solution until a blue color persisted. O₃ bubbling was stopped and replaced with argon until the blue color disappeared. The mixture was kept under argon and triphenylphosphine (529 mg, 2.0 mmol, 1.2 equiv.) was added in one portion at -78 °C. The mixture was kept at this temperature for 1h before being allowed to reach room temperature. It was stirred for a further 3h after which the volatiles were removed under reduced pressure. The purification was then made via flash column chromatography using 50% EtOAc in pet. ether. The product obtained is a white solid (434 mg, 86%).

¹H-NMR (400 MHz; CDCl₃, 293K): δ 9.79 (s, 1H), 8.27 (s, 2H), 8.04 (s, 1H), 7.14 (br s, 1H), 4.49 (d, *J* = 4.8 Hz, 2H).

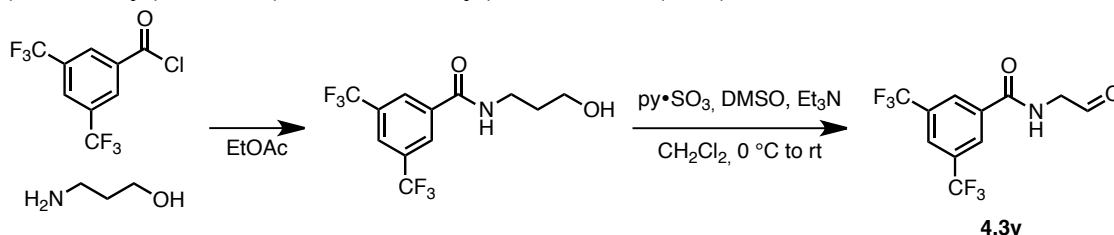
¹³C NMR (100 MHz, CDCl₃, 293K): δ 195.5, 164.7, 135.5, 132.4 (q, *J* = 34.0 Hz), 127.6-127.4 (m), 125.6-125.4 (m), 122.84 (d, *J* = 272.8 Hz), 50.9

IR (ν_{max}/cm⁻¹): 3324, 1652, 1559, 1279, 1089

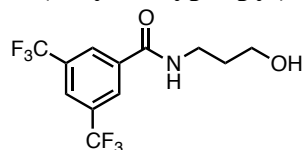
HRMS calculated for C₁₁H₇F₅NO₂ (M-F⁺): 280.0397; Found 280.0402

R_f: 0.38 with 50% EtOAc in pet. ether

N-(2-oxoethyl)-3,5-bis(trifluoromethyl)benzamide (4.3v)



N-(3-hydroxypropyl)-3,5-bis(trifluoromethyl)benzamide



3,5-bis(trifluoromethyl)benzoyl chloride (700 μ L, 3.9 mmol, 1 equiv.) was added to a mixture of allylamine (887 μ L, 11.6 mmol, 3 equiv.) in EtOAc at 0 °C. After addition, the mixture was allowed to reach room temperature. It was then stirred for a further 2 h after which TLC showed complete conversion. The mixture was diluted with more EtOAc, washed 2x with 10% HCl, 1x with NaHCO₃ and 1x with brine. The organic phase was then dried over MgSO₄, filtered and evaporated under reduced pressure. The resulting oil was filtered over a plug of silica while washing with 20% EtOAc in pet. ether. The solvent was evaporated to afford a thick oil that eventually solidified (1.18 g, 97%).

¹H-NMR (400 MHz; CDCl₃, 293K): δ 8.24 (s, 2H), 7.98 (s, 1H), 7.70 (s, 1H), 3.79 (t, J = 5.5 Hz, 2H), 3.66 (q, J = 6.0 Hz, 2H), 3.34 (s, 1H), 1.86 (quintet, J = 5.8 Hz, 2H).

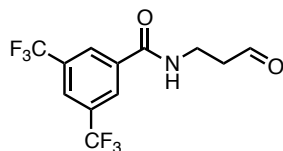
¹³C NMR (100 MHz, CDCl₃, 293K): δ 165.4, 136.3, 132.1 (q, J = 33.9 Hz), 127.4, 125.2-124.9 (m), 122.9 (q, J = 272.9 Hz), 60.5, 38.3, 31.4

IR ($\nu_{\max}/\text{cm}^{-1}$): 3310, 2949, 1652, 1556, 1278, 1134

HRMS calculated for C₁₂H₁₁F₆NO₂ (M⁺): 315.0694; Found 315.0706

R_f: 0.11 with 40% EtOAc in pet. ether

***N*-(3-oxopropyl)-3,5-bis(trifluoromethyl)benzamide (4.3v)**



A mixture of DMSO (1.13 mL, 15.9 mmol, 10.0 equiv.) and py•SO₃ (1.09 g, 6.8 mmol, 4.3 equiv.) was pre-mixed for 10 min before being added at 0 °C to a mixture of *N*-(3-hydroxypropyl)-3,5-bis(trifluoromethyl)benzamide (500 mg, 1.6 mmol, 1.0 equiv.) and triethylamine (1.1 mL, 18.0 mmol, 4.9 equiv.) in CH₂Cl₂ (5 mL). The mixture was allowed to stir at 0 °C for 1 h before being brought to room temperature. It was stirred for a further 2 h after which TLC analysis showed complete conversion. The mixture was diluted with Et₂O and washed 3x with 10% HCl and 2x with brine. The organic phase was then dried over MgSO₄, filtered and evaporated under reduced pressure. The purification was made via flash column chromatography using 35% EtOAc in pet. ether as eluent. The product obtained is a white solid (408 mg, 82%).

¹H-NMR (400 MHz; CDCl₃, 293K): δ 9.86 (s, 1H), 8.21 (s, 2H), 7.98 (s, 1H), 7.33 (br s, 1H), 3.79 (q, J = 5.8 Hz, 2H), 2.92 (t, J = 5.7 Hz, 2H).

¹³C NMR (100 MHz, CDCl₃, 293K): δ 201.7, 164.9, 136.3, 132.15 (q, J = 33.9 Hz), 127.45 (m), 125.11 (m), 122.93 (q, J = 272.9 Hz), 43.4, 33.9

IR ($\nu_{\max}/\text{cm}^{-1}$): 1734, 1652, 1556, 1279, 1132

HRMS calculated for C₁₂H₉F₆NO₂ (M⁺): 313.0537; Found 313.0543

R_f: 0.36 with 40% EtOAc in pet. ether

5.4.8 RATE COMPARISON FOR 4.3T AND 4.3W

General Procedure

N-Benzylhydroxylamine (0.0616 g, 0.500 mmol, 1.00 equiv.) and 1,3,5-trimethoxy-benzene (the internal standard, 0.0280 g, 0.167 mmol) were weighted in a 1-dram vial. The vial was capped with a rubber septum and flushed with argon. DMSO-*d*₆ (0.500 mL) was then added, followed by the carbonyl catalyst (0.100 mmol, 20.0 mol%). The mixture was allowed to stir at room temperature for about 40 minutes after which allylbenzylamine (0.117 mL, 0.750 mmol) was added via syringe. The resulting mixture was then transferred in an NMR tube via pipette and the tube was quickly flushed with argon. The NMR tube was taken to the spectrometer and heated to 298 K. Using a custom program made by our NMR professional, Dr. Glenn Facey, a 8 scan spectrum was acquired every 20 minutes for a period of 230 minutes (first spectra taken 10 min after mixing reagents). The concentration of product formed was determined by integrating the product's peak ($\delta = 1.06$ ppm (d, 3H)) relative to the internal standard peak ($\delta = 6.13$ ppm).

Catalyst	time (min)	[product] (M)	V_0
3i	10	0	2.38E-6 M/s
	30	0.0027	
	50	0.0053	
	70	0.0073	
	90	0.0097	
	110	0.0128	
	130	0.0154	
	150	0.0194	
	170	0.0218	
	190	0.0243	
	210	0.0284	
	230	0.0315	

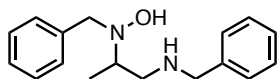
Catalyst	time (min)	[product] (M)	V_0
3j	10	0	6.91E-6 M/s (calculated from 150 to 230 min)
	30	0	
	50	0.0023	
	70	0.0057	
	90	0.0095	
	110	0.0155	
	130	0.0206	
	150	0.0276	
	170	0.0337	
	190	0.0423	
	210	0.0503	
	230	0.0607	

5.4.8 PARAFORMALDEHYDE-CATALYZED COPE-TYPE HYDROAMINATION OF ALLYLIC AMINES WITH N-ALKYLHYDROXYLAMINES

General Procedure

A 5-mL sealed tube was charged with a stir bar, amine (1.50 equiv.) paraformaldehyde (0.05-0.10 equiv.), hydroxylamine (1.00 equiv.) and *t*-BuOH (1.0 M). The reaction was stirred at 30 °C, and monitored by TLC or ¹H NMR. The crude reaction mixture was concentrated under reduced pressure and purified by column chromatography to give the corresponding *N,N*-dialkylhydroxylamine products.

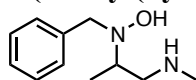
N-Benzyl-2-(benzyl(hydroxy)amino)propan-1-amine (4.4b)



The compound was prepared following the general procedure using *N*-benzylhydroxylamine (0.123 g, 1.00 mmol) and paraformaldehyde (0.05 equiv.). Isolated 0.230 g as a white solid (85%) after column chromatography (1 % Et₃N/ 1 % MeOH/CH₂Cl₂).

¹H NMR (300 MHz, CDCl₃) δ 7.37-7.24 (m, 10H), 3.93 (d, *J* = 13.2 Hz, 1H), 3.73 (d, *J* = 13.1 Hz, 1H), 3.72 (d, *J* = 13.3 Hz, 1H), 3.67 (d, *J* = 13.2 Hz, 1H), 3.08-3.02 (m, 1H), 2.80 (dd, *J* = 12.2, 8.5 Hz, 1H), 2.64 (dd, *J* = 12.2, 4.0 Hz, 1H), 1.11 (d, *J* = 6.5 Hz, 3H). Spectral data was consistent with literature.⁵

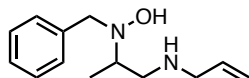
2-(Benzyl(hydroxy)amino)-*N*-methylpropan-1-amine (4.4c)



The compound was prepared following the general procedure using *N*-benzylhydroxylamine (0.123 g, 1.00 mmol) and paraformaldehyde (0.05 equiv.). Isolated 0.191 g as a pale yellow oil (98%) after column chromatography (1 % Et₃N/ 10 % MeOH/CH₂Cl₂).

¹H NMR (300 MHz, CDCl₃): δ 7.39-7.26 (m, 5H), 3.97 (d, *J* = 13.2 Hz, 1H), 3.72 (d, *J* = 13.2 Hz, 1H), 3.08-2.97 (m, 1H), 2.78 (dd, *J* = 12.2, 8.5 Hz, 1H), 2.56 (dd, *J* = 12.2, 4.0 Hz, 1H), 2.35 (s, 3H), 1.12 (d, *J* = 6.5 Hz, 3H). Spectral data was consistent with literature.¹⁸⁵

N-(2-(Benzyl(hydroxy)amino)propyl)prop-2-en-1-amine (4.4d)

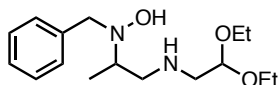


¹⁸⁵ MacDonald, M. J.; Schipper, D. J.; Ng, P. J.; Moran, J.; Beauchemin, A. M. *J. Am. Chem. Soc.* 2011, 133, 20100.

The compound was prepared following the general procedure using *N*-benzylhydroxylamine (0.123 g, 1.00 mmol) and paraformaldehyde (0.05 equiv.). Isolated 0.203 g as a pale yellow oil (92%) after column chromatography (1 % Et₃N/ 5 % MeOH/CH₂Cl₂).

¹H NMR (300 MHz, CDCl₃) δ 7.36- 7.24 (m, 5H), 5.74 (tdd, *J* = 16.4, 10.2, 6.2 Hz, 1H), 5.06 (dt, *J* = 17.1, 1.5 Hz, 2H), 3.92 (d, *J* = 13.0 Hz, 1H), 3.69 (d, *J* = 13.0 Hz, 1H), 3.02 (d, *J* = 5.8 Hz, 1H), 2.98-2.95 (m, 1H), 2.69 (dd, *J* = 12.4, 9.2 Hz, 1H), 2.43 (dd, *J* = 12.4, 4.1 Hz, 1H), 1.06 (d, *J* = 6.5 Hz, 3H). Spectral data was consistent with literature.¹⁸⁵

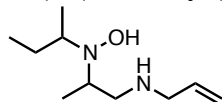
2-(Benzyl(hydroxy)amino)-*N*-(2,2-diethoxyethyl)propan-1-amine (4.4e)



The compound was prepared following the general procedure using *N*-benzylhydroxylamine (0.123 g, 1.00 mmol) and paraformaldehyde (0.10 equiv.). Isolated 0.196 g as a pale yellow oil (66%) after column chromatography (1 % Et₃N/ 5 % MeOH/CH₂Cl₂).

¹H NMR (300 MHz, CDCl₃) δ 7.39-7.38 (m, 5H), 4.58 (t, *J* = 5.6 Hz, 1H), 3.97 (d, *J* = 13.2 Hz, 1H), 3.72 (d, *J* = 13.2 Hz, 1H), 3.67 (tt, *J* = 8.9, 4.7 Hz, 2H), 3.51 (dq, *J* = 14.2, 7.1, 0.9 Hz, 2H), 3.07-2.96 (m, 1H), 2.86-2.67 (m, 4H), 1.20 (t, *J* = 7.0 Hz, 3H), 1.18 (t, *J* = 7.0 Hz, 3H), 1.11 (d, *J* = 6.5 Hz, 3H). Spectral data was consistent with literature.¹⁸⁵

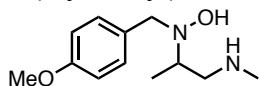
N-(2-(*sec*-Butyl(hydroxy)amino)propyl)prop-2-en-1-amine (4.4f)



The compound was prepared following the general procedure using *N*-(*sec*-butyl)hydroxylamine (0.089 g, 1.0 mmol) and paraformaldehyde (0.10 equiv.). Isolated 0.138 g as a pale yellow oil and mixture of 1:1 diastereomers (72%) after column chromatography (1 % Et₃N/ 10 % MeOH/CH₂Cl₂).

¹H NMR (300 MHz, CDCl₃) δ 5.88 [tdd, *J* = 16.4, 10.5, 6.0 Hz, 1H (mix)], 5.15 [d, *J* = 17.3 Hz, 1H (mix)], 5.08 [d, *J* = 10.2 Hz, 1H (mix)], 3.29-3.19 [m, 2H (mix)], 3.14-3.04 [m, 1H (mix)], 2.83-2.71 [m, 2H (mix)], 2.61-2.53 [m, 1H (mix)], 1.82-1.69 [m, 1H (minor)], 1.66-1.53 [m, 1H (major)], 1.11 [d, *J* = 6.3 Hz, 3H (first diastereomer)], 1.02 [d, *J* = 6.4 Hz, 3H (second diastereomer)], 0.97 [d, *J* = 6.3 Hz, 3H (first diastereomer)], 0.95 [d, *J* = 6.2 Hz, 3H (second diastereomer)], 0.88 [t, *J* = 7.4 Hz, 3H (first diastereomer)], 0.87 [t, *J* = 7.5 Hz, 3H (second diastereomer)]. Spectral data was consistent with literature.¹⁸⁵

2-(Hydroxy(4-methoxybenzyl)amino)-*N*-methylpropan-1-amine (4.4g)



The compound was prepared following the general procedure using *N*-(4-methoxybenzyl)hydroxylamine (0.153 g, 1.00 mmol) and paraformaldehyde (0.10 equiv.). Isolated 0.122 g as a pale yellow oil (80%) after column chromatography (1 % Et₃N/ 10 % MeOH/CH₂Cl₂).

¹H NMR (300 MHz, CDCl₃) δ 7.24 (d, *J* = 8.7 Hz, 2H), 6.82 (d, *J* = 8.7 Hz, 2H), 3.85 (d, *J* = 13.0 Hz, 1H), 3.75 (s, 3H), 3.61 (d, *J* = 13.0 Hz, 1H), 2.93 (m, 1H), 2.70 (m, 1H), 2.406 (m, 1H), 2.23 (s, 3H), 1.04 (s, *J* = 6.5 Hz, 3H). Spectral data was consistent with literature.¹⁸⁵

Appendix 1

Initial Steps Toward the Development of an Organocatalyzed Azide-Alkyne Huisgen Cycloaddition

A1.1 Introduction

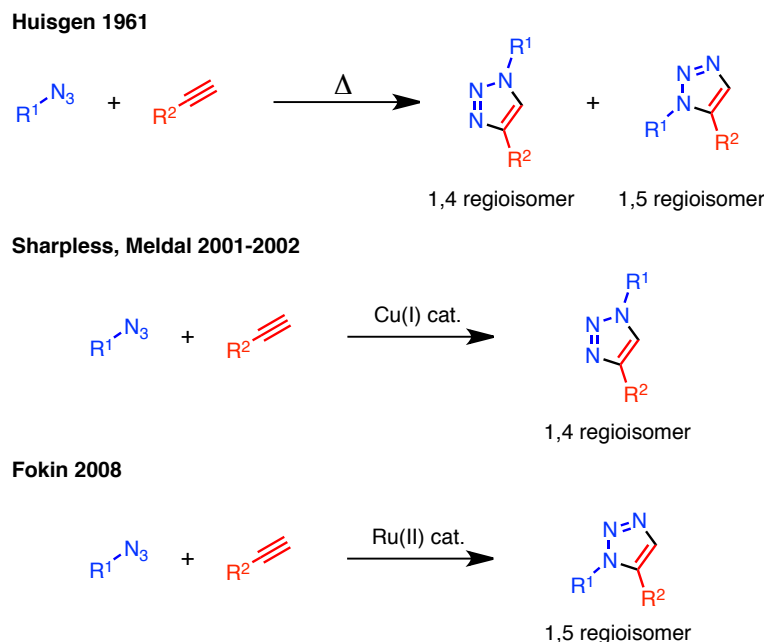
The Huisgen 1,3-dipolar cycloaddition reaction of organic azides and alkynes is thermodynamically a highly favoured process which leads to the formation of triazoles. Initially developed by Huisgen in the 1960's, the thermal version of this reaction is known to provide mixtures of 1,4- and 1,5-disubstituted triazoles when terminal alkynes are coupled with alkyl azides (Scheme A1.1). In part for this reason, the use of this reaction has been relatively modest until 2001-2002, where a copper-catalyzed version was discovered independently by Tornøe & Meldal^{186,187} and Sharpless.¹⁸⁸ This catalytic system enabled the mild and regioselective formation of 1,4-substituted triazoles. Given the exceptional efficiency and robustness of this reaction, Sharpless classified the Huisgen 1,3-dipolar

¹⁸⁶ Tornøe, C. W.; Meldal, M. Peptidotriazoles: Copper(I)-catalyzed 1,3-dipolar cycloadditions on solid-phase, Peptides 2001, Proc. Am. Pept. Symp.; American Peptide Society and Kluwer Academic Publishers: San Diego, 2001; pp 263-264.

¹⁸⁷ Tornøe, C. W.; Christensen, C.; Meldal, M. *J. Org. Chem.* **2002**, *67*, 3057.

¹⁸⁸ Rostovtsev, V. V.; Green, L. G.; Fokin, V. V.; Sharpless, B. K. *Angew. Chem., Int. Ed.* **2002**, *41*, 2596.

cycloaddition as part of "click chemistry".¹⁸⁹ It is now widely used in several spheres of science such as organic synthesis, drug discovery, bioconjugation, polymer chemistry and material science.¹⁹⁰



Scheme A1.1 Huisgen 1,3-Dipolar Cycloaddition of Azides and Terminal Alkynes

In 2005, Fokin reported the use of ruthenium catalysis to access the 1,5 regioisomer of the azide-alkyne cycloaddition reaction with high regioselectivity and under mild conditions.¹⁹¹ This approach nicely complements the work that was accomplished with copper catalysis.

While catalysis is typically required for the intermolecular Huisgen 1,3-dipolar cycloaddition reaction, some intramolecular examples were shown to proceed under relatively mild conditions upon heating in common organic solvent.¹⁹² Scheme A1.2

¹⁸⁹ Hartmuth, K. C.; Finn, M. G.; Sharpless, B. K. *Angew. Chem., Int. Ed.* **2001**, *40*, 2004.

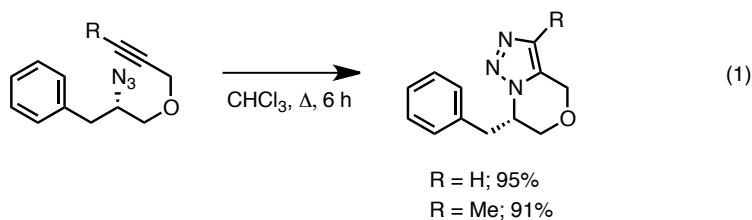
¹⁹⁰ For a review, see: (a) Meldal, M.; Tornøe, C. W. *Chem. Rev.* **2008**, *108*, 2952.

¹⁹¹ Zhang, L.; Chen, X.; Xue, P.; Sun, H. H. Y.; Williams, I. D.; Sharpless, K. B.; Fokin, V. V.; Jia, G. *J. Am. Chem. Soc.* **2005**, *127*, 15998.

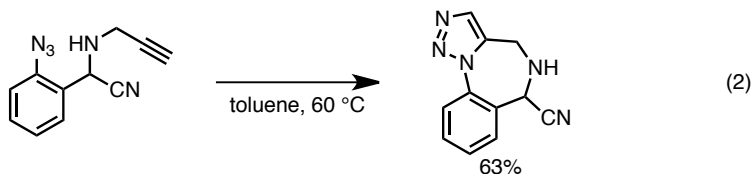
¹⁹² For a short review, see: Majumbar, K. C.; Ray, K. *Synthesis* **2011**, 3767

illustrates some of the mildest examples of this reactivity. Eq. 1 presents a system from Datta where a propargyl ether reacts with an azide in refluxing chloroform to afford a 6,5-fused heterocycle.¹⁹³ In Eq. 2, a propargylamine reacts intramolecularly with an aryl azide at 60 °C to form the corresponding 6,7,5-fused ring system.¹⁹⁴ Eq. 3 shows the formation of a 6,5-fused ring system from a tandem azidation/1,3-dipolar cycloaddition.¹⁹⁵ While the acetal azidation proceeds rapidly at room temperature, the cycloaddition requires a longer reaction time at a temperature of 50 °C. In contrast to most other intramolecular azide-alkyne cycloadditions, where the temperatures required to effect the transformation are typically over 100 °C, the reactions presented in Scheme A1.2 occur at relatively low temperatures. This is due to the electron-poor nature of the alkynes employed. The presence of a heteroatom at the propargylic position seems withdraw electrons and activate the alkyne toward cycloaddition.

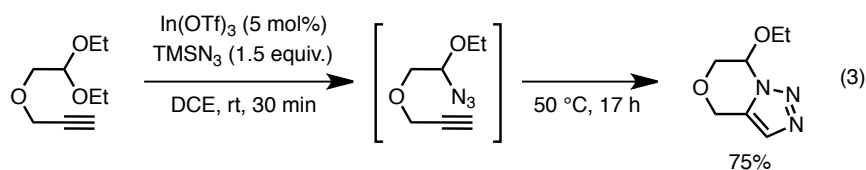
Datta 2009



Martin 2011



Taguchi 2005



¹⁹³ Li, R.; Jansen, D. J.; Datta, A. *Org. Biomol. Chem.* **2009**, *7*, 1921.

¹⁹⁴ Donald, J. R.; Martin, S. F. *Org. Lett.* **2011**, *13*, 852.

¹⁹⁵ Yanai, H.; Taguchi, T. *Tetrahedron Lett.* **2005**, *46*, 8639.

Scheme A1.2 Intramolecular 1,3-Dipolar Azide-Alkyne Cycloaddition

Taking into account that intermolecular azide-alkyne cycloadditions require biased alkynes and/or harsh reaction conditions while the intramolecular variant can be done under relatively mild conditions, we wondered if an organocatalytic tethering strategy analogous to the one presented in Chapter 4 could be applicable to this transformation. The envisioned catalytic cycle that would promote this transformation is depicted in Figure A1.1. Starting from an aldehyde catalyst, acid-catalyzed formation of an *O,O*-dipropargylacetal could occur to enter the catalytic cycle. Then, as demonstrated in the report from Taguchi (Scheme A1.2, Eq. 3), azidation of the acetal using a Lewis acid catalyst¹⁹⁶ could yield an α -azido ether that would be well suited to undergo the key cycloaddition reaction. A subsequent acid-catalyzed transacetalization would return the catalyst to its initial form.

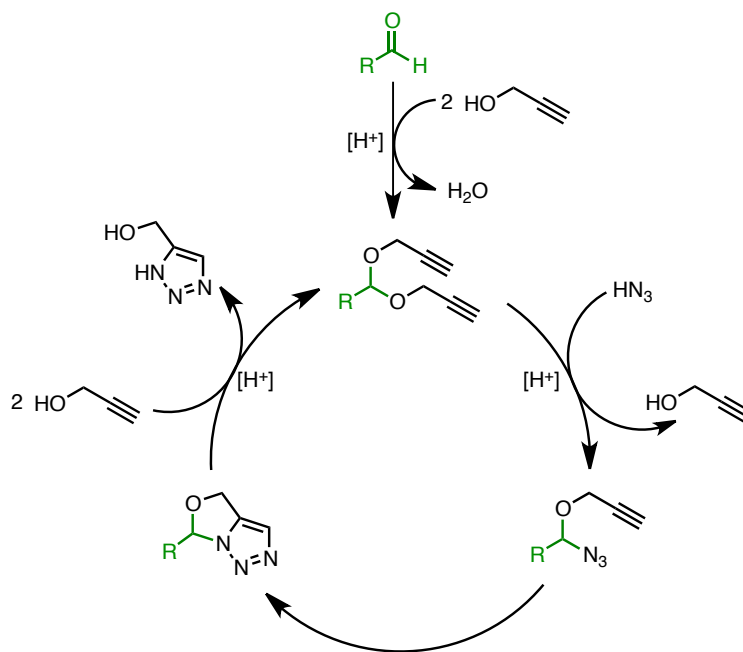


Figure A1.1 Design plan for an organocatalytic Huisgen 1,3-dipolar azide-alkyne cycloaddition

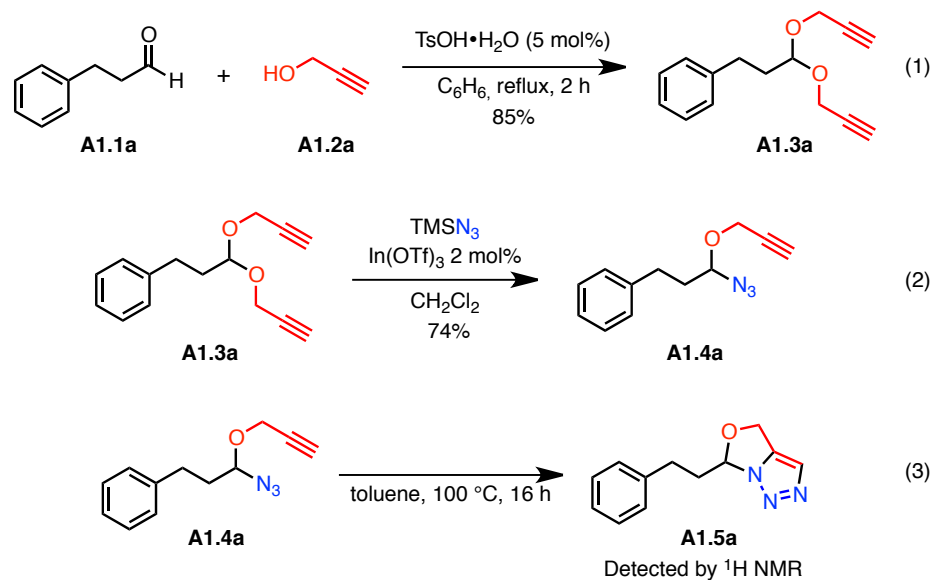
¹⁹⁶ Formation of α -azido ethers has been previously reported, see: (a) Ref. 195 (b) Hassner, A.; Fibiger, R.; Amarasekara, A. S. *J. Org. Chem.* **1988**, *53*, 22.

Some interesting features of this strategy include its selectivity to propargylic alkynes and its tolerance to the use of internal alkynes (terminal alkynes were drawn in Figure A1.1 for simplicity). The realization of this project should thus allow for a copper- or ruthenium-free site selective 1,3-dipolar cycloaddition.

A1.2 Results and Discussion

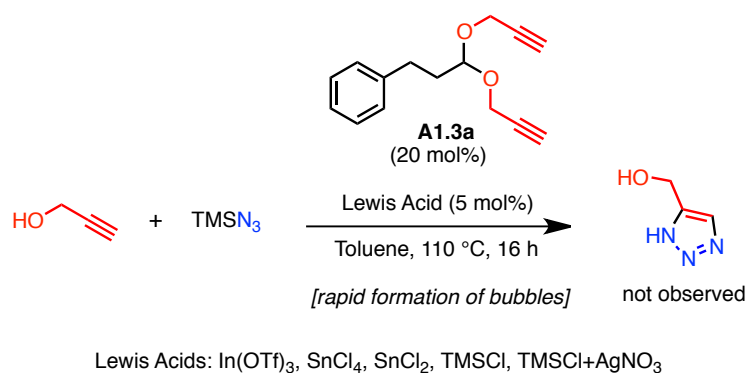
In order to determine whether this proposed design plan was viable, every step of the envisioned catalytic cycle was executed separately in a stoichiometric fashion. Scheme A1.3 summarizes the results obtained for this sequence. The first step (Eq. 1) is a simple acid-catalyzed acetal formation from aldehyde **A1.1a** and propargyl alcohol,¹⁹⁷ which affords compound **A1.3a** in 85% yield. Using the conditions developed by Taguchi (Scheme A1.2, Eq. 3), α -azido ether **A1.4a** could then be obtained in good yield using TMSN₃ and In(OTf)₃ as a Lewis acid. Upon heating **A1.4a** in toluene at 100 °C for 16 h, a compound consistent with the structure of **A1.5a** could be detected by ¹H NMR. Nonetheless, attempts at isolation of this compound via flash column chromatography failed. The acetal moiety presumably undergoes hydrolysis upon exposure to silica gel. These results however suggested that all the steps required to execute the proposed organocatalytic strategy could work successfully. More encouraging was the fact that every step of this catalytic cycle but the cycloaddition could be catalyzed by acid. The identification of a suitable acid would thus be very important to establish the desired reaction.

¹⁹⁷ Propargyl alcohol was used for simplicity and cost effectiveness to take the first steps into this chemistry.



Scheme A1.3 Individual Steps Leading to the Formation of Triazole A1.5a

Since the cycloaddition step was known to require a relatively elevated temperature (generally above 80 °C), our initial attempts at the organocatalyzed triazole formation were conducted in toluene at 110 °C. A set of experiments was performed using acetal **A1.3a** as a catalyst along with propargyl alcohol and TMSN_3 as substrates (Scheme A1.4). While screening Lewis acids under these conditions, it was noticed that bubbles were produced rapidly upon immersing the reaction flasks in the pre-heated oil bath. With all the Lewis acids tested, no desired product was observed by $^1\text{H NMR}$. The evolution of gas in the reaction mixtures suggests that the azide source is unstable under the reaction conditions. This phenomena was observed at temperatures as low as 50 °C.

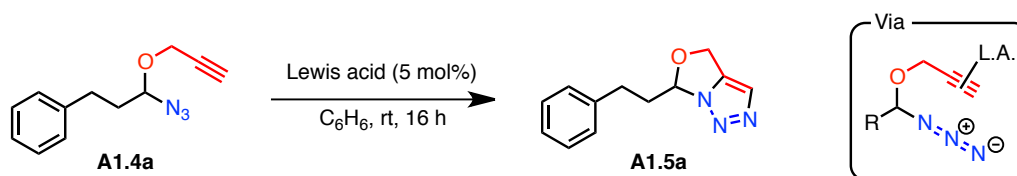


Scheme A1.4 Initial Attempts Toward Organocatalyzed Triazole Formation

Since there are high yielding room temperature literature precedents for all the steps of the proposed catalytic cycle but the intramolecular cycloaddition, we sought to find a way to catalyze this particular step so that it would occur under ambient conditions and therefore prevent the decomposition of TMSN₃. Given that electron-poor alkynes are well known to undergo 1,3-dipolar cycloaddition at lower temperature, we attempted to address the problem by reducing the electron density at the triple bond. To do so, a variety of Lewis acids that are known to activate alkynes were screened. The results are outlined in Table A1.1. In all instances, a large amount of starting material was unreacted after stirring for 16 h in benzene or acetonitrile. At best, only traces of what could correspond to the desired heterocycle were observed by ¹H NMR (Table A1.1, entries 1, 2, 7). In all other cases, the starting material was either intact or had undergone partial hydrolysis to afford aldehyde **A1.1a**.

Table A1.1 Lewis Acid Screen for an Intramolecular 1,3-Dipolar Cycloaddition

Leading to a 5,5-Fused Heterocycle



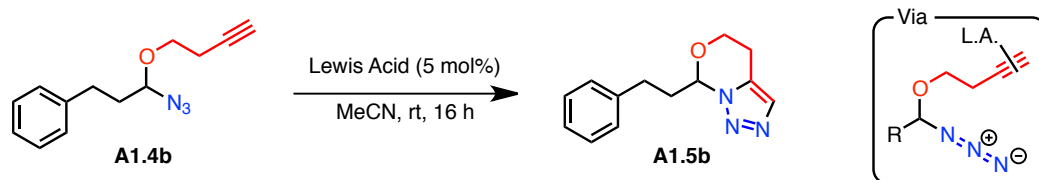
Entry	Lewis Acid	Qualitative Result
1 ^b	[(<i>i</i> PrNHC)Au(MeCN)][SbF ₆]	mostly A1.4a , traces product
2 ^b	[(JohnPhos)Au(MeCN)][SbF ₆]	mostly A1.4a , traces product
3	AuCl ₃	A1.4a and some hydrolysis product
4	CuSO ₄	Intact A1.4a
5 ^b	Cu(OTf) ₂	Almost intact A1.4a , traces of hydrolysis
6	ZnBr ₂	Intact A1.4a
7 ^b	Zn(OTf) ₂	Almost intact A1.4a , traces of product
8	In(NTf ₂) ₃	A1.4a and some hydrolysis product
9	Bi(OTf) ₃	A1.4a and some hydrolysis product
10	AgNO ₃	Intact A1.4a
11	LiBF ₄	Intact A1.4a
12	La(OTf) ₃	Intact A1.4a

^aConditions: **5.4a** (1 equiv.), Lewis acid (5 mol%), Benzene (0.4 M), rt, 16 h. ^bMeCN used as solvent instead of benzene

We then questioned whether the formation of a 5,5-fused heterocycle via intermolecular Huisgen 1,3-dipolar cycloaddition that we had tried so far was well suited for room temperature reactivity. We thus synthesized compound **A1.4b** (Table A1.2) using the same strategy as for **A1.4a**, but employing homopropargyl alcohol instead of propargyl alcohol. The intramolecular cycloaddition of this substrate would thus afford a 6,5-fused ring system. In order to promote this cyclization, mixed acetal **A1.4b** was subjected to several Lewis acids. The results obtained are summarized in Table A1.2. Similarly to what was observed with α -azido ether **A1.4a**, either intact or partially hydrolyzed **A1.4b** was found in the reaction mixture after stirring for 16 h in acetonitrile. Only the reaction using Cu(OTf)₂ as the Lewis acid may have given some trace of the desired product.

Table A1.2 Lewis Acid Screen for an Intramolecular 1,3-Dipolar Cycloaddition

Leading to a 5,6-Fused Heterocycle



Entry	Lewis Acid	Qualitative Result
1 ^b	[(<i>i</i> PrNHC)Au(MeCN)][SbF ₆]	Intact A1.4b
2 ^b	[(JohnPhos)Au(MeCN)][SbF ₆]	Intact A1.4b
3	Zn(OTf) ₂	Intact A1.4b
4	In(NTf ₂) ₃	A1.4b and some hydrolysis product
5 ^b	Cu(OTf) ₂	Almost intact A1.4a , may be traces of product

^aConditions: **5.4b** (1 equiv.), Lewis acid (5 mol%), benzene (0.4 M), rt, 16 h. ^bMeCN used as solvent instead of benzene

We then turned our attention toward the formation of an α -azido ether made from a ketone instead of an aldehyde. Analogously to what was presented in Chapter 4, we believed that the Thorpe-Ingold effect gained by employing such a substrate would allow the cyclization to proceed at a lower temperature.

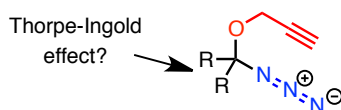


Figure A1.2 Potential Thorpe-Ingold effect to allow for a lower temperature cyclization

The formation of the necessary *bis*-propargyl acetal from several ketones proved difficult. Both the *trans*-acetalization strategy (from a dimethylacetal) and the Dean-Stark apparatus failed to provide the desired acetal. This is presumably due to the inherent generation of a thermodynamically disfavoured quaternary carbon center.

A1.3 Summary and Outlook

Although we have not found a solution to allow the intramolecular cycloaddition to occur at room temperature, a requisite for the organocatalytic tethering reaction we envisioned, we were able to highlight some loopholes in organic synthesis: no catalyst for the *intramolecular* Huisgen 1,3-dipolar cycloaddition has been discovered and no *organocatalyst* (other than base catalysts)¹⁹⁸ was found to promote the intermolecular version of this highly thermodynamically favoured reaction. It is still believed that these challenges can be addressed through an organocatalytic tethering strategy. However, an additional mode of activation would be required to facilitate the transformation. As it was alluded to in the preceding chapter, internal hydrogen bonding activation could constitute a potential solution. Indeed, given the relatively low temperature required to undergo the intramolecular cycloaddition in some previously established systems (Scheme A1.2), a small beneficial interaction could prove very advantageous in our case. Figure A1.3 illustrates a general design that we shall adopt in our future organocatalyst syntheses. It is believed that hydrogen bonding from an internal hydrogen bond donor to the oxygen of the propargyl ether could reduce the electron density of the alkyne via inductive effect. This should result in a lower energy barrier to cyclization, and potentially permit room temperature reactivity.

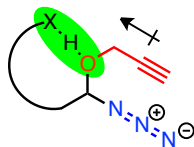


Figure A1.3 Internal hydrogen bonding activation

¹⁹⁸ A base-catalyzed formation of triazole from azides and terminal alkynes was developed by Fokin: Kwok, S. W.; Fotsing, J. R.; Fraser, R. J.; Rodionov, V. O.; Fokin, V. V. *Org. Lett.* **2010**, *12*, 4217.

In conclusion, we likely have a long way to go before being able to realize the complete catalytic cycle described in Figure A1.1. However it is very appealing to take what we learned about organocatalytic tethering strategies in the context of hydroamination and apply it to new challenges. The evolution of this general concept through the rational design of more potent organocatalysts should find application in hydroamination, in azide-alkyne cycloadditions as well as in a multitude of other reactions.

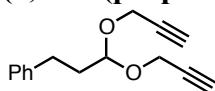
Supporting Information for Appendix 1

SYNTHESIS OF CYCLOADDITION PRECURSORS

General Information

All reagents were used as is from commercial sources. Unless otherwise noted below, all other compounds have been reported in the literature or are commercially available.

(3,3-bis(prop-2-yn-1-yloxy)propyl)benzene (A1.3a)



TsOH•H₂O (354 mg, 1.9 mmol, 0.05 equiv.) was added to a mixture of hydrocinnamaldehyde (5.00 g, 37.3 mmol, 1.00 equiv.) and propargylalcohol (8.70 mL, 149.1 mmol, 4.00 equiv.) in benzene (40 mL). The reaction flask was equipped with a Dean-Stark apparatus and refluxed for 2 h. At this point, the reaction mixture was dark brown. TLC showed high conversion. The mixture was cooled to room temperature, diluted with Et₂O, washed 2x with sat. NaHCO₃ and 1x with brine. The organic phase was dried over MgSO₄, filtered and evaporated under reduced pressure. The resulting oil obtained was clean as seen by ¹H NMR.

¹H-NMR (400 MHz; CDCl₃, 293K): δ 7.30-7.19 (m, 5H), 4.83 (t, *J* = 5.7 Hz, 1H), 4.25 (d, *J* = 2.4 Hz, 4H), 2.73 (dd, *J* = 9.1, 6.9 Hz, 2H), 2.44 (t, *J* = 2.4 Hz, 2H), 2.03-1.98 (m, 2H).

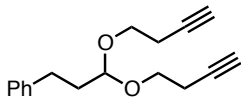
¹³C NMR (100 MHz, CDCl₃, 293K): δ 141.2, 128.4, 128.4, 125.9, 100.9, 79.7, 74.3, 53.2, 34.7, 30.6

IR (ν_{max}/cm⁻¹): 3291, 2928, 1454, 1121, 1042

HRMS calculated for C₁₅H₁₆O₂ (M⁺): 228.1150; Found 228.1116

R_f: 0.58 with 10% EtOAc in pet. ether

(3,3-bis(but-3-yn-1-yloxy)propyl)benzene (A1.3b)



TsOH•H₂O (238 mg, 1.3 mmol, 0.05 equiv.) was added to a mixture of hydrocinnamaldehyde (3.30 mL, 25.0 mmol, 1.00 equiv.) and homopropargylalcohol (7.57 mL, 100.0 mmol, 4.00 equiv.) in benzene (30 mL). The reaction flask was equipped with a Dean-Stark apparatus and refluxed for 2 h. The mixture was cooled to room temperature, diluted with Et₂O, washed 2x with sat. NaHCO₃ and 1x with brine. The organic phase was dried over MgSO₄, filtered and evaporated under reduced pressure. The mixture was then distilled under high vacuum using Kugelrohr. Leftover homopropargylalcohol was removed by distilling at 100 °C for 45 min. The temperature was then raised to 165 °C to distill the desired product. A good portion of the product collected had undergone rearrangement. The mixture was thus purified by flash column chromatography using 6-7% Et₂O in pet. ether as eluent. The product obtained is a clear oil (2.74 g, 43%).

¹H-NMR (400 MHz; CDCl₃, 293K): δ 7.29-7.18 (m, 5H), 4.58 (t, *J* = 5.8 Hz, 1H), 3.66 (ddt, *J* = 45.8, 9.3, 6.8 Hz, 4H), 2.70 (dd, *J* = 7.9, 7.9 Hz, 2H), 2.46 (td, *J* = 6.8, 2.7 Hz, 4H), 1.99-1.94 (m, 4H).

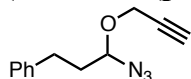
¹³C NMR (100 MHz, CDCl₃, 293K): δ 141.4, 128.4, 128.4, 125.9, 102.2, 81.4, 69.4, 63.3, 34.6, 30.9, 20.0

IR (ν_{max}/cm⁻¹): 3292, 2928, 2886, 1129, 640

HRMS calculated for C₁₇H₂₀O₂ (M⁺): 256.1463; Found 256.1476

R_f: 0.58 with 10% EtOAc in pet. ether

(3-azido-3-(prop-2-yn-1-yloxy)propyl)benzene (A1.4a)



TMSN₃ (1.73 mL, 13.14 mmol, 2.00 equiv.) was added to a suspension of In(OTf)₃ (73 mg, 0.13 mmol, 0.02 equiv.) in CH₂Cl₂ (30 mL) followed by a solution of **A1.3a** (1.50 g, 6.57 mmol, 1.00 equiv.) in CH₂Cl₂ (5 mL). The resulting mixture was allowed to stir at room temperature for 16 h. It was then diluted with CHCl₃, washed 2x with water and 1x with brine. The organic phase was then dried over MgSO₄, filtered and evaporated under reduced pressure. The purification was made via flash column chromatography using 2% Et₂O in pet. ether as eluent. The product obtained is a clear oil (1.05 g, 74%)

¹H-NMR (400 MHz; CDCl₃, 293K): δ 7.30-7.26 (m, 2H), 7.21-7.17 (m, 3H), 4.55 (t, *J* = 6.1 Hz, 1H), 4.36-4.26 (m, 2H), 2.81-2.68 (m, 2H), 2.45 (t, *J* = 2.4 Hz, 1H), 2.16-2.00 (m, 2H).

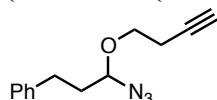
¹³C NMR (100 MHz, CDCl₃, 293K): δ 140.5, 128.5, 128.4, 126.2, 90.0, 78.5, 75.3, 55.8, 35.8, 30.8

IR (ν_{max}/cm⁻¹): 3297, 2108, 1219, 1099, 1088

HRMS calculated for C₁₂H₁₃O ((M-N₃)⁺): 173.0966; Found 173.0966

R_f: 0.29 with 2% Et₂O in pet. ether

(3-azido-3-(but-3-yn-1-yloxy)propyl)benzene (A1.4b)



TMSN₃ (1.54 mL, 11.70 mmol, 2.00 equiv.) was added to a suspension of In(OTf)₃ (99 mg, 0.18 mmol, 0.03 equiv.) in CH₂Cl₂ (20 mL) followed by a solution of **A1.3b** (1.50 g, 5.85 mmol, 1.00 equiv.) in CH₂Cl₂ (5 mL). The resulting mixture was allowed to stir at room temperature for 16 h. It was then diluted with CHCl₃, washed 2x with water and 1x with brine. The organic phase was then dried over MgSO₄, filtered and evaporated under reduced pressure. The purification was made via flash column chromatography using 4% Et₂O in pet. ether as eluent. The product obtained is a clear oil (1.01 g, 75%)

¹H-NMR (400 MHz; CDCl₃, 293K): δ 7.30-7.26 (m, 2H), 7.19 (m, 3H), 4.33 (t, *J* = 6.1 Hz, 1H), 3.86 (dt, *J* = 9.3, 6.6 Hz, 1H), 3.57 (dt, *J* = 9.3, 7.0 Hz, 1H), 2.80-2.68 (m, 2H), 2.49 (td, *J* = 6.8, 2.6 Hz, 2H), 2.15-1.97 (m, 3H).

¹³C NMR (100 MHz, CDCl₃, 293K): δ 140.6, 128.5, 128.4, 126.2, 91.7, 80.8, 69.7, 67.0, 35.8, 30.9, 19.8

IR ($\nu_{\max}/\text{cm}^{-1}$): 3303, 2107, 1106, 1090

HRMS calculated for $\text{C}_{13}\text{H}_{15}\text{O}$ ($(\text{M}-\text{N}_3)^+$): 187.1123; Found 187.1146

R_f: 0.52 with 5% Et_2O in pet. ether

General procedure for the screening of Lewis acids

5.4 (0.2 mmol, 1.00 equiv.) was placed in a test tube and dissolved in benzene or acetonitrile (0.5 mL). Lewis acid (0.01 mmol, 0.05 equiv.) was added after which the tube closed with a septa and flushed with argon. The mixture was allowed to stir overnight at room temperature. The next day, an aliquot was taken and volatiles evaporated under a flow of air. The mixture was taken up in CDCl_3 and analyzed by ^1H NMR. Results are shown in Table 5.1 and 5.2.

Appendix 2

Claims to Original Research

1. Development of conditions for the oxidative Rh(III)-catalyzed synthesis of isoquinolines from the coupling/cyclization of benzaldimines with internal alkynes
2. Preliminary mechanistic investigations into the Rh(III)-catalyzed isoquinoline synthesis mentioned above.
3. Development of mild conditions (low temperature, low catalyst loading) for the redox-neutral synthesis of isoquinolones from benzohydroxamic acids with alkynes (terminal or internal) or alkenes.
4. Mechanistic investigations into the redox-neutral Rh(III) catalyzed synthesis of isoquinolones mentioned above
5. Development of conditions for the Rh(III)-catalyzed redox-neutral synthesis of isoquinolines from the cross-coupling/cyclization of aryl oximes with alkynes
6. Mechanistic investigation into the Cope-type hydroamination of alkenes via tethering organocatalysis

Publications from this Work

1. *Isoquinoline Synthesis via Rhodium-Catalyzed Oxidative Cross-Coupling/Cyclization of Aryl Aldimines and Alkynes* Guimond, N.; Fagnou, K. *J. Am. Chem. Soc.* **2009**, *131*, 12050-12051.
2. *Rhodium(III)-Catalyzed Isoquinolone Synthesis: The N-O bond as a Handle for C-N Bond Formation and Catalyst Turnover* Guimond, N.; Gouliaras, C.; Fagnou, K. *J. Am. Chem. Soc.* **2010**, *132*, 6908-6909.
3. *Rhodium(III)-Catalyzed Heterocycle Synthesis Using An Internal Oxidant: Improved Reactivity and Mechanistic Studies* Guimond, N., Gorelsky, S.; Fagnou, K. *J. Am. Chem. Soc.* **2011**, *133*, 6449-6957.
4. *Catalysis Through Temporary Intramolecularity: Mechanistic Investigations on Aldehyde-Catalyzed Cope-Type Hydroamination Lead to the Discovery of a More Efficient Tethering Catalyst* Guimond, N.; MacDonald, M. J.; Lemieux, V.; Beauchemin, A. M. *Submitted*

Presentations from this Work

Oral presentation

1. Nicolas Guimond and Keith Fagnou. *Synthèse d'isoquinolines catalysée par le rhodium par couplage d'aldimine d'aryle avec des alcynes*. 77e congrès de l'Acfas, Université d'Ottawa, Ottawa, Ontario, Canada (2009)
2. Nicolas Guimond, Christina Gouliaras and Keith Fagnou. *Formation d'isoquinolones catalysée au Rh(III): le lien N-O comme outil pour la formation de lien C-N et la*

régénération du catalyseur. 78^e congrès de l'Acfas, Université de Montréal, Montréal, Québec, Canada (2010)

3. Nicolas Guimond and Keith Fagnou. *Rh(III)-Catalyzed Isoquinolone Formation: Mechanistic Investigations Lead to Discovery of Unexpected Reactivity*. QOMSBQC, Brock University, Ste-Catherines, Ontario, Canada (2010)

Poster Presentations

1. Nicolas Guimond and Keith Fagnou. *Isoquinoline Synthesis via Rhodium-Catalyzed Coupling of Aryl Aldimines and Alkynes*. Ottawa Carleton Chemistry Innovation Day (*1st prize winner for poster presentations*), Synthesis Day, University of Ottawa, Ottawa, Ontario, Canada (2009)
2. Nicolas Guimond, Christina Gouliaras and Keith Fagnou. *Nitrogen Containing Heterocycles Through Rhodium Catalyzed Processes*. QOMSBQC, Université Laval, Québec, Québec, Canada (2009)
3. Nicolas Guimond, Christina Gouliaras and Keith Fagnou. *Rh(III)-Catalyzed Isoquinolone Formation: the N-O Bond as a Handle for C-N Bond Formation and Catalyst Turnover*. Keith Fagnou Organic chemistry Symposium (KFOS), University of Ottawa, Ottawa, Ontario, Canada (2010)
4. Nicolas Guimond, and Keith Fagnou. *Rh(III)-Catalyzed Isoquinolone Formation: Mechanistic Investigations Lead to Discovery of Unexpected Reactivity*. AstraZeneca Symposium (*2nd prize poster presentation award*), Montréal, Québec, Canada (2010)
5. Nicolas Guimond and André Beauchemin. *Mechanistic Insights Into an Intermolecular Alkene Hydroamination Using an Organocatalytic Tethering*

- Strategy*. Ottawa Carleton Chemistry Innovation Day, University of Ottawa, Ottawa, Ontario, Canada (2011)
6. Nicolas Guimond, Melissa J. MacDonald, Peter J. Ng, Derek J. Schipper, Joseph Moran and André M. Beauchemin. *Intermolecular Alkene Hydroamination Using an Organocatalytic Tethering Strategy*. Gordon Research Conference – Heterocyclic Compounds, Newport, Rhode Island, United-States (2011)
 7. Nicolas Guimond and André Beauchemin. *Intermolecular made Intramolecular: Mechanistic Investigations on Cope-Type Alkene Hydroamination Using an Organocatalytic Tethering Strategy*. QOMSBOC (*best poster presentation award*), Concordia University, Montréal, Québec, Canada (2011)